공학박사학위논문

Selection of Optimal Liquefaction Process System considering Offshore Module Layout for LNG FPSO at FEED stage

해양 모듈 배치를 고려한 FEED 단계에서의 LNG FPSO 용 최적 액화 프로세스 시스템 선정 연구

2013년 2월

서울대학교대학원
조선해양공학과
황지현

Contents

Figures

Tables

Abstract

Selection of the Optimal Liquefaction Process System Considering the Offshore Module Layout for LNG FPSO at the FEED Stage

In this paper, the offshore selection criteria for the optimal liquefaction process system are studied to contribute to the future FEED engineering for the liquefied –natural -gas (LNG) floating, production, storage, and offloading (LNG FPSO) liquefaction process system.

From the foregoing, it is clear that offshore liquefaction plants have process requirements different from those of the traditional onshore liquefaction plants. While thermodynamic efficiency is the key technical process selection criterion for large onshore liquefaction plants, the high-efficiency pre-cooled mixed refrigerant and optimized cascade plants that dominate the onshore LNG installations are unlikely to meet the diverse technical and safety needs of offshore liquefaction facilities. Offshore liquefaction technology developers are rightly focusing on process simplicity, low weight, small footprint, and other criteria. The key criteria that influence process selection and plant optimization for the offshore liquefaction cycle lead to some trade-offs and compromises between efficiency and simplicity. In addition, other criteria for offshore liquefaction cycles should also be considered, such as flexibility, safety, vessel motion, refrigerant storage hazard, proven technology, simplicity of operation, ease of start-up/shutdown, and capital cost.

First of all, this paper proposes a generic mixed refrigerant (MR) liquefaction cycle based on four configuration strategies. The 27 feasible MR liquefaction cycles from such generic MR liquefaction cycle are configured for optimal synthesis. From the 27 MR liquefaction cycles, the top 10 are selected based on the minimum amount of power required for the compressors. Then, one MR liquefaction cycle is selected based on simplicity among the 10 MR process cycles, and this is called a "potential MR liquefaction cycle."

Second, three additional offshore liquefaction cycles — DMR for SHELL LNG FPSO, C_3MR for onshore projects, and the dual N2 expander for FLEX LNG FPSO — are considered for comparison with the potential MR liquefaction cycle for the selection of the optimal offshore liquefaction cycle.

Such four cycles are compared based on simplicity, efficiency, and other criteria. Therefore, the optimal operating conditions for each cycle with four LNG capacities (4.0, 3.0, 2.0, and 1.0 MTPA) are calculated with the minimum amount of power required for the compressors. Then the preliminary equipment module layout for the four cycles are designed as multi-deck instead of single-deck, and this equipment module layout should be optimized to reduce the area occupied by the topside equipment at the FEED stage. In this paper, the connectivity cost, the construction cost proportional to the deck area, and the distance of the main cryogenic heat exchanger (MCHE) and separators from the centerline of the hull are considered objective functions to be minimized. Moreover, the constraints are proposed to ensure the safety and considering the deck penetration of the long equipment across several decks. Considering the above, mathematical models were formulated for them. For example, the potential MR liquefaction cycle has a mathematical model consisting of 257 unknowns, 193 equality constraints, and 330

inequality constraints. The preliminary optimal equipment module layouts with four LNG capacities (4.0, 3.0, 2.0, and 1.0 MTPA) are then obtained using mixed-integer nonlinear programming (MINLP).

Based on the above optimal operating conditions and equipment module layouts for the four potential offshore liquefaction cycles, trade-offs between simplicity and efficiency are performed for actual offshore application, and finally, the potential MR liquefaction cycle is selected for the optimal liquefaction cycle for LNG FPSO.

Keywords: Offshore selection criteria, optimal offshore liquefaction cycle, offshore application, efficiency, simplicity, optimal synthesis, optimal operating conditions, equipment module layout, generic MR liquefaction cycle, LNG FPSO, FEED

Student number: 2007-30176

1. Introduction

1.1. Motivation

The demand for oil and gas will not abate in the near future. Peak oil is a fast-approaching reality, and the oil prices may rise again, destabilizing the oil market. On the other hand, the demand for fossil fuels is increasing exponentially, making countries and oil companies eager to explore new reserves. Smaller and difficult oil and gas fields, which were previously uneconomical, are looking more attractive as alternatives for fossil fuel production. Offshore floating liquefied natural gas (LNG) production is the key differential that may ensure the development of some of these fields.

LNG is one of the methods of transporting natural gas over long distances that have been introduced. Numerous projects and researches on issues related to it are currently being undertaken. The aim of these studies is to find new efficient methods of producing and transporting LNG. One of the conductive topics is floating, production, storage, and offloading (FPSO). The technical risk, equipment design and availability, topside design, ease of modularization, plant performance and operation, delivery schedule, and safety and environmental impact of offshore areas in this process have been evaluated. These engineering studies have further proven that this liquefaction technology is an outstanding candidate for offshore LNG projects (Michelle, 2007).

Critically, the cost of FPSO is massively greater than those of land-based LNG units. In addition, the technical challenges of FPSO are difficult to overcome, but FPSO is essentially the only option to extract natural resources for many fields. As the prices of oil and gas increase, the investment required for FPSO looks more attractive (Makhateb et al., 2008). With the realization of large FPSO facilities for oil production, and more recently, LPG production, LNG FPSO projects appear to be increasingly more likely in the future.

This study focused on the optimal liquefaction cycle to realize LNG FPSO in future projects. It is expected to contribute tremendously to actual offshore application.

1.2. LNG FPSO Topsides Process Systems

LNG FPSO consists of a hull, a turret, and a topside. The latter (topside) is divided into two parts: the process system and the utility system. The process system consists of separation, pretreatment, fractionation, and liquefaction, as shown in Figure 1-1 (Hwang et al., 2013).

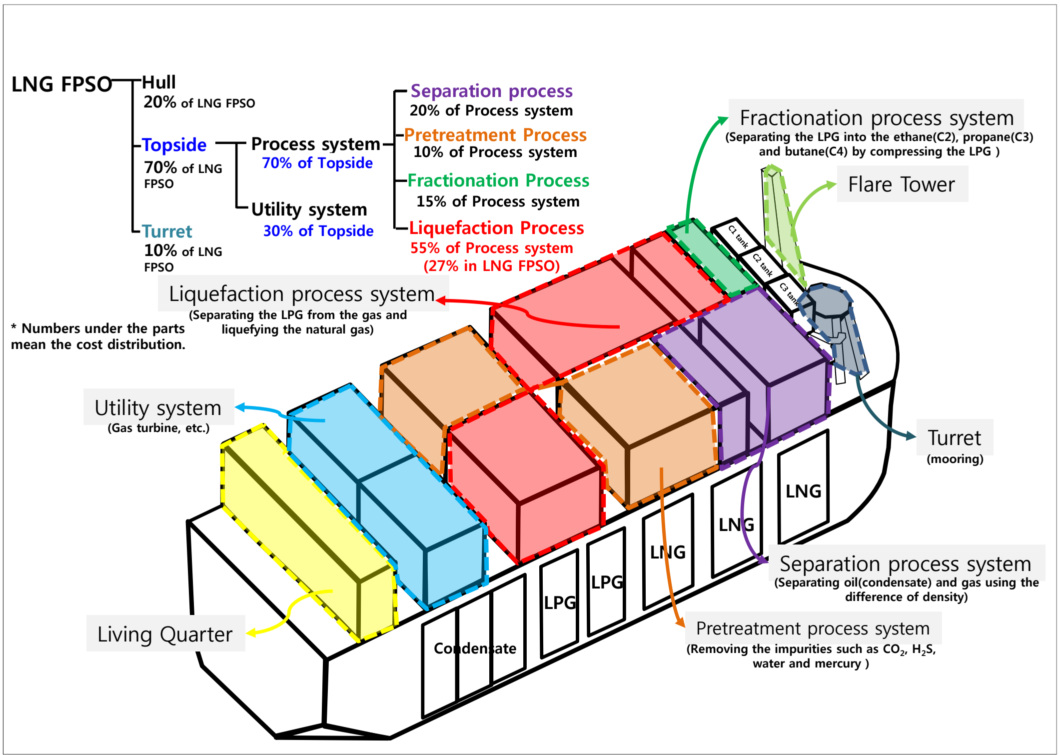

Figure 1-1 Configuration of LNG FPSO

In the liquefaction process system, the separated and pre-treated natural gas is condensed into a liquid (LNG) whose volume is about 1/600th the volume of natural gas. The resulting LNG is stored in atmospheric tanks ready for export by ships. Therefore, the liquefaction process is important in the LNG FPSO topside process system and typically accounts for 70% of the capital cost of the topside process system and 30-40%

of the overall plant cost (Shukri, 2004).

The products of the gas well are separated into natural gas (NG), liquefied petroleum gas (LPG), and condensate. They are stored separately in the LNG FPSO. The main component of NG is methane (CH_4), and the main components of LPG are propane (C_3H^8) and butane (C_4H_{10}). If a fuel is composed of ethane (C_2H_6), propane (C_3H_8), and butane (C_4H^{10}), it is called a “natural gas liquid (NGL).” As the boiling points of NG, LPG, and NGL at 1 atm are higher than room temperature (21℃), as shown in Table 1-1, they exist in the gas phase at 1 atm and room temperature. On the other hand, the condensate is composed of pentane (C_5H_{12}) and hexane (C_6H_{14}). As the boiling point of the condensate is higher than room temperature (21℃), as shown in Table 1-1, it exists in the liquid phase at 1 atm and room temperature, and is called “oil.”

Table 1-1 Gas well components

		Components	**Elementary Symbol**	**Boiling Point**
Natural gas (NG)		Methane	CH_4	-161.5℃
Natural gas liquid (NGL)		Ethane	C_2H_6	-88.6℃
	Liquefied petroleum gas (LPG)	Propane	C_3H_8	-42.1℃
		Isobutane	C_4H_{10}	-11.73℃
		Normal butane	C_4H_{10}	-0.5℃
Condensate		Isopentane	C_5H_{12}	27.88℃
		Normal pentane	C_5H_{12}	36.06℃
		Normal hexane	C_6H_{14}	68.73℃

The topside process system in LNG FPSO proceeds as follows. At first, as shown in Figure 1-2, the components of the mixture of water, condensate (liquid), and gas components of NGL and NG are separated using the difference in density, through the separation process system. The separation process system consists of a slug catcher (1-1 in Figure 1-2), a gas/liquid separator (1-2 in Figure 1-2), and a stabilizer (1-3 in Figure 1-2). The slug catcher stabilizes the slug flow from the gas well. The gas/liquid separator then separates the components of the mixture of water, condensate, and gas using the difference in density. As the gas components are not completely separated from the condensate in the gas/liquid separator, the stabilizer again separates the gas components from the condensate, returns them to the gas flow, and stores the condensate that is left in the condensate tank.

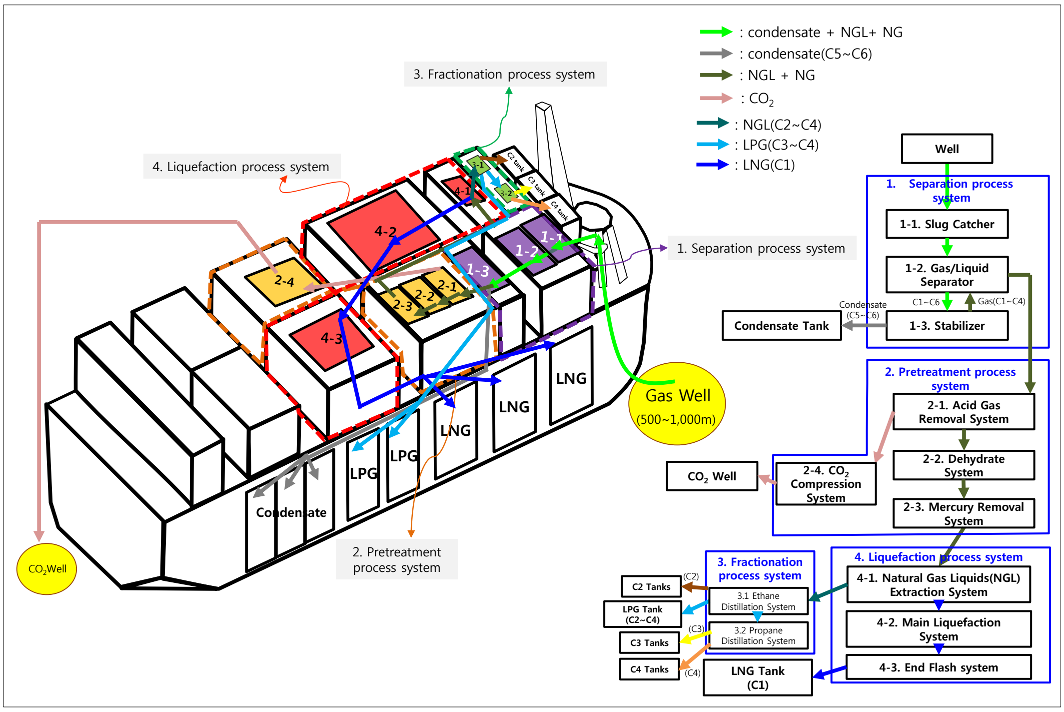

Figure 1-2 Topside process system of LNG FPSO

Second, the pretreatment process system removes impurities such as CO_2, H_2S, water, and mercury from the separated gas components. The pretreatment process system consists of the acid-gas removal system (2-1 in Figure 1-2), the dehydrate system (2-2 in Figure 1-2), the mercury removal system (2-3 in Figure 1-2), and the CO_2 compression system (2-4 in Figure 1-2). The acid-gas removal system removes acid gases such as H_2S and CO_2, which are corrosive to materials and toxic to humans. To prevent global warming, the CO_2 removed from the gas components is re-injected into the CO_2 well, which is separated from the gas well. The dehydrate system removes the water, which forms the ice. The mercury removal system removes the mercury, which can damage the equipment and pipes.

Third, the fractionation process system separates the NGL into ethane, propane, and butane through compression and the liquefaction process system separates the gas components into NGL and NG and then liquefies NG. The fraction process system consists of the ethane distillation system (3-1 in Figure 1-2) and the propane distillation system (3-2 in Figure 1-2). The liquefaction process system consists of the natural gas liquid (NGL) extraction system (4-1 in Figure 1-2), the main liquefaction system (4-2 in Figure 1-2), and the end flash system (4-3 in Figure 1-2). The gas components consisting of NGL and NG were separated into NGL and NG in the NGL extraction system by pre-cooling such components. The NGL was separated into ethane and LPG through the ethane distillation system. The ethane separated from the NGL was used as the refrigerant in the liquefaction system. Some of the LPG was stored in the LPG tank, and the rest was used in the propane distillation system. The propane distillation system separates LPG into propane and butane through compression, and uses them as the refrigerant in the liquefaction system. The natural gas separated from the gas components in the NGL extraction system is liquefied by using the refrigerant in the main liquefaction system. At this time, the pressure of LNG is 60 bars. To store the LNG in the LNG tank at atmospheric pressure (1.01 bar), the pressure of the LNG is reduced to the atmospheric pressure through the end flash system. Finally, the LNG is stored in the LNG tank.

1.3. Key Technical Process Selection Criteria between Offshore and Onshore Natural Gas Liquefaction

Offshore natural gas liquefaction has process requirements different from that of the traditional onshore liquefaction. While thermodynamic efficiency is arguably the most important process selection criteria for onshore natural gas liquefiers, other factors have become more important for offshore projects.

Thermodynamic efficiency is likely to remain critically important. For offshore applications, however, criteria such as compactness and process simplicity have become more significant considerations.

(1) Onshore liquefaction process

The logical starting point for any new LNG production scheme should be the existing industry and processes. The baseload LNG industry now has a more-than-40-year history, starting with the permanent operations of the Camel plant in Algeria in 1964. The earliest plants consisted of fairly simple liquefaction processes based on either the cascaded refrigeration or single mixed refrigerant (SMR) processes, and the train capacities were less than 1 MTPA. In 1972, Brunei Lumut 1 utilized the first two-cycle process using a propane pre-cooled mixed refrigerant (C_3MR) developed by Air Products and Chemicals Int. (APCI). This process became the dominant liquefaction process technology by the late 1970s and continues to be the workhorse of the LNG industry today. During this period, APCI and others have made significant improvements on the original C_3MR process. The economies of scale, improved process simulation tools, and improved equipment performance (i.e., liquid expanders and gas turbine drivers) have all dramatically decreased the installed liquefaction plant costs, improved the performance, and increased the capacity of the liquefaction trains. The continued development of the traditional LNG plant design can be seen by comparing the recently commissioned plants to the current and planned facilities. Less than five years ago, Foster Wheeler and Chiyoda Corp. of Japan completed an engineering, procurement, and construction (EPC) contract for Oman LNG. At the time of the start-up (February 2000 for Train 2), this plant had the largest trains in operation at 3.3 MTPA, and set a benchmark for process efficiency with a reported average specific power of 10.15 kW per tonne per day of LNG (McLachlan et al., 2002). Five years later, the installed train capacities were over 5 MTPA, with projects in development for 7.8 MTPA. The liquefaction process typically accounts for 30-40% of the capital of the overall plant and has a large impact on the utilities and operating costs. The selection of the appropriate cycle is critical for cost-effective LNG projects. Historically, liquefaction cycle selection was an easy choice to make: APCI C_3MR. Table 1 shows the baseload liquefaction trains currently operating, in various stages of construction, and the planned ones (in the case of AP-X).

Table 1-2 shows two key points (Shukri, 2004; Meyer, 2004; DOE/EIA, 2003).

Table 1-2 LNG trains by liquefaction process

Liquefaction Process	**Licensor**	**% of Market**
Propane pre-cooled MR	APCI	77 %
Optimized cascade	Conoco-Phillips	9 %
Single refrigerant MR	APCI	5 %
Classic cascade	Marathon/Phillips	1 %
Teal dual-pressure MR		1 %
Prico single-stage MR	Black & Veatch	2 %
MR processes (DMR)	Shell	4 %
Multifluid cascade	Linde-Statoil	1 %
AP-X process	APCI	0 %

First, the APCI C_3MR process dominates the industry; second, there has been a considerable diversification of liquefaction processes in the last five to seven years. This increased competition has led to increased train capacity, improved driver integration, and decreased capital costs. Four trains of APCI's new AP-X liquefaction process are being planned in Qatar for Qatargas II trains 4 and 5 and RasGas II trains 6 and 7. These planned plants represent the state-of-the-art land-based liquefaction process, featuring a single-train liquefaction capacity of 7.8 MTPA using an N_2 expander cycle to effect the subcooling of the LNG.

(2) Offshore liquefaction process

Offshore liquefaction facilities have technology selection criteria different from those of their onshore counterparts, leading to different optimal processes. Offshore facilities must be compact and light, must have a small footprint, and must offer high inherent process safety. They must also consider the additional constraints placed on the system in the marine environment, such as vessel motion, and must offer a high degree of modularity, ease of operation, low equipment count, quick start-up, and high availability. Additionally, as FPSOs will be processing gas from marginal fields, they must be tolerant of a variety of process conditions and must have a high degree of inherent process robustness. High process efficiency remains an important selection criterion because even with inexpensive feed gas, poor efficiency must be paid for with increased utilities, compressor capacity, and other major capital expenditure items. The technologies in use on the existing FPSOs, such as turbines, compressors, towers, and separators, have already set the groundwork for installing machinery on floating facilities. This development over the past 20 years allows the process to be taken to offshore LNG plants with a large number of already-proven components. Other factors that must be considered are LNG storage and offloading. The transport in LNG carriers is well established, but partial fill conditions in the LNG FPSO will occur as the LNG is being processed prior to offtake. This may result in sloshing, which is of particular concern in membrane tanks. The consideration of loss of containment must also be addressed when considering hull fabrication. The use of concrete for the hull provides benefits in the storage of cryogenic fluids as it retains its structural integrity when in contact with the LNG, but this must be measured against the potential cost reductions if traditional steel ship designs could be utilized. If offloading is considered with a typical spread-moored configuration, such as that which might be found offshore West Africa, side-by-side offloading can be considered. This provides a benefit because LNG carriers typically load at midship, therefore providing more flexibility. In less benign seas, however, weathervaning configurations are often used, possibly with tandem offloading being required. To facilitate a number of technologies, suppliers have looked at flexible loading arms for the transfer of LNG between the production vessel and the tanker, such as the SBM soft-yoke mooring and offloading (SYMO) system. These factors have all been examined in various studies, such as Project Azure and the Shell development work on FLNG and FONG (Sheffield, 2001; Faber, 2002).

2. Related Works

2.1. Offshore Front-End Engineering Design (FEED)

The engineering of offshore production plants is divided into two phases: the front-end engineering design (FEED) phase and the detailed engineering phase. Of these two phases, the FEED phase is more critical for determining the feasibility of specific well area development. An economic analysis of the development of a specific well area is performed based on the outputs of the FEED phase. Based on the results of this analysis, the detailed engineering phase is executed if the value of the development is sufficiently large. In other words, the FEED phase, which is the basis of the detailed engineering phase and of the feasibility of development on specific well areas, is the most important overall offshore plant phase, determining the project success. The final outputs of the FEED phase are the total costs, the weight, and the layout of an offshore plant. The feasibility of offshore plant projects is determined by these final outputs. The system capacity and size of each topside system are first determined to ascertain such final outputs as the total cost, weight, and layout. Offshore process engineering, one of the highest priority areas in engineering, is the most important component in calculating the system capacities and sizes of topside systems. The overall engineering for offshore topside systems includes the offshore process, piping, mechanical engineering, instrumentation, electrical engineering, and outfitting engineering. Major engineering data are derived through offshore process engineering, to obtain the final data for increasing the efficiency of the process.

While many offshore projects such as drillships, semi-submersible rigs, fixed platforms, and FPSOs have been constructed, the South Korean shipyards have concentrated more on construction and installation than on engineering in the early stages of these offshore projects. In the case of process engineering, the South Korean shipyards only have to perform the construction and installation according to the process engineering results obtained from sub-engineering contractors such as Technip (2012), Mustang Engineering (2012), and Doris Engineering (2012). For example, Technip was involved in major offshore FPSO projects such as Petrobras P-37, Elf Nkossa, Total Dalia, and Total Akpo while Mustang Engineering performed major offshore FPSO projects, including Chevron Agbami and Nexus Crux. Doris Engineering carried out CPTL Farwah FPSO projects.

While process engineering technology is partially understood by the South Korean shipyard workers due to the technical meetings between the South Korean shipyard representatives and the sub-engineering contractors during the construction stage of offshore projects, process engineering is still regarded as an exclusive technology of the top offshore engineering companies. Fortunately, a process engineering method with extreme limitations was introduced in recent offshore conferences and papers. The universities and research centers in South Korea, however, are not conducting process engineering studies of offshore plants; rather, research is being conducted in fields related to structural mechanics and fluid dynamics, such as the motion and hydroelastic responses of offshore structures (Shin et al., 2000; Lee et al., 2000), the reliability of fatigue and strength analyses of offshore structures (Lee et al., 1998; Kim et al., 2004), and the mooring systems of offshore structures (Na et al., 2004; Kim et al., 2006).

In overseas countries, specialized offshore engineering companies such as Technip, Mustang Engineering, and Doris Engineering are accumulating experience in process engineering through their involvement in several oil and gas development business consortiums. Universities and research centers in foreign countries, however, are conducting basic research related to structural and fluid dynamics and not actual studies related to the process engineering of offshore plants (Lake et al., 2000; Newman & Lee, 2002; Matsuura & Bernitsas, 2006).

2.2. Optimal Operating Conditions

For the related works on the design of the liquefaction cycle, two kinds of studies have been conducted so far. The first kind of studies focused on the configuration of the cycle and compared the proposed liquefaction cycle or some existing liquefaction cycles with other existing liquefaction cycles (Chang et al., 2010; Finn et al., 2000; Lee et al., 2010a; Lee et al., 2010b; Lim et al., 2010; Nogal et al., 2008; Remeljrej & Hoadley, 2006). The second kind of studies focused on finding the optimal operating conditions for a given commercial cycle (Chang et al., 2009; Jensen, 2008; Kim et al., 2010; Lee, 2002; Venkatarathnam, 2008). This study falls under the combination of the first and second kinds.

(1) Related works on the configuration of the liquefaction cycle

To compare the cycles with differing configurations, the operating conditions of each cycle should be the optimal value obtained from the analysis of the optimization of the cycle. Thus, in the following studies, whether the optimal operating conditions were used was checked.

Lee et al. (2010b) proposed a modified SMR cycle and compared the exergy efficiency of the cycle and the required compressor power in the cycle with those of the existing SMR cycle. For the comparison, the optimal operating conditions of the cycle were obtained by referring to the other studies (Venkatarathnam, 2008). Lim et al. (2010) proposed that the cycle be combined with the SMR cycle and with the N_2 expander cycle, and compared the required compressor power in the cycle with that in the other existing cycles. For the comparison, the operating conditions of the cycles were also obtained by referring to the patent. Lee et al. (2010a) compared the existing C_3MR cycle with the N_2 expander cycle according to the required compressor power in each cycle for the application of the liquefaction cycle of LNG FPSO. For the comparison, the operating conditions of the cycles were also obtained by referring to the patent. Chang et al. (2010) proposed the combined refrigerant-pre-cooled mixed refrigerant (CR-MR) cycle, whose pre-cooling part consists of the ethane and butane cycles, and compared the exergy efficiency of the cycle with those of the existing C_3MR and DMR cycles. For the comparison, the operating conditions of the cycles were obtained by referring to the existing optimal operating conditions obtained by Venkatarathnam (2008). Finn et al. (2000) compared the existing liquefaction cycles with one another, according to the required compressor power in each cycle and their complexity, sensitivity to vessel motion, compactness, and cost, for the application of the liquefaction cycle of offshore and midscale plants. For the comparison, the values of the aforementioned criteria for each cycle were obtained by referring to the other studies. Remeljrej and Hoadley (2006) compared the existing liquefaction cycles with one another according to their exergy efficiency and complexity, to propose that the new LNG open-loop cycle is good for offshore production. For the comparison, the operating conditions of the cycles were obtained by referring to the existing optimal operating conditions obtained in other studies. Nogal et al. (2008) proposed an approach for the optimal configuration of the SMR cycle and the MR cascade cycle, according to the required compressor power in each configuration. For the comparison of the cycles, the operating conditions of the cycles were obtained using the properties of the Aspen simulators — the commercial process simulators made by AspenTech for the calculation of thermodynamic properties — and the GA in the study.

(2) Related works on the analysis optimization of the liquefaction cycle

Lee et al. (2002) obtained the optimal operating conditions of the SMR cycle to minimize the required compressor power in the cycle by formulating a mathematical model of the cycle. Jensen (2008) also obtained the optimal operating conditions of the SMR cycle to minimize its required compressor power by formulating a mathematical model of it. While one case of the mathematical model of the SMR cycle was focused on in the study conducted by Lee et al. (2002), nine cases of such were formulated, and the optimal operating conditions of each case were obtained. Venkatarathnam (2008) obtained the optimal operating conditions of the various cycles, including the DMR cycle, to maximize the exergy efficiency. Instead of formulating a mathematical model of the cycle, ASPEN Plus was used. Further, the optimization problem was solved by via SQP. Kim et al. (2010) only formulated an objective function and design variables for the C_3MR cycle and did not obtain the optimal operating conditions. Cha et al. (2010) formulated a mathematical model of the reverse Brayton cycle to minimize the required compressor power, and obtained the optimal operating conditions. Chang et al. (2009) obtained the optimal operating conditions, including the optimal heat exchanger size, in the reverse Brayton cycle. A mathematical model of the cycle was formulated, and the objective function was the exergy efficiency.

In this study, the optimal operating conditions of the potential offshore liquefaction cycles were obtained to minimize the required compressor power in the cycle. Table 2-1 shows the comparison of the formulation of the optimization problem between this paper and other past papers

Table 2-1 Comparison of the formulation of the operating conditions optimization problem between this study and past studies

Study	**Cycle**	**Formulation of the Optimization Problem**		
		Constraints	**Objective function**	**Optimization method**
Chang et al. (2009)	Reverse Brayton cycle	Derived	Exergy efficiency	Self-optimization[1]
Cha et al. (2010)	Reverse Brayton cycle	Derived	Required compressor power for the compressors	Hybrid optimization method (SQP+GA)
Jensen (2008)	SMR cycle	Derived	Required compressor power	Use of a commercial tool (gPROMS[2])
Lee et al (2002)	SMR cycle	Derived	Required compressor power	Nonlinear programming
Nogal et al. (2008)	SMR cycle and MR cascade cycle	Derived	Required compressor power	GA
Venkatarathnam (2008)	Various cycles, including the DMR cycle	Use of a commercial process simulator (ASPEN Plus[3])	Exergy efficiency	SQP
This study (2013)	Potential offshore liquefaction cycles	Derived	Required compressor power	Self-optimization[1]

---

[1] By selecting a controlled variable and varying this variable by keeping the other variables at a constant setpoint, the optimal value of the variable that is being controlled to minimize the objective function can be obtained.

[2] The commercial process simulator used for the modeling and optimization of the process, made by Process Systems Enterprise Limited (PSE)

[3] The commercial process simulator used for the modeling and simulation of the process, made by AspenTech

2.3. Optimal Synthesis

The previous studies related to liquefaction cycle configuration can be classified into two groups. One group of studies examined the different numbers of cycles in the liquefaction process compared with the existing liquefaction processes. The other group examined the optimal synthesis of liquefaction cycles by changing the number of combinations of the equipment comprising the liquefaction cycle. Hence, optimal liquefaction cycles are derived from the comparison of feasible liquefaction cycles that can be configured according to the engineering intention.

(1) Related works on the number of cycles

Lim et al. (2010) proposed combining the dual cycle with the SMR and reverse Brayton cycles. They compared the power required for the compressors with that in other existing cycles, such as the SMR, reverse Brayton, C_3MR, dual expander, and cascade cycles.

Finn et al. (2000) and Lee et al. (2010b) compared the liquefaction process cycles already developed with the existing cycles. Lee et al. (2010b) quantitatively compared the power required for the compressors in the existing C_3MR cycle and the reverse Brayton cycle. Finn et al. (2000) qualitatively compared the existing liquefaction cycles, such as the SMR, reverse Brayton, C_3MR, DMR, dual expander, and cascade cycles. The comparison was made according to the power required for the compressors in each cycle, their complexity, the available area, the degree of explosion risk, the degree of operation difficulty, and the capital cost.

(2) Related works on optimal synthesis

A number of authors have proposed an optimal liquefaction cycle by changing the combinations of the equipment making up both a single liquefaction cycle and a dual liquefaction cycle. Nogal et al. (2008) proposed an optimal liquefaction cycle by combining three configuration strategies in the single and dual liquefaction cycles. The configuration strategies in the liquefaction cycle change the number and association of the equipment making up the cycle within a feasible range. The three configuration strategies proposed by Nogal et al. (2008) are “single cycle with regeneration,” “multi-stage compression with intercooling,” and “multi-stage refrigeration.” These strategies are explained in detail in the next chapter. The objective was to minimize the power required by the compressors.

In contrast, Rangaiah (2008) proposed an optimal liquefaction cycle considering only multi-stage refrigeration in the single liquefaction cycle, using expanders instead of expansion valves. The objective was to minimize the cost of the resources, such as the compressors, expanders, and electricity.

This study proposes a generic MR liquefaction cycle based on the configuration strategies of “single cycle with regeneration,” “multi-stage compression with intercooling,” and “multi-stage refrigeration” proposed by Nogal (2006) and Rangaiah (2008). In addition, “multi-stage compression refrigeration” is considered a generic liquefaction model for configuring the optimal liquefaction cycle for the liquefaction of natural gas. Through this generic MR liquefaction cycle, the optimal liquefaction cycle can be configured to consider all the configurations that are mechanically feasible. Table 2-2 shows a summary of the related works.

Table 2-2 Comparison of the formulation of the optimal synthesis between this study and previous studies

Studied by	**Cycle**	**Configuration of the Liquefaction Cycle**
Nogal	Single cycle Dual cycle	Single cycle with regeneration, multi-stage compression with intercooling, multi-stage refrigeration
Rangaiah	Single cycle	Multi-stage refrigeration
This thesis	Dual cycle	Single cycle with regeneration, multi-stage compression with intercooling, multi-stage refrigeration, multi-stage compression refrigeration

2.4. Optimal Layout

Penteado (1996) performed optimal equipment layout on a single-floor chemical process plant, considering safety. Equipment location, the land area finally requested after equipment layout, and the number of safety devices were defined as unknowns. The minimum distance between the equipment was defined as a safety constraint. The total layout cost, including the cost of the plant site area, the cost of piping between the equipment, the safety device cost, and the costs associated with the damage to the equipment through the TNT equivalency method, was defined as the objective function. The mathematical model derived from this concept was finally solved using mixed-integer nonlinear programming (MINLP) to determine the optimal layout of this plant.

Patsiatzis (2002) conducted optimal equipment layout on a multi-floor chemical process plant. The equipment location and land area finally requested after equipment layout were defined as unknowns. The layout cost considered by Penteado (1996) and the additional construction cost induced by the number of floors (multi-floors) were defined as objective functions. The mathematical model determined by this concept was solved using mixed-integer linear programming (MILP) to determine the optimal layout of the plant.

Park (2011) performed optimal equipment layout on a multi-floor chemical process plant, considering safety. The unknowns were the same as those in the study by Patsiatzis (2002). The total layout cost covered by Patsiazis (2002) and the costs associated with the damage to the equipment through the TNT equivalency method proposed by Penteado (1996) were defined as objective functions. The mathematical model determined through this concept was solved using MILP to determine the optimal layout of the plant.

Georgiadis (1999) studied optimal equipment layout on a multi-floor chemical process plant. Unlike other studies that addressed the multi-floor layout, this study included equipment that penetrated more than one floor. The equipment location and land area finally requested after the equipment layout were defined as unknowns. The layout cost proposed by Patsiazis (2002) and the upward and horizontal transportation costs (such as that of a pump for delivering liquid to higher locations) were defined as objective functions. The mathematical model determined based on these definitions was solved using MILP to determine the optimal layout of the plant.

This study presents an optimal module layout on potential offshore liquefaction cycles for LNG FPSO, considering long equipment (such as heat exchangers) that penetrate more than one floor. The equipment location and deck area finally requested after equipment layout were defined as unknowns, as in the study by Patsiatzis (2002). The connectivity cost, the construction cost proportional to the deck area, and the distance of the main cryogenic heat exchanger (MCHE) and separators from the centerline of the hull are considered objective functions to be minimized. Moreover, offshore constraints are proposed to ensure safety and considering the deck penetration of the long equipment across several decks. The mathematical model derived from these definitions was solved using MINLP to determine the optimal module layout of the plant. Table 2-3 summarizes the above related works and this study.

Table 2-3 Comparison of the formulation of the layout optimization problem between this study and previous studies

Study	**Object**	**Multi -Floor**	**Design Variables**
Penteado et al., 1996	EO plant[1)]	X (single	Position of each equipment, land area, safety devices that have to

		floor)	be installed at each equipment
Patsiatzis et al., 2002	Instant coffee processing plant, EO plant	O	Floor allocation, position and orientation of each equipment, land area
Park et al., 2011	EO plant, benzene production process plant	O	Floor allocation, position and orientation of each equipment, land area
Georgiadis et al., 1999	Instant coffee processing plant, industrial multipurpose batch plant	O	Floor allocation, position and orientation of each equipment, land area
This study	Potential offshore liquefaction cycles	O	Deck allocation, position and orientation of each equipment, deck area

Study	Additional Considerations		Objective Function	Optimization Method
	Offshore constraints	Equipment occupying more than one floor		
Penteado et al., 1996	X	X	Layout cost[2] + protection devices cost + financial risk cost	MINLP[3]
Patsiatzis et al., 2002	X	X	Layout cost	MILP[4]
Park et al., 2011	X	X	Layout cost + explosion damage cost	MILP
Georgiadis et al., 1999	X	O	Layout cost + upward and horizontal transportation cost[5]	MILP
This study	O	O	Connectivity cost + construction cost proportional to the deck area + efficiency cost due to the motion effects	MINLP

[1] EO plant: Ethylene oxide manufacturing plant

[2] Layout cost = total plant area cost + floor construction cost + connectivity cost involving cost of piping and other required connections between equipment (Patsiatzis et al., 2002)

[3] MINLP: Mixed integer nonlinear programming

[4] MILP: Mixed integer linear programming

[5] Upward and horizontal transportation costs: The pumping cost for moving materials to higher floors through the pipes.

3. Offshore Process FEED for the Offshore Liquefaction Process System

3.1. Offshore and Onshore Engineering

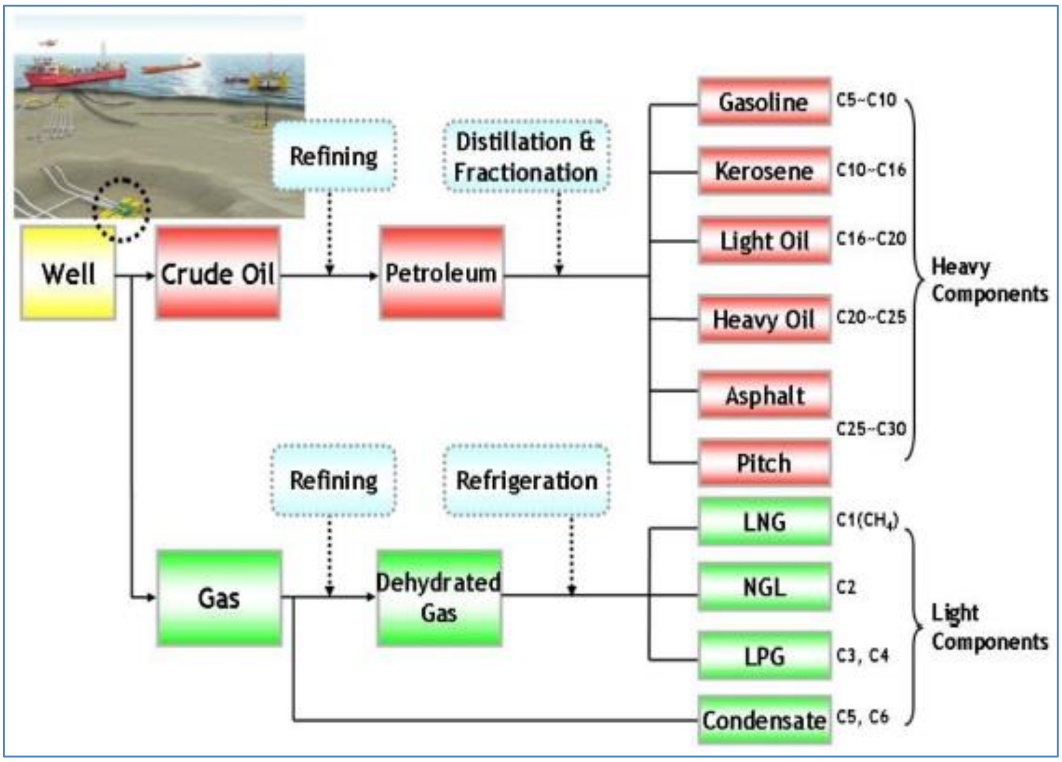

Figure 3-1 Production of oil and gas in offshore and onshore engineering

Shown in Figure 3-1 is the offshore and onshore engineering scheme for refining petroleum products from oil and gas. The main function of offshore engineering is to separate the light hydrocarbon components from the heavy hydrocarbon components, to refine each hydrocarbon component to meet the specifications for saleable oil and gas, and to transfer the oil and gas products to the onshore plants. The main function of onshore engineering is to convert oil and gas into petroleum products. Onshore engineering consists of two fields, one involving the refining of heavy hydrocarbon oil products through the distillation and fractionation processes, and the other pertaining to light hydrocarbon gas products obtained through the refrigeration processes. In the case of LNG FPSO, a liquefaction process that belongs to the onshore engineering field, it is applied to the offshore engineering field. As such, engineering technologies have gradually moved from onshore to offshore technologies, and great expansion of the offshore engineering field is expected in the future.

3.2. Offshore Process FEED Engineering

Offshore plants consist of two main systems: a topside system and a hull system. Topside systems, which are those that take place on the decks of offshore plants, are used for the production of oil and gas. Hull systems, which are located on the lower decks of offshore plants, are used for the storage of oil and gas. With regard to the main function of an FPSO, the importance of topside systems is far greater than that of hull systems. The fields of engineering related to topside systems include offshore process, piping, mechanical, instrumentation, electrical, and outfitting engineering. Among these, offshore process engineering comprises the majority of topside system engineering (Hwang et al., 2008).

Offshore process engineering consists of the FEED and detailed engineering. The specifications of process and utility systems, which are located on the topside parts of plants, are determined according to the client specifications, rules, and regulations. The determined specifications are thoroughly examined and actualized in the detailed engineering stage. That is, the duration of detailed engineering can fluctuate according to the results of FEED. Offshore plant projects can actually be canceled because of the

FEED results. As such, offshore process FEED is an engineering phase of great consequence because it can determine whether or not an offshore plant can be constructed.

(1) Definition of offshore process FEED activities

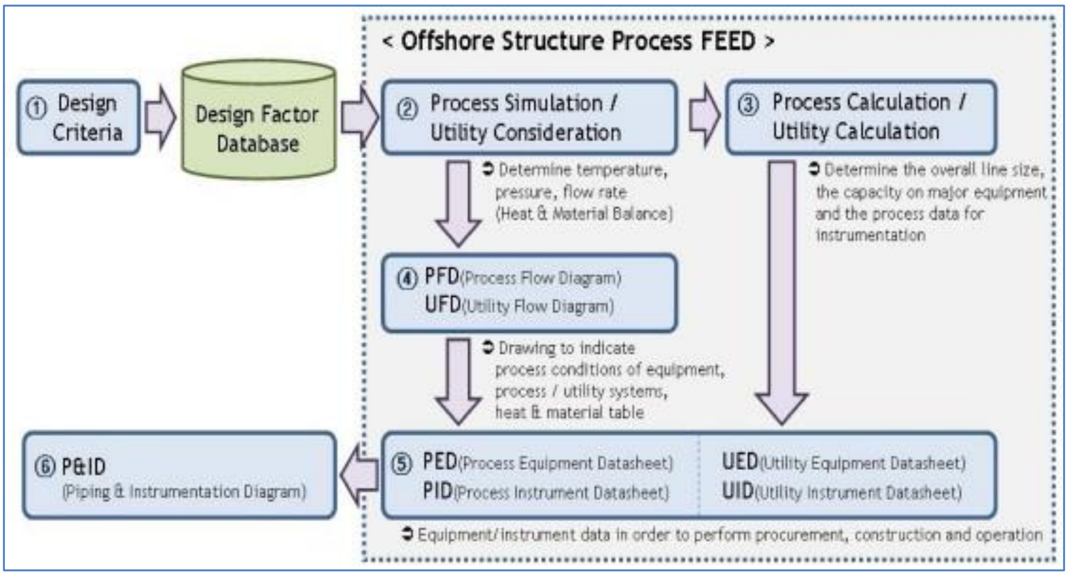

Figure 3-2 Offshore process FEED activities

The offshore process FEED activities are shown in Figure 3-2. The FEED results estimate the overall costs, weights, and layouts of offshore plants. The process FEED activities that yield the FEED results are as follows. Design criteria, such as the engineering considerations of equipment, instruments, and pipes on topside systems, are first determined after establishing the customer requirements (Figure 3-2①). Next, the overall process flow, which corresponds to the production flows of oil and gas, and the utility flow, which supports the process flow, are defined and simulated to calculate the physical and thermodynamic properties as well as the utility specifications for each process and utility system (Figure 3-2②). The specifications of the equipment, instruments, and pipes are then determined based on the results of the process simulation and on the utility considerations (Figure 3-2③). A process flow diagram (PFD) and a utility flow diagram (UFD), which represent the heat/material table and the overall safety and control logic, are also prepared based on the results of a process simulation and on the utility considerations (Figure 3-2④). Next, a process equipment datasheet (PED), a process instrument datasheet (PID), a utility equipment datasheet (UED), and a utility instrument datasheet (UID) are generated to obtain information on the equipment and instruments (Figure ⑤). Finally, a piping and instrumentation diagram (P&ID), which shows the safety, operation, and maintenance factors of each system and the vendor data for the equipment and instruments, are preliminarily prepared based on the PFD and UFD (Figure ⑥). The aim of the above-mentioned process activities is to obtain the overall costs, weights, and layouts of offshore plants so as to determine the feasibility of well developments in specific locations. If the economic feasibility is established based on the FEED results, detailed process engineering is performed.

(2) Purpose of process FEED

The first goal in performing process FEED is to determine the sizes of the equipment and instruments which are the main components of topside systems. This is achieved by calculating the overall capacities of a topside system and receiving suitable information from specific vendors. The second aim is to calculate the sizes of the pipes, which connect the components of topside systems, through process simulation and utility considerations. By calculating the sizes of the equipment, instruments, and pipes, the overall layout of a topside system can be efficiently determined. The various cranes, which are necessary for constructing and installing topside systems and pipes, can also be selected by examining the weight information. Most importantly, the total cost of a topside system and its pipes can be estimated. Therefore, the process FEED results are the most important factors to consider when performing overall engineering, construction, and installation of an offshore plant, and can ultimately affect the success or failure of an offshore project.

3.3. Offshore Process FEED Engineering Method

Figure 3-3 shows the overall offshore process engineering stages, and Figure 3-4, the overall schematic of the offshore process FEED method. Through this FEED method, the capacities and sizes of topside systems and pipes can be efficiently determined without unnecessary time-consuming engineering work. Engineering data from the vendors can be received based on the overall capacity and size of a topside system. In the long run, the potential feasibility of specific well development can be rapidly determined because the total costs, weights, and effective layout of an offshore plant topside system can be obtained via the offshore process FEED method.

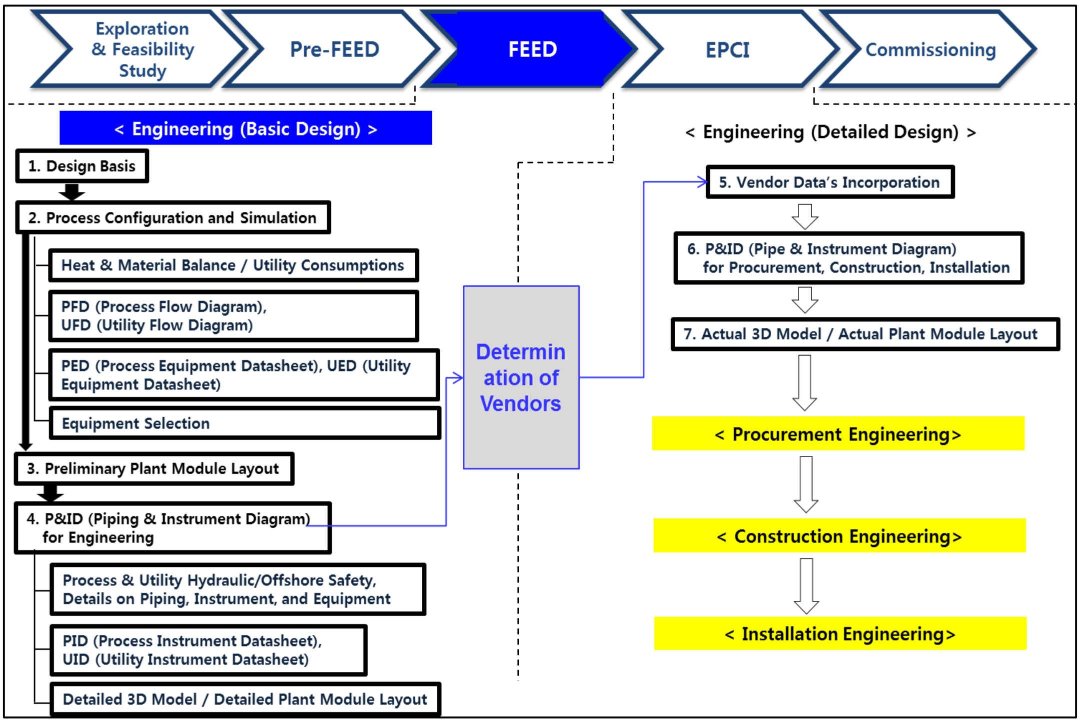

Figure 3-3 Overall offshore process engineering stages

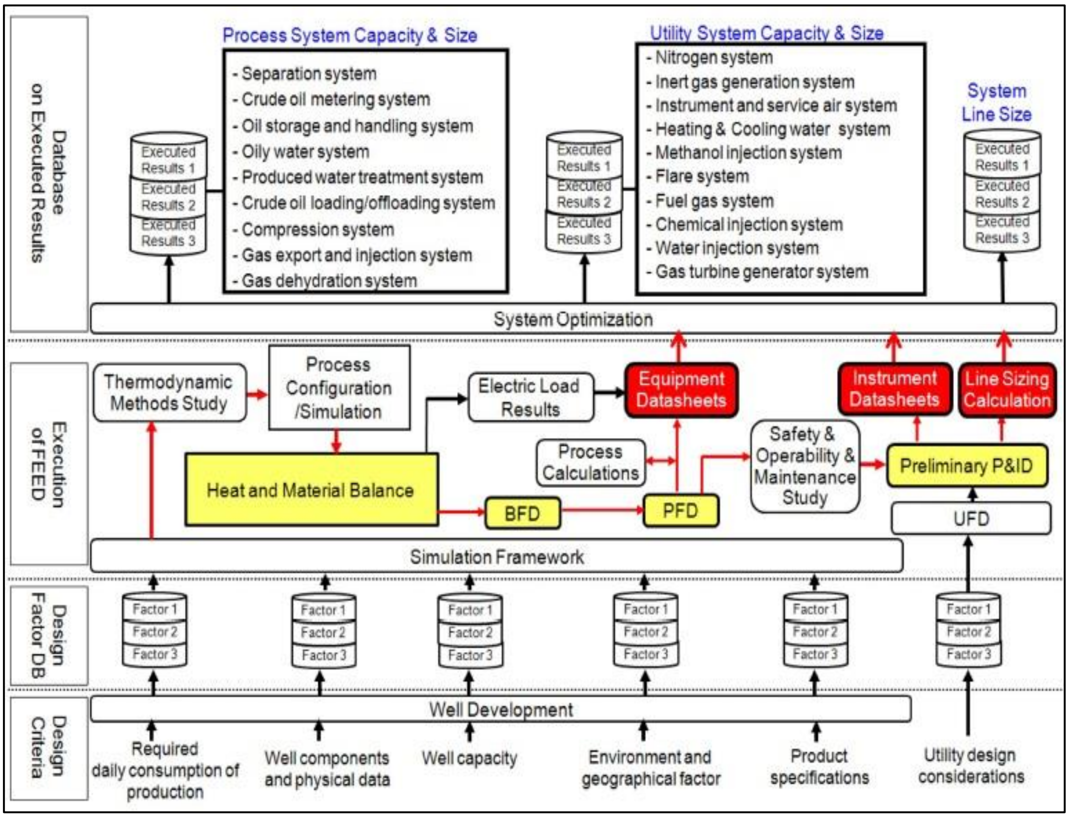

Figure 3-4 Schematic of the offshore process FEED engineering method

(1) Thermodynamic method study

In physics and thermodynamics, an equation of state is a relationship between the state variables. More specifically, an equation of state is a thermodynamic equation describing the state of matter under a given set of physical conditions. It is a constitutive equation that provides a mathematical relationship between two or more state functions associated with matter, such as its temperature, pressure, volume, or internal energy. Equations of state are useful in describing the properties of fluids, mixtures of fluids, solids, and even the interior of stars. The Peng-Robinson equation is widely used as a mathematical model to calculate fluid phase equilibrium. The Peng-Robinson equation was developed in 1976 to attain the following goals:

$$P = \frac{RT}{V_m - b} - \frac{a_c[1 + m(1 - (\frac{T}{T_c})^{0.5})]^2}{V_m(V_m + b) + b(V_m - b)}$$

$$a_c = 0.45724\frac{R^2 T_c^{\ 2.5}}{P_c}, \quad b = 0.07780\frac{RT_c}{P_c}$$

$$m = 0.37464 + 1.54226w - 0.26992w^2$$

First, the parameters should be expressible in terms of the critical properties and the acentric factor. Second, the model should provide reasonable accuracy near the critical point, particularly for calculations of the compressibility factor and liquid density. Third, the mixing rules should not employ more than a single binary interaction parameter, which should be independent of the temperature, pressure, and composition. Finally, the equation should be applicable to the calculations of all fluid properties in the natural gas processes. For the most part, the Peng-Robinson equation exhibits a performance similar to that of the Soave equation, although it is generally superior in predicting the liquid densities of many materials, especially nonpolar substances

(2) Process and utility configuration/simulation study

The purpose of performing the process and utility configuration and the simulation using the above-mentioned thermodynamic methods is to calculate the physical properties for each stream based on a unit operation at the operating conditions. Case studies are performed according to major considerations, such as the temperature, pressure, flow rate, and mole fraction from well reservoirs, as well as the efficient configuration of the main topside systems. The case that satisfies the most severe condition for each system is then considered the design case. The simulation study and configuration comprise the most important stage when determining the specifications of the equipment, instruments, and piping in offshore process FEED engineering. Therefore, optimized methods pertaining to the simulation and configuration study should be developed to determine the optimal operating conditions and configurations. This will in turn lead to successful FEED results in offshore production projects.

(3) Heat and material balance

Heat and material balance is the process of calculating the physical properties and electric loads of each topside process system through process simulation and configuration. The heat and material balance provides the most important data in topside process system engineering. The specifications of the equipment, instruments, and pipes for the topside process systems are determined based on the heat and material balance. Therefore, the heat and material balance should be exactly and rapidly determined to be able to produce successful FEED results in the early stage. Thus, the process data should be rapidly and efficiently calculated and managed in the early FEED stage. This is critical when performing FEED engineering in oil and gas production plants.

(4) Block flow diagram (BFD)

A BFD is a drawing that shows the overall flow in a topside system. The organic relationships among the oil processing systems, gas processing systems, and water processing systems can be illustrated through a BFD. All the engineers involved in a project can use the BFD to understand a topside system in a specific oil and gas production plant.

(5) Process flow diagram (PFD)

A PFD is a drawing that shows the safety and control logic of a topside process system as well as the heat and material tables, which present the engineering data (temperature, pressure, flow rate, and mole fraction) for each topside process system for a specific design case. Engineering information on all the process equipment from a specific vendor can be obtained based on the PFD. The PFD is expanded to a P&ID by incorporating the safety, operation, and maintenance factors of all the topside process systems. To be more specific, a PFD is a schematic drawing of a process or utility unit that shows all the relevant physical and other process data, the main utility characteristics, the basic process control elements, and the main dimensions of the process equipment. A PFD should contain a list of included equipment items, identified by tag numbers in the drawing title block. A process or utility engineer is responsible for the preparation of PFDs, and no modifications to a PFD should be made without the engineer's authorization. If a design provides for different modes of operation, such as different crudes, feedstocks, or cut points, a distinction should be made through the use of letters (e.g., mode of operation A, B, etc.). For more complicated cases, separate PFDs should be prepared for each mode of operation. PFDs provided by process licensors or other third parties should be redrawn with symbols and identifications in accordance with specific rules and regulations. PFDs for pressure relief systems should indicate the relief quantities, physical characteristics, and conditions for each relief valve and depressurization valve for each individual and general emergency case.

(6) Utility balance

Utility systems play an important role in supporting process systems. The engineering data for each topside utility system are determined after fixing the engineering conditions of each process system. Utility balance is the process of calculating the physical properties and electric loads of each topside utility system through utility considerations. The utility balance is the most important factor in topside utility system engineering. The specifications of the equipment, instruments, and pipes of topside utility systems are determined based on the utility balance. Therefore, the utility balance should be exactly and rapidly determined after fixing the process concepts and process data.

(7) Utility flow diagram (UFD)

A UFD is a drawing that shows the safety and control logic of a topside utility system as well as the utility balance tables, which present the engineering data (temperature, pressure, flow rate, and mole fraction) for each topside utility system after all the utility systems, such as the instrument air, utility air, seawater, freshwater, cooling water, diesel oil, and lube oil, have been diagrammed. Engineering information on all the utility equipment from a specific vendor can be obtained based on the UFD. The UFD is expanded to a P&ID by incorporating the safety, operation, and maintenance factors for all topside utility systems.

(8) Process and utility calculations

Process calculation is the optimized engineering of the equipment, piping, and instruments of a topside system based on the results of the process configuration/ simulation. Normally, specific references from API, ASME, NACE, ISO, NFPA, etc. can be used when process and utility calculations are performed. The following calculations should be considered. First, design parameters such as the design pressure, temperature, and design factors should be calculated according to specific rules and regulations. Next, the equipment design of vessels, heat exchangers, equipment nozzles, and lever controls, and the material and corrosion allowance, should be considered. Third, the piping design has to be considered, including the material and corrosion allowance, insulation and tracing, minimum pipe size, and line sizing. Fourth, flare and vent design should be performed according to specific rules and regulations. Finally, other specific systems pertaining to the drain, instrument air, sea and cooling water, steam generation, fuel gas, glycol dehydration, and chemical injection should be considered as special activities in the process and utility calculations.

(9) Equipment datasheets

Datasheets for the equipment in a topside system are prepared based on the process configuration/simulation and process calculations. Process datasheets containing only the equipment process data should first be prepared so that they can be sent to specific equipment vendors. Several equipment vendors should then be considered in potential vendor lists. Finally, one vendor of specific equipment should be selected as the contractor after the performance of technical evaluations. Detailed equipment data from the selected vendor can then be received, and the equipment datasheets can be finalized. Therefore, all the necessary data for the procurement, installation, and operation of equipment are contained in the equipment datasheets.

(10) Safety/operability/maintenance study

Safety and operability studies of topside systems (e.g., hazard operability studies) are performed based on the engineering data from PFD and UFD, to consider all the potential hazardous factors in topside process engineering. A maintenance study on the equipment and instruments of a topside system is then performed so that the lifetime requirements of the systems can be met. A P&ID can subsequently be developed according to the results of the safety, operability, and maintenance studies.

(11) Preliminary P&ID

The PFD and UFD can be expanded to P&IDs for each topside system after incorporating the results of the safety, operability, and maintenance studies and after receiving the vendor data. The P&ID shows all the data, such as the operating conditions, process control, and safety logic, for all the equipment, instruments, and pipes. To be more specific, a P&ID is a pictorial representation of a process or utility unit that shows all the equipment, including the installed spares and the associated piping and piping components, instrumentation, heat tracing, and insulation. An elevated view is normally shown, although tank farms are usually shown in the plane view. All the piping and piping components should be shown with their sizes, piping classes, and tag numbers. The equipment, piping, and instrument numbering should logically follow the process flow and should preferably be drawn from left to right and from top to bottom on vertical equipment, except for column trays. The schematics should show the specific engineering requirements necessary for the design, such as sloping lines, minimum straight pipe lengths, equipment elevations, no pockets, enter at the top of the line, and minimum or maximum distances. These requirements must be stated in words (or with symbols), as a

P&ID is not an isometric representation. Process conditions and physical data should not be shown on the P&ID. The column above the title block of a P&ID should be reserved for the following:

- reference to the legends sheet accompanying the P&ID;
- notes indicating that the P&ID should start from the top of the page and should be numbered from 1 (if a note is deleted, the number should not be used for another note but should instead be shown as “deleted”; notes should cover non-standard instructions);
- list of equipment shown on the P&ID; and
- register of revisions and P&ID issues.

A separate P&ID should be prepared for each utility system, such as those for cooling water, steam (high, medium, and low pressure), condensate, air, and water. Combining several systems on one P&ID is subject to the approval of the principal. P&IDs are prepared under the supervision of process or utility engineers, in close consultation with the process control engineers. No modifications should be made to a P&ID without the authorization of the responsible process or utility engineer.

(12) Instrument datasheet

Instrument datasheets on all topside system instruments are prepared based on the process configuration/simulation, process calculations, and P&IDs. Process datasheets for instruments containing only process data should be prepared so that they can be sent to specific instrument vendors. Several instrument vendors should then be considered in potential vendor lists. Finally, one vendor of a specific instrument should be selected as the contractor after the performance of technical evaluations. Detailed instrument data from the selected vendor can then be received, and the instrument datasheets can be finalized. All the data necessary for the procurement, installation, and operation of instruments should be represented in the instrument datasheets.

(13) Line size calculations

Line size calculation is the optimized size engineering of pipes in a topside system based on the results of process configuration/simulation. It is performed when the velocity and pressure drop at the operating conditions (type of fluid, flow rate, pressure, temperature) have been investigated. Line sizing should be performed according to the guidelines put forward in specific rules and regulations. A suitable line size should be selected by considering the following aspects:

- achieving a pressure drop compatible with the service considered (e.g., a very low ÄP is required for the main gas process line while a higher ΔP may be acceptable for the compressor discharge line);
- seeking the most economical pipe size considering the configuration in place (e.g., for a pump discharge line, it is sometimes more economical to increase the pump head than to increase the pipe size, which may have an impact on the supports, layout, and routing);
- the conditions that arise during a transient phase (e.g., start-up, shutdown, process upset), such as pressure surges (e.g., water hammer) and vibrations;
- pipe erosion and corrosion;
- minimum speeds to prevent the deposition of the suspended solids;
- flow patterns in the two-phase flow; and
- mechanical strength of the pipework.

4. Optimal Synthesis for Potential Offshore Liquefaction Process Cycles

4.1. Generic MR (Mixed Refrigerant) Liquefaction Process Cycle

4.1.1. Configuration of the liquefaction cycle

(1) Configuration and basic principle of the liquefaction cycle

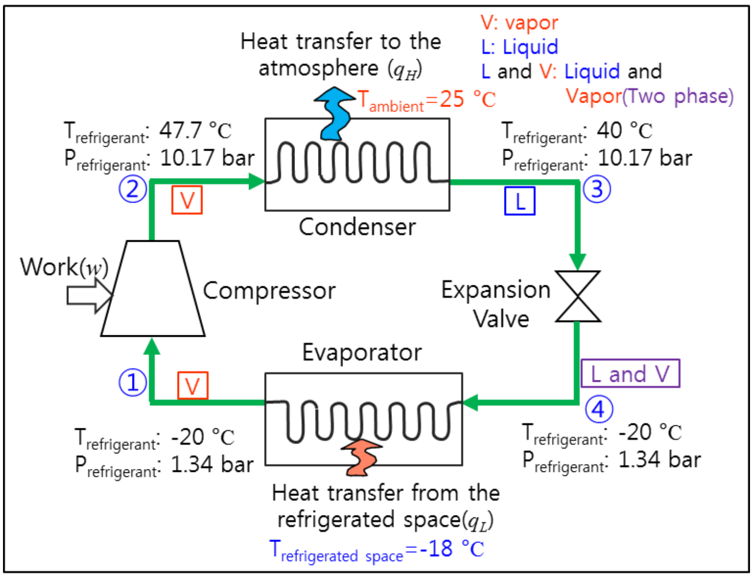

Figure 4-1 Single cycle (refrigerator)

Figure 4-1 and 4-2 illustrate the single cycle used in a refrigerator, which is helpful in understanding the liquefaction cycle as their basic principles are the same. The main equipment in a refrigerator cycle is a compressor, a condenser, an expansion valve, and an evaporator. The condenser and evaporator are heat exchanger types, and a condenser that uses seawater is called "seawater cooler" in the liquefaction cycle. The refrigerant flows in a clockwise direction, and the principle of operation in a refrigerator is as follows (Hwang et al., 2012):

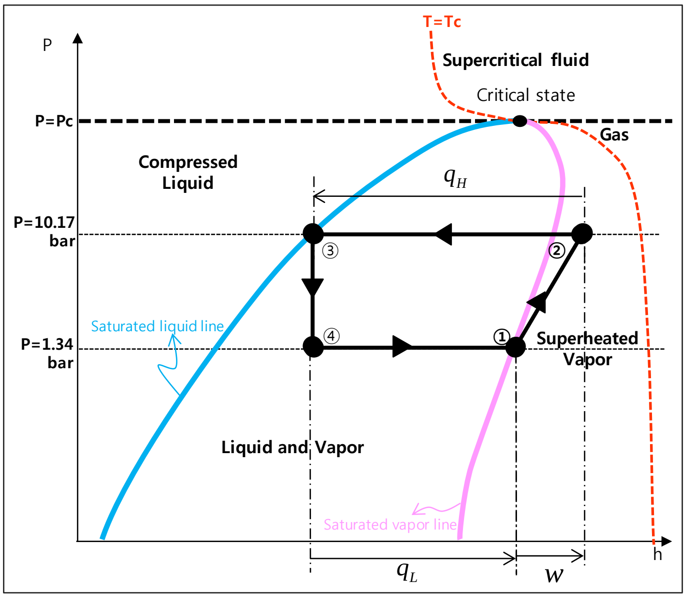

Figure 4-2 Pressure (P)-enthalpy(h) diagram of a single cycle (refrigerator)

<u>Process 1-2</u>

In process 1-2, the refrigerant in the vapor phase is compressed by the compressor and is changed to a superheated vapor at a high temperature and pressure. This refrigerant compression process is assumed to be reversible, without heat exchange with the external environment (i.e., reversible adiabatic compression).

<u>Process 2-3</u>

The refrigerant in the vapor phase at a high temperature and pressure loses heat through the condenser and is changed to liquid from vapor as the temperature of the refrigerant decreases. At this point in the process, no change in the refrigerant pressure is assumed to occur (i.e., isobaric condensation).

Process 3-4

The refrigerant in the liquid phase is expanded through an expansion valve and is then converted to mixed vapor (i.e., liquid and vapor) with the decrease in the pressure and temperature of the refrigerant. No heat exchange with the external environment is assumed to occur in this process (i.e., adiabatic expansion).

Process 4-1

The refrigerant in the two-phase refrigerant at a low temperature passes over an evaporator and absorbs the heat inside the refrigerator. At this point, the refrigerant is changed to vapor through vaporization in the refrigerator. This process is the same as the liquefaction cycle under cryogenic conditions. In this process, it is assumed that there is no change in the refrigerant pressure (i.e., isobaric evaporation).

(2) Configuration strategies of the liquefaction cycle

All liquefaction cycles follow the basic principles addressed in the previous chapter. Furthermore, the order of the main equipment cannot be changed when liquefaction cycles are configured. Instead, various types of liquefaction cycles can be configured by changing the numbers of the main equipment pieces, without changing the equipment order. Configuration strategies in the liquefaction cycle are used to change the number and association of the equipment used in the liquefaction cycle to within a feasible range. Four strategies are considered for the configuration of liquefaction cycles, which are explained below.

Single cycle with regeneration

The single cycle with regeneration (Figure 4-3) has an additional counterflow heat exchanger for subcooling before expanding the refrigerant at a low temperature and high pressure through a condenser (Cengel, 2011).

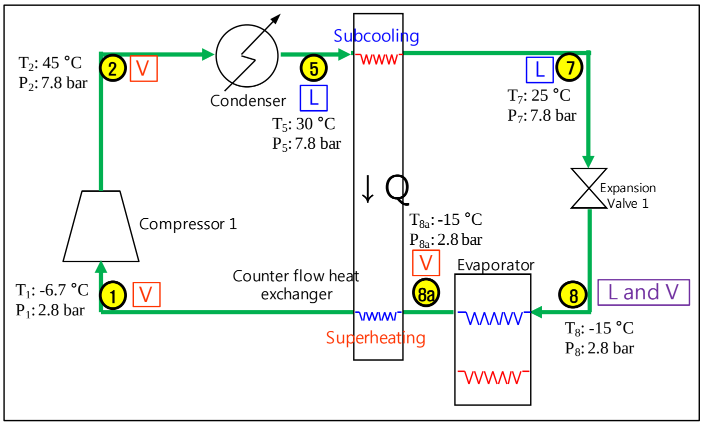

Figure 4-3 Single cycle with regeneration (refrigerator)

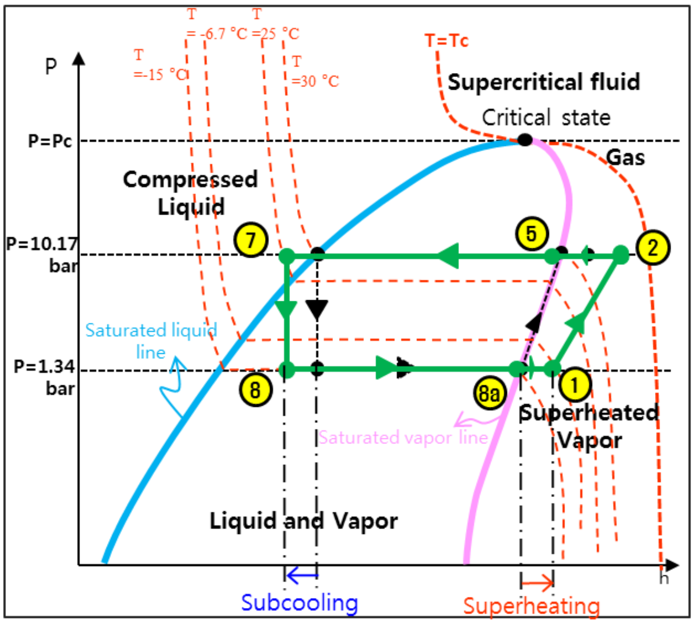

Figure 4-4 Pressure (P)-enthalpy(h) diagram of a single cycle with regeneration (refrigerator)

Thus, the cooling capacity of the cycle is increased due to subcooling before expanding the refrigerant. If the liquid enters the compressor, severe mechanical damage can occur. Figure 4-4 shows that the inlet refrigerant status of the compressor (①) is saturated vapor, whose temperature and pressure are such that any compression of its volume at a constant temperature will cause it to condense to liquid at a rate sufficient to maintain a constant pressure. It is difficult, however, for the status of the refrigerant to fit the status of the saturated vapor. To prevent the liquid from entering the compressor, a counterflow heat exchanger is also installed in the refrigerator cycle, which causes superheated vapor flows (⑧a→①) by absorbing its own heat (⑤→⑦). Unlike the above-mentioned refrigerator cycle, a common heat exchanger is represented in Figure 4-5, integrating an evaporator and a counterflow heat exchanger in the liquefaction cycle.

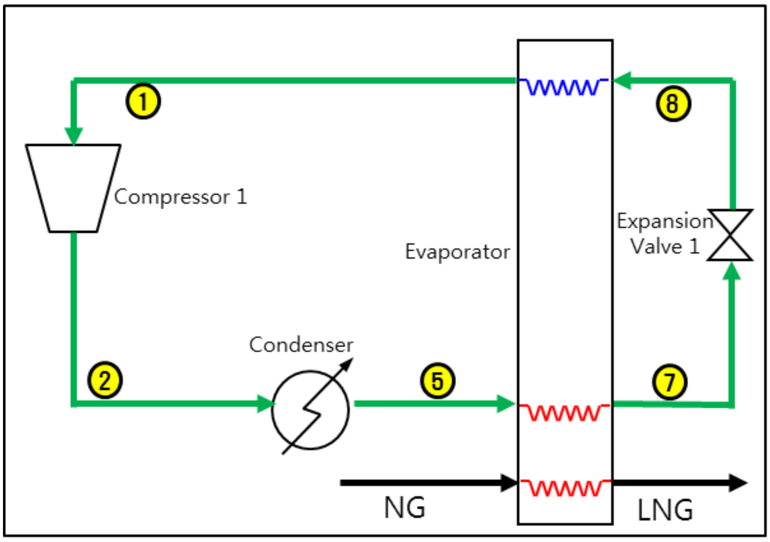

Figure 4-5 Single cycle with regeneration (liquefaction cycle)

Multi-stage compression with intercooling

In multi-stage compression with intercooling, the refrigerant is compressed across multiple stages, as shown in Figure 4-6. For multiple stages, new compressors are installed downstream of the existing compressor, and intercoolers are installed between the compressors. Figure 4-6 shows two-stage compression with intercooling, which includes additional compressors and intercoolers.

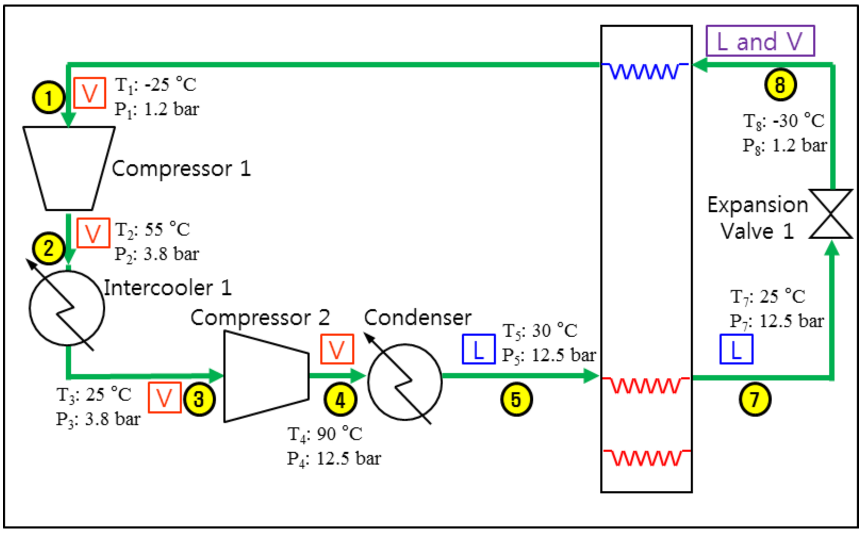

Figure 4-6 Single cycle with regeneration + two-stage compression with intercooling (refrigerator)

To obtain a low temperature of less than -30℃ using one compressor, the reduced pressure of the refrigerant in the expansion valve must be much lower than the atmospheric pressure. Therefore, increasing the pressure to the level of the condensing pressure will make the compression ratio too large and will reduce the efficiency of the compressor due to the increased temperature of the refrigerant. Furthermore, the life of the compressor will be shortened due to the increased temperature. Thus, for the required temperature range of the refrigerant, multi-stage compression, which installs two or more compressors, has been shown to improve these defects (Choi, 2008). As industrial compressors have a practical maximum stage compression ratio of 4-5, performing compression tasks in multiple stages is very common (Nogal et al., 2008). When the refrigerant is compressed by splitting it into multiple stages using multiple compressors, an intercooler is installed between the compressors to cool the refrigerant before it enters the next compressor. The lower temperature of the partially compressed gas lowers the volumetric flow rate and consequently requires less compression power in the next stage (Nogal et al., 2008). The P-h diagram in Figure 4-7 confirms that a compressor power reduction is required.

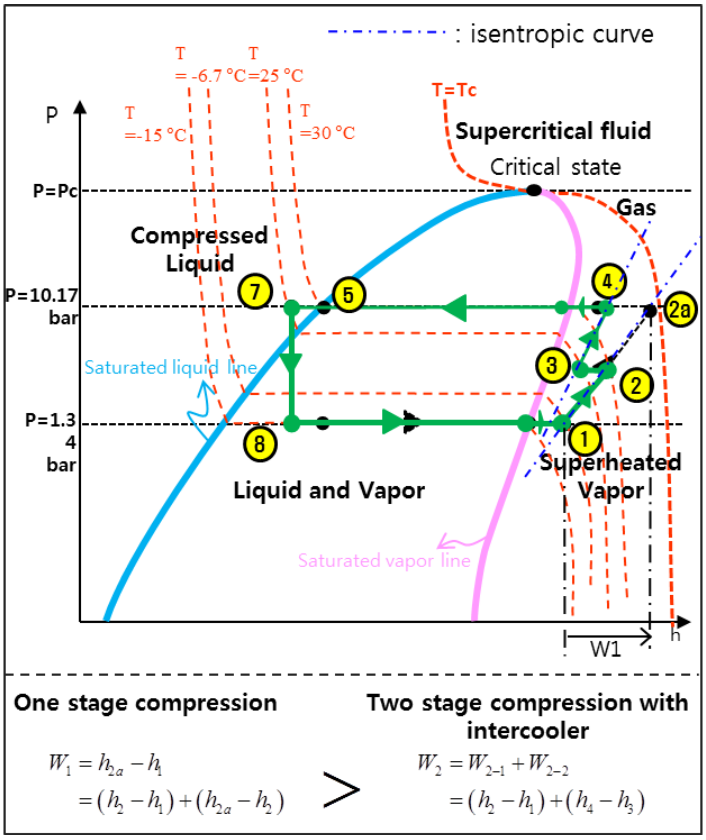

Figure 4-7 Pressure (P)-enthalpy (h) diagram of a single cycle with regeneration + two-stage compression with intercooling (refrigerator)

Multi-stage compression refrigeration

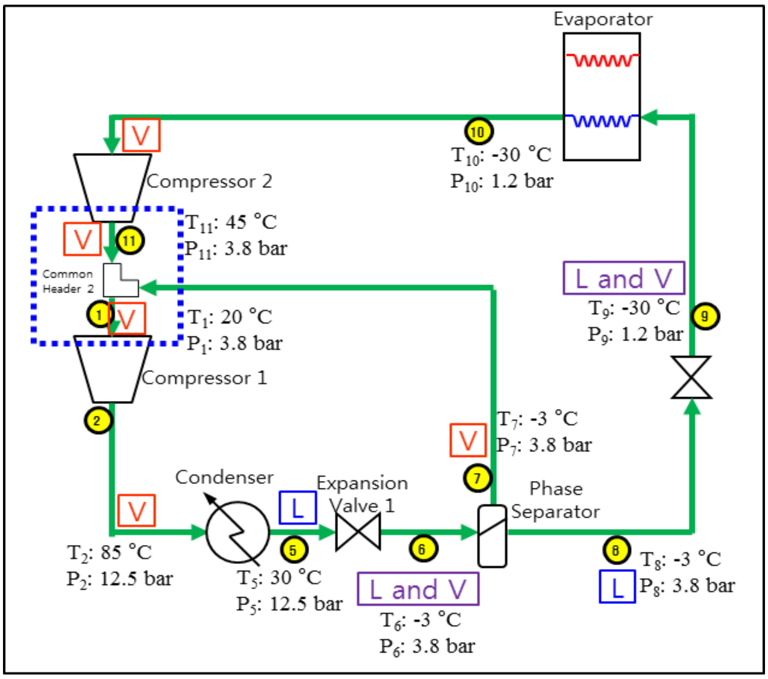

Figure 4-8 Single cycle + two-stage compression refrigeration (refrigerator)

As shown in Figure 4-8, multi-stage compression refrigeration uses additional compressors with common headers and phase separators instead of intercoolers. Figure 4-8 illustrates a form of two-stage compression refrigeration with an additional phase separator and a common header. The phase separator equipment is split into two flows of liquid and vapor from the liquid vapor mixture of the refrigerant flow. The phase separator downstream of the condenser has the ability to form two flows (liquid and vapor) from the vapor mixture. The vapor flow from the phase separator is combined with the refrigerant flow rate at the outlet of compressor 2. At this point, as shown in Figure 4-9, the refrigerant outlet temperature of compressor 2 (⑪) is 45°C, the temperature of the separated vapor refrigerant (⑦) is –3°C, and the combined temperature in the common header (①) is 20°C. Therefore, the common header used to combine two streams into one plays the role of the intercooler, as shown in Figure 4-6. As in multi-stage compression with intercooling, compared with one-stage compression, multi-stage compression refrigeration can reduce the power required by the compressors. The P-h diagram in Figure 4-9 confirms that the power required in two-stage compression refrigeration is less than that required in one-stage compression refrigeration.

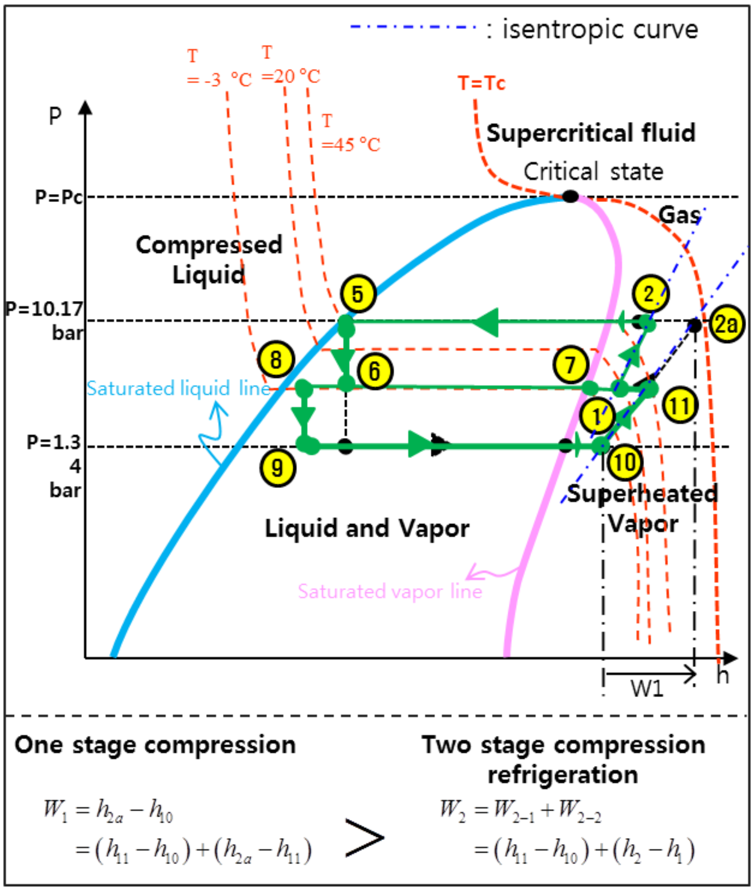

Figure 4-9 Pressure (P)-enthalpy (h) diagram of a single cycle + two-stage compression refrigeration (refrigerator)

<u>Multi-stage refrigeration</u>

As shown in Figure 4-10, in multi-stage refrigeration, each step along the multi-stage process uses a phase separator, a common header, an expansion valve, and an evaporator (see Nogal et al.). Figure 4-10 shows a typical liquefaction cycle in two-stage refrigeration with an additional phase separator, a common header, an expansion valve, and an evaporator.

In the case where the difference between the inlet temperature of the refrigerant in the evaporator and the temperature cooled by the condenser increases, the overall cooling effect decreases because the rate of the refrigerant vapor increases in the liquefaction cycle with one expansion and greater than two-stage compression. Therefore, a greater refrigerant flow rate is required to liquefy the same amount of natural gas, which increases the power required by the compressors. To resolve this problem, as shown in Figure 4-10, a phase separator, an expansion valve, and an evaporator can be installed in the liquefaction cycle. The operation principle in two-stage refrigeration (Figure 4-10) is described below.

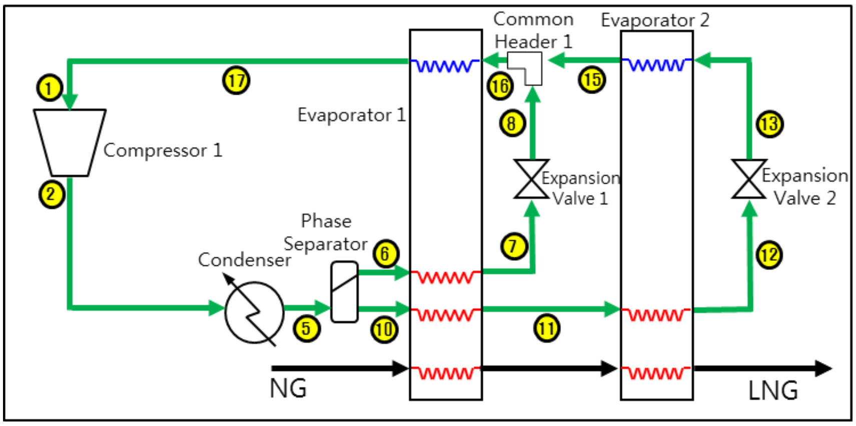

Figure 4-10 Single cycle + two-stage refrigeration (liquefaction cycle)

In a vapor-liquid mixed state, the refrigerant in the condenser (⑤) is divided by the phase separator into the flow of the liquid state (⑥) and that of the vapor state (⑩). The two flows are cooled by a cryogenic refrigerator through expansion valve 1 in evaporator 1. Between the two flows in the phase separator, the flow of the liquid state (⑥) is cooled by an evaporator (subcooling, ⑦). It then changes to a low-pressure cryogenic state (⑧) in expansion valve 1. The flow of the vapor state (⑩) changes the state of the liquid vapor mixture (⑪) in evaporator 1 and finally changes to a low-pressure cryogenic state in evaporator 2, according to the same principles (⑪→⑫→⑬). The two split cryogenic flows are recombined into common header 1. The cryogenic flows of the refrigerant play a role in reducing the temperature in the evaporators, in addition to liquefying the natural gas contained within (with regeneration).

In the case of the liquid-only status in the condenser (⑤), according to the properties of the refrigerant, the phase separator is replaced by a tee. According to the engineer's intention, the tee can split one flow into two, in contrast to the phase separator function, which divides the liquid flow and the vapor flow in relation to the vapor fraction of the flow rate.

4.1.2. Generic MR (Mixed Refrigerant) liquefaction process cycle

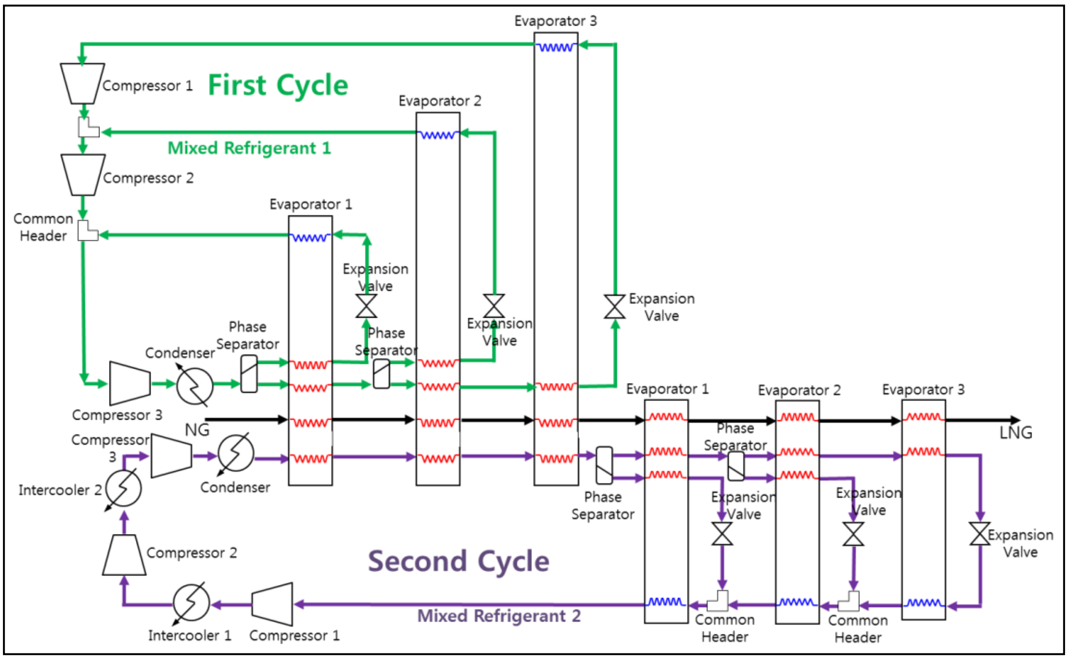

Figure 4-11 Proposed generic MR liquefaction process cycle

Considering the above-mentioned configuration strategies (i.e., single cycle with regeneration, multi-stage compression with intercooling, multi-stage compression refrigeration, and multi-stage refrigeration), a generic liquefaction model is proposed as shown in Figure 4-11. The generic MR liquefaction process cycle is limited to the dual cycle to implement offshore applications. The reasons for limiting the model to the dual cycle are as follows: the dual mixed refrigerant (DMR) cycle is now being considered for application in LNG FPSO, and the C_3MR cycle is one of the most commonly used in onshore applications, along with the dual cycle. Therefore, the dual cycle is considered a generic liquefaction model for offshore application in terms of reliability. In addition, the maximum number available for each main piece of equipment (compressor, expansion valve, condenser, and evaporator) is three per cycle, taking into account offshore requirements, such as the compactness (related to energy efficiency), motion effects, and module layout. Actual LNG FPSO (SHELL FLNG) is now being verified and developed based on the offshore requirements. Thus, the following equipment is considered in each dual cycle, as shown in Figure 4-11:

- total of six compressors: three for the first cycle + three for the second cycle;
- total of three evaporators: for the first cycle (pre-cooling);
- total of one evaporator with three different temperature distributions: for the second cycle (main cooling);
- total of six expansion valves: three for the first cycle + three for the second cycle;
- total of four heat exchangers: one for the first cycle + three for the second cycle;
- total of four common headers: two for the first cycle + two for the second cycle; and
- total of four phase separators: two for the first cycle + two for the second cycle.

As shown in Figure 4-11, the first cycle performs pre-cooling to liquefy the natural gas. The type of evaporator selected is the printed cryogenic heat exchanger (PCHE). A maximum of three PCHEs can be configured in the first cycle, and three compressors are used to compress each refrigerant from each PCHE (i.e., the strategies of multi-stage compression refrigeration + single cycle with regeneration).

The second cycle performs main cooling to liquefy the natural gas, and the type of evaporator selected is the spiral wounded heat exchanger (SWHE), which is widely used in onshore liquefaction plants and has high reliability. Considering the features of SWHE, one SWHE with a maximum of three temperature distributions can be configured in the second cycle (i.e., the strategies of multi-stage refrigeration and single cycle with regeneration). In the evaporators, the combined refrigerant is finally compressed using a maximum of three compressors in series (i.e., the strategy of multi-stage compression with intercooling). The above-mentioned strategies are the bases of the proposed generic MR liquefaction process cycle in this study.

4.2. Selection of Top 10 Feasible MR Liquefaction Process Cycles considering Efficiency

4.2.1. Feasible MR liquefaction process cycles

With regard to the mechanical feasibility of the liquefaction cycles, there are 27 model cases available from the authors' generic MR liquefaction process cycles. In the first cycle, three cases can be considered for potential configuration. In the case of multi-stage compression refrigeration, the combination of an evaporator and a compressor cannot be separated, and therefore, three cases are available for the first cycle. In the second cycle, nine cases can be considered for the possible liquefaction cycles. For multi-stage refrigeration + multi-stage compression with intercooling, the separated configurations of the evaporators and compressors can be considered for the potential liquefaction cycles. Therefore, each of the three cases is available for the evaporators and compressors, and 27 cases are feasible for the potential optimal liquefaction cycle, computed as follows:

3 cases (combination of a maximum of 3 evaporators and compressors from pre-cooling) × 3 cases (maximum of 3 evaporators from main cooling) × 3 cases (maximum of 3 compressors from main cooling) = total of 27 cases.

The 27 feasible MR liquefaction process cycles are shown in Figure 4-12, 4-13, and 4-14.

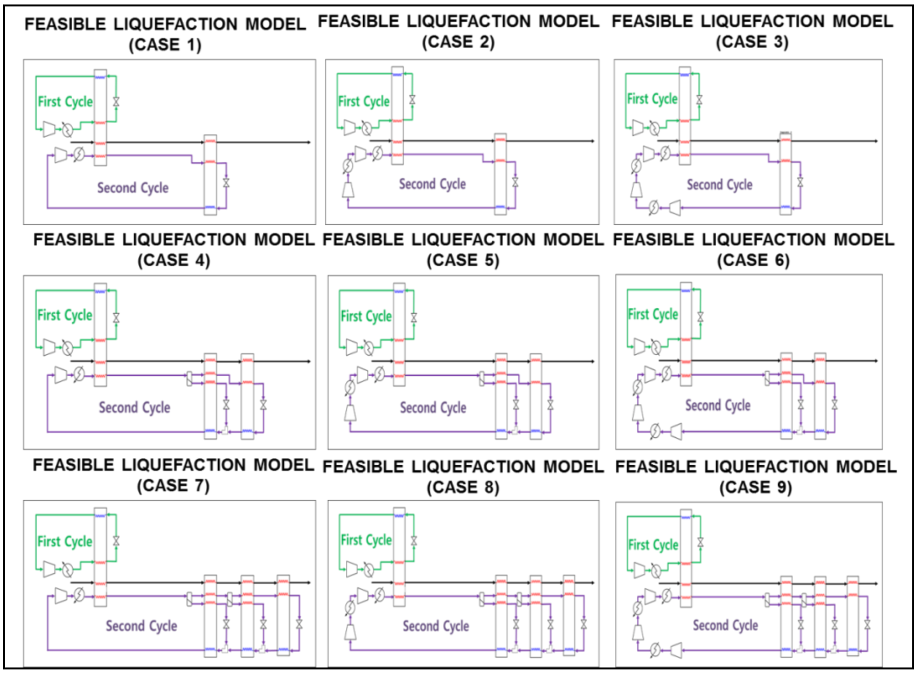

Figure 4-12 Feasible MR liquefaction process cycles (cases 1-9)

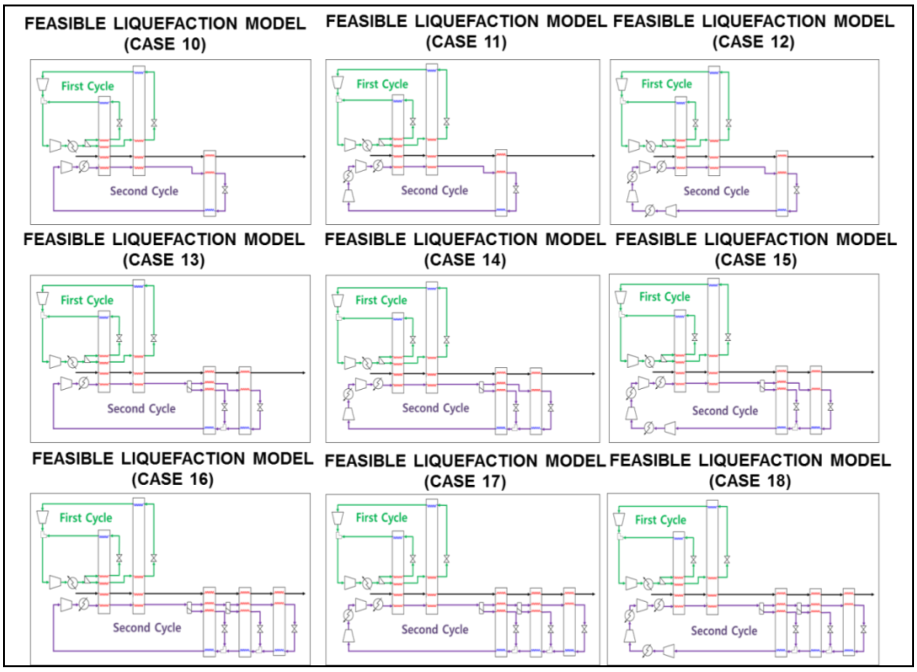

Figure 4-13 Feasible MR liquefaction process cycles (cases 10-18)

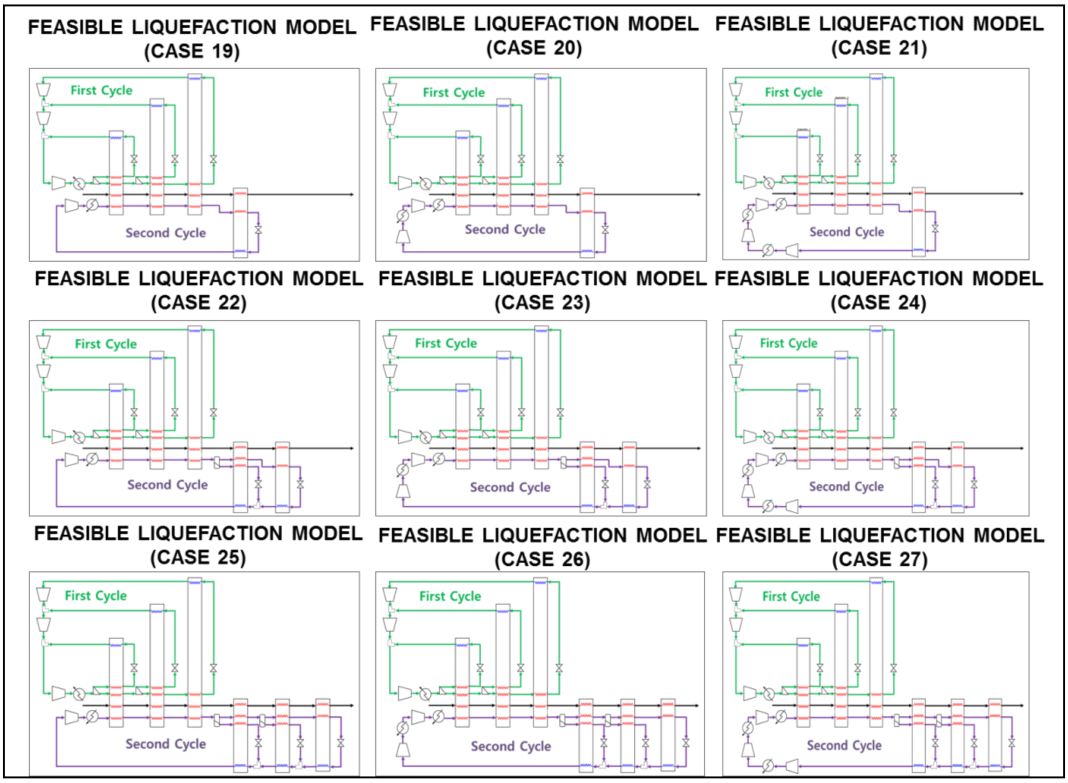

Figure 4-14 Feasible MR liquefaction process cycles (cases 19-27)

4.2.2. Optimal operating conditions of feasible MR liquefaction process cycles by HYSYS

All the feasible MR liquefaction cycles from the proposed generic MR liquefaction process cycle are considered the optimal synthesis for selecting the ten most feasible MR liquefaction process cycles.

Before the optimization of the 27 feasible liquefaction models by HYSYS, the unknowns are given as follows: NG flow rate [479,500 kg/h = 4.0 MTPA (million ton per annum)]; NG pressure (84.21 bar); temperature (24ºC); composition of the natural gas feed (nitrogen, 0.00279; methane, 0.7873; ethane, 0.05179; propane, 0.01803; n-butane, 0.00558; i-butane, 0.00329; i-pentane, 0.00199; n-pentane, 0.00199), temperature of the LNG (-160.15ºC); pressure of the LNG (74.21 bar) before pressure let-down in the LNG expander; compressor efficiency (80%); and temperature of the refrigerant leaving the seawater cooler (35ºC). For the optimal synthesis in this study, actual operating values are selected and considered for offshore application.

All the optimal operating conditions, such as the pressure, temperature, volume, flow rate, and compositions of the refrigerant at the inlet and outlet of each piece of equipment in the 27 cases, are calculated to minimize the power required by the compressors.

To compare the required compressor power for all the cycles proposed in this study, the required power of the compressor (W) for the cycle per unit production of LNG (kg/s) was calculated, and the values are compared in Table 4-1.

Table 4-1 Comparison of the required power of the compressors for all the feasible liquefaction cycles

Cases	**Required Power of Compressor for the Cycle per Production of LNG (kW)**	**Ranking**
Case 1	181,200	27
Case 2	178,100	26
Case 3	174,700	25
Case 4	159,200	24
Case 5	156,800	23
Case 6	153,700	21
Case 7	151,100	19
Case 8	148,000	17
Case 9	145,100	15
Case 10	154,800	22
Case 11	151,200	20
Case 12	148,300	18

Case 13	136,900	12
Case 14	133,100	10
Case 15	129,700	7
Case 16	134,100	11
Case 17	131,300	8
Case 18	128,100	6
Case 19	145,300	16
Case 20	141,100	14
Case 21	137,200	13
Case 22	132,900	9
Case 23	126,700	5
Case 24	123,200	4
Case 25	119,800	3
Case 26	114,211	2
Case 27	111,056	1

The optimal operating conditions for all the feasible liquefaction cycles are shown in Figure 4-15 to 4-41 and in Table 4-2 to 4-28.

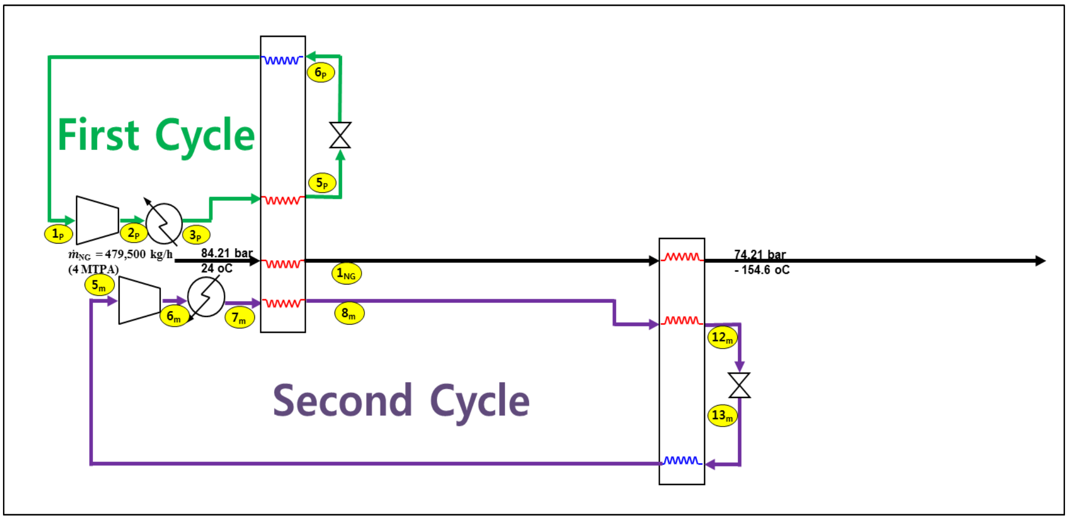

Figure 4-15 Configuration of the feasible liquefaction cycle - case 1

Table 4-2 Optimal operating conditions for the feasible liquefaction cycle - case 1

P1NG	79.71	P5m	3.48														
T1NG	-55	T5m	-58														
F1NG	479,500	F5m	638,400														
P1p	3.26	P6m	43.75														
T1p	-31.3	T6m	305														
F1p	1,603,000	F6m	638,400													Zpre_Methane	0.0075
P2p	33.66	P7m	43.35													Zpre_Ethane	0.745493
T2p	285	T7m	7.273													Zpre_Propane	0.244508
F2p	1,603,000	F7m	638,400													Zpre_i-Butane	0.00225
P3p	32.86	P8m	37.35													Zpre_n-Butane	000025
T3p	24	T8m	-55													Zmain_Nitrogen	0.160811
F3p	1,603,000	F8m	638,400													Zmain_Methane	0.696517
P5p	22.36	P12m	30.95													Zmain_Ethane	0.138704
T5p	-55	T12m	-155.1													Zmain_Propane	0.003955
F5p	1,603,000	F12m	638,400													Zmain_i-Butane	0.000007
P6p	3.56	P13m	3.88													Zmain_n-Butane	0.000005
T6p	-57.57	T13m	-161.3													Objective Function(work) [kW]	181,200
F6p	1,603,000	F13m	638,400														

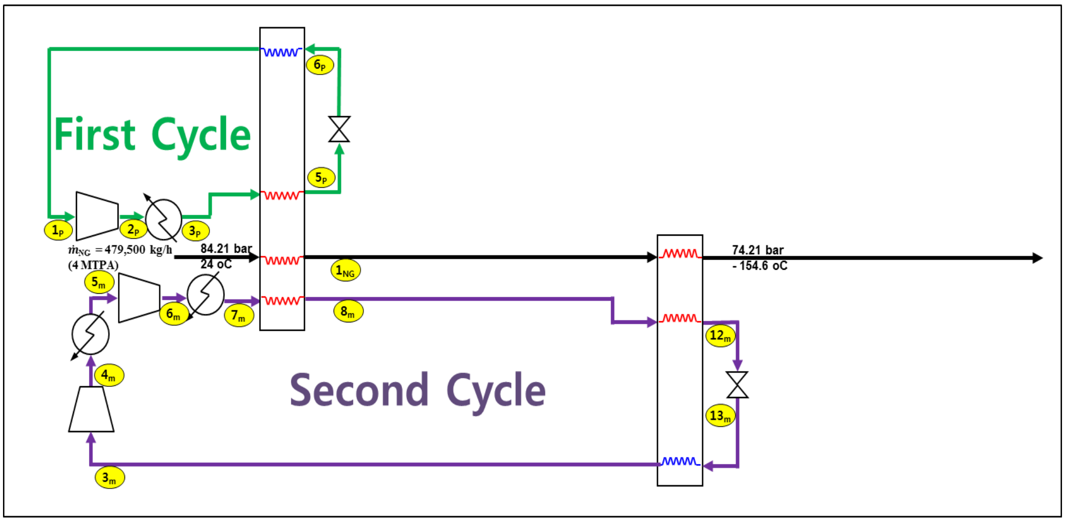

Figure 4-16 Configuration of the feasible liquefaction cycle - case 2

Table 4-3 Optimal operating conditions for the feasible liquefaction cycle - case 2

P1NG	79.71	P3m	3.48	P12m	30.95												
T1NG	-55	T3m	-58	T12m	-155.1												
F1NG	479,500	F3m	638,400	F12m	638,400												
P1p	3.26	P4m	15.75	P13m	3.88												
T1p	-31.3	T4m	42.46	T13m	-161.3												
F1p	1,603,000	F4m	638,400	F13m	638,400											Zpre_Methane	0.0075
P2p	33.66	P5m	15.75													Zpre_Ethane	0.745493
T2p	285	T5m	24													Zpre_Propane	0.244508
F2p	1,603,000	F5m	638,400													Zpre_i-Butane	0.00225
P3p	32.86	P6m	43.75													Zpre_n-Butane	000025
T3p	24	T6m	104.3													Zmain_Nitrogen	0.160811
F3p	1,603,000	F6m	638,400													Zmain_Methane	0.696517
P5p	22.36	P7m	43.35													Zmain_Ethane	0.138704
T5p	-55	T7m	7.273													Zmain_Propane	0.003955
F5p	1,603,000	F7m	638,400													Zmain_i-Butane	0.000007
P6p	3.56	P8m	37.35													Zmain_n-Butane	0.000005
T6p	-57.57	T8m	-55													Objective Function(work) [kW]	178,100
F6p	1,603,000	F8m	638,400														

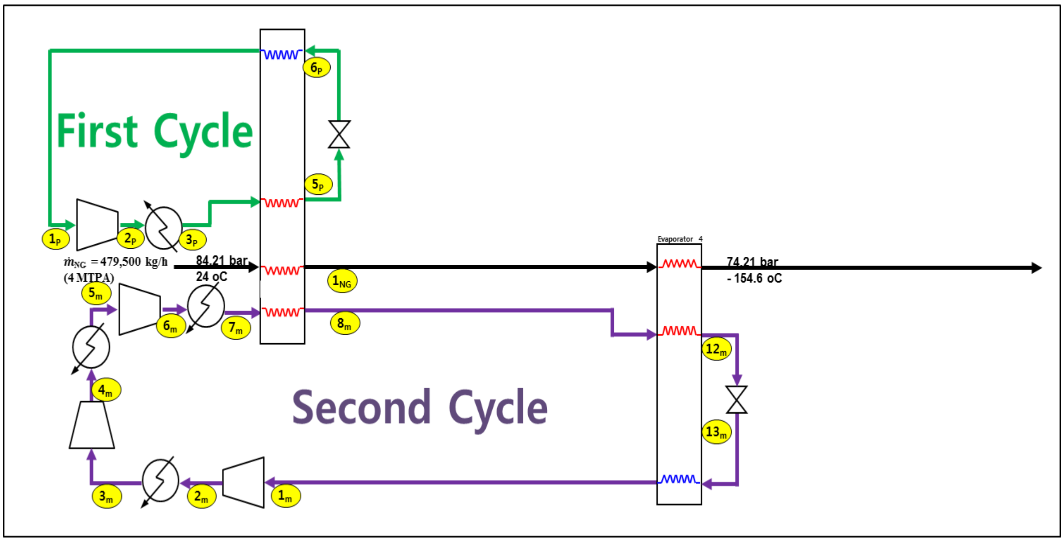

Figure 4-17 Configuration of the feasible liquefaction cycle - case 3

Table 4-4 Optimal operating conditions for the feasible liquefaction cycle - case 3

P1NG	79.71	P1m	3.48	P7m	43.35												
T1NG	-55	T1m	-58	T7m	7.273												
F1NG	479,500	F1m	638,400	F7m	638,400												
P1p	3.26	P2m	10.02	P8m	37.35												
T1p	-31.3	T2m	26	T8m	-55												
F1p	1,603,000	F2m	638,400	F8m	638,400											Zpre_Methane	0.0075
P2p	33.66	P3m	10.02	P12m	30.95											Zpre_Ethane	0.745493
T2p	285	T3m	24	T12m	-155.1											Zpre_Propane	0.244508
F2p	1,603,000	F3m	638,400	F12m	638,400											Zpre_i-Butane	0.00225
P3p	32.86	P4m	20.2	P13m	3.88											Zpre_n-Butane	000025
T3p	24	T4m	78	T13m	-161.3											Zmain_Nitrogen	0.160811
F3p	1,603,000	F4m	638,400	F13m	638,400											Zmain_Methane	0.696517
P5p	22.36	P5m	20.2													Zmain_Ethane	0.138704
T5p	-55	T5m	24													Zmain_Propane	0.003955
F5p	1,603,000	F5m	638,400													Zmain_i-Butane	0.000007
P6p	3.56	P6m	43.75													Zmain_n-Butane	0.000005
T6p	-57.57	T6m	88													Objective Function(work) [kW]	174,700
F6p	1,603,000	F6m	638,400														

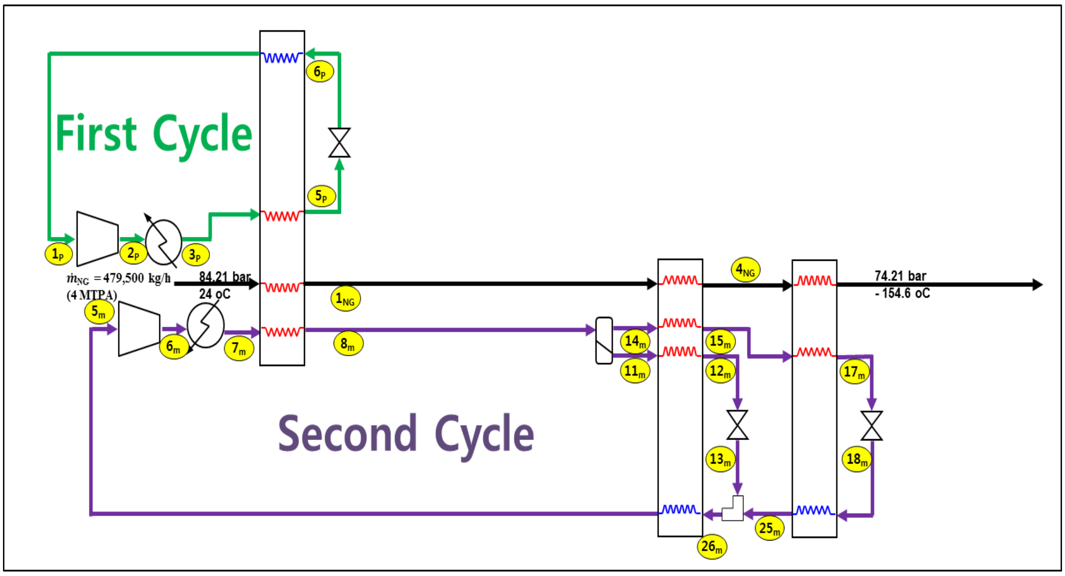

Figure 4-18 Configuration of the feasible liquefaction cycle - case 4

Table 4-5 Optimal operating conditions for the feasible liquefaction cycle - case 4

P1NG	79.71	P6p	3.56	P12m	32.45	P25m	3.78										
T1NG	-55	T6p	-57.57	T12m	-134	T25m	-142.6										
F1NG	479,500	F6p	1,603,000	F12m	434,300	F25m	204,100										
P4NG	76.96	P5m	3.48	P13m	3.78	P26m	3.78										
T4NG	-134	T5m	-58	T13m	-135.9	T26m	-136.7										
F4NG	479,500	F5m	638,400	F13m	434,300	F26m	638,400									Zpre_Methane	0.0075
P1p	3.26	P6m	43.75	P14m	37.25											Zpre_Ethane	0.745493
T1p	-31.3	T6m	305	T14m	-55.06											Zpre_Propane	0.244508
F1p	1,603,000	F6m	638,400	F14m	204,100											Zpre_i-Butane	0.00225
P2p	33.66	P7m	43.35	P15m	34.1											Zpre_n-Butane	000025
T2p	285	T7m	7.273	T15m	-134											Zmain_Nitrogen	0.160811
F2p	1,603,000	F7m	638,400	F15m	204,100											Zmain_Methane	0.696517
P3p	32.86	P8m	37.35	P17m	30.95											Zmain_Ethane	0.138704
T3p	24	T8m	-55	T17m	-155.1											Zmain_Propane	0.003955
F3p	1,603,000	F8m	638,400	F17m	204,100											Zmain_i-Butane	0.000007
P5p	22.36	P11m	37.25	P18m	3.88											Zmain_n-Butane	0.000005
T5p	-55	T11m	-55.06	T18m	-161.3											Objective Function(work) [kW]	159,200
F5p	1,603,000	F11m	434,300	F18m	204,100												

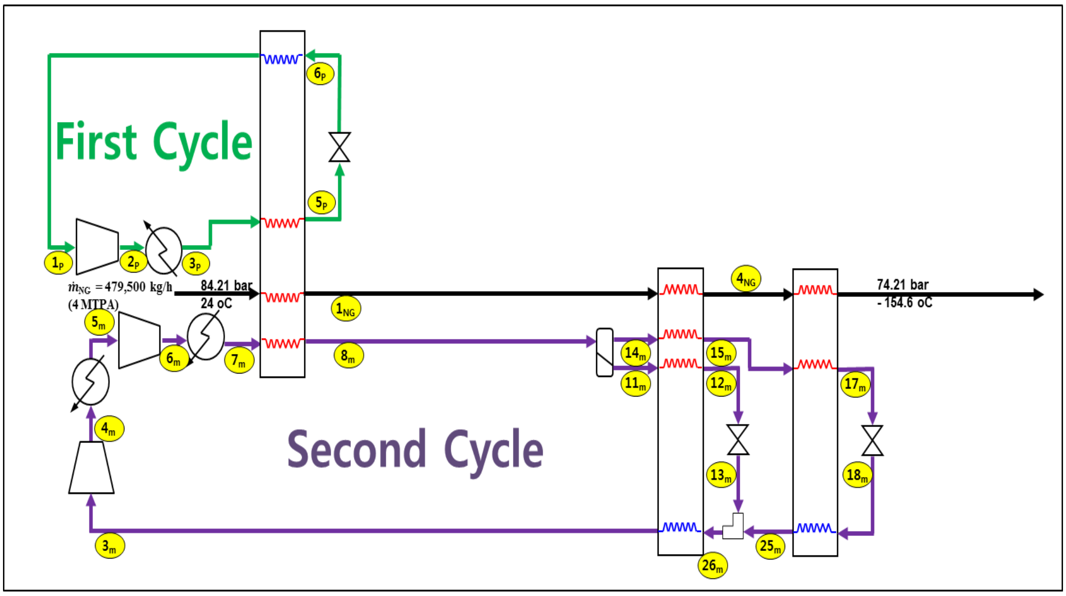

Figure 4-19 Configuration of the feasible liquefaction cycle - case 5

Table 4-6 Optimal operating conditions for the feasible liquefaction cycle - case 5

P1NG	79.71	P6p	3.56	P8m	37.35	P17m	30.95										
T1NG	-55	T6p	-57.57	T8m	-55	T17m	-155.1										
F1NG	479,500	F6p	1,603,000	F8m	638,400	F17m	204,100										
P4NG	76.96	P3m	3.48	P11m	37.25	P18m	3.88										
T4NG	-134	T3m	-58	T11m	-55.06	T18m	-161.3										
F4NG	479,500	F3m	638,400	F11m	434,300	F18m	204,100									Zpre_Methane	0.0075
P1p	3.26	P4m	15.75	P12m	32.45	P25m	3.78									Zpre_Ethane	0.745493
T1p	-31.3	T4m	42.46	T12m	-134	T25m	-142.6									Zpre_Propane	0.244508
F1p	1,603,000	F4m	638,400	F12m	434,300	F25m	204,100									Zpre_i-Butane	0.00225
P2p	33.66	P5m	15.75	P13m	3.78	P26m	3.78									Zpre_n-Butane	000025
T2p	285	T5m	24	T13m	-135.9	T26m	-136.7									Zmain_Nitrogen	0.160811
F2p	1,603,000	F5m	638,400	F13m	434,300	F26m	638,400									Zmain_Methane	0.696517
P3p	32.86	P6m	43.75	P14m	37.25											Zmain_Ethane	0.138704
T3p	24	T6m	104.3	T14m	-55.06											Zmain_Propane	0.003955
F3p	1,603,000	F6m	638,400	F14m	204,100											Zmain_i-Butane	0.000007
P5p	22.36	P7m	43.35	P15m	34.1											Zmain_n-Butane	0.000005
T5p	-55	T7m	7.273	T15m	-134											Objective Function(work) [kW]	156,800
F5p	1,603,000	F7m	638,400	F15m	204,100												

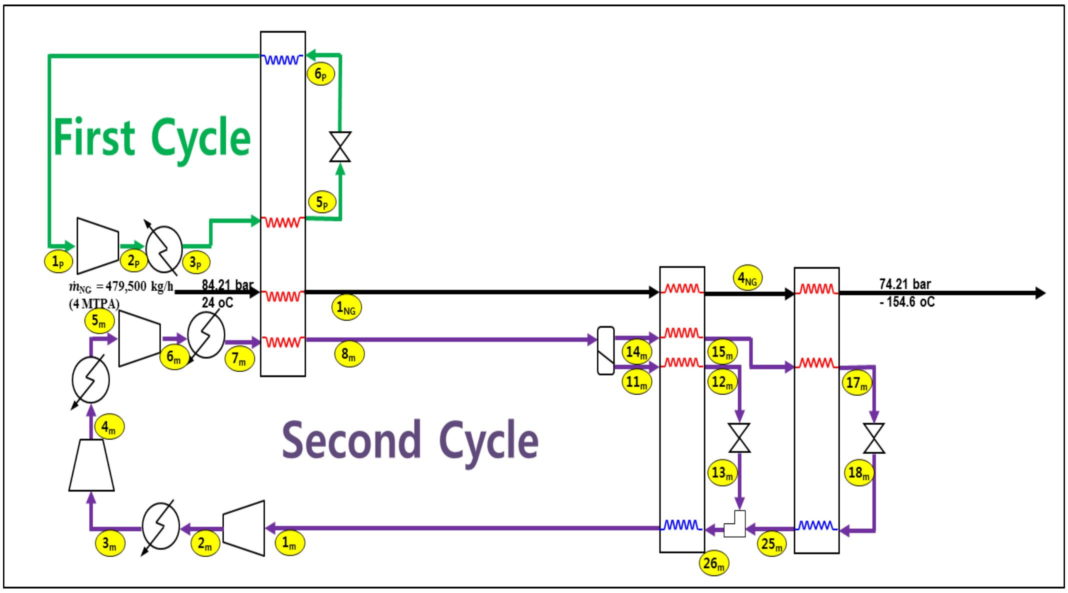

Figure 4-20 Configuration of the feasible liquefaction cycle - case 6

Table 4-7 Optimal operating conditions for the feasible liquefaction cycle - case 6

P1NG	79.71	P6p	3.56	P6m	43.75	P14m	37.25										
T1NG	-55	T6p	-57.57	T6m	88	T14m	-55.06										
F1NG	479,500	F6p	1,603,000	F6m	638,400	F14m	204,100										
P4NG	76.96	P1m	3.48	P7m	43.35	P15m	34.1										
T4NG	-134	T1m	-58	T7m	7.273	T15m	-134										
F4NG	479,500	F1m	638,400	F7m	638,400	F15m	204,100									Zpre_Methane	0.0075
P1p	3.26	P2m	10.02	P8m	37.35	P17m	30.95									Zpre_Ethane	0.745493
T1p	-31.3	T2m	26	T8m	-55	T17m	-155.1									Zpre_Propane	0.244508
F1p	1,603,000	F2m	638,400	F8m	638,400	F17m	204,100									Zpre_i-Butane	0.00225
P2p	33.66	P3m	10.02	P11m	37.25	P18m	3.88									Zpre_n-Butane	000025
T2p	285	T3m	24	T11m	-55.06	T18m	-161.3									Zmain_Nitrogen	0.160811
F2p	1,603,000	F3m	638,400	F11m	434,300	F18m	204,100									Zmain_Methane	0.696517
P3p	32.86	P4m	20.2	P12m	32.45	P25m	3.78									Zmain_Ethane	0.138704
T3p	24	T4m	78	T12m	-134	T25m	-142.6									Zmain_Propane	0.003955
F3p	1,603,000	F4m	638,400	F12m	434,300	F25m	204,100									Zmain_i-Butane	0.000007
P5p	22.36	P5m	20.2	P13m	3.78	P26m	3.78									Zmain_n-Butane	0.000005
T5p	-55	T5m	24	T13m	-135.9	T26m	-136.7									Objective Function(work) [kW]	153,700
F5p	1,603,000	F5m	638,400	F13m	434,300	F26m	638,400										

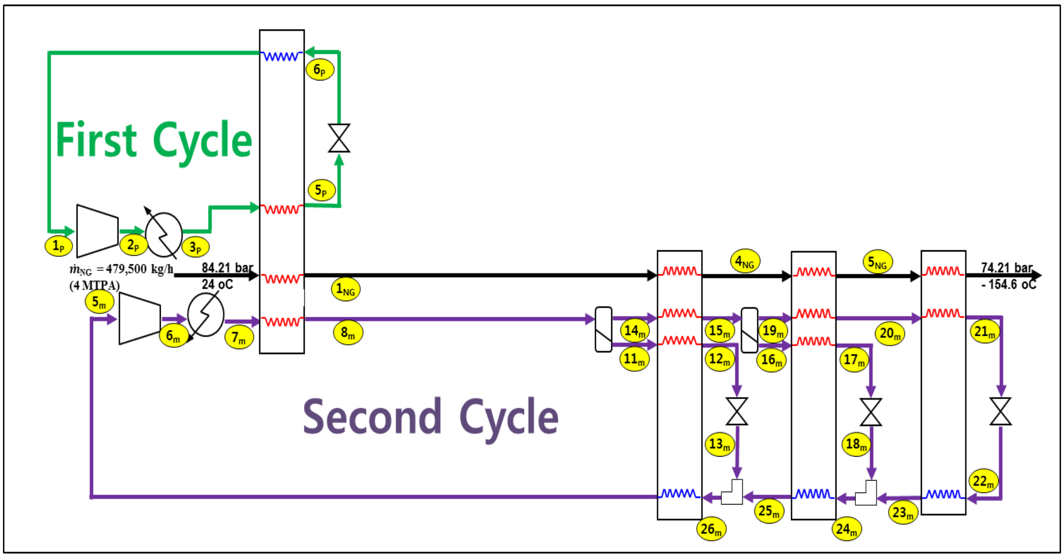

Figure 4-21 Configuration of the feasible liquefaction cycle - case 7

Table 4-8 Optimal operating conditions for the feasible liquefaction cycle - case 7

P1NG	79.71	P5p	22.36	P11m	37.25	P17m	32.45	P23m	3.78								
T1NG	-55	T5p	-55	T11m	-55.06	T17m	-134	T23m	-142.6								
F1NG	479,500	F5p	1,603,000	F11m	301,300	F17m	201,100	F23m	136,000								
P4NG	77.86	P6p	3.56	P12m	34.75	P18m	3.78	P24m	3.78								
T4NG	-110	T6p	-57.57	T12m	-110	T18m	-135.9	T24m	-136.7								
F4NG	479,500	F6p	1,603,000	F12m	301,300	F18m	201,100	F24m	337,100							Zpre_Methane	0.0075
P5NG	75.96	P5m	3.48	P13m	3.68	P19m	34.75	P25m	3.68							Zpre_Ethane	0.745493
T5NG	-134	T5m	-58	T13m	-114	T19m	-110	T25m	-120							Zpre_Propane	0.244508
F5NG	479,500	F5m	638,400	F13m	301,300	F19m	136,000	F25m	337,100							Zpre_i-Butane	0.00225
P1p	3.26	P6m	43.75	P14m	37.25	P20m	32.45	P26m	3.68							Zpre_n-Butane	000025
T1p	-31.3	T6m	305	T14m	-55.06	T20m	-134	T26m	-116							Zmain_Nitrogen	0.160811
F1p	1,603,000	F6m	638,400	F14m	337,100	F20m	136,000	F26m	638,400							Zmain_Methane	0.696517
P2p	33.66	P7m	43.35	P15m	34.75	P21m	30.95									Zmain_Ethane	0.138704
T2p	285	T7m	7.273	T15m	-110	T21m	-155.1									Zmain_Propane	0.003955
F2p	1,603,000	F7m	638,400	F15m	337,100	F21m	136,000									Zmain_i-Butane	0.000007
P3p	32.86	P8m	37.35	P16m	34.75	P22m	3.88									Zmain_n-Butane	0.000005
T3p	24	T8m	-55	T16m	-110	T22m	-161.3									Objective Function(work) [kW]	151,100
F3p	1,603,000	F8m	638,400	F16m	201,100	F22m	136,000										

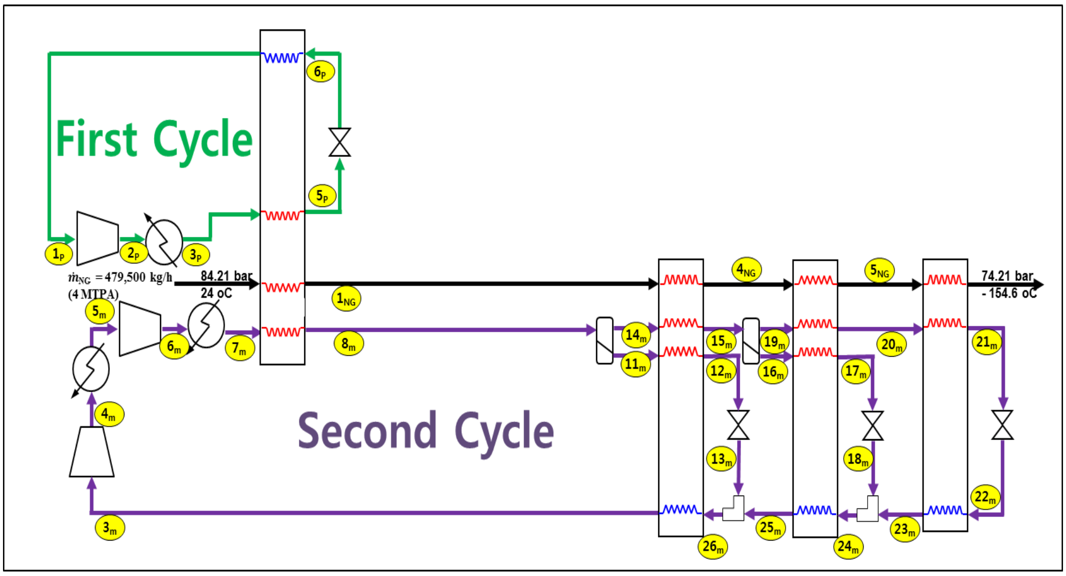

Figure 4-22 Configuration of the feasible liquefaction cycle - case 8

Table 4-9 Optimal operating conditions for the feasible liquefaction cycle - case 8

P1NG	79.71	P5p	22.36	P7m	43.35	P15m	34.75	P21m	30.95								
T1NG	-55	T5p	-55	T7m	7.273	T15m	-110	T21m	-155.1								
F1NG	479,500	F5p	1,603,000	F7m	638,400	F15m	337,100	F21m	136,000								
P4NG	77.86	P6p	3.56	P8m	37.35	P16m	34.75	P22m	3.88								
T4NG	-110	T6p	-57.57	T8m	-55	T16m	-110	T22m	-161.3								
F4NG	479,500	F6p	1,603,000	F8m	638,400	F16m	201,100	F22m	136,000							Zpre_Methane	0.0075
P5NG	75.96	P3m	10.02	P11m	37.25	P17m	32.45	P23m	3.78							Zpre_Ethane	0.745493
T5NG	-134	T3m	24	T11m	-55.06	T17m	-134	T23m	-142.6							Zpre_Propane	0.244508
F5NG	479,500	F3m	638,400	F11m	301,300	F17m	201,100	F23m	136,000							Zpre_i-Butane	0.00225
P1p	3.26	P4m	20.2	P12m	34.75	P18m	3.78	P24m	3.78							Zpre_n-Butane	000025
T1p	-31.3	T4m	78	T12m	-110	T18m	-135.9	T24m	-136.7							Zmain_Nitrogen	0.160811
F1p	1,603,000	F4m	638,400	F12m	301,300	F18m	201,100	F24m	337,100							Zmain_Methane	0.696517
P2p	33.66	P5m	20.2	P13m	3.68	P19m	34.75	P25m	3.68							Zmain_Ethane	0.138704
T2p	285	T5m	24	T13m	-114	T19m	-110	T25m	-120							Zmain_Propane	0.003955
F2p	1,603,000	F5m	638,400	F13m	301,300	F19m	136,000	F25m	337,100							Zmain_i-Butane	0.000007
P3p	32.86	P6m	43.75	P14m	37.25	P20m	32.45	P26m	3.68							Zmain_n-Butane	0.000005
T3p	24	T6m	88	T14m	-55.06	T20m	-134	T26m	-116							Objective Function(work) [kW]	148,000
F3p	1,603,000	F6m	638,400	F14m	337,100	F20m	136,000	F26m	638,400								

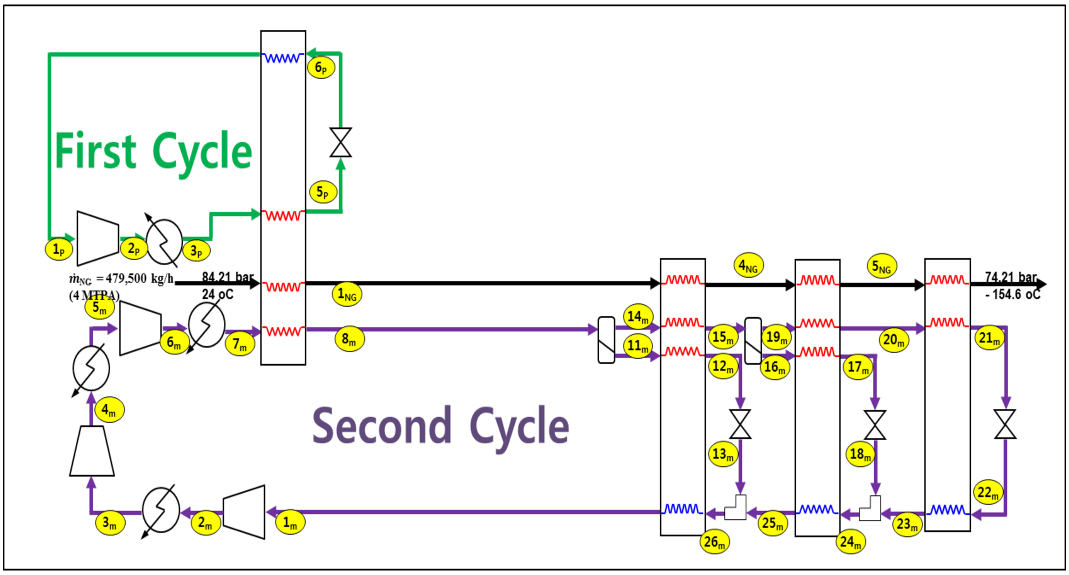

Figure 4-23 Configuration of the feasible liquefaction cycle - case 9

Table 4-10 Optimal operating conditions for the feasible liquefaction cycle - case 9

P1NG	79.71	P5p	22.36	P5m	20.2	P13m	3.68	P19m	34.75	P25m	3.68						
T1NG	-55	T5p	-55	T5m	24	T13m	-114	T19m	-110	T25m	-120						
F1NG	479,500	F5p	1,603,000	F5m	638,400	F13m	301,300	F19m	136,000	F25m	337,100						
P4NG	77.86	P6p	3.56	P6m	43.75	P14m	37.25	P20m	32.45	P26m	3.68						
T4NG	-110	T6p	-57.57	T6m	88	T14m	-55.06	T20m	-134	T26m	-116						
F4NG	479,500	F6p	1,603,000	F6m	638,400	F14m	337,100	F20m	136,000	F26m	638,400					Zpre_Methane	0.0075
P5NG	75.96	P1m	3.48	P7m	43.35	P15m	34.75	P21m	30.95							Zpre_Ethane	0.745493
T5NG	-134	T1m	-58	T7m	7.273	T15m	-110	T21m	-155.1							Zpre_Propane	0.244508
F5NG	479,500	F1m	638,400	F7m	638,400	F15m	337,100	F21m	136,000							Zpre_i-Butane	0.00225
P1p	3.26	P2m	10.02	P8m	37.35	P16m	34.75	P22m	3.88							Zpre_n-Butane	000025
T1p	-31.3	T2m	26	T8m	-55	T16m	-110	T22m	-161.3							Zmain_Nitrogen	0.160811
F1p	1,603,000	F2m	638,400	F8m	638,400	F16m	201,100	F22m	136,000							Zmain_Methane	0.696517
P2p	33.66	P3m	10.02	P11m	37.25	P17m	32.45	P23m	3.78							Zmain_Ethane	0.138704
T2p	285	T3m	24	T11m	-55.06	T17m	-134	T23m	-142.6							Zmain_Propane	0.003955
F2p	1,603,000	F3m	638,400	F11m	301,300	F17m	201,100	F23m	136,000							Zmain_i-Butane	0.000007
P3p	32.86	P4m	20.2	P12m	34.75	P18m	3.78	P24m	3.78							Zmain_n-Butane	0.000005
T3p	24	T4m	78	T12m	-110	T18m	-135.9	T24m	-136.7							Objective Function(work) [kW]	145,100
F3p	1,603,000	F4m	638,400	F12m	301,300	F18m	201,100	F24m	337,100								

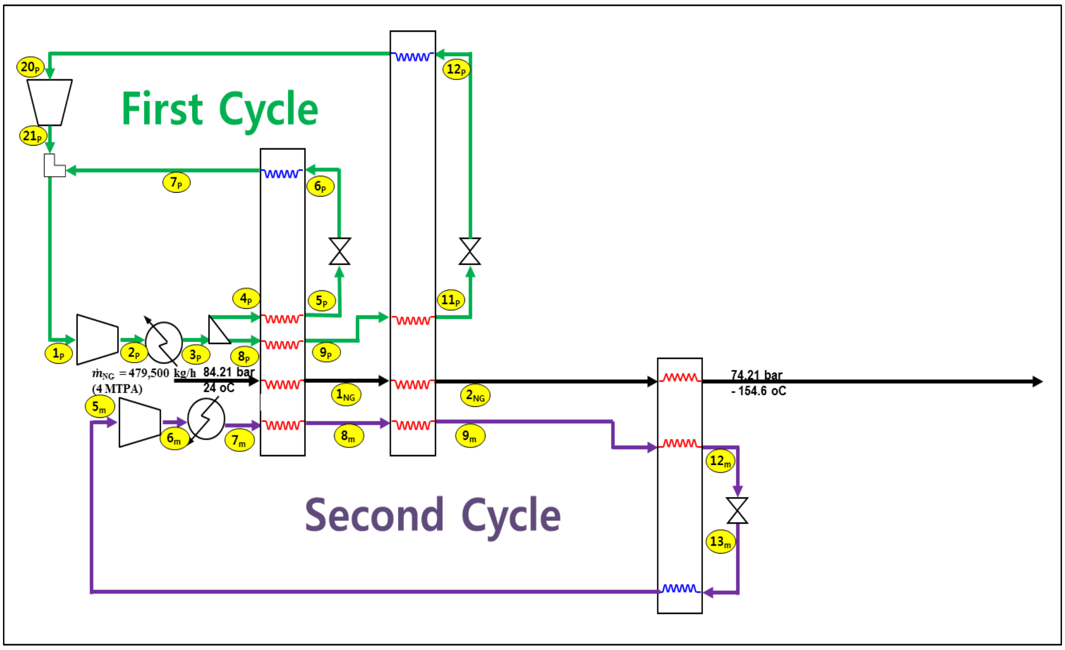

Figure 4-24 Configuration of the feasible liquefaction cycle - case 10

Table 4-11 Optimal operating conditions for the feasible liquefaction cycle - case 10

P1NG	82.71	P5p	27.36	P12p	3.56	P8m	41.35										
T1NG	-15.5	T5p	-15.5	T12p	-57.57	T8m	-15.5										
F1NG	479,500	F5p	810,200	F12p	792,800	F8m	638,400										
P2NG	79.71	P6p	10.5	P20p	3.26	P9m	37.35										
T2NG	-55	T6p	-18.5	T20p	-31.3	T9m	-55										
F2NG	479,500	F6p	810,200	F20p	792,800	F9m	638,400									Zpre_Methane	0.0075
P1p	10.2	P7p	10.2	P21p	10.2	P12m	30.95									Zpre_Ethane	0.745493
T1p	28.3	T7p	21	T21p	33.79	T12m	-155.1									Zpre_Propane	0.244508
F1p	1,603,000	F7p	810,200	F21p	792,800	F12m	638,400									Zpre_i-Butane	0.00225
P2p	33.66	P8p	32.86	P5m	3.48	P13m	3.88									Zpre_n-Butane	000025
T2p	125	T8p	24	T5m	-58	T13m	-161.3									Zmain_Nitrogen	0.160811
F2p	1,603,000	F8p	792,800	F5m	638,400	F13m	638,400									Zmain_Methane	0.696517
P3p	32.86	P9p	27.36	P6m	43.75											Zmain_Ethane	0.138704
T3p	24	T9p	-15.5	T6m	305											Zmain_Propane	0.003955
F3p	1,603,000	F9p	792,800	F6m	638,400											Zmain_i-Butane	0.000007
P4p	32.86	P11p	22.36	P7m	43.35											Zmain_n-Butane	0.000005
T4p	24	T11p	-55	T7m	7.273											Objective Function(work) [kW]	154,800
F4p	810,200	F11p	792,800	F7m	638,400												

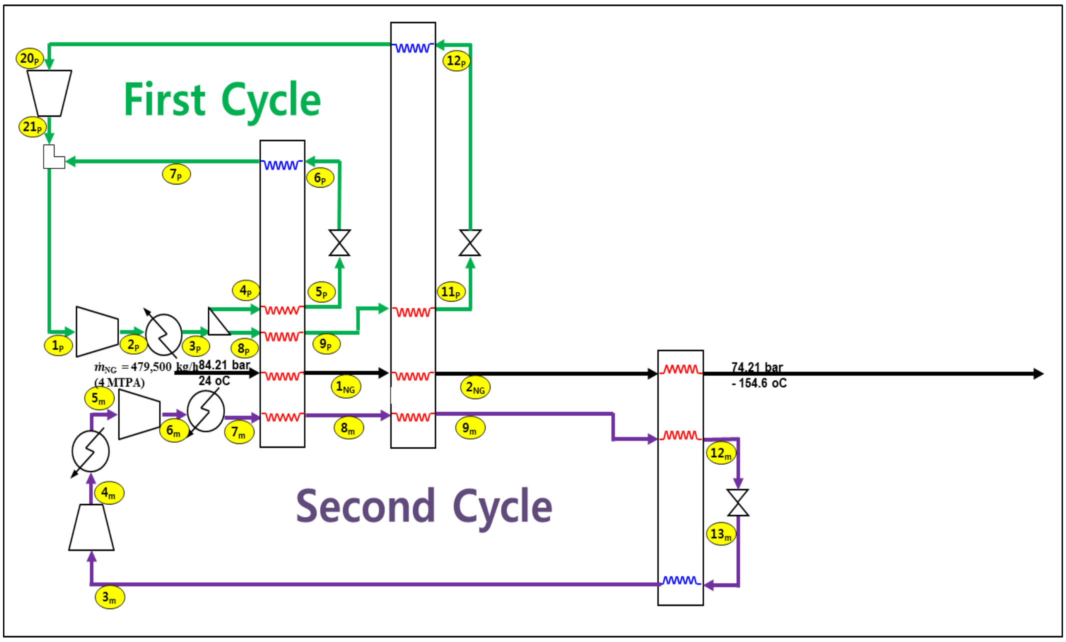

Figure 4-25 Configuration of the feasible liquefaction cycle - case 11

Table 4-12 Optimal operating conditions for the feasible liquefaction cycle - case 11

P1NG	82.71	P5p	27.36	P12p	3.56	P6m	43.75										
T1NG	-15.5	T5p	-15.5	T12p	-57.57	T6m	104.3										
F1NG	479,500	F5p	810,200	F12p	792,800	F6m	638,400										
P2NG	79.71	P6p	10.5	P20p	3.26	P7m	43.35										
T2NG	-55	T6p	-18.5	T20p	-31.3	T7m	7.273										
F2NG	479,500	F6p	810,200	F20p	792,800	F7m	638,400									Zpre_Methane	0.0075
P1p	10.2	P7p	10.2	P21p	10.2	P8m	41.35									Zpre_Ethane	0.745493
T1p	28.3	T7p	21	T21p	33.79	T8m	-15.5									Zpre_Propane	0.244508
F1p	1,603,000	F7p	810,200	F21p	792,800	F8m	638,400									Zpre_i-Butane	0.00225
P2p	33.66	P8p	32.86	P3m	3.48	P9m	37.35									Zpre_n-Butane	000025
T2p	125	T8p	24	T3m	-58	T9m	-55									Zmain_Nitrogen	0.160811
F2p	1,603,000	F8p	792,800	F3m	638,400	F9m	638,400									Zmain_Methane	0.696517
P3p	32.86	P9p	27.36	P4m	15.75	P12m	30.95									Zmain_Ethane	0.138704
T3p	24	T9p	-15.5	T4m	42.46	T12m	-155.1									Zmain_Propane	0.003955
F3p	1,603,000	F9p	792,800	F4m	638,400	F12m	638,400									Zmain_i-Butane	0.000007
P4p	32.86	P11p	22.36	P5m	15.75	P13m	3.88									Zmain_n-Butane	0.000005
T4p	24	T11p	-55	T5m	24	T13m	-161.3										
F4p	810,200	F11p	792,800	F5m	638,400	F13m	638,400									Objective Function(work) [kW]	151,200

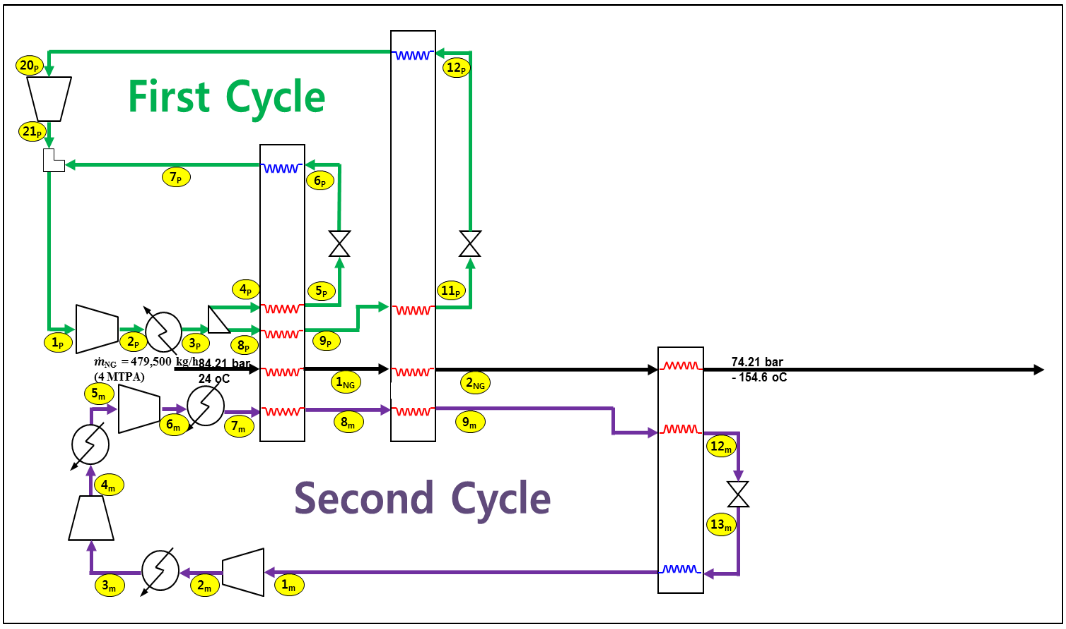

Figure 4-26 Configuration of the feasible liquefaction cycle - case 12

Table 4-13 Optimal operating conditions for the feasible liquefaction cycle - case 12

P1NG	82.71	P5p	27.36	P12p	3.56	P4m	20.2	P12m	30.95								
T1NG	-15.5	T5p	-15.5	T12p	-57.57	T4m	78	T12m	-155.1								
F1NG	479,500	F5p	810,200	F12p	792,800	F4m	638,400	F12m	638,400								
P2NG	79.71	P6p	10.5	P20p	3.26	P5m	20.2	P13m	3.88								
T2NG	-55	T6p	-18.5	T20p	-31.3	T5m	24	T13m	-161.3								
F2NG	479,500	F6p	810,200	F20p	792,800	F5m	638,400	F13m	638,400							Zpre_Methane	0.0075
P1p	10.2	P7p	10.2	P21p	10.2	P6m	43.75									Zpre_Ethane	0.745493
T1p	28.3	T7p	21	T21p	33.79	T6m	88									Zpre_Propane	0.244508
F1p	1,603,000	F7p	810,200	F21p	792,800	F6m	638,400									Zpre_i-Butane	0.00225
P2p	33.66	P8p	32.86	P1m	3.48	P7m	43.35									Zpre_n-Butane	000025
T2p	125	T8p	24	T1m	-58	T7m	7.273									Zmain_Nitrogen	0.160811
F2p	1,603,000	F8p	792,800	F1m	638,400	F7m	638,400									Zmain_Methane	0.696517
P3p	32.86	P9p	27.36	P2m	10.02	P8m	41.35									Zmain_Ethane	0.138704
T3p	24	T9p	-15.5	T2m	26	T8m	-15.5									Zmain_Propane	0.003955
F3p	1,603,000	F9p	792,800	F2m	638,400	F8m	638,400									Zmain_i-Butane	0.000007
P4p	32.86	P11p	22.36	P3m	10.02	P9m	37.35									Zmain_n-Butane	0.000005
T4p	24	T11p	-55	T3m	24	T9m	-55										
F4p	810,200	F11p	792,800	F3m	638,400	F9m	638,400									Objective Function(work) [kW]	148,300

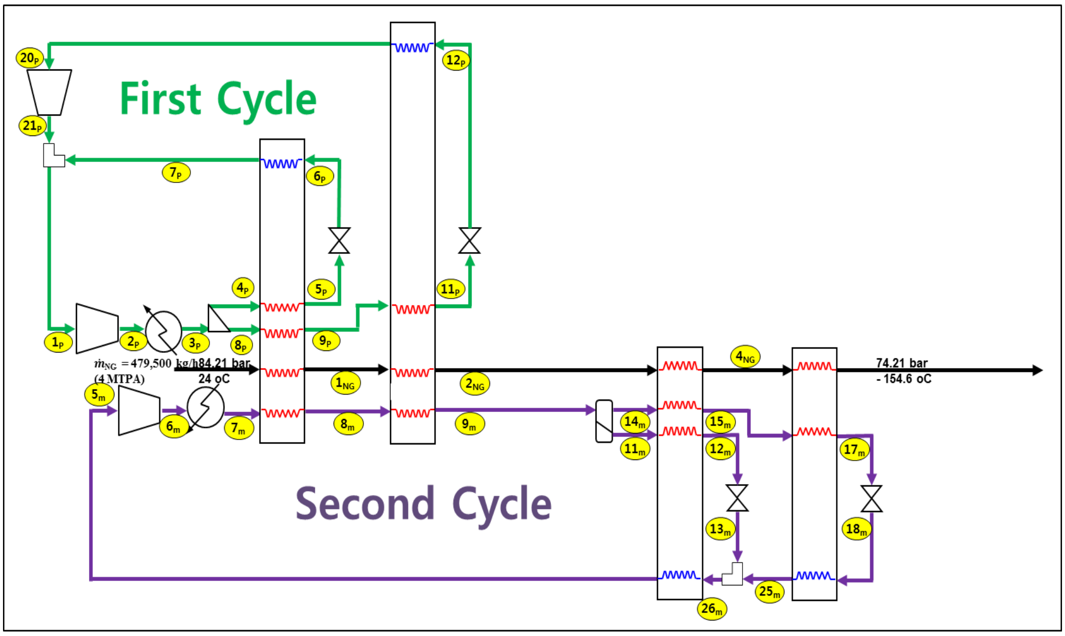

Figure 4-27 Configuration of the feasible liquefaction cycle - case 13

Table 4-14 Optimal operating conditions for the feasible liquefaction cycle - case 13

P1NG	82.71	P4p	32.86	P11p	22.36	P7m	43.35	P14m	37.25								
T1NG	-15.5	T4p	24	T11p	-55	T7m	7.273	T14m	-55.06								
F1NG	479,500	F4p	810,200	F11p	792,800	F7m	638,400	F14m	204,100								
P2NG	79.71	P5p	27.36	P12p	3.56	P8m	41.35	P15m	34.1								
T2NG	-55	T5p	-15.5	T12p	-57.57	T8m	-15.5	T15m	-134								
F2NG	479,500	F5p	810,200	F12p	792,800	F8m	638,400	F15m	204,100							Zpre_Methane	0.0075
P4NG	76.96	P6p	10.5	P20p	3.26	P9m	37.35	P17m	30.95							Zpre_Ethane	0.745493
T4NG	-134	T6p	-18.5	T20p	-31.3	T9m	-55	T17m	-155.1							Zpre_Propane	0.244508
F4NG	479,500	F6p	810,200	F20p	792,800	F9m	638,400	F17m	204,100							Zpre_i-Butane	0.00225
P1p	10.2	P7p	10.2	P21p	10.2	P11m	37.25	P18m	3.88							Zpre_n-Butane	000025
T1p	28.3	T7p	21	T21p	33.79	T11m	-55.06	T18m	-161.3							Zmain_Nitrogen	0.160811
F1p	1,603,000	F7p	810,200	F21p	792,800	F11m	434,300	F18m	204,100							Zmain_Methane	0.696517
P2p	33.66	P8p	32.86	P5m	3.48	P12m	32.45	P25m	3.78							Zmain_Ethane	0.138704
T2p	125	T8p	24	T5m	-58	T12m	-134	T25m	-142.6							Zmain_Propane	0.003955
F2p	1,603,000	F8p	792,800	F5m	638,400	F12m	434,300	F25m	204,100							Zmain_i-Butane	0.000007
P3p	32.86	P9p	27.36	P6m	43.75	P13m	3.78	P26m	3.78							Zmain_n-Butane	0.000005
T3p	24	T9p	-15.5	T6m	305	T13m	-135.9	T26m	-136.7							Objective Function(work) [kW]	136,900
F3p	1,603,000	F9p	792,800	F6m	638,400	F13m	434,300	F26m	638,400								

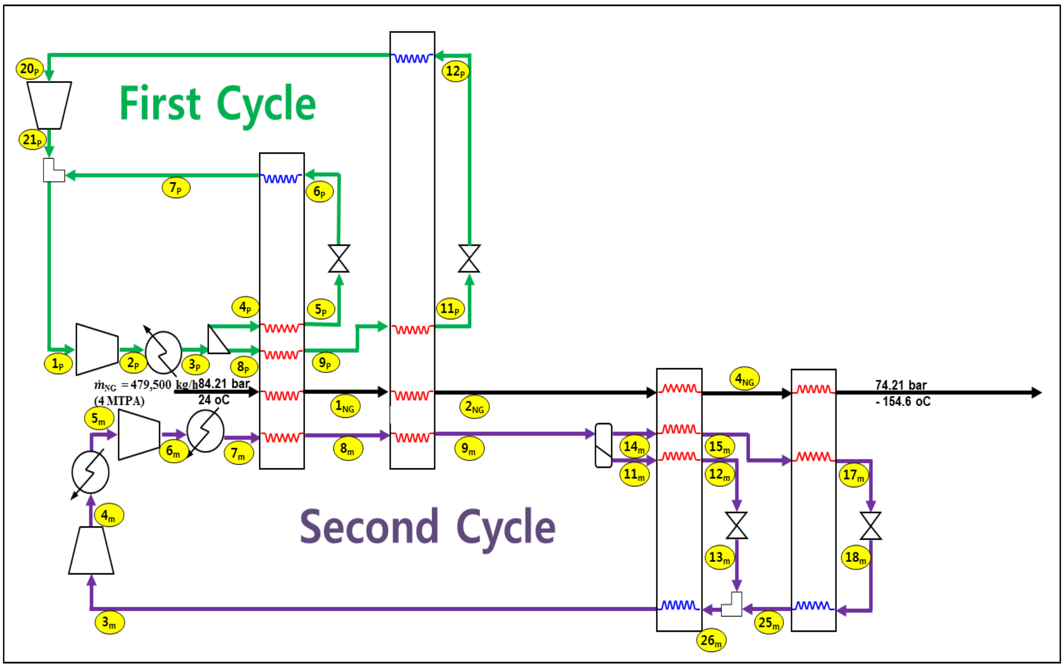

Figure 4-28 Configuration of the feasible liquefaction cycle - case 14

Table 4-15 Optimal operating conditions for the feasible liquefaction cycle - case 14

P1NG	82.71	P4p	32.86	P11p	22.36	P5m	20.2	P12m	32.45	P25m	3.78						
T1NG	-15.5	T4p	24	T11p	-55	T5m	24	T12m	-134	T25m	-142.6						
F1NG	479,500	F4p	810,200	F11p	792,800	F5m	638,400	F12m	434,300	F25m	204,100						
P2NG	79.71	P5p	27.36	P12p	3.56	P6m	43.75	P13m	3.78	P26m	3.78						
T2NG	-55	T5p	-15.5	T12p	-57.57	T6m	88	T13m	-135.9	T26m	-136.7						
F2NG	479,500	F5p	810,200	F12p	792,800	F6m	638,400	F13m	434,300	F26m	638,400					Zpre_Methane	0.0075
P4NG	76.96	P6p	10.5	P20p	3.26	P7m	43.35	P14m	37.25							Zpre_Ethane	0.745493
T4NG	-134	T6p	-18.5	T20p	-31.3	T7m	7.273	T14m	-55.06							Zpre_Propane	0.244508
F4NG	479,500	F6p	810,200	F20p	792,800	F7m	638,400	F14m	204,100							Zpre_i-Butane	0.00225
P1p	10.2	P7p	10.2	P21p	10.2	P8m	41.35	P15m	34.1							Zpre_n-Butane	000025
T1p	28.3	T7p	21	T21p	33.79	T8m	-15.5	T15m	-134							Zmain_Nitrogen	0.160811
F1p	1,603,000	F7p	810,200	F21p	792,800	F8m	638,400	F15m	204,100							Zmain_Methane	0.696517
P2p	33.66	P8p	32.86	P3m	10.02	P9m	37.35	P17m	30.95							Zmain_Ethane	0.138704
T2p	125	T8p	24	T3m	24	T9m	-55	T17m	-155.1							Zmain_Propane	0.003955
F2p	1,603,000	F8p	792,800	F3m	638,400	F9m	638,400	F17m	204,100							Zmain_i-Butane	0.000007
P3p	32.86	P9p	27.36	P4m	20.2	P11m	37.25	P18m	3.88							Zmain_n-Butane	0.000005
T3p	24	T9p	-15.5	T4m	78	T11m	-55.06	T18m	-161.3							Objective Function(work) [kW]	133,100
F3p	1,603,000	F9p	792,800	F4m	638,400	F11m	434,300	F18m	204,100								

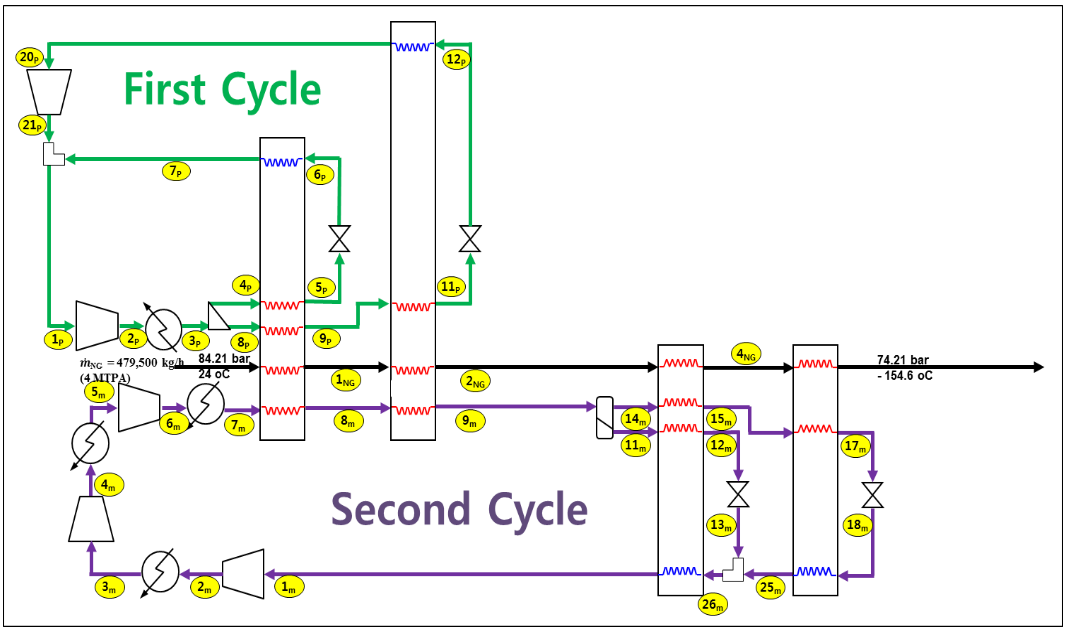

Figure 4-29 Configuration of the feasible liquefaction cycle - case 15

Table 4-16 Optimal operating conditions for the feasible liquefaction cycle - case 15

P1NG	82.71	P4p	32.86	P11p	22.36	P3m	10.02	P9m	37.35	P17m	30.95						
T1NG	-15.5	T4p	24	T11p	-55	T3m	24	T9m	-55	T17m	-155.1						
F1NG	479,500	F4p	810,200	F11p	792,800	F3m	638,400	F9m	638,400	F17m	204,100						
P2NG	79.71	P5p	27.36	P12p	3.56	P4m	20.2	P11m	37.25	P18m	3.88						
T2NG	-55	T5p	-15.5	T12p	-57.57	T4m	78	T11m	-55.06	T18m	-161.3						
F2NG	479,500	F5p	810,200	F12p	792,800	F4m	638,400	F11m	434,300	F18m	204,100					Zpre_Methane	0.0075
P4NG	76.96	P6p	10.5	P20p	3.26	P5m	20.2	P12m	32.45	P25m	3.78					Zpre_Ethane	0.745493
T4NG	-134	T6p	-18.5	T20p	-31.3	T5m	24	T12m	-134	T25m	-142.6					Zpre_Propane	0.244508
F4NG	479,500	F6p	810,200	F20p	792,800	F5m	638,400	F12m	434,300	F25m	204,100					Zpre_i-Butane	0.00225
P1p	10.2	P7p	10.2	P21p	10.2	P6m	43.75	P13m	3.78	P26m	3.78					Zpre_n-Butane	000025
T1p	28.3	T7p	21	T21p	33.79	T6m	88	T13m	-135.9	T26m	-136.7					Zmain_Nitrogen	0.160811
F1p	1,603,000	F7p	810,200	F21p	792,800	F6m	638,400	F13m	434,300	F26m	638,400					Zmain_Methane	0.696517
P2p	33.66	P8p	32.86	P1m	3.48	P7m	43.35	P14m	37.25							Zmain_Ethane	0.138704
T2p	125	T8p	24	T1m	-58	T7m	7.273	T14m	-55.06							Zmain_Propane	0.003955
F2p	1,603,000	F8p	792,800	F1m	638,400	F7m	638,400	F14m	204,100							Zmain_i-Butane	0.000007
P3p	32.86	P9p	27.36	P2m	10.02	P8m	41.35	P15m	34.1							Zmain_n-Butane	0.000005
T3p	24	T9p	-15.5	T2m	26	T8m	-15.5	T15m	-134							Objective Function(work) [kW]	129,700
F3p	1,603,000	F9p	792,800	F2m	638,400	F8m	638,400	F15m	204,100								

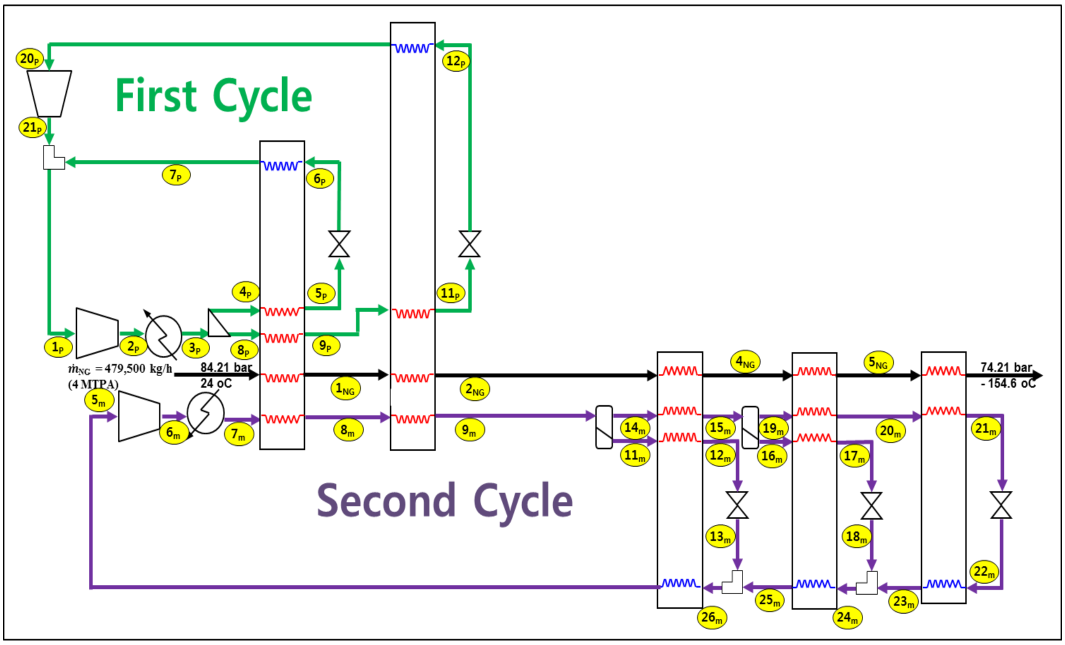

Figure 4-30 Configuration of the feasible liquefaction cycle - case 16

Table 4-17 Optimal operating conditions for the feasible liquefaction cycle - case 16

P1NG	82.71	P3p	32.86	P9p	27.36	P6m	43.75	P13m	3.68	P19m	34.75	P25m	3.68				
T1NG	-15.5	T3p	24	T9p	-15.5	T6m	305	T13m	-114	T19m	-110	T25m	-120				
F1NG	479,500	F3p	1,603,000	F9p	792,800	F6m	638,400	F13m	301,300	F19m	136,000	F25m	337,100				
P2NG	79.71	P4p	32.86	P11p	22.36	P7m	43.35	P14m	37.25	P20m	32.45	P26m	3.68				
T2NG	-55	T4p	24	T11p	-55	T7m	7.273	T14m	-55.06	T20m	-134	T26m	-116				
F2NG	479,500	F4p	810,200	F11p	792,800	F7m	638,400	F14m	337,100	F20m	136,000	F26m	638,400			Zpre_Methane	0.0075
P4NG	77.86	P5p	27.36	P12p	3.56	P8m	41.35	P15m	34.75	P21m	30.95					Zpre_Ethane	0.745493
T4NG	-110	T5p	-15.5	T12p	-57.57	T8m	-15.5	T15m	-110	T21m	-155.1					Zpre_Propane	0.244508
F4NG	479,500	F5p	810,200	F12p	792,800	F8m	638,400	F15m	337,100	F21m	136,000					Zpre_i-Butane	0.00225
P5NG	75.96	P6p	10.5	P20p	3.26	P9m	37.35	P16m	34.75	P22m	3.88					Zpre_n-Butane	000025
T5NG	-134	T6p	-18.5	T20p	-31.3	T9m	-55	T16m	-110	T22m	-161.3					Zmain_Nitrogen	0.160811
F5NG	479,500	F6p	810,200	F20p	792,800	F9m	638,400	F16m	201,100	F22m	136,000					Zmain_Methane	0.696517
P1p	10.2	P7p	10.2	P21p	10.2	P11m	37.25	P17m	32.45	P23m	3.78					Zmain_Ethane	0.138704
T1p	28.3	T7p	21	T21p	33.79	T11m	-55.06	T17m	-134	T23m	-142.6					Zmain_Propane	0.003955
F1p	1,603,000	F7p	810,200	F21p	792,800	F11m	301,300	F17m	201,100	F23m	136,000					Zmain_i-Butane	0.000007
P2p	33.66	P8p	32.86	P5m	3.48	P12m	34.75	P18m	3.78	P24m	3.78					Zmain_n-Butane	0.000005
T2p	125	T8p	24	T5m	-58	T12m	-110	T18m	-135.9	T24m	-136.7					Objective Function(work) [kW]	134,100
F2p	1,603,000	F8p	792,800	F5m	638,400	F12m	301,300	F18m	201,100	F24m	337,100						

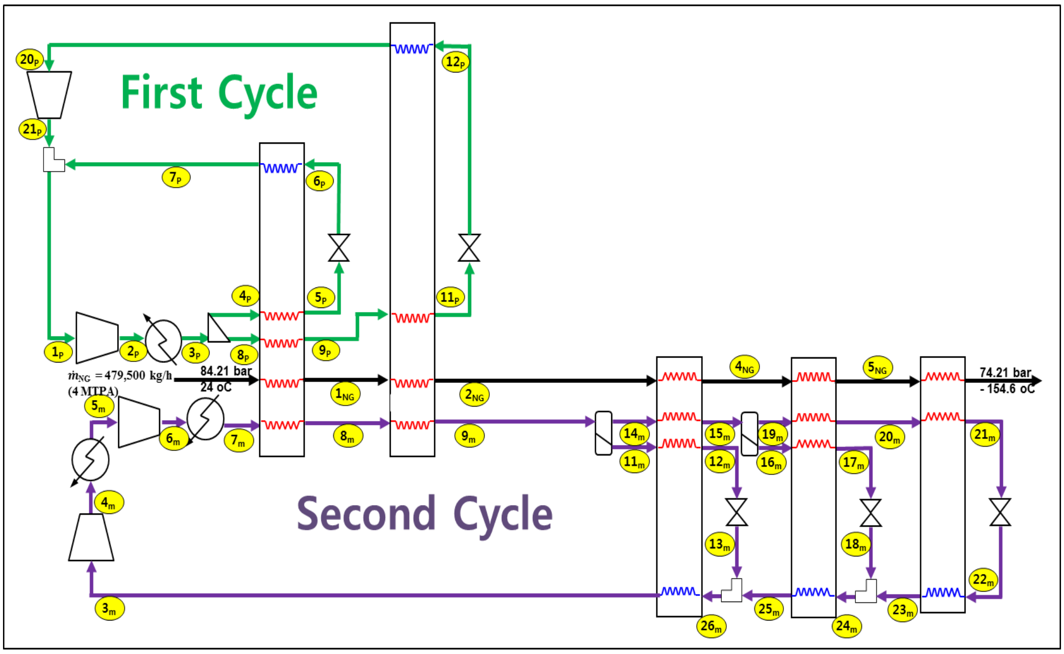

Figure 4-31 Configuration of the feasible liquefaction cycle - case 17

Table 4-18 Optimal operating conditions for the feasible liquefaction cycle - case 17

P1NG	82.71	P3p	32.86	P9p	27.36	P4m	15.75	P11m	37.25	P17m	32.45	P23m	3.78				
T1NG	-15.5	T3p	24	T9p	-15.5	T4m	42.46	T11m	-55.06	T17m	-134	T23m	-142.6				
F1NG	479,500	F3p	1,603,000	F9p	792,800	F4m	638,400	F11m	301,300	F17m	201,100	F23m	136,000				
P2NG	79.71	P4p	32.86	P11p	22.36	P5m	15.75	P12m	34.75	P18m	3.78	P24m	3.78				
T2NG	-55	T4p	24	T11p	-55	T5m	24	T12m	-110	T18m	-135.9	T24m	-136.7				
F2NG	479,500	F4p	810,200	F11p	792,800	F5m	638,400	F12m	301,300	F18m	201,100	F24m	337,100			Zpre_Methane	0.0075
P4NG	77.86	P5p	27.36	P12p	3.56	P6m	43.75	P13m	3.68	P19m	34.75	P25m	3.68			Zpre_Ethane	0.745493
T4NG	-110	T5p	-15.5	T12p	-57.57	T6m	104.3	T13m	-114	T19m	-110	T25m	-120			Zpre_Propane	0.244508
F4NG	479,500	F5p	810,200	F12p	792,800	F6m	638,400	F13m	301,300	F19m	136,000	F25m	337,100			Zpre_i-Butane	0.00225
P5NG	75.96	P6p	10.5	P20p	3.26	P7m	43.35	P14m	37.25	P20m	32.45	P26m	3.68			Zpre_n-Butane	000025
T5NG	-134	T6p	-18.5	T20p	-31.3	T7m	7.273	T14m	-55.06	T20m	-134	T26m	-116			Zmain_Nitrogen	0.160811
F5NG	479,500	F6p	810,200	F20p	792,800	F7m	638,400	F14m	337,100	F20m	136,000	F26m	638,400			Zmain_Methane	0.696517
P1p	10.2	P7p	10.2	P21p	10.2	P8m	41.35	P15m	34.75	P21m	30.95					Zmain_Ethane	0.138704
T1p	28.3	T7p	21	T21p	33.79	T8m	-15.5	T15m	-110	T21m	-155.1					Zmain_Propane	0.003955
F1p	1,603,000	F7p	810,200	F21p	792,800	F8m	638,400	F15m	337,100	F21m	136,000					Zmain_i-Butane	0.000007
P2p	33.66	P8p	32.86	P3m	3.48	P9m	37.35	P16m	34.75	P22m	3.88					Zmain_n-Butane	0.000005
T2p	125	T8p	24	T3m	-58	T9m	-55	T16m	-110	T22m	-161.3					Objective Function(work) [kW]	131,300
F2p	1,603,000	F8p	792,800	F3m	638,400	F9m	638,400	F16m	201,100	F22m	136,000						

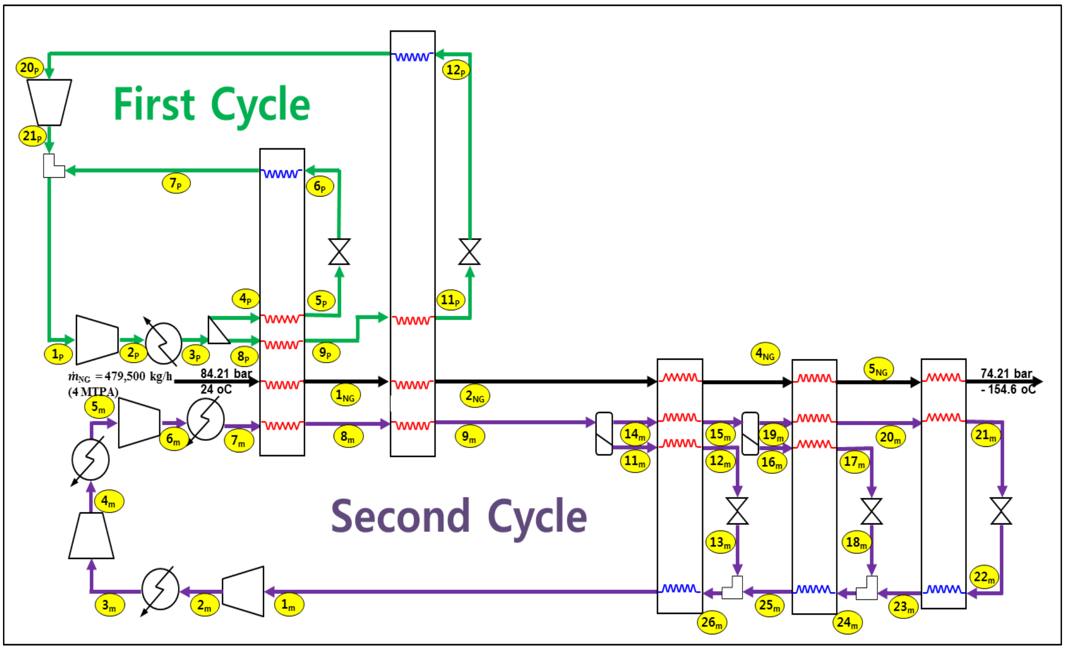

Figure 4-32 Configuration of the feasible liquefaction cycle - case 18

Table 4-19 Optimal operating conditions for the feasible liquefaction cycle - case 18

P1NG	82.71	P3p	32.86	P9p	27.36	P2m	10.02	P8m	41.35	P15m	34.75	P21m	30.95				
T1NG	-15.5	T3p	24	T9p	-15.5	T2m	26	T8m	-15.5	T15m	-110	T21m	-155.1				
F1NG	479,500	F3p	1,603,000	F9p	792,800	F2m	638,400	F8m	638,400	F15m	337,100	F21m	136,000				
P2NG	79.71	P4p	32.86	P11p	22.36	P3m	10.02	P9m	37.35	P16m	34.75	P22m	3.88				
T2NG	-55	T4p	24	T11p	-55	T3m	24	T9m	-55	T16m	-110	T22m	-161.3				
F2NG	479,500	F4p	810,200	F11p	792,800	F3m	638,400	F9m	638,400	F16m	201,100	F22m	136,000			Zpre_Methane	0.0075
P4NG	77.86	P5p	27.36	P12p	3.56	P4m	20.2	P11m	37.25	P17m	32.45	P23m	3.78			Zpre_Ethane	0.745493
T4NG	-110	T5p	-15.5	T12p	-57.57	T4m	78	T11m	-55.06	T17m	-134	T23m	-142.6			Zpre_Propane	0.244508
F4NG	479,500	F5p	810,200	F12p	792,800	F4m	638,400	F11m	301,300	F17m	201,100	F23m	136,000			Zpre_i-Butane	0.00225
P5NG	75.96	P6p	10.5	P20p	3.26	P5m	20.2	P12m	34.75	P18m	3.78	P24m	3.78			Zpre_n-Butane	000025
T5NG	-134	T6p	-18.5	T20p	-31.3	T5m	24	T12m	-110	T18m	-135.9	T24m	-136.7			Zmain_Nitrogen	0.160811
F5NG	479,500	F6p	810,200	F20p	792,800	F5m	638,400	F12m	301,300	F18m	201,100	F24m	337,100			Zmain_Methane	0.696517
P1p	10.2	P7p	10.2	P21p	10.2	P6m	43.75	P13m	3.68	P19m	34.75	P25m	3.68			Zmain_Ethane	0.138704
T1p	28.3	T7p	21	T21p	33.79	T6m	88	T13m	-114	T19m	-110	T25m	-120			Zmain_Propane	0.003955
F1p	1,603,000	F7p	810,200	F21p	792,800	F6m	638,400	F13m	301,300	F19m	136,000	F25m	337,100			Zmain_i-Butane	0.000007
P2p	33.66	P8p	32.86	P1m	3.48	P7m	43.35	P14m	37.25	P20m	32.45	P26m	3.68			Zmain_n-Butane	0.000005
T2p	125	T8p	24	T1m	-58	T7m	7.273	T14m	-55.06	T20m	-134	T26m	-116			Objective Function(work) [kW]	128,100
F2p	1,603,000	F8p	792,800	F1m	638,400	F7m	638,400	F14m	337,100	F20m	136,000	F26m	638,400				

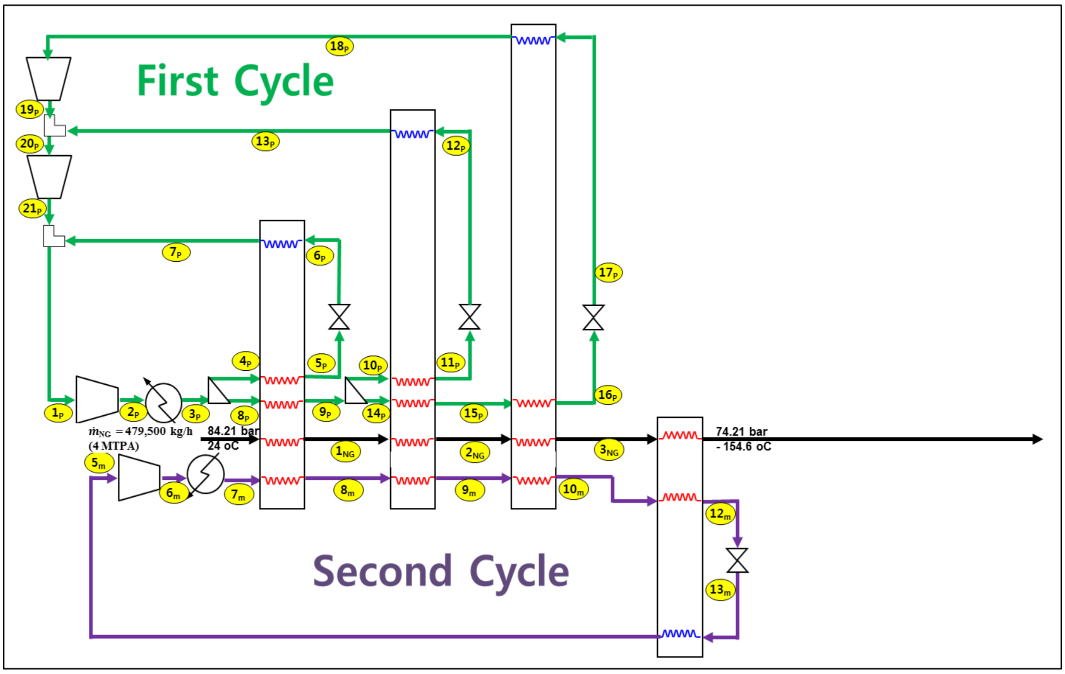

Figure 4-33 Configuration of the feasible liquefaction cycle - case 19

Table 4-20 Optimal operating conditions for the feasible liquefaction cycle - case 19

P1NG	82.71	P4p	32.86	P10p	29.36	P16p	22.36	P5m	3.48	P12m	30.95						
T1NG	-3.75	T4p	24	T10p	-3.75	T16p	-55	T5m	-58	T12m	-155.1						
F1NG	479,500	F4p	543,200	F10p	582,600	F16p	476,800	F5m	638,400	F12m	638,400						
P2NG	81.21	P5p	29.36	P11p	25.86	P17p	3.56	P6m	43.75	P13m	3.88						
T2NG	-28.3	T5p	-3.75	T11p	-28.3	T17p	-57.57	T6m	305	T13m	-161.3						
F2NG	479,500	F5p	543,200	F11p	582,600	F17p	476,800	F6m	638,400	F13m	638,400					Zpre_Methane	0.0075
P3NG	79.71	P6p	15.41	P12p	8.29	P18p	3.26	P7m	43.35							Zpre_Ethane	0.745493
T3NG	-55	T6p	-8.53	T12p	-31.73	T18p	-31.3	T7m	7.273							Zpre_Propane	0.244508
F3NG	479,500	F6p	543,200	F12p	582,600	F18p	476,800	F7m	638,400							Zpre_i-Butane	0.00225
P1p	14.96	P7p	14.96	P13p	7.99	P19p	7.99	P8m	41.35							Zpre_n-Butane	000025
T1p	33.79	T7p	20.78	T13p	-6.75	T19p	16.84	T8m	-3.75							Zmain_Nitrogen	0.160811
F1p	1,603,000	F7p	543,200	F13p	582,600	F19p	476,800	F8m	638,400							Zmain_Methane	0.696517
P2p	33.66	P8p	32.86	P14p	29.36	P20p	7.99	P9m	39.35							Zmain_Ethane	0.138704
T2p	85.3	T8p	24	T14p	-3.75	T20p	3.962	T9m	-28.3							Zmain_Propane	0.003955
F2p	1,603,000	F8p	1,059,000	F14p	476,800	F20p	1,059,400	F9m	638,400							Zmain_i-Butane	0.000007
P3p	32.86	P9p	29.36	P15p	25.86	P21p	14.96	P10m	37.35							Zmain_n-Butane	0.000005
T3p	24	T9p	-3.75	T15p	-28.3	T21p	33.79	T10m	-55							Objective Function(work) [kW]	145,300
F3p	1,603,000	F9p	1,059,000	F15p	476,800	F21p	1,059,400	F10m	638,400								

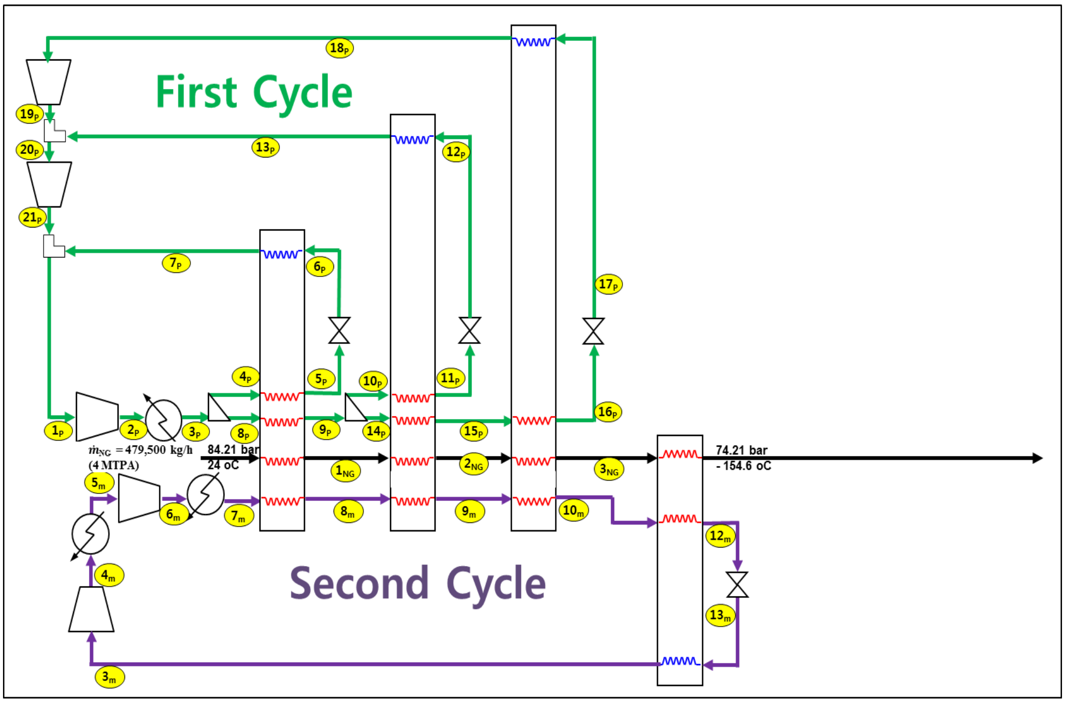

Figure 4-34 Configuration of the feasible liquefaction cycle - case 20

Table 4-21 Optimal operating conditions for the feasible liquefaction cycle - case 20

P1NG	82.71	P4p	32.86	P10p	29.36	P16p	22.36	P3m	3.48	P9m	39.35						
T1NG	-3.75	T4p	24	T10p	-3.75	T16p	-55	T3m	-58	T9m	-28.3						
F1NG	479,500	F4p	543,200	F10p	582,600	F16p	476,800	F3m	638,400	F9m	638,400						
P2NG	81.21	P5p	29.36	P11p	25.86	P17p	3.56	P4m	15.75	P10m	37.35						
T2NG	-28.3	T5p	-3.75	T11p	-28.3	T17p	-57.57	T4m	42.46	T10m	-55						
F2NG	479,500	F5p	543,200	F11p	582,600	F17p	476,800	F4m	638,400	F10m	638,400					Zpre_Methane	0.0075
P3NG	79.71	P6p	15.41	P12p	8.29	P18p	3.26	P5m	15.75	P12m	30.95					Zpre_Ethane	0.745493
T3NG	-55	T6p	-8.53	T12p	-31.73	T18p	-31.3	T5m	24	T12m	-155.1					Zpre_Propane	0.244508
F3NG	479,500	F6p	543,200	F12p	582,600	F18p	476,800	F5m	638,400	F12m	638,400					Zpre_i-Butane	0.00225
P1p	14.96	P7p	14.96	P13p	7.99	P19p	7.99	P6m	43.75	P13m	3.88					Zpre_n-Butane	000025
T1p	33.79	T7p	20.78	T13p	-6.75	T19p	16.84	T6m	104.3	T13m	-161.3					Zmain_Nitrogen	0.160811
F1p	1,603,000	F7p	543,200	F13p	582,600	F19p	476,800	F6m	638,400	F13m	638,400					Zmain_Methane	0.696517
P2p	33.66	P8p	32.86	P14p	29.36	P20p	7.99	P7m	43.35							Zmain_Ethane	0.138704
T2p	85.3	T8p	24	T14p	-3.75	T20p	3.962	T7m	7.273							Zmain_Propane	0.003955
F2p	1,603,000	F8p	1,059,000	F14p	476,800	F20p	1,059,400	F7m	638,400							Zmain_i-Butane	0.000007
P3p	32.86	P9p	29.36	P15p	25.86	P21p	14.96	P8m	41.35							Zmain_n-Butane	0.000005
T3p	24	T9p	-3.75	T15p	-28.3	T21p	33.79	T8m	-3.75							Objective Function(work) [kW]	141,100
F3p	1,603,000	F9p	1,059,000	F15p	476,800	F21p	1,059,400	F8m	638,400								

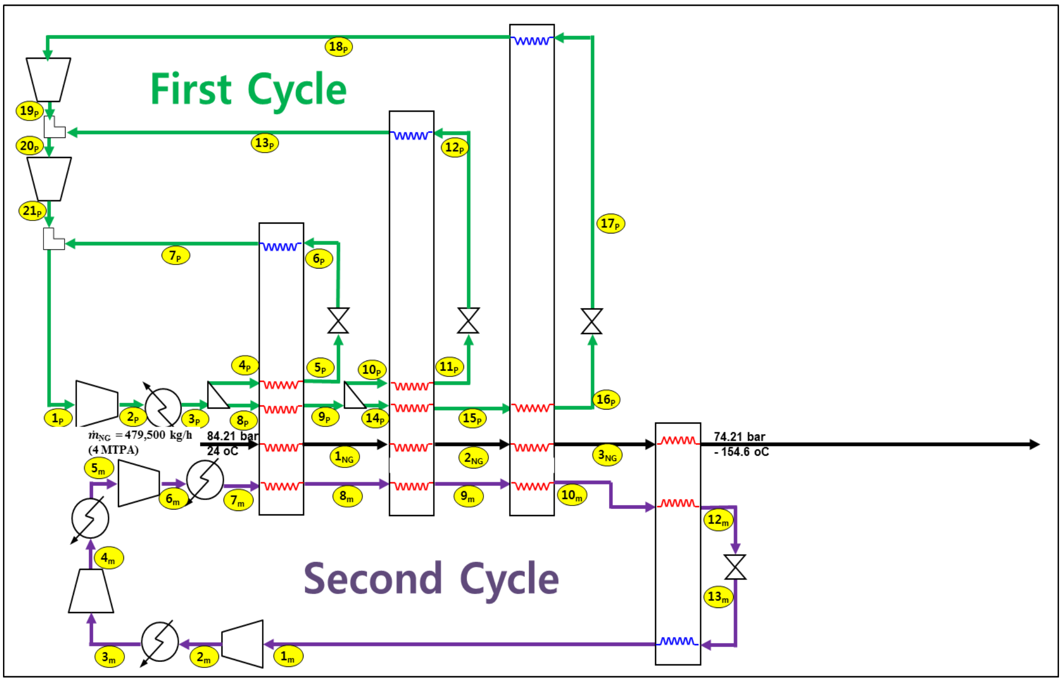

Figure 4-35 Configuration of the feasible liquefaction cycle - case 21

Table 4-22 Optimal operating conditions for the feasible liquefaction cycle - case 21

P1NG	82.71	P4p	32.86	P10p	29.36	P16p	22.36	P1m	3.48	P7m	43.35						
T1NG	-3.75	T4p	24	T10p	-3.75	T16p	-55	T1m	-58	T7m	7.273						
F1NG	479,500	F4p	543,200	F10p	582,600	F16p	476,800	F1m	638,400	F7m	638,400						
P2NG	81.21	P5p	29.36	P11p	25.86	P17p	3.56	P2m	10.02	P8m	41.35						
T2NG	-28.3	T5p	-3.75	T11p	-28.3	T17p	-57.57	T2m	26	T8m	-3.75						
F2NG	479,500	F5p	543,200	F11p	582,600	F17p	476,800	F2m	638,400	F8m	638,400					Zpre_Methane	0.0075
P3NG	79.71	P6p	15.41	P12p	8.29	P18p	3.26	P3m	10.02	P9m	39.35					Zpre_Ethane	0.745493
T3NG	-55	T6p	-8.53	T12p	-31.73	T18p	-31.3	T3m	24	T9m	-28.3					Zpre_Propane	0.244508
F3NG	479,500	F6p	543,200	F12p	582,600	F18p	476,800	F3m	638,400	F9m	638,400					Zpre_i-Butane	0.00225
P1p	14.96	P7p	14.96	P13p	7.99	P19p	7.99	P4m	20.2	P10m	37.35					Zpre_n-Butane	000025
T1p	33.79	T7p	20.78	T13p	-6.75	T19p	16.84	T4m	78	T10m	-55					Zmain_Nitrogen	0.160811
F1p	1,603,000	F7p	543,200	F13p	582,600	F19p	476,800	F4m	638,400	F10m	638,400					Zmain_Methane	0.696517
P2p	33.66	P8p	32.86	P14p	29.36	P20p	7.99	P5m	20.2	P12m	30.95					Zmain_Ethane	0.138704
T2p	85.3	T8p	24	T14p	-3.75	T20p	3.962	T5m	24	T12m	-155.1					Zmain_Propane	0.003955
F2p	1,603,000	F8p	1,059,000	F14p	476,800	F20p	1,059,400	F5m	638,400	F12m	638,400					Zmain_i-Butane	0.000007
P3p	32.86	P9p	29.36	P15p	25.86	P21p	14.96	P6m	43.75	P13m	3.88					Zmain_n-Butane	0.000005
T3p	24	T9p	-3.75	T15p	-28.3	T21p	33.79	T6m	88	T13m	-161.3					Objective Function(work) [kW]	137,200
F3p	1,603,000	F9p	1,059,000	F15p	476,800	F21p	1,059,400	F6m	638,400	F13m	638,400						

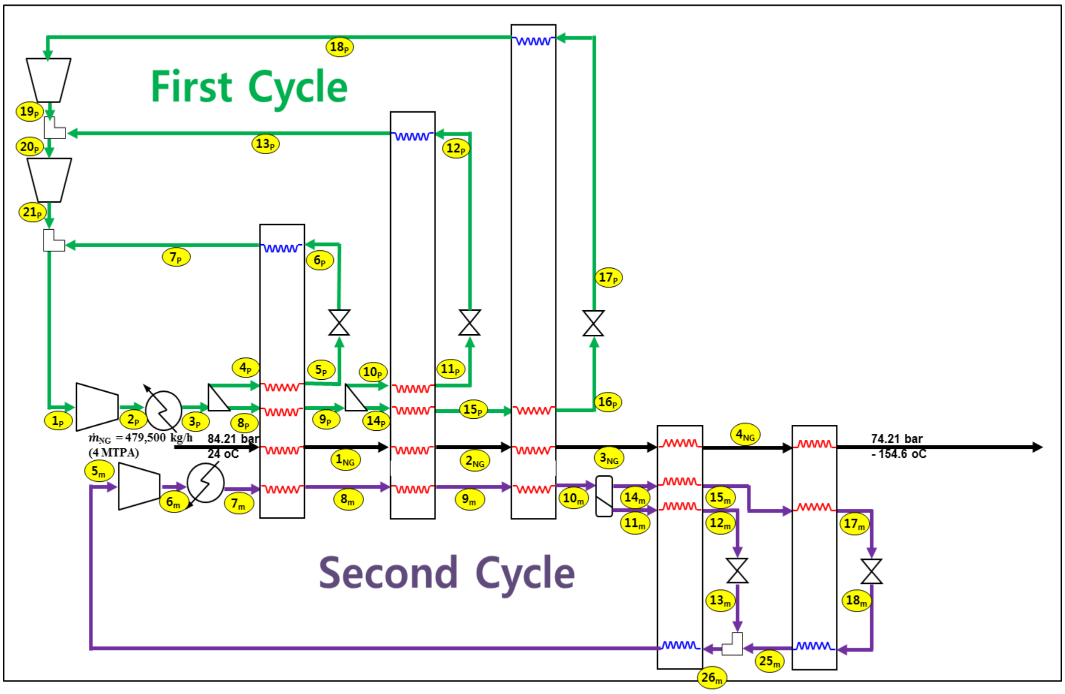

Figure 4-36 Configuration of the feasible liquefaction cycle - case 22

Table 4-23 Optimal operating conditions for the feasible liquefaction cycle - case 22

P1NG	82.71	P3p	32.86	P9p	29.36	P15p	25.86	P21p	14.96	P10m	37.35	P17m	30.95				
T1NG	-3.75	T3p	24	T9p	-3.75	T15p	-28.3	T21p	33.79	T10m	-55	T17m	-155.1				
F1NG	479,500	F3p	1,603,000	F9p	1,059,000	F15p	476,800	F21p	1,059,400	F10m	638,400	F17m	204,100				
P2NG	81.21	P4p	32.86	P10p	29.36	P16p	22.36	P5m	3.48	P11m	37.25	P18m	3.88				
T2NG	-28.3	T4p	24	T10p	-3.75	T16p	-55	T5m	-58	T11m	-55.06	T18m	-161.3				
F2NG	479,500	F4p	543,200	F10p	582,600	F16p	476,800	F5m	638,400	F11m	434,300	F18m	204,100			Zpre_Methane	0.0075
P3NG	79.71	P5p	29.36	P11p	25.86	P17p	3.56	P6m	43.75	P12m	32.45	P25m	3.78			Zpre_Ethane	0.745493
T3NG	-55	T5p	-3.75	T11p	-28.3	T17p	-57.57	T6m	305	T12m	-134	T25m	-142.6			Zpre_Propane	0.244508
F3NG	479,500	F5p	543,200	F11p	582,600	F17p	476,800	F6m	638,400	F12m	434,300	F25m	204,100			Zpre_i-Butane	0.00225
P4NG	76.96	P6p	15.41	P12p	8.29	P18p	3.26	P7m	43.35	P13m	3.78	P26m	3.78			Zpre_n-Butane	000025
T4NG	-134	T6p	-8.53	T12p	-31.73	T18p	-31.3	T7m	7.273	T13m	-135.9	T26m	-136.7			Zmain_Nitrogen	0.160811
F4NG	479,500	F6p	543,200	F12p	582,600	F18p	476,800	F7m	638,400	F13m	434,300	F26m	638,400			Zmain_Methane	0.696517
P1p	14.96	P7p	14.96	P13p	7.99	P19p	7.99	P8m	41.35	P14m	37.25					Zmain_Ethane	0.138704
T1p	33.79	T7p	20.78	T13p	-6.75	T19p	16.84	T8m	-3.75	T14m	-55.06					Zmain_Propane	0.003955
F1p	1,603,000	F7p	543,200	F13p	582,600	F19p	476,800	F8m	638,400	F14m	204,100					Zmain_i-Butane	0.000007
P2p	33.66	P8p	32.86	P14p	29.36	P20p	7.99	P9m	39.35	P15m	34.1					Zmain_n-Butane	0.000005
T2p	85.3	T8p	24	T14p	-3.75	T20p	3.962	T9m	-28.3	T15m	-134					Objective Function(work) [kW]	132,900
F2p	1,603,000	F8p	1,059,000	F14p	476,800	F20p	1,059,400	F9m	638,400	F15m	204,100						

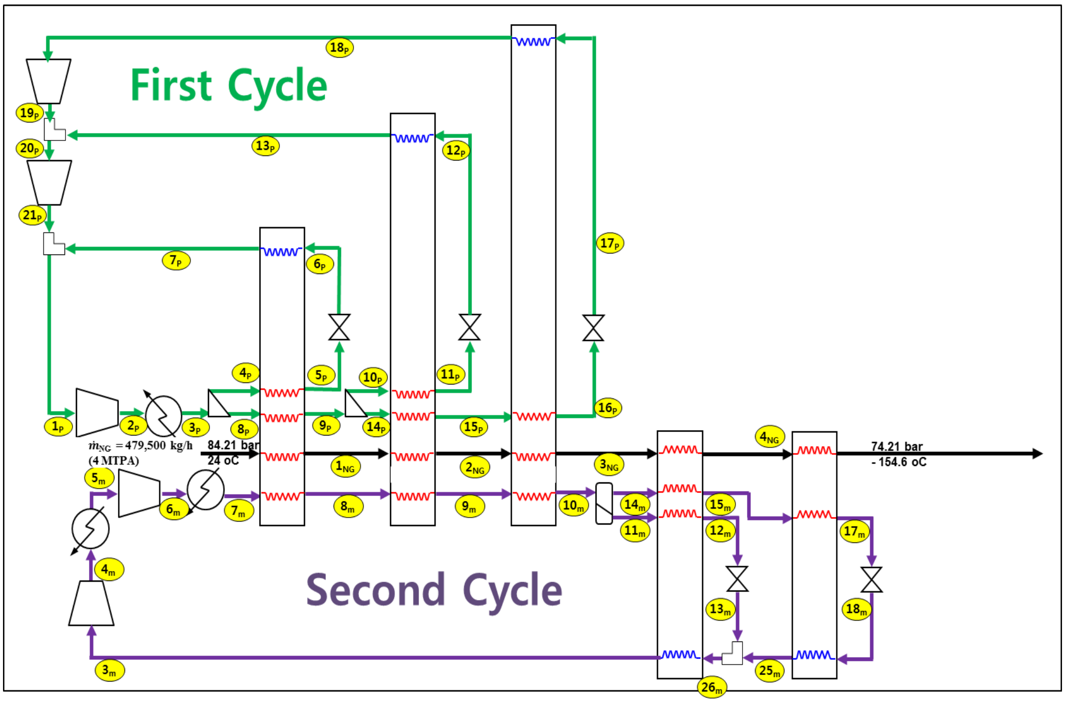

Figure 4-37 Configuration of the feasible liquefaction cycle - case 23

Table 4-24 Optimal operating conditions for the feasible liquefaction cycle - case 23

P1NG	82.71	P3p	32.86	P9p	29.36	P15p	25.86	P21p	14.96	P8m	41.35	P14m	37.25				
T1NG	-3.75	T3p	24	T9p	-3.75	T15p	-28.3	T21p	33.79	T8m	-3.75	T14m	-55.06				
F1NG	479,500	F3p	1,603,000	F9p	1,059,000	F15p	476,800	F21p	1,059,400	F8m	638,400	F14m	204,100				
P2NG	81.21	P4p	32.86	P10p	29.36	P16p	22.36	P3m	3.48	P9m	39.35	P15m	34.1				
T2NG	-28.3	T4p	24	T10p	-3.75	T16p	-55	T3m	-58	T9m	-28.3	T15m	-134				
F2NG	479,500	F4p	543,200	F10p	582,600	F16p	476,800	F3m	638,400	F9m	638,400	F15m	204,100			Zpre_Methane	0.0075
P3NG	79.71	P5p	29.36	P11p	25.86	P17p	3.56	P4m	15.75	P10m	37.35	P17m	30.95			Zpre_Ethane	0.745493
T3NG	-55	T5p	-3.75	T11p	-28.3	T17p	-57.57	T4m	42.46	T10m	-55	T17m	-155.1			Zpre_Propane	0.244508
F3NG	479,500	F5p	543,200	F11p	582,600	F17p	476,800	F4m	638,400	F10m	638,400	F17m	204,100			Zpre_i-Butane	0.00225
P4NG	76.96	P6p	15.41	P12p	8.29	P18p	3.26	P5m	15.75	P11m	37.25	P18m	3.88			Zpre_n-Butane	000025
T4NG	-134	T6p	-8.53	T12p	-31.73	T18p	-31.3	T5m	24	T11m	-55.06	T18m	-161.3			Zmain_Nitrogen	0.160811
F4NG	479,500	F6p	543,200	F12p	582,600	F18p	476,800	F5m	638,400	F11m	434,300	F18m	204,100			Zmain_Methane	0.696517
P1p	14.96	P7p	14.96	P13p	7.99	P19p	7.99	P6m	43.75	P12m	32.45	P25m	3.78			Zmain_Ethane	0.138704
T1p	33.79	T7p	20.78	T13p	-6.75	T19p	16.84	T6m	104.3	T12m	-134	T25m	-142.6			Zmain_Propane	0.003955
F1p	1,603,000	F7p	543,200	F13p	582,600	F19p	476,800	F6m	638,400	F12m	434,300	F25m	204,100			Zmain_i-Butane	0.000007
P2p	33.66	P8p	32.86	P14p	29.36	P20p	7.99	P7m	43.35	P13m	3.78	P26m	3.78			Zmain_n-Butane	0.000005
T2p	85.3	T8p	24	T14p	-3.75	T20p	3.962	T7m	7.273	T13m	-135.9	T26m	-136.7			Objective Function(work) [kW]	126,700
F2p	1,603,000	F8p	1,059,000	F14p	476,800	F20p	1,059,400	F7m	638,400	F13m	434,300	F26m	638,400				

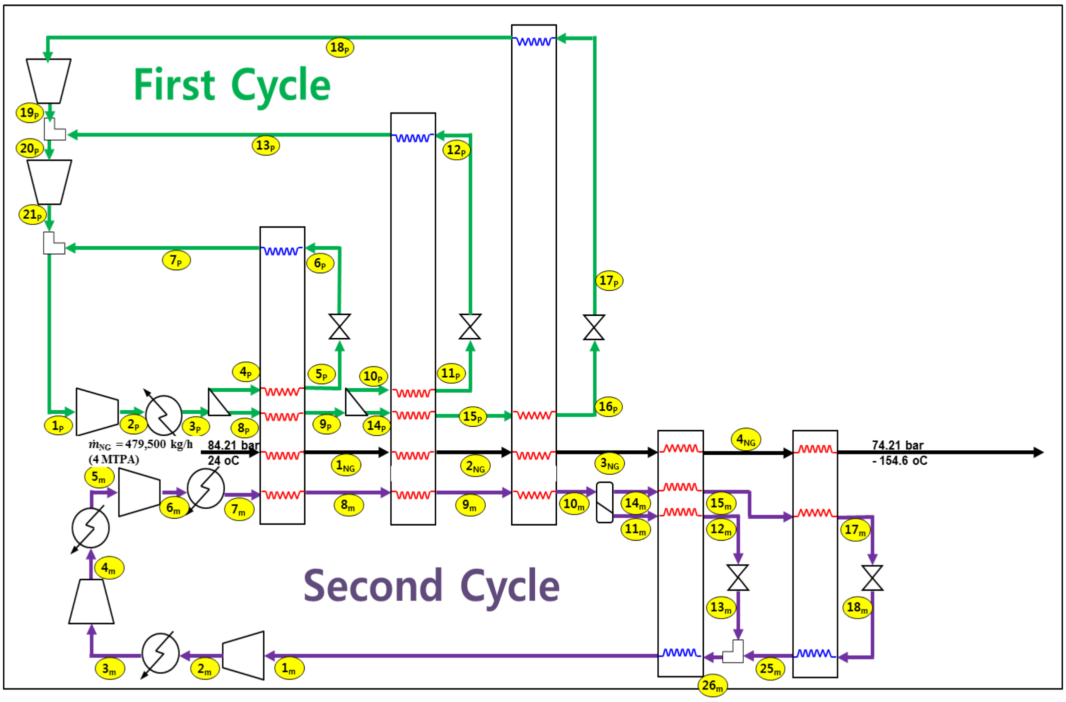

Figure 4-38 Configuration of the feasible liquefaction cycle - case 24

Table 4-25 Optimal operating conditions for the feasible liquefaction cycle - case 24

P1NG	82.71	P3p	32.86	P9p	29.36	P15p	25.86	P21p	14.96	P6m	43.75	P12m	32.45	P25m	3.78		
T1NG	-3.75	T3p	24	T9p	-3.75	T15p	-28.3	T21p	33.79	T6m	88	T12m	-134	T25m	-142.6		
F1NG	479,500	F3p	1,603,000	F9p	1,059,000	F15p	476,800	F21p	1,059,400	F6m	638,400	F12m	434,300	F25m	204,100		
P2NG	81.21	P4p	32.86	P10p	29.36	P16p	22.36	P1m	3.48	P7m	43.35	P13m	3.78	P26m	3.78		
T2NG	-28.3	T4p	24	T10p	-3.75	T16p	-55	T1m	-58	T7m	7.273	T13m	-135.9	T26m	-136.7		
F2NG	479,500	F4p	543,200	F10p	582,600	F16p	476,800	F1m	638,400	F7m	638,400	F13m	434,300	F26m	638,400	Zpre_Methane	0.0075
P3NG	79.71	P5p	29.36	P11p	25.86	P17p	3.56	P2m	10.02	P8m	41.35	P14m	37.25			Zpre_Ethane	0.745493
T3NG	-55	T5p	-3.75	T11p	-28.3	T17p	-57.57	T2m	26	T8m	-3.75	T14m	-55.06			Zpre_Propane	0.244508
F3NG	479,500	F5p	543,200	F11p	582,600	F17p	476,800	F2m	638,400	F8m	638,400	F14m	204,100			Zpre_i-Butane	0.00225
P4NG	76.96	P6p	15.41	P12p	8.29	P18p	3.26	P3m	10.02	P9m	39.35	P15m	34.1			Zpre_n-Butane	000025
T4NG	-134	T6p	-8.53	T12p	-31.73	T18p	-31.3	T3m	24	T9m	-28.3	T15m	-134			Zmain_Nitrogen	0.160811
F4NG	479,500	F6p	543,200	F12p	582,600	F18p	476,800	F3m	638,400	F9m	638,400	F15m	204,100			Zmain_Methane	0.696517
P1p	14.96	P7p	14.96	P13p	7.99	P19p	7.99	P4m	20.2	P10m	37.35	P17m	30.95			Zmain_Ethane	0.138704
T1p	33.79	T7p	20.78	T13p	-6.75	T19p	16.84	T4m	78	T10m	-55	T17m	-155.1			Zmain_Propane	0.003955
F1p	1,603,000	F7p	543,200	F13p	582,600	F19p	476,800	F4m	638,400	F10m	638,400	F17m	204,100			Zmain_i-Butane	0.000007
P2p	33.66	P8p	32.86	P14p	29.36	P20p	7.99	P5m	20.2	P11m	37.25	P18m	3.88			Zmain_n-Butane	0.000005
T2p	85.3	T8p	24	T14p	-3.75	T20p	3.962	T5m	24	T11m	-55.06	T18m	-161.3			Objective Function(work) [kW]	123,200
F2p	1,603,000	F8p	1,059,000	F14p	476,800	F20p	1,059,400	F5m	638,400	F11m	434,300	F18m	204,100				

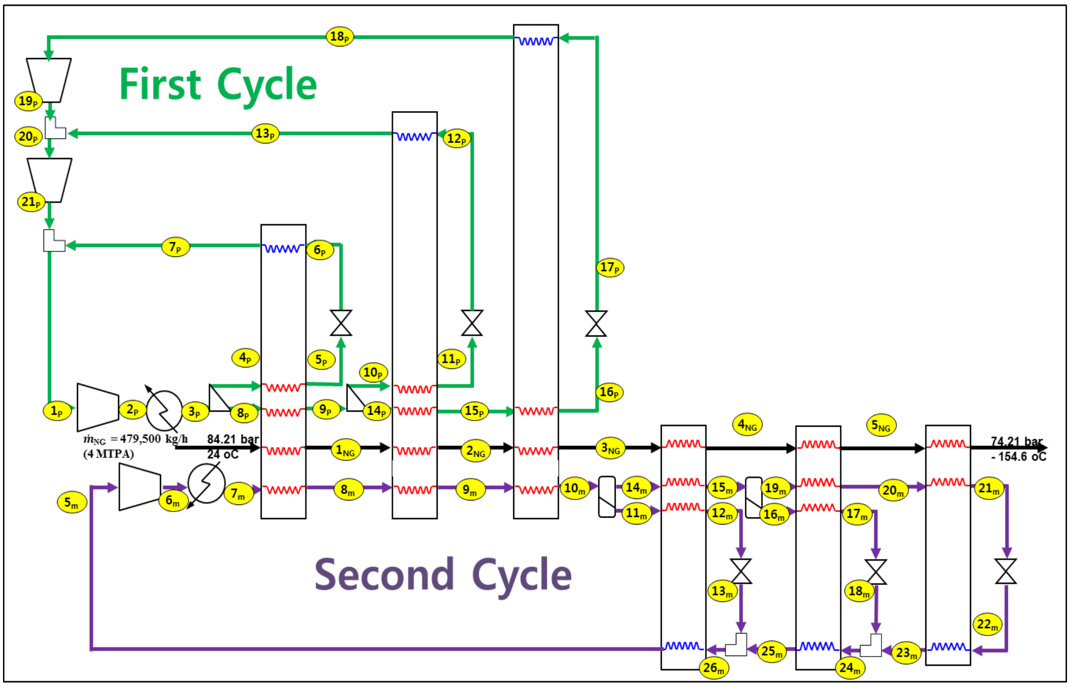

Figure 4-39 Configuration of the feasible liquefaction cycle - case 25

Table 4-26 Optimal operating conditions for the feasible liquefaction cycle - case 25

P1NG	82.71	P2p	33.66	P8p	32.86	P14p	29.36	P20p	7.99	P9m	39.35	P15m	34.75	P21m	30.95		
T1NG	-3.75	T2p	85.3	T8p	24	T14p	-3.75	T20p	3.962	T9m	-28.3	T15m	-110	T21m	-155.1		
F1NG	479,500	F2p	1,603,000	F8p	1,059,000	F14p	476,800	F20p	1,059,400	F9m	638,400	F15m	337,100	F21m	136,000		
P2NG	81.21	P3p	32.86	P9p	29.36	P15p	25.86	P21p	14.96	P10m	37.35	P16m	34.75	P22m	3.88		
T2NG	-28.3	T3p	24	T9p	-3.75	T15p	-28.3	T21p	33.79	T10m	-55	T16m	-110	T22m	-161.3		
F2NG	479,500	F3p	1,603,000	F9p	1,059,000	F15p	476,800	F21p	1,059,400	F10m	638,400	F16m	201,100	F22m	136,000	Zpre_Methane	0.0075
P3NG	79.71	P4p	32.86	P10p	29.36	P16p	22.36	P5m	3.48	P11m	37.25	P17m	32.45	P23m	3.78	Zpre_Ethane	0.745493
T3NG	-55	T4p	24	T10p	-3.75	T16p	-55	T5m	-58	T11m	-55.06	T17m	-134	T23m	-142.6	Zpre_Propane	0.244508
F3NG	479,500	F4p	543,200	F10p	582,600	F16p	476,800	F5m	638,400	F11m	301,300	F17m	201,100	F23m	136,000	Zpre_i-Butane	0.00225
P4NG	77.86	P5p	29.36	P11p	25.86	P17p	3.56	P6m	43.75	P12m	34.75	P18m	3.78	P24m	3.78	Zpre_n-Butane	000025
T4NG	-110	T5p	-3.75	T11p	-28.3	T17p	-57.57	T6m	305	T12m	-110	T18m	-135.9	T24m	-136.7	Zmain_Nitrogen	0.160811
F4NG	479,500	F5p	543,200	F11p	582,600	F17p	476,800	F6m	638,400	F12m	301,300	F18m	201,100	F24m	337,100	Zmain_Methane	0.696517
P5NG	75.96	P6p	15.41	P12p	8.29	P18p	3.26	P7m	43.35	P13m	3.68	P19m	34.75	P25m	3.68	Zmain_Ethane	0.138704
T5NG	-134	T6p	-8.53	T12p	-31.73	T18p	-31.3	T7m	7.273	T13m	-114	T19m	-110	T25m	-120	Zmain_Propane	0.003955
F5NG	479,500	F6p	543,200	F12p	582,600	F18p	476,800	F7m	638,400	F13m	301,300	F19m	136,000	F25m	337,100	Zmain_i-Butane	0.000007
P1p	14.96	P7p	14.96	P13p	7.99	P19p	7.99	P8m	41.35	P14m	37.25	P20m	32.45	P26m	3.68	Zmain_n-Butane	0.000005
T1p	33.79	T7p	20.78	T13p	-6.75	T19p	16.84	T8m	-3.75	T14m	-55.06	T20m	-134	T26m	-116	Objective Function(work) [kW]	119,800
F1p	1,603,000	F7p	543,200	F13p	582,600	F19p	476,800	F8m	638,400	F14m	337,100	F20m	136,000	F26m	638,400		

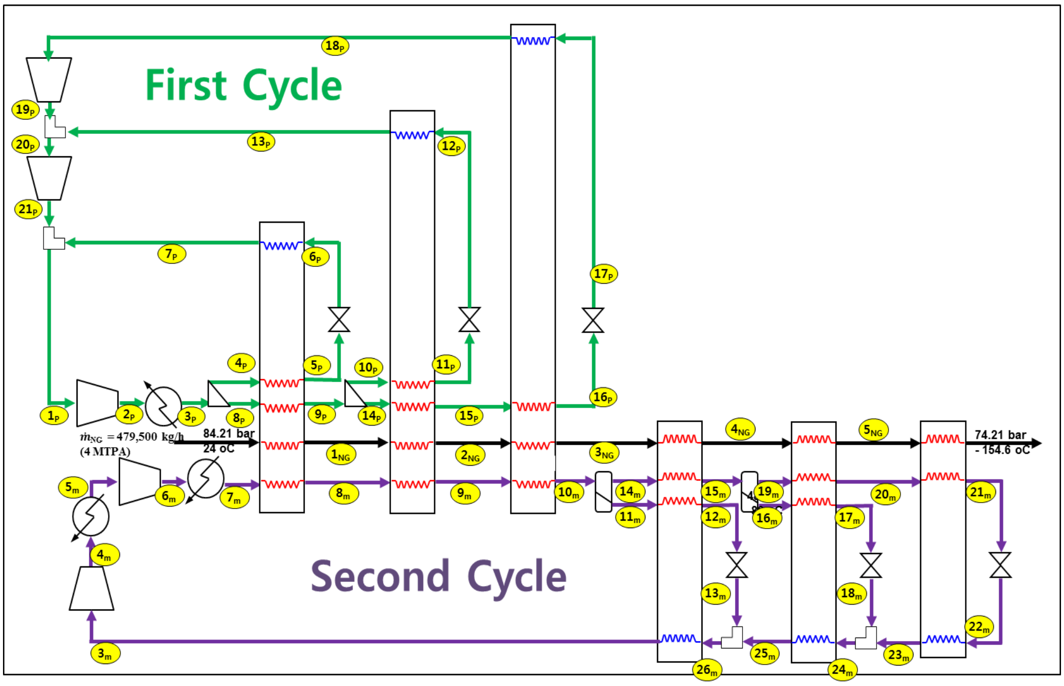

Figure 4-40 Configuration of the feasible liquefaction cycle - case 26

Table 4-27 Optimal operating conditions for the feasible liquefaction cycle - case 26

P1NG	82.71	P2p	33.66	P8p	32.86	P14p	29.36	P20p	7.99	P7m	43.35	P13m	3.68	P19m	34.75	P25m	3.68		
T1NG	-3.75	T2p	85.3	T8p	24	T14p	-3.75	T20p	3.962	T7m	7.273	T13m	-114	T19m	-110	T25m	-120		
F1NG	479,500	F2p	1,603,000	F8p	1,059,000	F14p	476,800	F20p	1,059,400	F7m	638,400	F13m	301,300	F19m	136,000	F25m	337,100		
P2NG	81.21	P3p	32.86	P9p	29.36	P15p	25.86	P21p	14.96	P8m	41.35	P14m	37.25	P20m	32.45	P26m	3.68		
T2NG	-28.3	T3p	24	T9p	-3.75	T15p	-28.3	T21p	33.79	T8m	-3.75	T14m	-55.06	T20m	-134	T26m	-116		
F2NG	479,500	F3p	1,603,000	F9p	1,059,000	F15p	476,800	F21p	1,059,400	F8m	638,400	F14m	337,100	F20m	136,000	F26m	638,400	Zpre_Methane	0.0075
P3NG	79.71	P4p	32.86	P10p	29.36	P16p	22.36	P3m	3.48	P9m	39.35	P15m	34.75	P21m	30.95			Zpre_Ethane	0.745493
T3NG	-55	T4p	24	T10p	-3.75	T16p	-55	T3m	-58	T9m	-28.3	T15m	-110	T21m	-155.1			Zpre_Propane	0.244508
F3NG	479,500	F4p	543,200	F10p	582,600	F16p	476,800	F3m	638,400	F9m	638,400	F15m	337,100	F21m	136,000			Zpre_i-Butane	0.00225
P4NG	77.86	P5p	29.36	P11p	25.86	P17p	3.56	P4m	15.75	P10m	37.35	P16m	34.75	P22m	3.88			Zpre_n-Butane	000025
T4NG	-110	T5p	-3.75	T11p	-28.3	T17p	-57.57	T4m	42.46	T10m	-55	T16m	-110	T22m	-161.3			Zmain_Nitrogen	0.160811
F4NG	479,500	F5p	543,200	F11p	582,600	F17p	476,800	F4m	638,400	F10m	638,400	F16m	201,100	F22m	136,000			Zmain_Methane	0.696517
P5NG	75.96	P6p	15.41	P12p	8.29	P18p	3.26	P5m	15.75	P11m	37.25	P17m	32.45	P23m	3.78			Zmain_Ethane	0.138704
T5NG	-134	T6p	-8.53	T12p	-31.73	T18p	-31.3	T5m	24	T11m	-55.06	T17m	-134	T23m	-142.6			Zmain_Propane	0.003955
F5NG	479,500	F6p	543,200	F12p	582,600	F18p	476,800	F5m	638,400	F11m	301,300	F17m	201,100	F23m	136,000			Zmain_i-Butane	0.000007
P1p	14.96	P7p	14.96	P13p	7.99	P19p	7.99	P6m	43.75	P12m	34.75	P18m	3.78	P24m	3.78			Zmain_n-Butane	0.000005
T1p	33.79	T7p	20.78	T13p	-6.75	T19p	16.84	T6m	104.3	T12m	-110	T18m	-135.9	T24m	-136.7			Objective Function(work) [kW]	114,211
F1p	1,603,000	F7p	543,200	F13p	582,600	F19p	476,800	F6m	638,400	F12m	301,300	F18m	201,100	F24m	337,100				

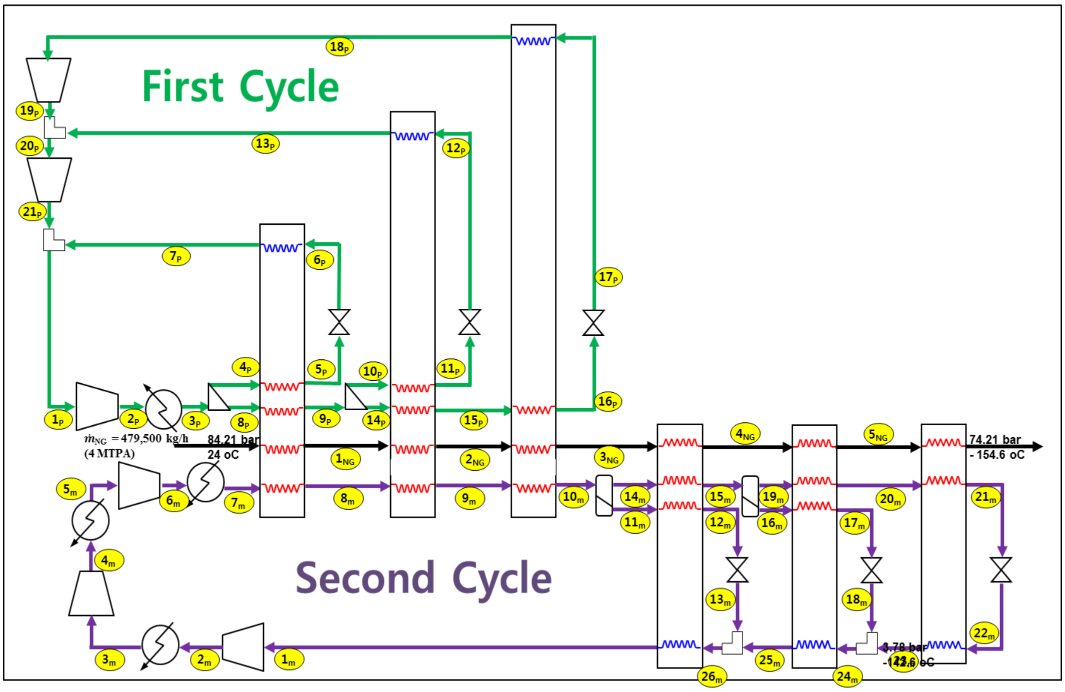

Figure 4-41 Configuration of the feasible liquefaction cycle - case 27

Table 4-28 Optimal operating conditions for the feasible liquefaction cycle - case 27

P1NG	82.71	P2p	33.66	P8p	32.86	P14p	29.36	P20p	7.99	P5m	20.2	P11m	37.25	P17m	32.45	P23m	3.78		
T1NG	-3.75	T2p	85.3	T8p	24	T14p	-3.75	T20p	3.962	T5m	24	T11m	-55.06	T17m	-134	T23m	-142.6		
F1NG	479,500	F2p	1,603,000	F8p	1,059,000	F14p	476,800	F20p	1,059,400	F5m	638,400	F11m	301,300	F17m	201,100	F23m	136,000		
P2NG	81.21	P3p	32.86	P9p	29.36	P15p	25.86	P21p	14.96	P6m	43.75	P12m	34.75	P18m	3.78	P24m	3.78		
T2NG	-28.3	T3p	24	T9p	-3.75	T15p	-28.3	T21p	33.79	T6m	88	T12m	-110	T18m	-135.9	T24m	-136.7		
F2NG	479,500	F3p	1,603,000	F9p	1,059,000	F15p	476,800	F21p	1,059,400	F6m	638,400	F12m	301,300	F18m	201,100	F24m	337,100	Zpre_Methane	0.0075
P3NG	79.71	P4p	32.86	P10p	29.36	P16p	22.36	P1m	3.48	P7m	43.35	P13m	3.68	P19m	34.75	P25m	3.68	Zpre_Ethane	0.745493
T3NG	-55	T4p	24	T10p	-3.75	T16p	-55	T1m	-58	T7m	7.273	T13m	-114	T19m	-110	T25m	-120	Zpre_Propane	0.244508
F3NG	479,500	F4p	543,200	F10p	582,600	F16p	476,800	F1m	638,400	F7m	638,400	F13m	301,300	F19m	136,000	F25m	337,100	Zpre_i-Butane	0.00225
P4NG	77.86	P5p	29.36	P11p	25.86	P17p	3.56	P2m	10.02	P8m	41.35	P14m	37.25	P20m	32.45	P26m	3.68	Zpre_n-Butane	000025
T4NG	-110	T5p	-3.75	T11p	-28.3	T17p	-57.57	T2m	26	T8m	-3.75	T14m	-55.06	T20m	-134	T26m	-116	Zmain_Nitrogen	0.160811
F4NG	479,500	F5p	543,200	F11p	582,600	F17p	476,800	F2m	638,400	F8m	638,400	F14m	337,100	F20m	136,000	F26m	638,400	Zmain_Methane	0.696517
P5NG	75.96	P6p	15.41	P12p	8.29	P18p	3.26	P3m	10.02	P9m	39.35	P15m	34.75	P21m	30.95			Zmain_Ethane	0.138704
T5NG	-134	T6p	-8.53	T12p	-31.73	T18p	-31.3	T3m	24	T9m	-28.3	T15m	-110	T21m	-155.1			Zmain_Propane	0.003955
F5NG	479,500	F6p	543,200	F12p	582,600	F18p	476,800	F3m	638,400	F9m	638,400	F15m	337,100	F21m	136,000			Zmain_i-Butane	0.000007
P1p	14.96	P7p	14.96	P13p	7.99	P19p	7.99	P4m	20.2	P10m	37.35	P16m	34.75	P22m	3.88			Zmain_n-Butane	0.000005
T1p	33.79	T7p	20.78	T13p	-6.75	T19p	16.84	T4m	78	T10m	-55	T16m	-110	T22m	-161.3			Objective Function(work) [kW]	111,056
F1p	1,603,000	F7p	543,200	F13p	582,600	F19p	476,800	F4m	638,400	F10m	638,400	F16m	201,100	F22m	136,000				

4.2.3. Top 10 feasible MR liquefaction process cycles considering efficiency

The ten most feasible MR liquefaction process cycles with the minimum required compressor power are selected for the potential MR liquefaction cycle in Table 4-29.

Table 4-29 Selection of the ten most feasible MR liquefaction process cycles

Cases	Required Power of Compressor for the Cycle per Production of LNG (kW)	Ranking
Case 14	133,100	10
Case 15	129,700	7
Case 17	131,300	8
Case 18	128,100	6
Case 22	132,900	9
Case 23	126,700	5
Case 24	123,200	4
Case 25	119,800	3
Case 26	114,211	2
Case 27	111,056	1

4.3. Selection of Potential MR Liquefaction Cycle considering simplicity

The offshore liquefaction technology developers are rightly focusing on process simplicity, low weight, and small footprint. Some technologies already deployed and proven for onshore peak-shaving application are attractive in this regard. Considering that all the process technologies deal with the thermodynamic constraints imposed by the natural-gas composition, the technologies that best fit the tried and tested machinery are those that are most likely to succeed commercially. The key criteria that influence process selection and plant optimization for offshore liquefaction unavoidably lead to some trade-offs and compromises between efficiency and simplicity.

Before presenting the equipment module layouts of liquefaction cycles in the next chapter (Chapter 5), the equipment counts of the ten most feasible liquefaction process cycles are considered based on their simplicity, for the selection of a potential MR liquefaction cycle. Optimal equipment module layout is performed in Chapter 5, however, to realize the simplicity of the potential offshore liquefaction cycles. Table 4-30 shows the preliminary trade-offs between efficiency and simplicity for the ten most feasible liquefaction process cycles, for the selection of a potential MR liquefaction cycle.

Table 4-30 Preliminary trade-offs between efficiency and simplicity for the ten most feasible liquefaction process cycles

Cases	**Compressor Power (kW)**	**Equipment Counts**	**Equipment Module Layout**
Criteria	Efficiency	Simplicity	
Case 27	111,056	29	Not considered in this chapter
Case 26	114,211	28	Not considered in this chapter

Case 25	119,800	27	Not considered in this chapter
Case 24	123,200	27	Not considered in this chapter
Case 23	126,700	26	Not considered in this chapter
Case 18	128,100	25	Not considered in this chapter
Case 15	129,700	23	Not considered in this chapter
Case 17	131,300	24	Not considered in this chapter
Case 22	132,900	25	Not considered in this chapter
Case 14	133,100	22	Not considered in this chapter

Based on the above preliminary trade-offs between efficiency and simplicity, case 14 is selected as the potential MR liquefaction cycle for offshore application, and is considered for one of the potential offshore liquefaction cycles.

4.4. Potential Offshore Liquefaction Cycles

The potential MR liquefaction cycle (case 14), which is one of the potential offshore liquefaction cycles, is selected for actual offshore application, considering its simplicity and efficiency.

This paper considers the following additional offshore liquefaction cycles as potential offshore liquefaction cycles: SHELL DMR for SHELL LNG FPSO, C_3MR for onshore projects, and the dual N_2 expander for FLEX LNG FPSO. They are considered for comparison with the potential MR liquefaction cycle (case 14) for selecting the optimal offshore liquefaction cycle. Figure 42-45 show the configurations of the potential offshore liquefaction cycles considered in this paper.

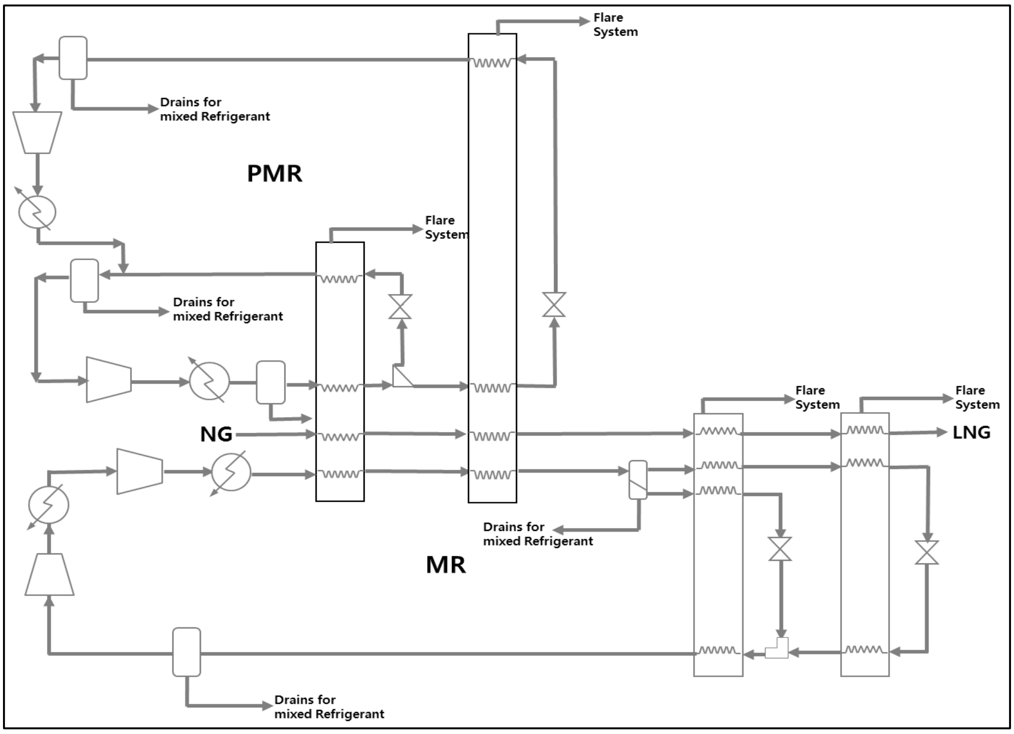

Figure 4-42 Configuration of the potential MR liquefaction cycle – case 14

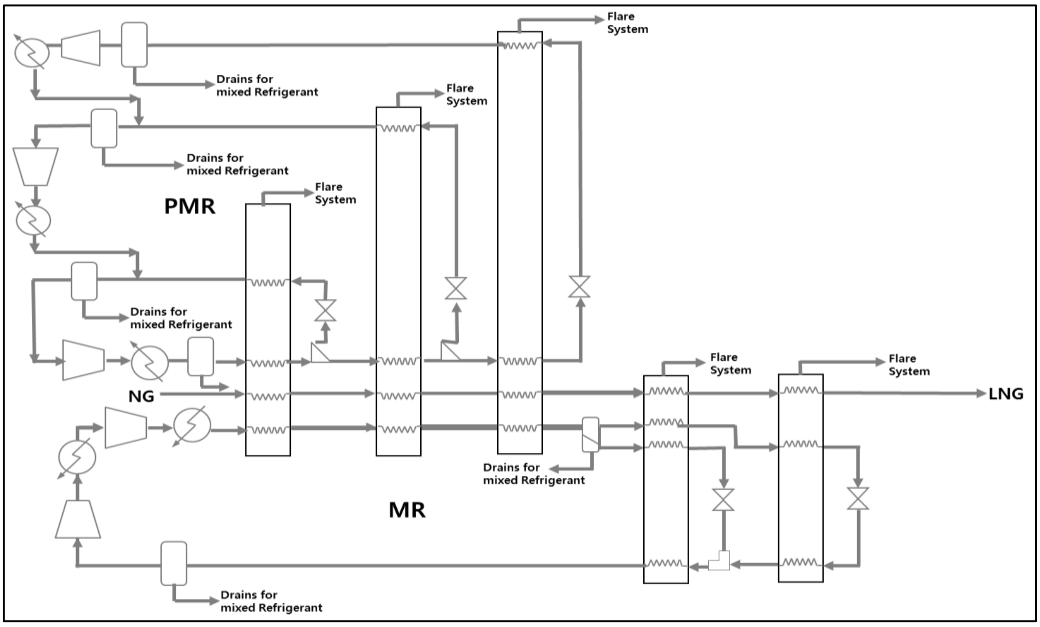

Figure 4-43 Configuration of the DMR cycle

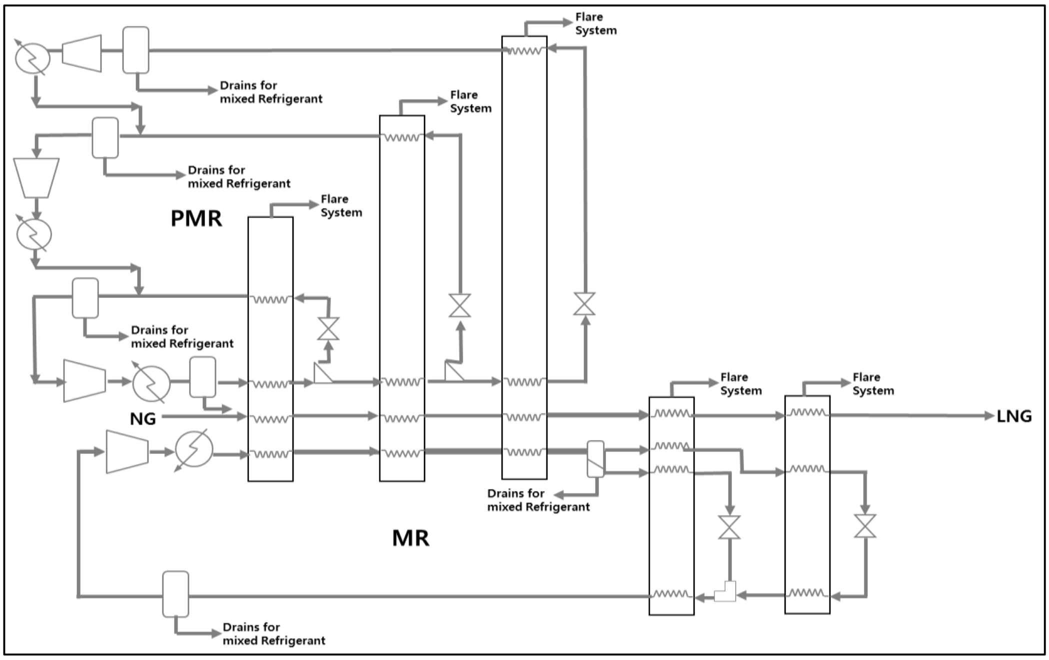

Figure 4-44 Configuration of the C_3MR cycle

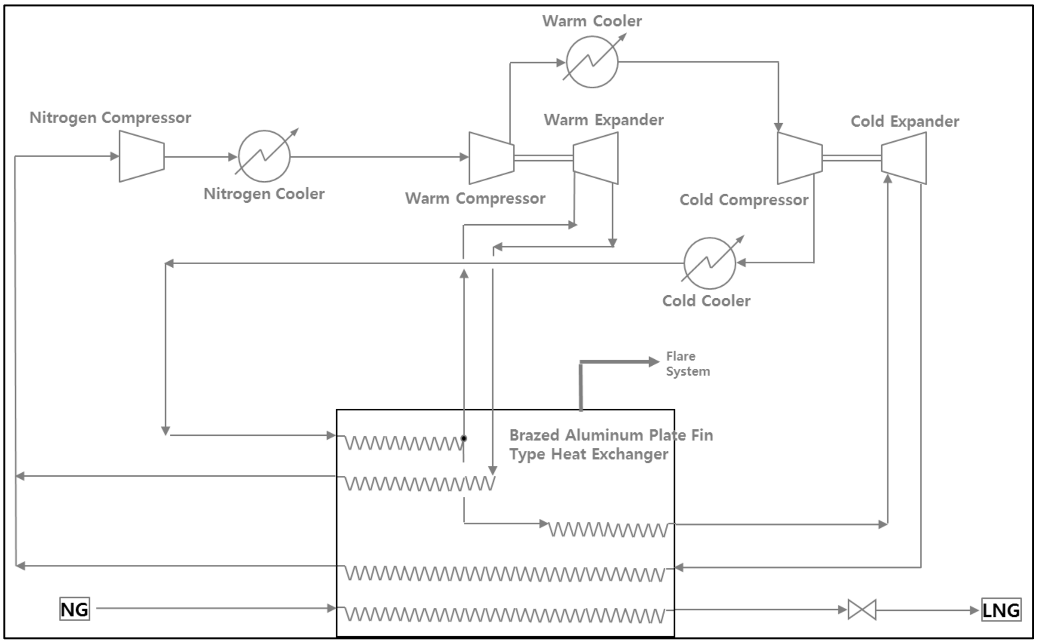

Figure 4-45 Configuration of the dual N2 expander cycle

4.5. Dermination of the Optimal Operating Conditions of the Potential Offshore Liquefaction Cycles Using HYSYS

To determine the optimal operating conditions of the potential offshore liquefaction cycles using HYSYS, the unknowns are given as follows: NG flow rate (479,500 kg/h = 4.0, 3.0, 2.0, and 1.0 MTPA); NG pressure (84.21 bar); temperature (24^{o}C); composition of the natural gas feed (nitrogen, 0.00279; methane, 0.7873; ethane, 0.05179; propane, 0.01803; n-butane, 0.00558; i-butane, 0.00329; i-pentane, 0.00199; n-pentane, 0.00199); temperature of the LNG (-160.15^{o}C); pressure of the LNG (74.21 bar) before pressure let-down in the LNG expander; compressor efficiency (80%); and temperature of the refrigerant leaving the seawater cooler (35^{o}C).

All the operating conditions, such as the pressure, temperature, volume, flow rate, and compositions of the refrigerant at the inlet and outlet of each piece of equipment in the potential offshore liquefaction cycles, are calculated to minimize the power required by the compressors.

To compare the required compressor power for the potential offshore liquefaction cycles proposed in this study, the required power of the compressor (W) for the cycle per unit production of LNG (kg/s) was calculated, and the values are compared in Table 4-31 to 4-34.

Table 4-31 Comparison of the required power of the compressors for the potential offshore liquefaction cycles (4.0 MTPA)

Cases	Required Power of Compressor for the Cycle per Production of LNG (kW)	Ranking
Case 14	133,100	3

DMR	126,700	1
C3 MR	132,900	2
Daul N2 Expander	225,210	4

Table 4-32 Comparison of the required power of the compressors for the potential offshore liquefaction cycles (3.0 MTPA)

Cases	Required Power of Compressor for the Cycle per Production of LNG (kW)	Ranking
Case 14	94,501	3
DMR	88,690	1
C3 MR	90,372	2
Daul N2 Expander	137,378	4

Table 4-33 Comparison of the required power of the compressors for the potential offshore liquefaction cycles (2.0 MTPA)

Cases	Required Power of Compressor for the Cycle per Production of LNG (kW)	Ranking
Case 14	61,226	3
DMR	55,748	1
C3 MR	59,805	2
Daul N2 Expander	81,075	4

Table 4-34 Comparison of the required power of the compressors for the potential offshore liquefaction cycles (1.0 MTPA)

Cases	Required Power of Compressor for the Cycle per Production of LNG (kW)	Ranking
Case 14	30,613	3
DMR	26,607	1
C3 MR	29,238	2
Dual N2 Expander	38,286	4

The operating conditions for the potential offshore liquefaction cycles are shown in Figure 4-46 to 4-49 and in Table 4-35 to 4-38.

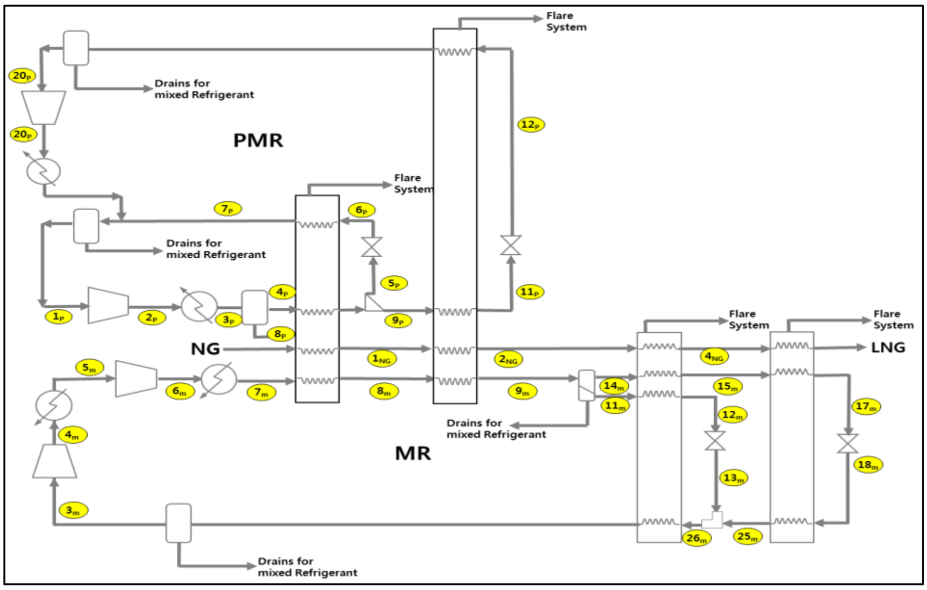

Figure 4-46 Potential MR liquefaction cycle –case 14

Table 4-35 Optimal operating conditions for the potential MR liquefaction cycle – case 14 (4.0 MTPA)

P1NG	82.71	P4p	32.86	P11p	22.36	P5m	20.2	P12m	32.45	P25m	3.78						
T1NG	-15.5	T4p	24	T11p	-55	T5m	24	T12m	-134	T25m	-142.6						
F1NG	479,500	F4p	810,200	F11p	792,800	F5m	638,400	F12m	434,300	F25m	204,100						
P2NG	79.71	P5p	27.36	P12p	3.56	P6m	43.75	P13m	3.78	P26m	3.78						
T2NG	-55	T5p	-15.5	T12p	-57.57	T6m	88	T13m	-135.9	T26m	-136.7						
F2NG	479,500	F5p	810,200	F12p	792,800	F6m	638,400	F13m	434,300	F26m	638,400					Zpre_Methane	0.0075
P4NG	76.96	P6p	10.5	P20p	3.26	P7m	43.35	P14m	37.25							Zpre_Ethane	0.745493
T4NG	-134	T6p	-18.5	T20p	-31.3	T7m	7.273	T14m	-55.06							Zpre_Propane	0.244508
F4NG	479,500	F6p	810,200	F20p	792,800	F7m	638,400	F14m	204,100							Zpre_i-Butane	0.00225
P1p	10.2	P7p	10.2	P21p	10.2	P8m	41.35	P15m	34.1							Zpre_n-Butane	000025
T1p	28.3	T7p	21	T21p	33.79	T8m	-15.5	T15m	-134							Zmain_Nitrogen	0.160811
F1p	1,603,000	F7p	810,200	F21p	792,800	F8m	638,400	F15m	204,100							Zmain_Methane	0.696517
P2p	33.66	P8p	32.86	P3m	10.02	P9m	37.35	P17m	30.95							Zmain_Ethane	0.138704
T2p	125	T8p	24	T3m	24	T9m	-55	T17m	-155.1							Zmain_Propane	0.003955
F2p	1,603,000	F8p	792,800	F3m	638,400	F9m	638,400	F17m	204,100							Zmain_i-Butane	0.000007
P3p	32.86	P9p	27.36	P4m	20.2	P11m	37.25	P18m	3.88							Zmain_n-Butane	0.000005
T3p	24	T9p	-15.5	T4m	78	T11m	-55.06	T18m	-161.3							Objective Function(work) [kW]	133,100
F3p	1,603,000	F9p	792,800	F4m	638,400	F11m	434,300	F18m	204,100								

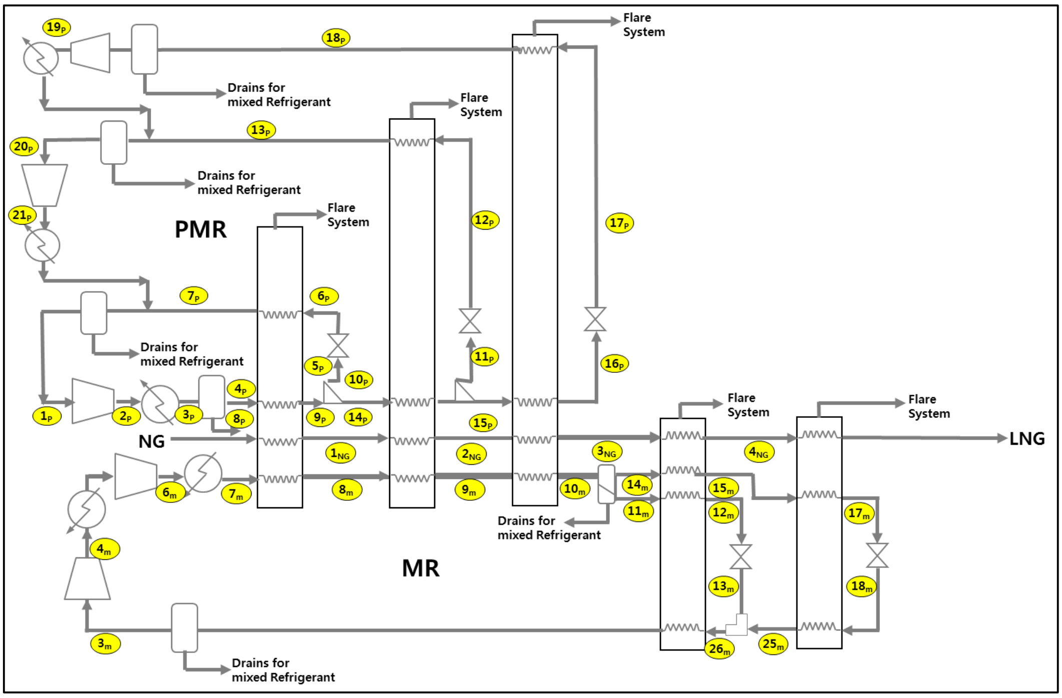

Figure 4-47 DMR cycle

Table 4-36 Optimal operating conditions for the DMR cycle (4.0 MTPA)

P1NG	82.71	P3p	32.86	P9p	29.36	P15p	25.86	P21p	14.96	P8m	41.35	P14m	37.25				
T1NG	-3.75	T3p	24	T9p	-3.75	T15p	-28.3	T21p	33.79	T8m	-3.75	T14m	-55.06				
F1NG	479,500	F3p	1,603,000	F9p	1,059,000	F15p	476,800	F21p	1,059,400	F8m	638,400	F14m	204,100				
P2NG	81.21	P4p	32.86	P10p	29.36	P16p	22.36	P3m	3.48	P9m	39.35	P15m	34.1				
T2NG	-28.3	T4p	24	T10p	-3.75	T16p	-55	T3m	-58	T9m	-28.3	T15m	-134				
F2NG	479,500	F4p	543,200	F10p	582,600	F16p	476,800	F3m	638,400	F9m	638,400	F15m	204,100			Zpre_Methane	0.0075
P3NG	79.71	P5p	29.36	P11p	25.86	P17p	3.56	P4m	15.75	P10m	37.35	P17m	30.95			Zpre_Ethane	0.745493
T3NG	-55	T5p	-3.75	T11p	-28.3	T17p	-57.57	T4m	42.46	T10m	-55	T17m	-155.1			Zpre_Propane	0.244508
F3NG	479,500	F5p	543,200	F11p	582,600	F17p	476,800	F4m	638,400	F10m	638,400	F17m	204,100			Zpre_i-Butane	0.00225
P4NG	76.96	P6p	15.41	P12p	8.29	P18p	3.26	P5m	15.75	P11m	37.25	P18m	3.88			Zpre_n-Butane	000025
T4NG	-134	T6p	-8.53	T12p	-31.73	T18p	-31.3	T5m	24	T11m	-55.06	T18m	-161.3			Zmain_Nitrogen	0.160811
F4NG	479,500	F6p	543,200	F12p	582,600	F18p	476,800	F5m	638,400	F11m	434,300	F18m	204,100			Zmain_Methane	0.696517
P1p	14.96	P7p	14.96	P13p	7.99	P19p	7.99	P6m	43.75	P12m	32.45	P25m	3.78			Zmain_Ethane	0.138704
T1p	33.79	T7p	20.78	T13p	-6.75	T19p	16.84	T6m	104.3	T12m	-134	T25m	-142.6			Zmain_Propane	0.003955
F1p	1,603,000	F7p	543,200	F13p	582,600	F19p	476,800	F6m	638,400	F12m	434,300	F25m	204,100			Zmain_i-Butane	0.000007
P2p	33.66	P8p	32.86	P14p	29.36	P20p	7.99	P7m	43.35	P13m	3.78	P26m	3.78			Zmain_n-Butane	0.000005
T2p	85.3	T8p	24	T14p	-3.75	T20p	3.962	T7m	7.273	T13m	-135.9	T26m	-136.7			Objective Function(work) [kW]	126,700
F2p	1,603,000	F8p	1,059,000	F14p	476,800	F20p	1,059,400	F7m	638,400	F13m	434,300	F26m	638,400				

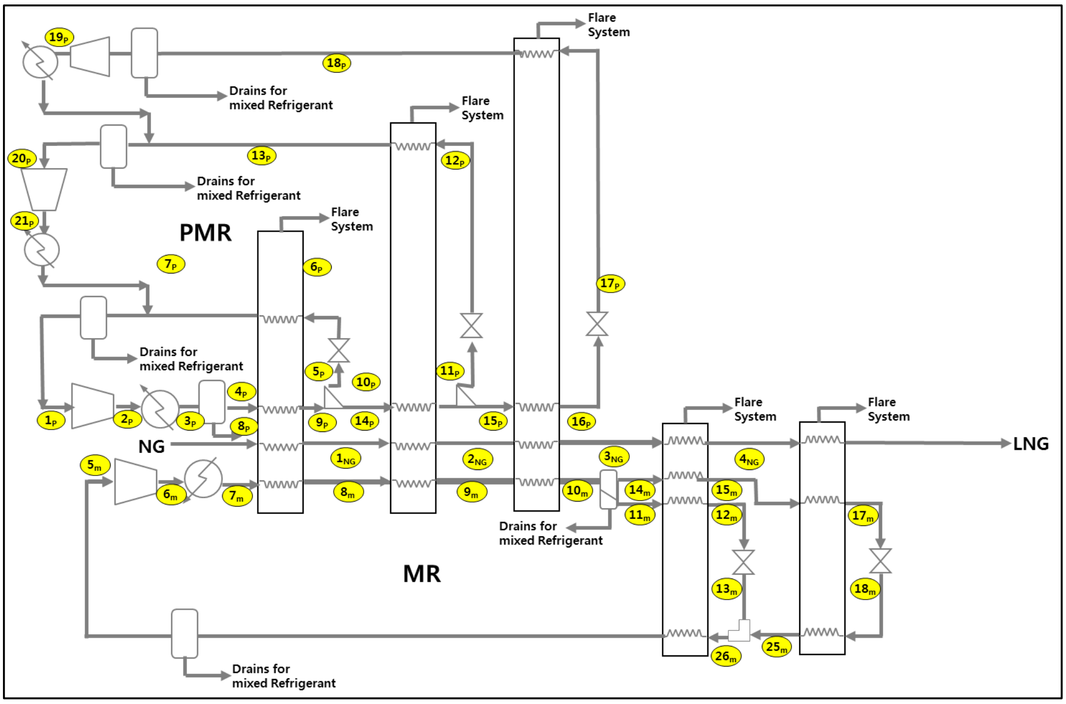

Figure 4-48 C_3MR cycle

Table 4-37 Optimal operating conditions for the C_3MR cycle (4.0 MTPA)

P1NG	82.71	P3p	32.86	P9p	29.36	P15p	25.86	P21p	14.96	P10m	37.35	P17m	30.95				
T1NG	-3.75	T3p	24	T9p	-3.75	T15p	-28.3	T21p	33.79	T10m	-55	T17m	-155.1				
F1NG	479,500	F3p	1,603,000	F9p	1,059,000	F15p	476,800	F21p	1,059,400	F10m	638,400	F17m	204,100				
P2NG	81.21	P4p	32.86	P10p	29.36	P16p	22.36	P5m	3.48	P11m	37.25	P18m	3.88				
T2NG	-28.3	T4p	24	T10p	-3.75	T16p	-55	T5m	-58	T11m	-55.06	T18m	-161.3				
F2NG	479,500	F4p	543,200	F10p	582,600	F16p	476,800	F5m	638,400	F11m	434,300	F18m	204,100			Zpre_Methane	0.0075
P3NG	79.71	P5p	29.36	P11p	25.86	P17p	3.56	P6m	43.75	P12m	32.45	P25m	3.78			Zpre_Ethane	0.745493
T3NG	-55	T5p	-3.75	T11p	-28.3	T17p	-57.57	T6m	305	T12m	-134	T25m	-142.6			Zpre_Propane	0.244508
F3NG	479,500	F5p	543,200	F11p	582,600	F17p	476,800	F6m	638,400	F12m	434,300	F25m	204,100			Zpre_i-Butane	0.00225
P4NG	76.96	P6p	15.41	P12p	8.29	P18p	3.26	P7m	43.35	P13m	3.78	P26m	3.78			Zpre_n-Butane	000025
T4NG	-134	T6p	-8.53	T12p	-31.73	T18p	-31.3	T7m	7.273	T13m	-135.9	T26m	-136.7			Zmain_Nitrogen	0.160811
F4NG	479,500	F6p	543,200	F12p	582,600	F18p	476,800	F7m	638,400	F13m	434,300	F26m	638,400			Zmain_Methane	0.696517
P1p	14.96	P7p	14.96	P13p	7.99	P19p	7.99	P8m	41.35	P14m	37.25					Zmain_Ethane	0.138704
T1p	33.79	T7p	20.78	T13p	-6.75	T19p	16.84	T8m	-3.75	T14m	-55.06					Zmain_Propane	0.003955
F1p	1,603,000	F7p	543,200	F13p	582,600	F19p	476,800	F8m	638,400	F14m	204,100					Zmain_i-Butane	0.000007
P2p	33.66	P8p	32.86	P14p	29.36	P20p	7.99	P9m	39.35	P15m	34.1					Zmain_n-Butane	0.000005
T2p	85.3	T8p	24	T14p	-3.75	T20p	3.962	T9m	-28.3	T15m	-134					Objective Function(work) [kW]	132,900
F2p	1,603,000	F8p	1,059,000	F14p	476,800	F20p	1,059,400	F9m	638,400	F15m	204,100						

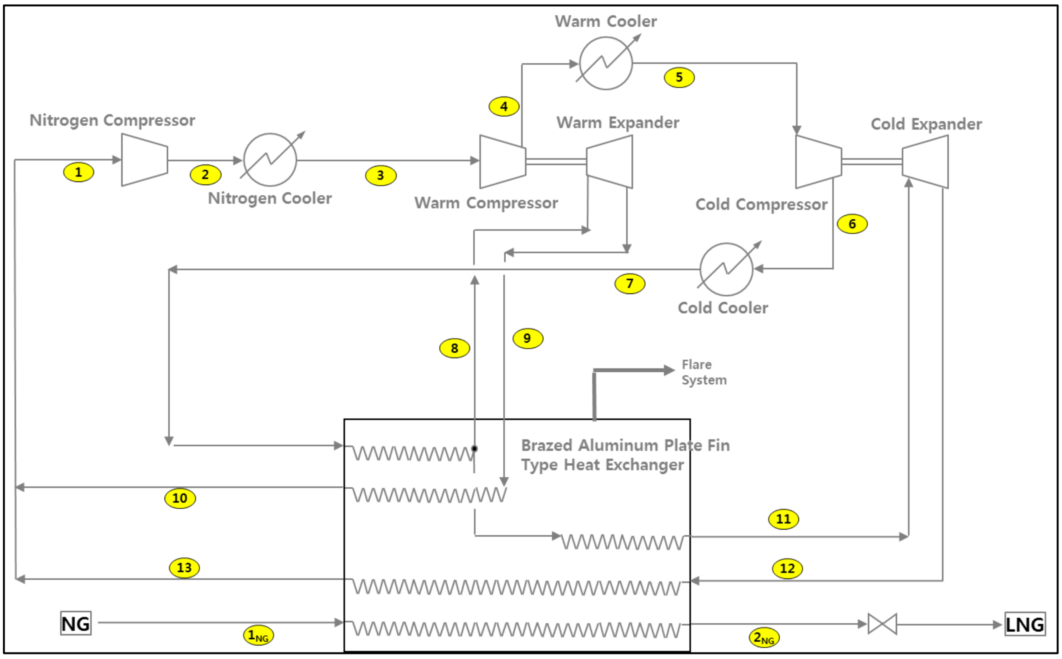

Figure 4-49 Dual N_2 expander cycle

Table 4-38 Optimal operating conditions for the dual N2 expander cycle (4.0 MTPA)

P1NG	82.71	P5	48	P11	77												
T1NG	-15.5	T5	24	T11	-38.7												
F1NG	479,500	F5	3,403,000	F11	1,020,900												
P2NG	79.71	P6	80.76	P12	13												
T2NG	-55	T6	115	T12	-163.2												
F2NG	479,500	F6	3,403,000	F12	1,020,900												
P1	10.2	P7	80	P13	10.2												
T1	28.3	T7	24	T13	28.3												
F1	3,403,000	F7	3,403,000	F13	1,020,900												
P2	25.66	P8	77														
T2	125	T8	-15														
F2	3,403,000	F8	2,382,100														
P3	25	P9	13														
T3	24	T9	-89														
F3	3,403,000	F9	2,382,100														
P4	48.86	P10	10.2														
T4	138	T10	28.3													Objective Function(work) [kW]	225,210
F4	3,403,000	F10	2,382,100														

4.6. Equipment Selection of the Potential Offshore Liquefaction Cycles

In the selection of liquefaction equipment, the mechanical integrity, especially that of the liquefaction heat exchangers, has been a concern. It is necessary to increase the shell side design pressure to make it higher than those of the land-based plants, to minimize the incidental flares required for the temporary trips of the plant. Also, mechanical devices may need to be installed to guarantee that maldistribution can be minimized and avoided altogether. Some of the major cryogenic equipment may need to have their mechanical integrity verified at a scaled-down size. Due to the offshore location, it will be necessary to reduce the height of the unusually high tower by using multiple units. Modularization, whenever possible, needs to be considered. Again, the flexibility and reliability of the equipment need to be emphasized.

To select equipment consisting of potential offshore liquefaction cycles, their operating conditions should be given to several potential vendors that can provide the suitable equipment. Based on the vendors' equipment data, the relevant equipment selection can be done. Thus, there are no references for estimating the equipment sizes without the vendors' data because the vendors' equipment models and blinded methods have high uncertainties. Therefore, this paper assumed that the equipment sizes for the potential offshore liquefaction cycles are proportional to those of the baseline design according to the compressor power ratio. If possible, this assumption can be modified in the future, according to more suitable methods for the equipment size estimation. Table 4-39 to 4-42 show the proportional method of estimating the equipment sizes for the potential offshore liquefaction cycles in this paper. In accordance with such method, the equipment sizes for the potential offshore liquefaction cycles are shown in Figure 4-50 to 4-53 and in Table 4-43 to 4-58. These equipment sizes are considered for their optimal module layouts in Chapter 5.

Table 4-39 Equipment size selection for the potential offshore liquefaction cycles (4.0 MTPA)

Potential Offshore Liquefaction Cycles	Required Power of Compressor for the Cycle per Production of LNG (kW)	Power Ratio	Equipment Size Selection
Base Line Design	134,400	1	Base Size
Case 14	133,100	0.9903	Base Size ×0.9903
DMR	126,700	0.9427	Base Size ×0.9427
C3 MR	132,900	0.9888	Base Size ×0.9888
Dual N2 Expander	225,210	1.6756	Base Size ×1.6756

Table 4-40 Equipment size selection for the potential offshore liquefaction cycles (3.0 MTPA)

Potential Offshore Liquefaction Cycles	Required Power of Compressor for the Cycle per Production of LNG (kW)	Power Ratio	Equipment Size Selection
Base Line Design	134,400	1	Base Size
Case 14	94,501	0.703	Base Size × 0.703
DMR	88,690	0.66	Base Size × 0.66
C3 MR	90,372	0.672	Base Size × 0.672
Dual N2 Expander	137,378	1.022	Base Size × 1.022

Table 4-41 Equipment size selection for the potential offshore liquefaction cycles (2.0 MTPA)

Potential Offshore Liquefaction Cycles	Required Power of Compressor for the Cycle per Production of LNG (kW)	Power Ratio	Equipment Size Selection
Base Line Design	134,400	1	Base Size
Case 14	61,226	0.4555	Base Size × 0.4555
DMR	55,748	0.4148	Base Size ×

			0.4148
C3 MR	59,805	0.445	Base Size × 0.445
Dual N2 Expander	81,075	0.603	Base Size × 0.603

Table 4-42 Equipment size selection for the potential offshore liquefaction cycles (1.0 MTPA)

Potential Offshore Liquefaction Cycles	Required Power of Compressor for the Cycle per Production of LNG (kW)	Power Ratio	Equipment Size Selection
Base Line Design	134,400	1	Base Size
Case 14	30,613	0.2278	Base Size × 0.2278
DMR	26,607	0.198	Base Size × 0.198
C3 MR	29,238	0.2175	Base Size × 0.2175
Dual N2 Expander	38,286	0.285	Base Size × 0.285

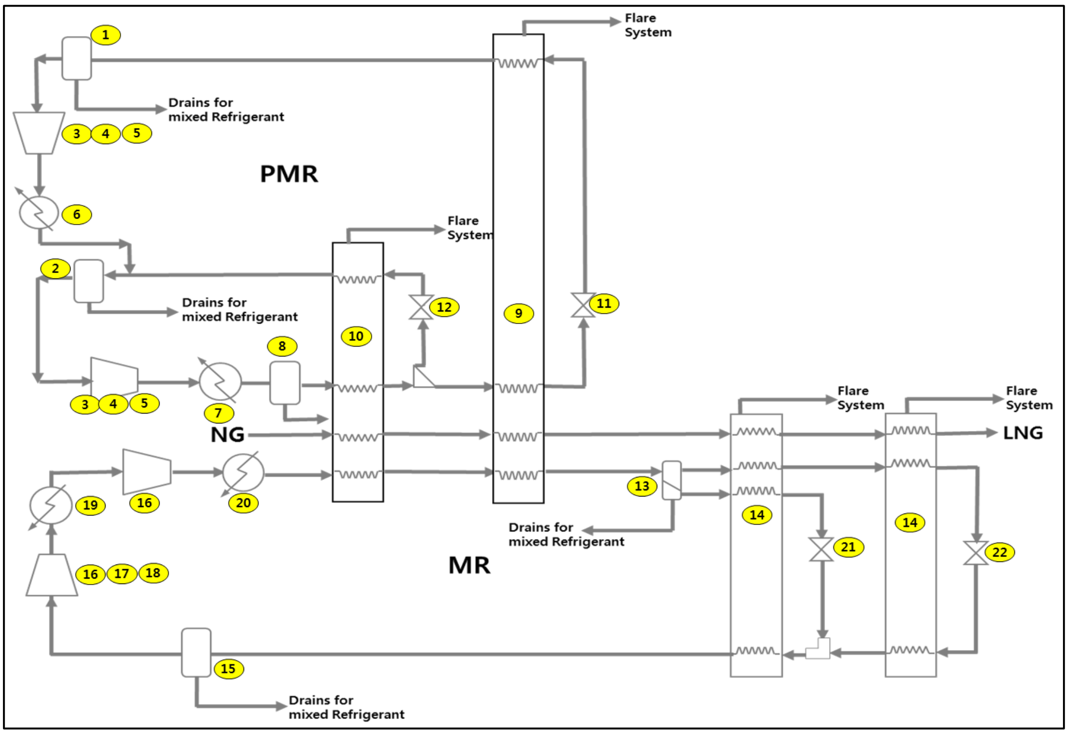

Figure 4-50 Equipment for the potential MR liquefaction cycle – case 14

Table 4-43 Equipment sizes for the potential MR liquefaction cycle – case 14 (4.0 MTPA)

No.	Name	Dimension of the Equipment			
		Length	Breadth /Diameter	Height	Module
1	PMR comp. LP suction drum	3.613	3.613	4.603	PMR Module 1
2	PMR comp. HP suction drum	3.217	3.217	4.900	
3	PMR Compressor	18.809	5.939	5.741	
4	Cooler for PMR com.	2.969	1.979	2.969	
5	Overhead crane for PMR com.	22.769	15.839	5.939	
6	SW cooler 1	7.919	1.979	4.949	
7	SW cooler 2	7.919	1.979	4.949	
8	PMR Receiver	4.157	4.157	9.800	PMR Module 2
9	LP Precool Exchanger	4.157	4.157	21.086	
10	HP Precool Exchanger	4.355	4.355	21.779	
11	Joule-Thomson Valve 1	0.989	0.989	0.989	
12	Joule-Thomson Valve 2	0.989	0.989	0.989	
13	MR Separator 1	4.454	4.454	12.869	MR Module
14	MCHE	5.642	5.642	41.579	
15	MR Comp. Suction Drum	5.444	5.444	8.909	
16	MR Comp.	17.126	5.939	5.939	
17	Cooler for MR comp.	2.969	1.979	2.969	
18	Overhead crane	22.769	15.839	5.939	
19	SW cooler 3	3.959	2.474	2.969	
20	SW cooler 4	3.959	2.474	2.969	
21	Joule-Thomson Valve 3	1.484	1.484	1.484	
22	Joule-Thomson Valve 4	1.484	1.484	1.484	

Table 4-44 Equipment sizes for the potential MR liquefaction cycle – case 14 (3.0 MTPA)

No.	Name	Dimension of the Equipment			
		Length	Breadth /Diameter	Height	Module
1	PMR comp. LP suction drum	2.56	2.56	3.27	PMR Module 1
2	PMR comp. HP suction drum	2.28	2.28	3.48	
3	PMR Compressor	13.35	4.22	4.08	
4	Cooler for PMR com.	2.11	1.40	2.11	
5	Overhead crane for PMR com.	16.16	11.24	4.22	
6	SW cooler 1	5.62	1.40	3.51	
7	SW cooler 2	5.62	1.40	3.51	
8	PMR Receiver	2.95	2.95	6.96	PMR Module 2
9	LP Precool Exchanger	2.95	2.95	14.97	
10	HP Precool Exchanger	3.09	3.09	15.46	
11	Joule-Thomson Valve 1	0.70	0.70	0.70	
12	Joule-Thomson Valve 2	0.70	0.70	0.70	
13	MR Separator 1	3.16	3.16	9.14	MR Module
14	MCHE	4.01	4.01	29.52	
15	MR Comp. Suction Drum	3.86	3.86	6.32	
16	MR Comp.	12.16	4.22	4.22	
17	Cooler for MR comp.	2.11	1.40	2.11	
18	Overhead crane	16.16	11.24	4.22	
19	SW cooler 3	2.81	1.76	2.11	
20	SW cooler 4	2.81	1.76	2.11	
21	Joule-Thomson Valve 3	1.05	1.05	1.05	
22	Joule-Thomson Valve 4	1.05	1.05	1.05	

Table 4-45 Equipment sizes for the potential MR liquefaction cycle – case 14 (2.0 MTPA)

No.	Name	Dimension of the Equipment			
		Length	Breadth /Diameter	Height	Module
1	PMR comp. LP suction drum	1.66	1.66	2.12	PMR Module 1
2	PMR comp. HP suction drum	1.48	1.48	2.25	
3	PMR Compressor	8.65	2.73	2.64	
4	Cooler for PMR com.	1.37	0.91	1.37	
5	Overhead crane for PMR com.	10.47	7.29	2.73	
6	SW cooler 1	3.64	0.91	2.28	
7	SW cooler 2	3.64	0.91	2.28	
8	PMR Receiver	1.91	1.91	4.51	PMR Module 2
9	LP Precool Exchanger	1.91	1.91	9.70	
10	HP Precool Exchanger	2.00	2.00	10.02	
11	Joule-Thomson Valve 1	0.45	0.45	0.45	
12	Joule-Thomson Valve 2	0.45	0.45	0.45	
13	MR Separator 1	2.05	2.05	5.92	MR Module
14	MCHE	2.60	2.60	19.13	
15	MR Comp. Suction Drum	2.50	2.50	4.10	
16	MR Comp.	7.88	2.73	2.73	
17	Cooler for MR comp.	1.37	0.91	1.37	
18	Overhead crane	10.47	7.29	2.73	
19	SW cooler 3	1.82	1.14	1.37	
20	SW cooler 4	1.82	1.14	1.37	
21	Joule-Thomson Valve 3	0.68	0.68	0.68	
22	Joule-Thomson Valve 4	0.68	0.68	0.68	

Table 4-46 Equipment sizes for the potential MR liquefaction cycle – case 14 (1.0 MTPA)

No.	Name	Dimension of the Equipment			
		Length	Breadth /Diameter	Height	Module
1	PMR comp. LP suction drum	0.83	0.83	1.06	PMR Module 1
2	PMR comp. HP suction drum	0.74	0.74	1.13	
3	PMR Compressor	4.33	1.37	1.32	
4	Cooler for PMR com.	0.68	0.46	0.68	
5	Overhead crane for PMR com.	5.24	3.64	1.37	
6	SW cooler 1	1.82	0.46	1.14	
7	SW cooler 2	1.82	0.46	1.14	
8	PMR Receiver	0.96	0.96	2.25	PMR Module 2
9	LP Precool Exchanger	0.96	0.96	4.85	
10	HP Precool Exchanger	1.00	1.00	5.01	
11	Joule-Thomson Valve 1	0.23	0.23	0.23	
12	Joule-Thomson Valve 2	0.23	0.23	0.23	
13	MR Separator 1	1.02	1.02	2.96	MR Module
14	MCHE	1.30	1.30	9.56	
15	MR Comp. Suction Drum	1.25	1.25	2.05	
16	MR Comp.	3.94	1.37	1.37	
17	Cooler for MR comp.	0.68	0.46	0.68	
18	Overhead crane	5.24	3.64	1.37	
19	SW cooler 3	0.91	0.57	0.68	
20	SW cooler 4	0.91	0.57	0.68	
21	Joule-Thomson Valve 3	0.34	0.34	0.34	
22	Joule-Thomson Valve 4	0.34	0.34	0.34	

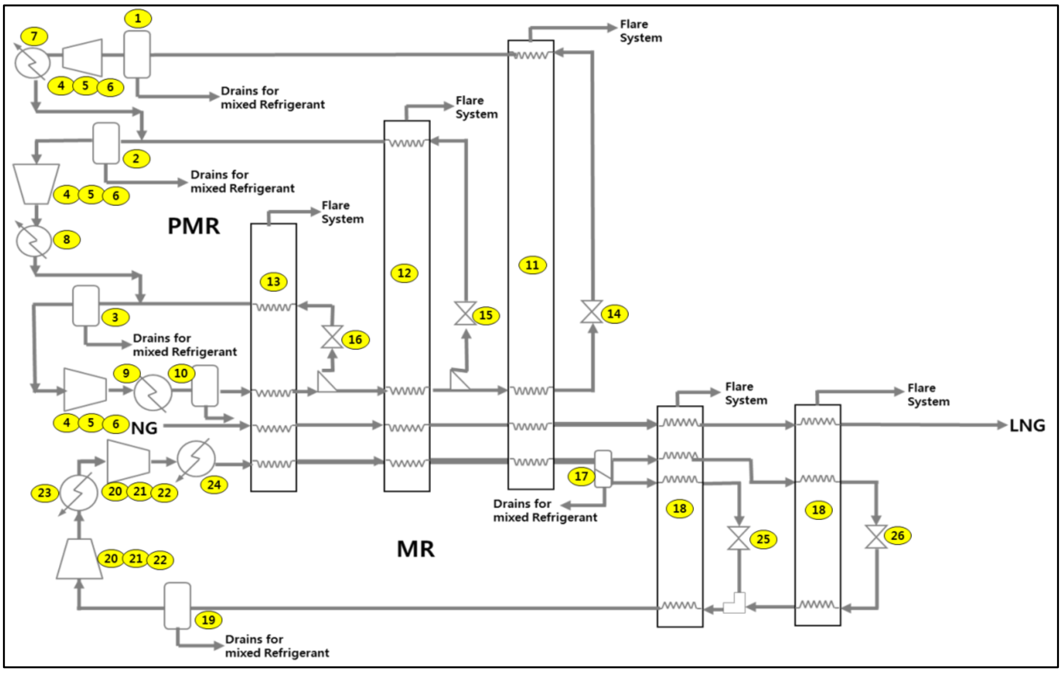

Figure 4-51 Equipment for the DMR cycle

Table 4-47 Equipment sizes for the DMR cycle (4.0 MTPA)

No.	Name	Dimension of the Equipment			
		Length	**Breadth /Diameter**	**Height**	**Module**
1	PMR comp. LP suction drum	3.4392	3.4392	4.3816	PMR Module 1
2	PMR comp. MP suction drum	3.2150	3.2150	4.501	
3	PMR comp. HP suction drum	3.0622	3.0622	4.664	
4	PMR Compressor	17.904	5.633	5.465	
5	Cooler for PMR com.	2.826	1.884	2.826	
6	Overhead crane for PMR com.	21.673	15.077	5.653	
7	SW cooler 1	7.538	1.884	4.711	
8	SW cooler 2	7.538	1.884	4.711	
9	SW cooler 3	7.538	1.884	4.711	
10	PMR Receiver	3.957	3.957	9.328	PMR Module 2
11	LP Precool Exchanger	3.957	3.957	20.072	
12	MP Precool Exchanger	4.025	4.025	20.521	
13	HP Precool Exchanger	4.145	4.145	20.731	
14	Joule-Thomson Valve 1	0.9414	0.9414	0.9414	
15	Joule-Thomson Valve 2	0.9414	0.9414	0.9414	
16	Joule-Thomson Valve 3	0.9414	0.9414	0.9414	
17	MR Separator 1	4.2397	4.2397	12.25	MR Module
18	MCHE	5.3706	5.3706	39.579	
19	MR Comp. Suction Drum	5.1821	5.1821	8.4805	
20	MR Comp.	16.3022	5.6533	5.6533	
21	Cooler for MR comp.	2.8262	1.884	2.8262	
22	Overhead crane	21.6738	15.0771	5.6533	
23	SW cooler 4	3.7686	2.355	2.8262	
24	SW cooler 5	3.7686	2.355	2.8262	
25	Joule-Thomson Valve 4	1.413	1.413	1.413	
26	Joule-Thomson Valve 5	1.413	1.413	1.413	

Table 4-48 Equipment sizes for the DMR cycle (3.0 MTPA)

No.	Name	Dimension of the Equipment			
		Length	Breadth /Diameter	Height	Module
1	PMR comp. LP suction drum	2.41	2.41	3.07	PMR Module 1
2	PMR comp. MP suction drum	2.25	2.25	3.15	
3	PMR comp. HP suction drum	2.14	2.14	3.27	
4	PMR Compressor	12.53	3.94	3.83	
5	Cooler for PMR com.	1.98	1.32	1.98	
6	Overhead crane for PMR com.	15.17	10.56	3.96	
7	SW cooler 1	5.28	1.32	3.30	
8	SW cooler 2	5.28	1.32	3.30	
9	SW cooler 3	5.28	1.32	3.30	
10	PMR Receiver	2.77	2.77	6.53	PMR Module 2
11	LP Precool Exchanger	2.77	2.77	14.05	
12	MP Precool Exchanger	2.82	2.82	14.37	
13	HP Precool Exchanger	2.90	2.90	14.51	
14	Joule-Thomson Valve 1	0.66	0.66	0.66	
15	Joule-Thomson Valve 2	0.66	0.66	0.66	
16	Joule-Thomson Valve 3	0.66	0.66	0.66	
17	MR Separator 1	2.97	2.97	8.58	MR Module
18	MCHE	3.76	3.76	27.71	
19	MR Comp. Suction Drum	3.63	3.63	5.94	
20	MR Comp.	11.41	3.96	3.96	
21	Cooler for MR comp.	1.98	1.32	1.98	
22	Overhead crane	15.17	10.56	3.96	
23	SW cooler 4	2.64	1.65	1.98	
24	SW cooler 5	2.64	1.65	1.98	
25	Joule-Thomson Valve 4	0.99	0.99	0.99	
26	Joule-Thomson Valve 5	0.99	0.99	0.99	

Table 4-49 Equipment sizes for the DMR cycle (2.0 MTPA)

No.	Name	Dimension of the Equipment			
		Length	Breadth /Diameter	Height	Module
1	PMR comp. LP suction drum	1.51	1.51	1.93	PMR Module 1
2	PMR comp. MP suction drum	1.41	1.41	1.98	
3	PMR comp. HP suction drum	1.35	1.35	2.05	
4	PMR Compressor	7.88	2.48	2.40	
5	Cooler for PMR com.	1.24	0.83	1.24	
6	Overhead crane for PMR com.	9.54	6.63	2.49	
7	SW cooler 1	3.32	0.83	2.07	
8	SW cooler 2	3.32	0.83	2.07	
9	SW cooler 3	3.32	0.83	2.07	
10	PMR Receiver	1.74	1.74	4.10	PMR Module 2
11	LP Precool Exchanger	1.74	1.74	8.83	
12	MP Precool Exchanger	1.77	1.77	9.03	
13	HP Precool Exchanger	1.82	1.82	9.12	
14	Joule-Thomson Valve 1	0.41	0.41	0.41	
15	Joule-Thomson Valve 2	0.41	0.41	0.41	
16	Joule-Thomson Valve 3	0.41	0.41	0.41	
17	MR Separator 1	1.87	1.87	5.39	MR Module
18	MCHE	2.36	2.36	17.41	
19	MR Comp. Suction Drum	2.28	2.28	3.73	
20	MR Comp.	7.17	2.49	2.49	
21	Cooler for MR comp.	1.24	0.83	1.24	
22	Overhead crane	9.54	6.63	2.49	
23	SW cooler 4	1.66	1.04	1.24	
24	SW cooler 5	1.66	1.04	1.24	
25	Joule-Thomson Valve 4	0.62	0.62	0.62	
26	Joule-Thomson Valve 5	0.62	0.62	0.62	

Table 4-50 Equipment sizes for the DMR cycle (1.0 MTPA)

No.	Name	Dimension of the Equipment			
		Length	**Breadth /Diameter**	**Height**	**Module**
1	PMR comp. LP suction drum	0.72	0.72	0.92	PMR Module 1
2	PMR comp. MP suction drum	0.68	0.68	0.95	
3	PMR comp. HP suction drum	0.64	0.64	0.98	
4	PMR Compressor	3.76	1.18	1.15	
5	Cooler for PMR com.	0.59	0.40	0.59	
6	Overhead crane for PMR com.	4.55	3.17	1.19	
7	SW cooler 1	1.58	0.40	0.99	
8	SW cooler 2	1.58	0.40	0.99	
9	SW cooler 3	1.58	0.40	0.99	
10	PMR Receiver	0.83	0.83	1.96	PMR Module 2
11	LP Precool Exchanger	0.83	0.83	4.22	
12	MP Precool Exchanger	0.85	0.85	4.31	
13	HP Precool Exchanger	0.87	0.87	4.35	
14	Joule-Thomson Valve 1	0.20	0.20	0.20	
15	Joule-Thomson Valve 2	0.20	0.20	0.20	
16	Joule-Thomson Valve 3	0.20	0.20	0.20	
17	MR Separator 1	0.89	0.89	2.57	MR Module
18	MCHE	1.13	1.13	8.31	
19	MR Comp. Suction Drum	1.09	1.09	1.78	
20	MR Comp.	3.42	1.19	1.19	
21	Cooler for MR comp.	0.59	0.40	0.59	
22	Overhead crane	4.55	3.17	1.19	
23	SW cooler 4	0.79	0.49	0.59	
24	SW cooler 5	0.79	0.49	0.59	
25	Joule-Thomson Valve 4	0.30	0.30	0.30	
26	Joule-Thomson Valve 5	0.30	0.30	0.30	

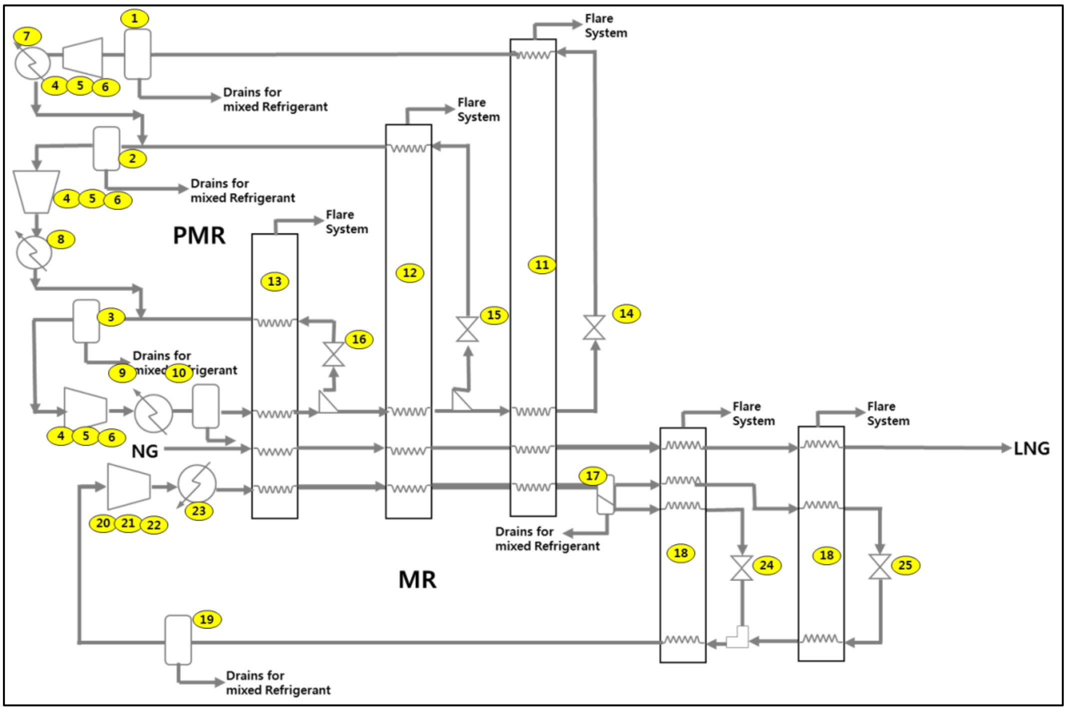

Figure 4-52 Equipment for the C_3MR cycle.

Table 4-51 Equipment sizes for the C_3MR cycle (4.0 MTPA)

No.	Name	Dimension of the Equipment			
		Length	**Breadth /Diameter**	**Height**	**Module**
1	PMR comp. LP suction drum	3.6075	3.608	4.596	PMR Module 1
2	PMR comp. MP suction drum	3.3723	3.372	4.721	
3	PMR comp. HP suction drum	3.2120	3.212	4.892	
4	PMR Compressor	18.7801	5.909	5.732	
5	Cooler for PMR com.	2.9643	1.976	2.964	
6	Overhead crane for PMR com.	22.734	15.815	5.93	
7	SW cooler 1	7.907	1.9762	4.942	
8	SW cooler 2	7.907	1.9762	4.942	
9	SW cooler 3	7.907	1.9762	4.942	
10	PMR Receiver	4.151	4.151	9.784	PMR Module 2
11	LP Precool Exchanger	4.151	4.151	21.054	
12	MP Precool Exchanger	4.222	4.222	21.525	
13	HP Precool Exchanger	4.348	4.348	21.745	
14	Joule-Thomson Valve 1	0.987	0.9875	0.9875	
15	Joule-Thomson Valve 2	0.987	0.9875	0.9875	
16	Joule-Thomson Valve 3	0.987	0.9875	0.9875	
17	MR Separator 1	4.447	4.447	12.849	MR Module
18	MCHE	5.633	5.633	41.516	
19	MR Comp. Suction Drum	5.436	5.436	8.8955	
20	MR Comp.	17.1	5.93	5.93	
21	Cooler for MR comp.	2.964	1.976	2.9645	
22	Overhead crane	22.734	15.815	5.93	
23	SW cooler 4	3.953	2.47	2.9645	
24	Joule-Thomson Valve 4	1.482	1.482	1.482	
25	Joule-Thomson Valve 5	1.482	1.482	1.482	

Table 4-52 Equipment sizes for the C_3MR cycle (3.0 MTPA)

No.	Name	Dimension of the Equipment			
		Length	Breadth /Diameter	Height	Module
1	PMR comp. LP suction drum	2.45	2.45	3.12	PMR Module 1
2	PMR comp. MP suction drum	2.29	2.29	3.21	
3	PMR comp. HP suction drum	2.18	2.18	3.32	
4	PMR Compressor	12.76	4.02	3.90	
5	Cooler for PMR com.	2.01	1.34	2.01	
6	Overhead crane for PMR com.	15.45	10.75	4.03	
7	SW cooler 1	5.37	1.34	3.36	
8	SW cooler 2	5.37	1.34	3.36	
9	SW cooler 3	5.37	1.34	3.36	
10	PMR Receiver	2.82	2.82	6.65	PMR Module 2
11	LP Precool Exchanger	2.82	2.82	14.31	
12	MP Precool Exchanger	2.87	2.87	14.63	
13	HP Precool Exchanger	2.95	2.95	14.78	
14	Joule-Thomson Valve 1	0.67	0.67	0.67	
15	Joule-Thomson Valve 2	0.67	0.67	0.67	
16	Joule-Thomson Valve 3	0.67	0.67	0.67	
17	MR Separator 1	3.02	3.02	8.73	MR Module
18	MCHE	3.83	3.83	28.21	
19	MR Comp. Suction Drum	3.69	3.69	6.05	
20	MR Comp.	11.62	4.03	4.03	
21	Cooler for MR comp.	2.01	1.34	2.01	
22	Overhead crane	15.45	10.75	4.03	
23	SW cooler 4	2.69	1.68	2.01	
24	Joule-Thomson Valve 4	1.01	1.01	1.01	
25	Joule-Thomson Valve 5	1.01	1.01	1.01	

Table 4-53 Equipment sizes for the C_3MR cycle (2.0 MTPA)

No.	Name	Dimension of the Equipment			
		Length	Breadth /Diameter	Height	Module
1	PMR comp. LP suction drum	1.62	1.62	2.07	PMR Module 1
2	PMR comp. MP suction drum	1.52	1.52	2.12	
3	PMR comp. HP suction drum	1.45	1.45	2.20	
4	PMR Compressor	8.45	2.66	2.58	
5	Cooler for PMR com.	1.33	0.89	1.33	
6	Overhead crane for PMR com.	10.23	7.12	2.67	
7	SW cooler 1	3.56	0.89	2.22	
8	SW cooler 2	3.56	0.89	2.22	
9	SW cooler 3	3.56	0.89	2.22	
10	PMR Receiver	1.87	1.87	4.40	PMR Module 2
11	LP Precool Exchanger	1.87	1.87	9.47	
12	MP Precool Exchanger	1.90	1.90	9.69	
13	HP Precool Exchanger	1.96	1.96	9.79	
14	Joule-Thomson Valve 1	0.44	0.44	0.44	
15	Joule-Thomson Valve 2	0.44	0.44	0.44	
16	Joule-Thomson Valve 3	0.44	0.44	0.44	
17	MR Separator 1	2.00	2.00	5.78	MR Module
18	MCHE	2.53	2.53	18.68	
19	MR Comp. Suction Drum	2.45	2.45	4.00	
20	MR Comp.	7.70	2.67	2.67	
21	Cooler for MR comp.	1.33	0.89	1.33	
22	Overhead crane	10.23	7.12	2.67	
23	SW cooler 4	1.78	1.11	1.33	
24	Joule-Thomson Valve 4	0.67	0.67	0.67	
25	Joule-Thomson Valve 5	0.67	0.67	0.67	

Table 4-54 Equipment sizes for the C_3MR cycle (1.0 MTPA)

No.	Name	Dimension of the Equipment			
		Length	**Breadth /Diameter**	**Height**	**Module**
1	PMR comp. LP suction drum	0.79	0.79	1.01	PMR Module 1
2	PMR comp. MP suction drum	0.74	0.74	1.04	
3	PMR comp. HP suction drum	0.71	0.71	1.08	
4	PMR Compressor	4.13	1.30	1.26	
5	Cooler for PMR com.	0.65	0.43	0.65	
6	Overhead crane for PMR com.	5.00	3.48	1.30	
7	SW cooler 1	1.74	0.43	1.09	
8	SW cooler 2	1.74	0.43	1.09	
9	SW cooler 3	1.74	0.43	1.09	
10	PMR Receiver	0.91	0.91	2.15	PMR Module 2
11	LP Precool Exchanger	0.91	0.91	4.63	
12	MP Precool Exchanger	0.93	0.93	4.74	
13	HP Precool Exchanger	0.96	0.96	4.78	
14	Joule-Thomson Valve 1	0.22	0.22	0.22	
15	Joule-Thomson Valve 2	0.22	0.22	0.22	
16	Joule-Thomson Valve 3	0.22	0.22	0.22	
17	MR Separator 1	0.98	0.98	2.83	MR Module
18	MCHE	1.24	1.24	9.13	
19	MR Comp. Suction Drum	1.20	1.20	1.96	
20	MR Comp.	3.76	1.30	1.30	
21	Cooler for MR comp.	0.65	0.43	0.65	
22	Overhead crane	5.00	3.48	1.30	
23	SW cooler 4	0.87	0.54	0.65	
24	Joule-Thomson Valve 4	0.33	0.33	0.33	
25	Joule-Thomson Valve 5	0.33	0.33	0.33	

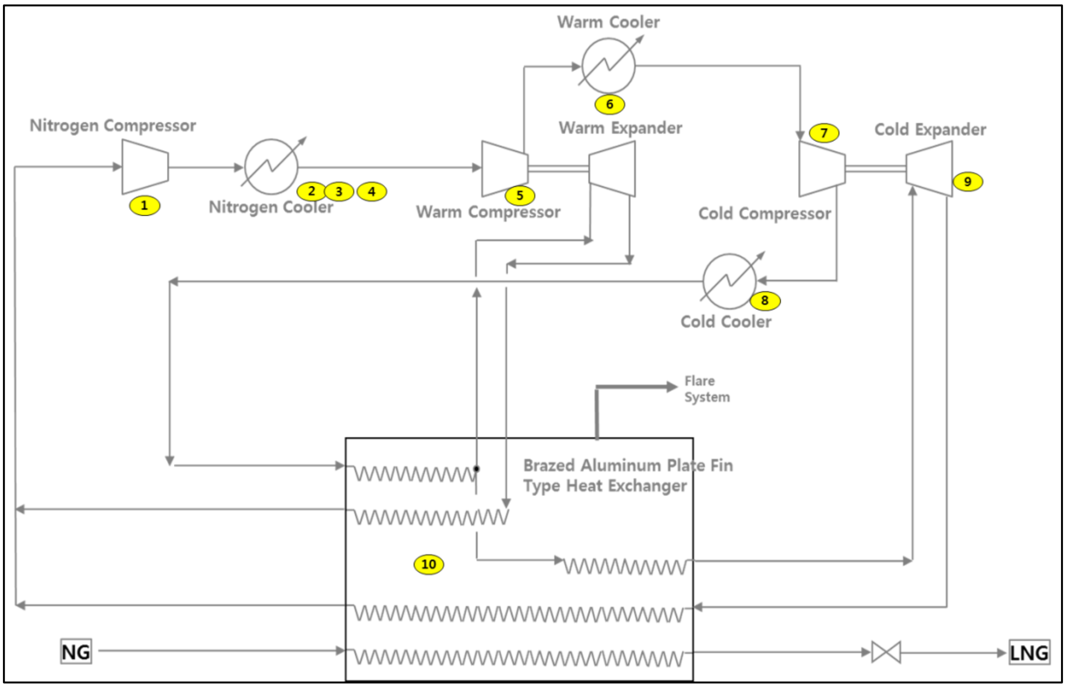

Figure 4-53 Equipment for the dual N_2 expander cycle

Table 4-55 Equipment sizes for the dual N_2 expander cycle (4.0 MTPA)

No.	Name	Dimension of the Equipment			
		Length	Breadth /Diameter	Height	Module
1	Nitrogen Compressor	39.929	12.608	12.187	Refrigerant Module 1
2	Nitrogen Cooler	16.811	4.201	10.506	
3	Cooler for PMR com.	6.303	4.201	6.303	
4	Overhead crane for PMR com.	39.929	20.502	5.939	
5	Warm Compressor	27.95	8.825	8.531	Refrigerant Module 2
6	Warm Cooler	11.767	2.941	7.354	
7	Warm Expander	27.95	8.825	8.531	
8	Cold Compressor	25.01	7.52	7.42	
9	Cold Cooler	5.04	1.26	3.152	
10	Cold Expander	11.98	3.782	3.656	
11	Brazed Aluminum Plate Fin Type Heat Exchanger	17.1	17.1	43	

Table 4-56 Equipment sizes for the dual N_2 expander cycle (3.0 MTPA)

No.	**Name**	**Dimension of the Equipment**			
		Length	**Breadth /Diameter**	**Height**	**Module**
1	Nitrogen Compressor	24.35	7.69	7.43	Refrigerant Module 1
2	Nitrogen Cooler	10.25	2.56	6.41	
3	Cooler for PMR com.	3.84	2.56	3.84	
4	Overhead crane for PMR com.	24.35	12.50	3.62	
5	Warm Compressor	17.05	5.38	5.20	Refrigerant Module 2
6	Warm Cooler	7.18	1.79	4.49	
7	Warm Expander	17.05	5.38	5.20	
8	Cold Compressor	15.25	4.59	4.53	
9	Cold Cooler	3.07	0.77	1.92	
10	Cold Expander	7.31	2.31	2.23	
11	Brazed Aluminum Plate Fin Type Heat Exchanger	10.43	10.43	26.23	

Table 4-57 Equipment sizes for the dual N_2 expander cycle (2.0 MTPA)

No.	**Name**	**Dimension of the Equipment**			
		Length	**Breadth /Diameter**	**Height**	**Module**
1	Nitrogen Compressor	14.38	4.54	4.39	Refrigerant Module 1
2	Nitrogen Cooler	6.05	1.51	3.78	
3	Cooler for PMR com.	2.27	1.51	2.27	
4	Overhead crane for PMR com.	14.38	7.38	2.14	
5	Warm Compressor	10.06	3.18	3.07	Refrigerant Module 2
6	Warm Cooler	4.24	1.06	2.65	
7	Warm Expander	10.06	3.18	3.07	
8	Cold Compressor	9.00	2.71	2.67	
9	Cold Cooler	1.81	0.45	1.13	
10	Cold Expander	4.31	1.36	1.32	
11	Brazed Aluminum Plate Fin Type Heat Exchanger	6.16	6.16	15.48	

Table 4-58 Equipment sizes for the dual N_2 expander cycle (1.0 MTPA)

No.	Name	Dimension of the Equipment			
		Length	Breadth /Diameter	Height	Module
1	Nitrogen Compressor	6.79	2.14	2.07	Refrigerant Module 1
2	Nitrogen Cooler	2.86	0.71	1.79	
3	Cooler for PMR com.	1.07	0.71	1.07	
4	Overhead crane for PMR com.	6.79	3.49	1.01	
5	Warm Compressor	4.75	1.50	1.45	Refrigerant Module 2
6	Warm Cooler	2.00	0.50	1.25	
7	Warm Expander	4.75	1.50	1.45	
8	Cold Compressor	4.25	1.28	1.26	
9	Cold Cooler	0.86	0.21	0.54	
10	Cold Expander	2.04	0.64	0.62	
11	Brazed Aluminum Plate Fin Type Heat Exchanger	2.91	2.91	7.31	

5. Optimal Equipment Module Layout for Potential Offshore Liquefaction Cycles

5.1. Introduction

The constraints related to offshore projects such as LNG FPSO have been considered more important than those related to onshore projects because topside process systems are located on a limited hull space (Li, 2010). Therefore, the equipment module layout of LNG FPSO topside equipment should be designed as multi-deck instead of single-deck, and this module layout should be optimized to reduce the area occupied by the topside equipment at the FEED stage.

In the liquefaction process, the separated and pre-treated natural gas is condensed into LNG, which takes up about $1/600^{th}$ the volume of gaseous natural gas. The resulting LNG is stored in atmospheric tanks ready for export by ships. Therefore, the liquefaction process is important in the LNG FPSO topside process system and typically accounts for 70% of the capital cost of such system and 30-40% of the overall plant cost (Shukri, 2004). This study describes an optimal equipment module layout for potential offshore liquefaction cycles. For this purpose, equipment to be placed on the liquefaction process modules is introduced. After that, a mathematical model of the equipment module layout problem is formulated, and the optimal module layouts for the potential offshore liquefaction cycles are determined using MINLP. The layouts obtained for them are compared for simplicity analysis.

5.2. Equipment Module Layout for Potential Offshore Liquefaction Cycles

The liquefaction process cycles can be largely classified as three types of cycles: the cascade liquefaction, MR, and turbine-based cycles (Venkatarathnam, 2008). The DMR cycle as a sort of MR cycle is currently being examined for possible application to LNG FPSO. The DMR cycle pre-cools natural gas with the MRs of ethane, propane, butane, and methane and then liquefies the natural gas with another set of MRs (nitrogen, methane, ethane, and propane), which are responsible for liquefaction and subcooling. This process is well known for having the highest efficiency among the liquefaction cycles (Barclay & Shukri, 2000).

In this paper, the potential MR liquefaction cycle (case 14) from the proposed generic MR liquefaction cycle is considered for the optimal equipment module layout. Three offshore liquefaction cycles — DMR for SHELL LNG FPSO, C_3MR for onshore projects, and the dual N_2 expander for FLEX LNG FPSO — are also considered for comparison with the potential MR liquefaction cycle (case 14), for selecting the optimal offshore liquefaction cycle. The above four liquefaction cycles can be called “potential offshore liquefaction cycles.

5.2.1. Potential MR liquefaction cycle (case 14)

The potential MR LNG liquefaction cycle derived from the proposed generic MR liquefaction cycle is shown in Figure 5-1. The main equipment comprising the potential MR liquefaction cycle are compressors, heat exchangers, seawater coolers, an MR separator, JT valves, tees, and common headers. Additional equipment should be considered for the module layout of the potential MR liquefaction cycle. First of all, a compressor suction drum, dedicated compressor coolers, and an overhead crane are the additional equipment for compressors. The compressor suction drum is installed upstream of a compressor to remove the liquid refrigerant from the two-phase refrigerant, to prevent compressor failure from the incoming liquid flow.

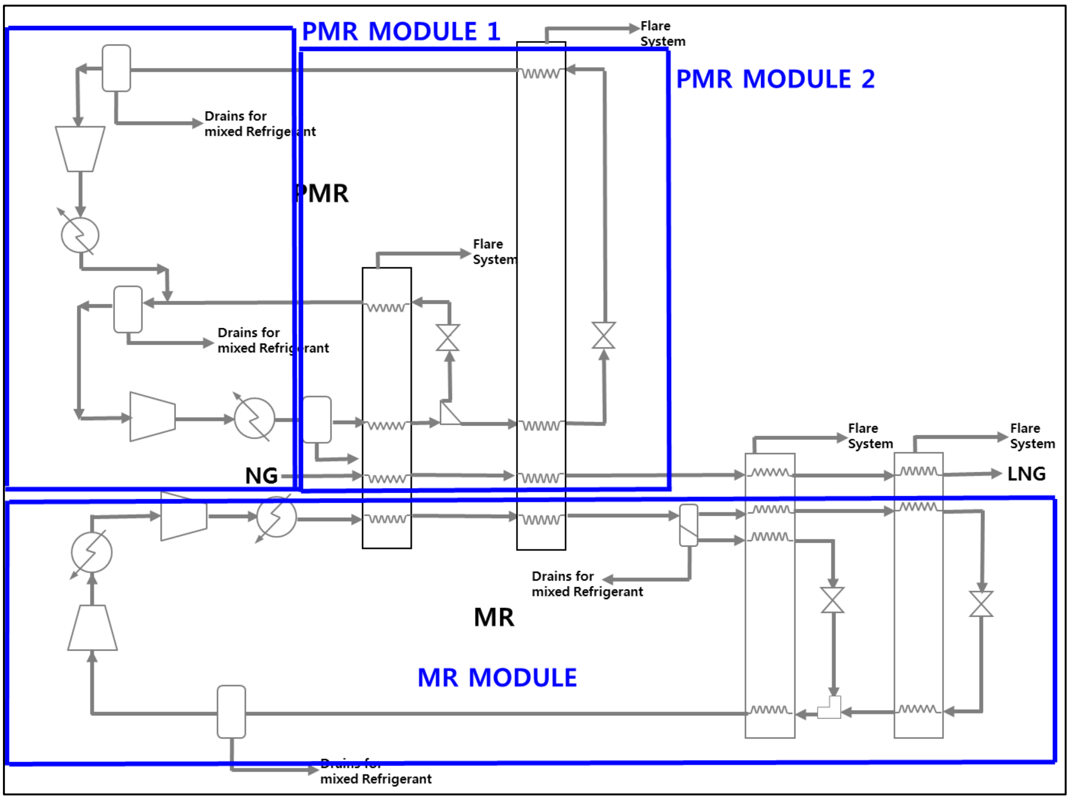

Figure 5-1 Equipment module configurations of the potential MR liquefaction cycle

The dedicated compressor coolers located at the bottom of a compressor can remove the heat from the compressor itself. An overhead crane installed at the upper deck of the compressor can be used to maneuver a very large compressor for maintenance. The additional equipment with respect to heat exchangers is a PMR receiver. A PMR receiver installed between the compressors and heat exchangers has a buffer function, which enables it to continuously supply MRs to the heat exchangers for two to three minutes if the compressors are shut down, and which protects the pipelines from surge impact. In addition, the PMR receiver is used to replace the refrigerant lost through pipe and equipment leakage.

Therefore, the following equipment is considered for the module layout of the potential MR liquefaction cycle. In PMR modules 1 and 2, there is one compressor that has two-stage compression using two impellers, one overhead crane, one dedicated compressor cooler, two suction drums, two seawater coolers, one PMR receiver, two heat exchangers, and two JT valves. The approximate sizes and connection information of this equipment are shown in Figure 5-2 to 5-5 and in Table 5-1 to 5-8.

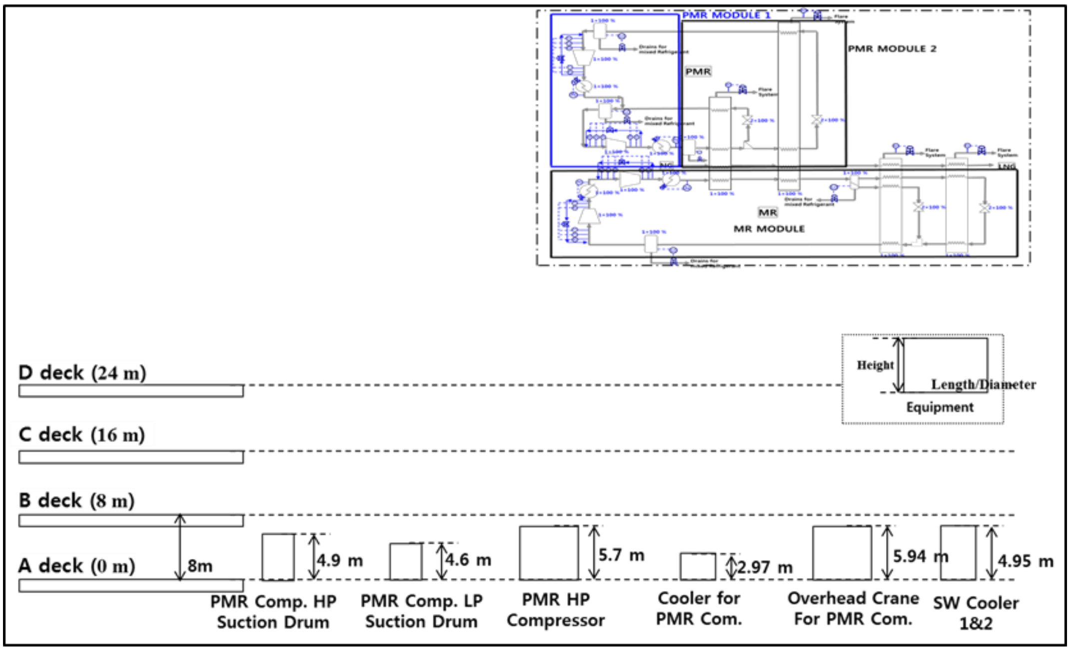

Figure 5-2 Elevated view of PMR module 1 of the potential MR liquefaction cycle

Table 5-1 Equipment sizes for PMR module 1 of the potential MR liquefaction cycle (4.0 MTPA)

No.	Name	Dimension of the Equipment			
		Length	Breadth /Diameter	Height	Module
1	PMR comp. LP suction drum	3.613	3.613	4.603	PMR Module 1
2	PMR comp. HP suction drum	3.217	3.217	4.900	
3	PMR Compressor	18.809	5.939	5.741	
4	Cooler for PMR com.	2.969	1.979	2.969	
5	Overhead crane for PMR com.	22.769	15.839	5.939	
6	SW cooler 1	7.919	1.979	4.949	
7	SW cooler 2	7.919	1.979	4.949	

Table 5-2 Equipment sizes for PMR module 1 of the potential MR liquefaction cycle (3.0 MTPA)

No.	Name	Dimension of the Equipment			
		Length	Breadth /Diameter	Height	Module
1	PMR comp. LP suction drum	2.56	2.56	3.27	PMR Module 1
2	PMR comp. HP suction drum	2.28	2.28	3.48	
3	PMR Compressor	13.35	4.22	4.08	
4	Cooler for PMR com.	2.11	1.40	2.11	
5	Overhead crane for PMR com.	16.16	11.24	4.22	
6	SW cooler 1	5.62	1.40	3.51	
7	SW cooler 2	5.62	1.40	3.51	

Table 5-3 Equipment sizes for PMR module 1 of the potential MR liquefaction cycle (2.0 MTPA)

No.	Name	Dimension of the Equipment			
		Length	Breadth /Diameter	Height	Module
1	PMR comp. LP suction drum	1.66	1.66	2.12	PMR Module 1
2	PMR comp. HP suction drum	1.48	1.48	2.25	
3	PMR Compressor	8.65	2.73	2.64	
4	Cooler for PMR com.	1.37	0.91	1.37	

5	Overhead crane for PMR com.	10.47	7.29	2.73	
6	SW cooler 1	3.64	0.91	2.28	
7	SW cooler 2	3.64	0.91	2.28	

Table 5-4 Equipment sizes for PMR module 1 of the potential MR liquefaction cycle (1.0 MTPA)

No.	**Name**	**Dimension of the Equipment**			
		Length	**Breadth /Diameter**	**Height**	**Module**
1	PMR comp. LP suction drum	0.83	0.83	1.06	PMR Module 1
2	PMR comp. HP suction drum	0.74	0.74	1.13	
3	PMR Compressor	4.33	1.37	1.32	
4	Cooler for PMR com.	0.68	0.46	0.68	
5	Overhead crane for PMR com.	5.24	3.64	1.37	
6	SW cooler 1	1.82	0.46	1.14	
7	SW cooler 2	1.82	0.46	1.14	

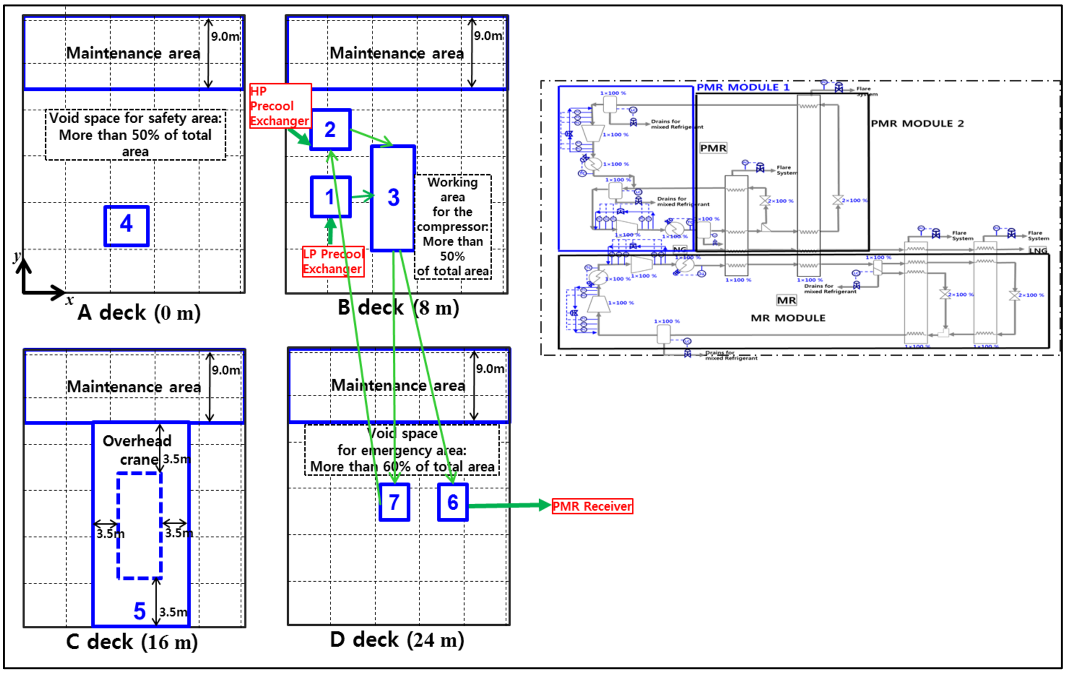

Figure 5-3 Connection information of PMR module 1 of the potential MR liquefaction cycle

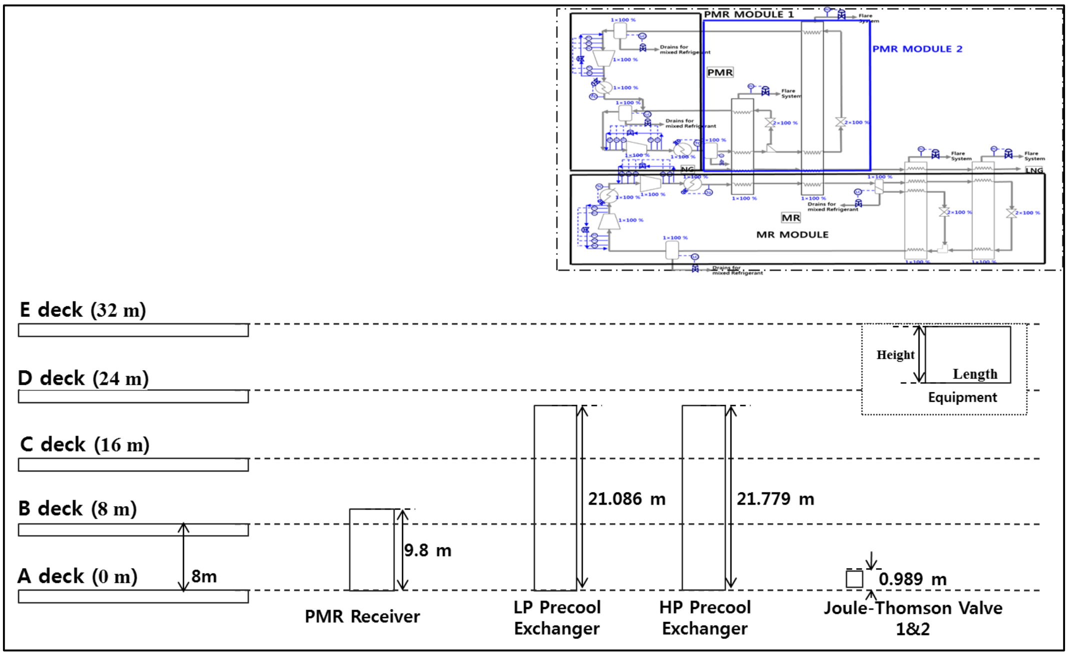

Figure 5-4 Elevated view of PMR module 2 of the potential MR liquefaction cycle

Table 5-5 Equipment sizes for PMR module 2 of the potential MR liquefaction cycle (4.0 MTPA)

No.	Name	Dimension of the Equipment			
		Length	Breadth /Diameter	Height	Module
1	PMR Receiver	4.157	4.157	9.800	PMR Module 2
2	LP Precool Exchanger	4.157	4.157	21.086	
3	HP Precool Exchanger	4.355	4.355	21.779	
4	Joule-Thomson Valve 1	0.989	0.989	0.989	
5	Joule-Thomson Valve 2	0.989	0.989	0.989	

Table 5-6 Equipment sizes for PMR module 2 of the potential MR liquefaction cycle (3.0 MTPA)

No.	Name	Dimension of the Equipment			
		Length	Breadth /Diameter	Height	Module
1	PMR Receiver	2.95	2.95	6.96	PMR

2	LP Precool Exchanger	2.95	2.95	14.97	Module 2
3	HP Precool Exchanger	3.09	3.09	15.46	
4	Joule-Thomson Valve 1	0.70	0.70	0.70	
5	Joule-Thomson Valve 2	0.70	0.70	0.70	

Table 5-7 Equipment sizes for PMR module 2 of the potential MR liquefaction cycle (2.0 MTPA)

No.	**Name**	**Dimension of the Equipment**			
		Length	**Breadth /Diameter**	**Height**	**Module**
1	PMR Receiver	1.91	1.91	4.51	PMR Module 2
2	LP Precool Exchanger	1.91	1.91	9.70	
3	HP Precool Exchanger	2.00	2.00	10.02	
4	Joule-Thomson Valve 1	0.45	0.45	0.45	
5	Joule-Thomson Valve 2	0.45	0.45	0.45	

Table 5-8 Equipment sizes for PMR module 2 of the potential MR liquefaction cycle (1.0 MTPA)

No.	**Name**	**Dimension of the Equipment**			
		Length	**Breadth /Diameter**	**Height**	**Module**
1	PMR Receiver	0.96	0.96	2.25	PMR Module 2
2	LP Precool Exchanger	0.96	0.96	4.85	
3	HP Precool Exchanger	1.00	1.00	5.01	
4	Joule-Thomson Valve 1	0.23	0.23	0.23	
5	Joule-Thomson Valve 2	0.23	0.23	0.23	

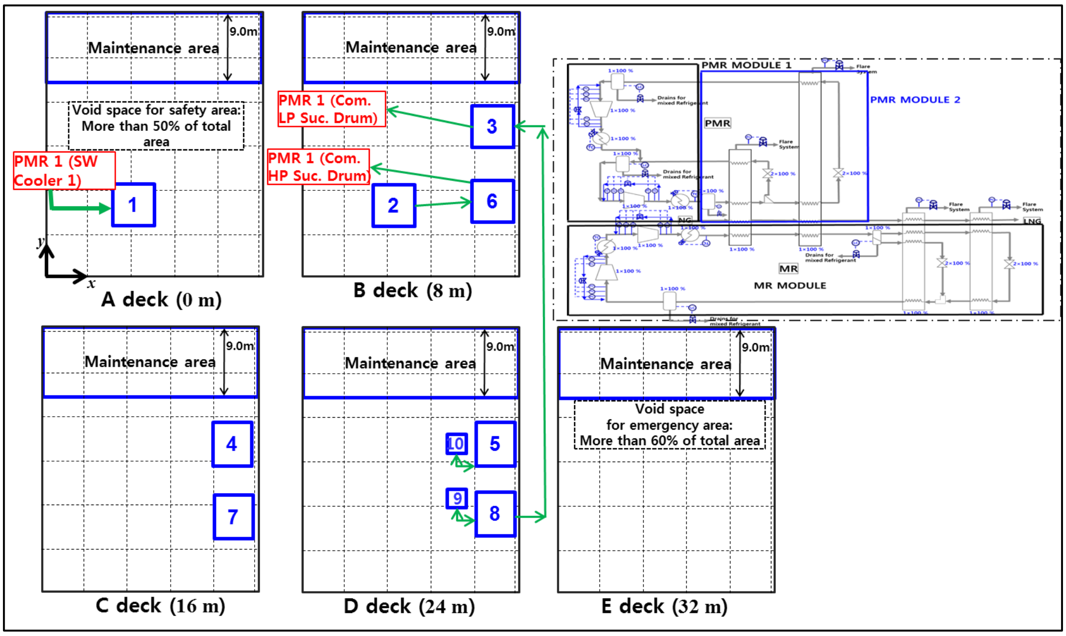

Figure 5-5 Connection information of PMR module 2 of the potential MR liquefaction cycle

The MR module, which takes care of the liquefaction and subcooling, has one compressor with two-stage compression using two impellers, one overhead crane, one dedicated compressor cooler, one suction drum, two seawater coolers, one heat exchanger, two JT valves, and one MR separator. The approximate sizes of this equipment are shown in Figure 5-6 and 5-7 and in Table 5-9 to 5-12.

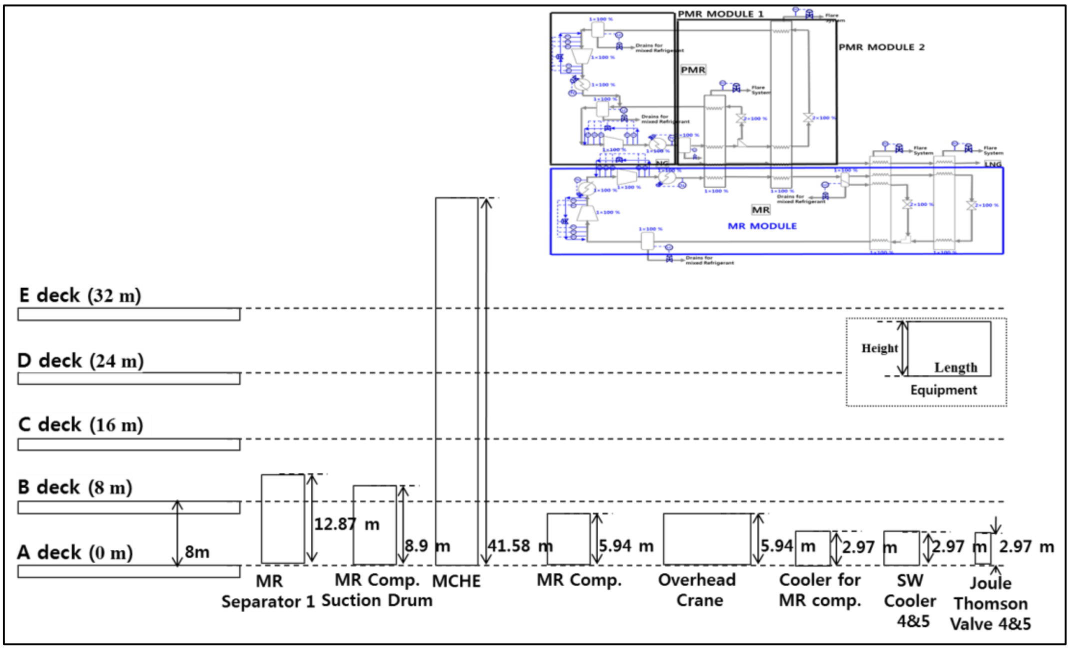

Figure 5-6 Elevated view of the MR module of the potential MR liquefaction cycle

Table 5-9 Equipment sizes for the MR module of the potential MR liquefaction cycle (4.0 MTPA)

No.	Name	Dimension of the Equipment			
		Length	Breadth /Diameter	Height	Module
1	MR Separator 1	4.454	4.454	12.869	MR Module
2	MCHE	5.642	5.642	41.579	
3	MR Comp. Suction Drum	5.444	5.444	8.909	
4	MR Comp.	17.126	5.939	5.939	
5	Cooler for MR comp.	2.969	1.979	2.969	
6	Overhead crane	22.769	15.839	5.939	
7	SW cooler 3	3.959	2.474	2.969	
8	SW cooler 4	3.959	2.474	2.969	
9	Joule-Thomson Valve 3	1.484	1.484	1.484	
10	Joule-Thomson Valve 4	1.484	1.484	1.484	

Table 5-10 Equipment sizes for the MR module of the potential MR liquefaction cycle (3.0 MTPA)

No.	Name	Dimension of the Equipment			
		Length	Breadth /Diameter	Height	Module
1	MR Separator 1	3.16	3.16	9.14	MR Module
2	MCHE	4.01	4.01	29.52	
3	MR Comp. Suction Drum	3.86	3.86	6.32	
4	MR Comp.	12.16	4.22	4.22	
5	Cooler for MR comp.	2.11	1.40	2.11	
6	Overhead crane	16.16	11.24	4.22	
7	SW cooler 3	2.81	1.76	2.11	
8	SW cooler 4	2.81	1.76	2.11	
9	Joule-Thomson Valve 3	1.05	1.05	1.05	
10	Joule-Thomson Valve 4	1.05	1.05	1.05	

Table 5-11 Equipment sizes for the MR module of the potential MR liquefaction cycle (2.0 MTPA)

No.	Name	Dimension of the Equipment			
		Length	Breadth /Diameter	Height	Module
1	MR Separator 1	2.05	2.05	5.92	MR Module
2	MCHE	2.60	2.60	19.13	
3	MR Comp. Suction Drum	2.50	2.50	4.10	
4	MR Comp.	7.88	2.73	2.73	
5	Cooler for MR comp.	1.37	0.91	1.37	
6	Overhead crane	10.47	7.29	2.73	
7	SW cooler 3	1.82	1.14	1.37	
8	SW cooler 4	1.82	1.14	1.37	
9	Joule-Thomson Valve 3	0.68	0.68	0.68	
10	Joule-Thomson Valve 4	0.68	0.68	0.68	

Table 5-12 Equipment sizes for the MR module of the potential MR liquefaction cycle (1.0 MTPA)

No.	Name	Dimension of the Equipment			
		Length	Breadth /Diameter	Height	Module
1	MR Separator 1	1.02	1.02	2.96	MR Module
2	MCHE	1.30	1.30	9.56	
3	MR Comp. Suction Drum	1.25	1.25	2.05	
4	MR Comp.	3.94	1.37	1.37	
5	Cooler for MR comp.	0.68	0.46	0.68	
6	Overhead crane	5.24	3.64	1.37	
7	SW cooler 3	0.91	0.57	0.68	
8	SW cooler 4	0.91	0.57	0.68	
9	Joule-Thomson Valve 3	0.34	0.34	0.34	
10	Joule-Thomson Valve 4	0.34	0.34	0.34	

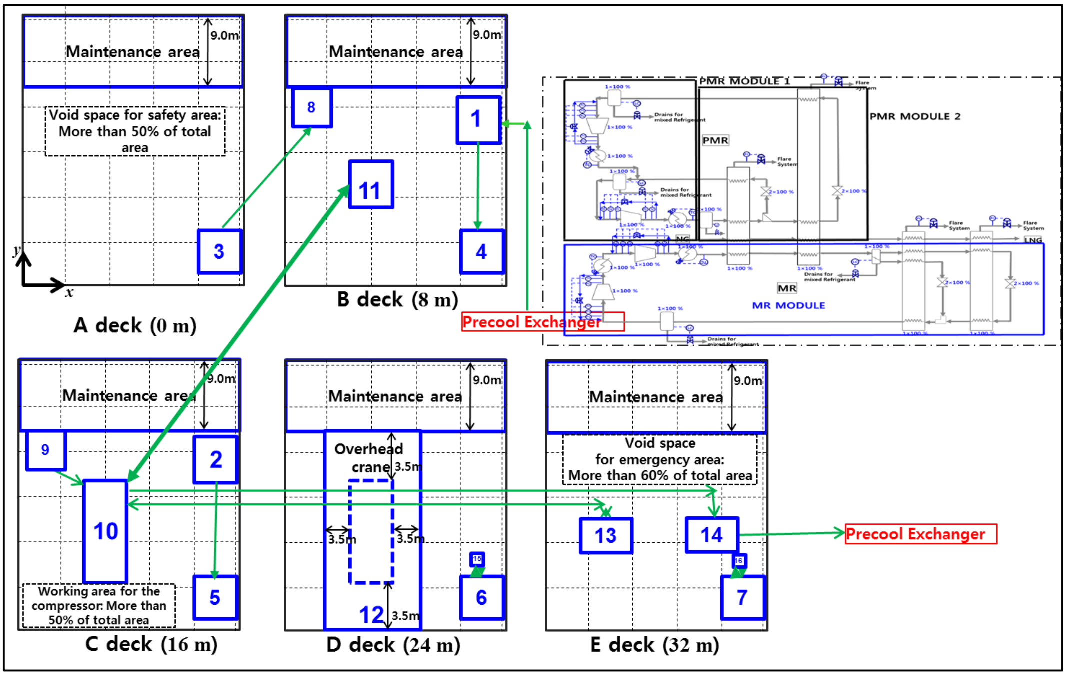

Figure 5-7 Connection information of the MR module of the potential MR liquefaction cycle

The equipment with the same functions should be located on the same module when the equipment is placed topside (Mechlenburgh, 1985), and the equipment should be optimally placed within each module to minimize the available area in each module. As shown in Figure 5-1, the potential MR liquefaction cycle is separately placed on three modules. The first pre-cooling module consists of a two-stage compression compressor, an overhead crane, a dedicated compressor cooler, two suction drums, and two seawater coolers. This module is called "PMR module 1." The second pre-cooling module has a PMR receiver, two PMR heat exchangers, and two JT valves. It is called "PMR module 2." The last module, the main cooling part, consists of a two-stage compression compressor, an overhead crane, a dedicated compressor cooler, a suction drum, two seawater coolers, an MCHE, two JT valves, and an MR separator. This module is called "MR module."

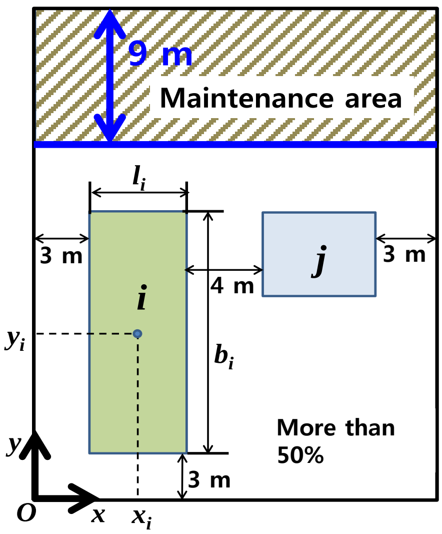

Figure 5-8 Plane view of deck A in the MR module, which has equipment items i and j.

Each module consists of multiple decks, each separated by an 8 m height. PMR module 2 and the MR module are available from deck A to deck E, and PMR module 1 is available from deck A to deck D.

The maintenance area is located from the end of the y direction to 9 m in the direction of origin, to maintain the equipment in each deck (part of the slash-through in Figure 5-8). It is assumed that no equipment can be placed on this maintenance area. Deck A, the lowest deck, and deck C for the MR compressor, make up over 50% of the deck area that is not intended for maintenance or equipment so that there will be a workspace for the workers (uncolored portion in Figure 5-8).

Deck E, the highest deck, has over 60% of the deck area not allocated to maintenance or equipment, for the installation of safety facilities like pressure safety valves (PSVs) and related instrumentation to relieve abnormal pressure in emergency cases.

The minimum distance between the equipment is assumed to be 4 m, and that between the equipment and the deck boundary is assumed to be 3 m, as shown in Figure 5-8. The minimum distance between the maintenance area and the equipment is not considered in this study.

When equipment are to be placed on each module, coolers are considered for the highest decks for each module due to the ventilation of hydrocarbon, and sensitive equipment induced by motion impact (MCHE, pre-cooling heat exchangers, and separators) should be considered for the centerline of the hull, to reduce the motion impact.

5.2.2. DMR cycle

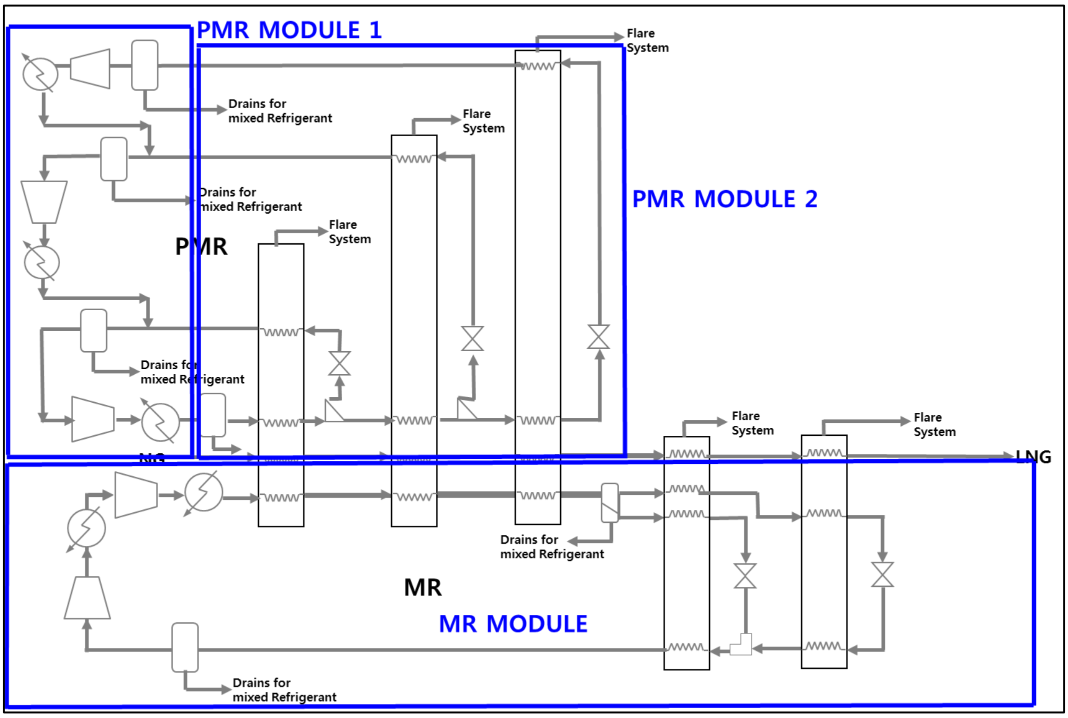

Figure 5-9 Equipment module configurations of the DMR cycle

The DMR cycle that is now being applied for SHELL LNG FPSO is shown in Figure 5-9. The main equipment comprising the DMR cycle includes compressors, heat exchangers, seawater coolers, an MR separator, JT valves, tees, and common headers. Additional equipment should be considered for the module layouts of the DMR cycle. First of all, a compressor suction drum, dedicated compressor coolers, and an overhead crane are the additional equipment for the compressors. The compressor suction drum is installed upstream of a compressor to remove the liquid refrigerant from the two-phase refrigerant so as to prevent compressor failure from the incoming liquid flow. The dedicated compressor coolers located at the bottom of a compressor can remove the heat from the compressor itself. An overhead crane installed at the upper deck of the compressor can be used to maneuver a very large compressor for maintenance. The additional equipment with respect to heat exchangers is a PMR receiver. A PMR receiver installed between the compressors and heat exchangers has a buffer function, which enables it to continuously supply MRs to the heat exchangers for two to three minutes if the compressors are shut down, and which protects the pipelines from surge impact. In addition, the PMR receiver is used to replace the refrigerant lost through pipe and equipment leakage.

Therefore, the following equipment is considered for the module layouts of the DMR cycle. In PMR modules 1 and 2, there is one compressor that has three-stage compression using three impellers, one overhead crane, one dedicated compressor cooler, three suction drums, three seawater coolers, one PMR receiver, three heat exchangers, and three JT valves. The approximate sizes and connection information of this equipment are shown in Figure 5-10 to 5-13 and in Table 5-13 to 5-20.

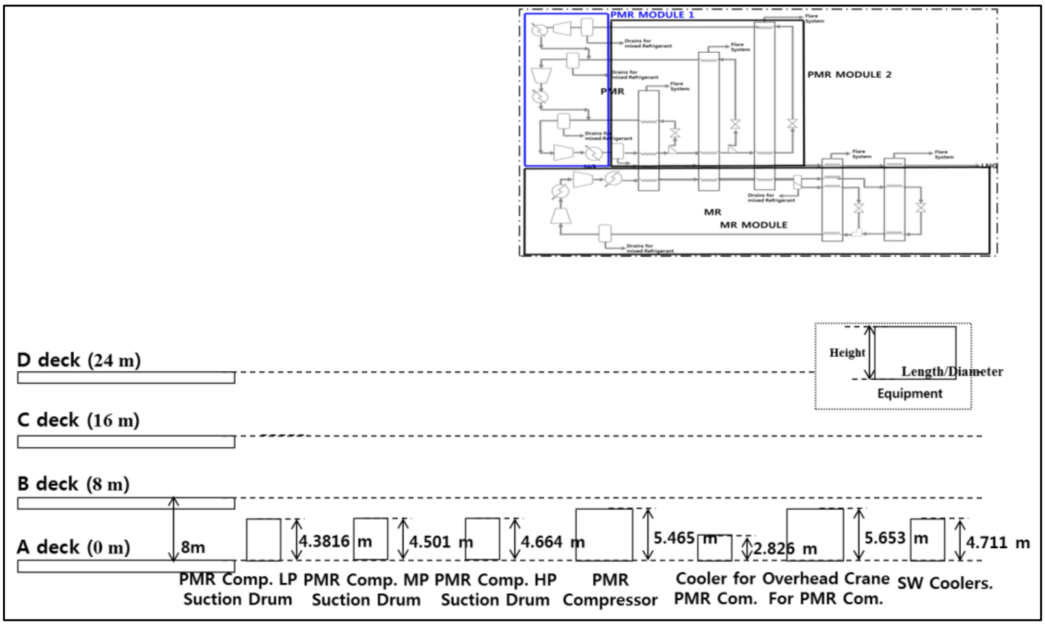

Figure 5-10 Elevated view of PMR module 1 of the DMR cycle

Table 5-13 Equipment sizes for PMR module 1 of the DMR cycle (4.0 MTPA)

No.	Name	Dimension of the Equipment			
		Length	Breadth /Diameter	Height	Module
1	PMR comp. LP suction drum	3.4392	3.4392	4.3816	PMR Module 1
2	PMR comp. MP suction drum	3.2150	3.2150	4.501	
3	PMR comp. HP suction drum	3.0622	3.0622	4.664	
4	PMR Compressor	17.904	5.633	5.465	
5	Cooler for PMR com.	2.826	1.884	2.826	
6	Overhead crane for PMR com.	21.673	15.077	5.653	
7	SW cooler 1	7.538	1.884	4.711	
8	SW cooler 2	7.538	1.884	4.711	
9	SW cooler 3	7.538	1.884	4.711	

Table 5-14 Equipment sizes for PMR module 1 of the DMR cycle (3.0 MTPA)

No.	Name	Dimension of the Equipment			
		Length	Breadth /Diameter	Height	Module
1	PMR comp. LP suction drum	2.41	2.41	3.07	PMR Module 1
2	PMR comp. MP suction drum	2.25	2.25	3.15	
3	PMR comp. HP suction drum	2.14	2.14	3.27	
4	PMR Compressor	12.53	3.94	3.83	
5	Cooler for PMR com.	1.98	1.32	1.98	
6	Overhead crane for PMR com.	15.17	10.56	3.96	
7	SW cooler 1	5.28	1.32	3.30	
8	SW cooler 2	5.28	1.32	3.30	
9	SW cooler 3	5.28	1.32	3.30	

Table 5-15 Equipment sizes for PMR module 1 of the DMR cycle (2.0 MTPA)

No.	Name	Dimension of the Equipment			
		Length	Breadth /Diameter	Height	Module
1	PMR comp. LP suction drum	1.51	1.51	1.93	PMR Module 1
2	PMR comp. MP suction drum	1.41	1.41	1.98	
3	PMR comp. HP suction drum	1.35	1.35	2.05	
4	PMR Compressor	7.88	2.48	2.40	
5	Cooler for PMR com.	1.24	0.83	1.24	
6	Overhead crane for PMR com.	9.54	6.63	2.49	
7	SW cooler 1	3.32	0.83	2.07	
8	SW cooler 2	3.32	0.83	2.07	
9	SW cooler 3	3.32	0.83	2.07	

Table 5-16 Equipment sizes for PMR module 1 of the DMR cycle (1.0 MTPA)

No.	Name	Dimension of the Equipment			
		Length	Breadth /Diameter	Height	Module
1	PMR comp. LP suction drum	0.72	0.72	0.92	PMR Module 1
2	PMR comp. MP suction drum	0.68	0.68	0.95	
3	PMR comp. HP suction drum	0.64	0.64	0.98	
4	PMR Compressor	3.76	1.18	1.15	
5	Cooler for PMR com.	0.59	0.40	0.59	
6	Overhead crane for PMR com.	4.55	3.17	1.19	
7	SW cooler 1	1.58	0.40	0.99	
8	SW cooler 2	1.58	0.40	0.99	
9	SW cooler 3	1.58	0.40	0.99	

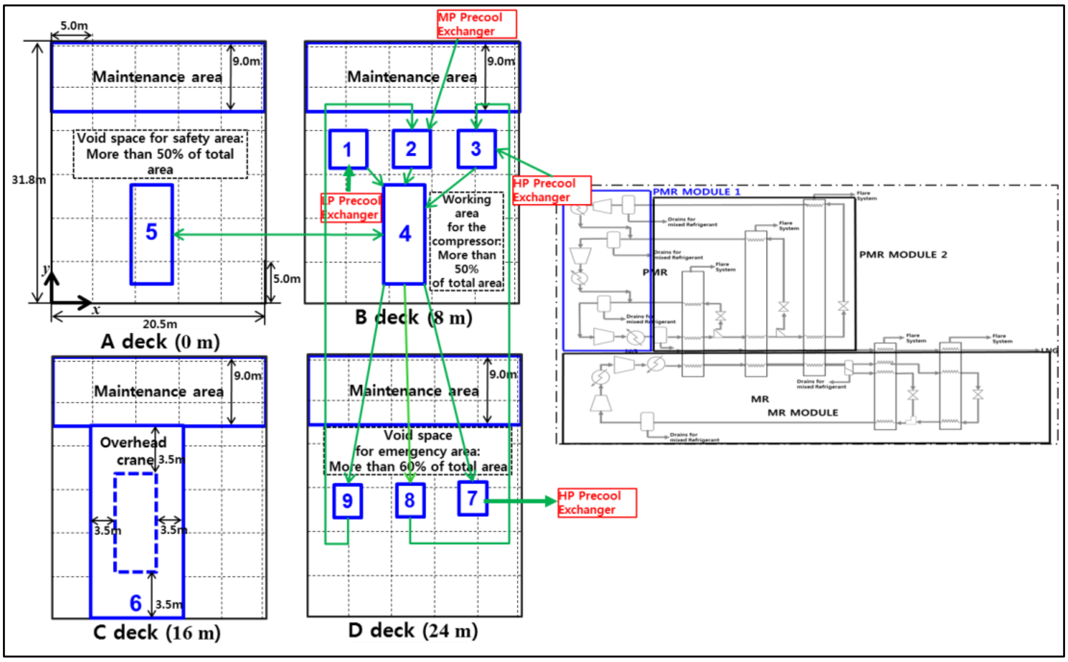

Figure 5-11 Connection information of PMR module 1 of the DMR cycle.

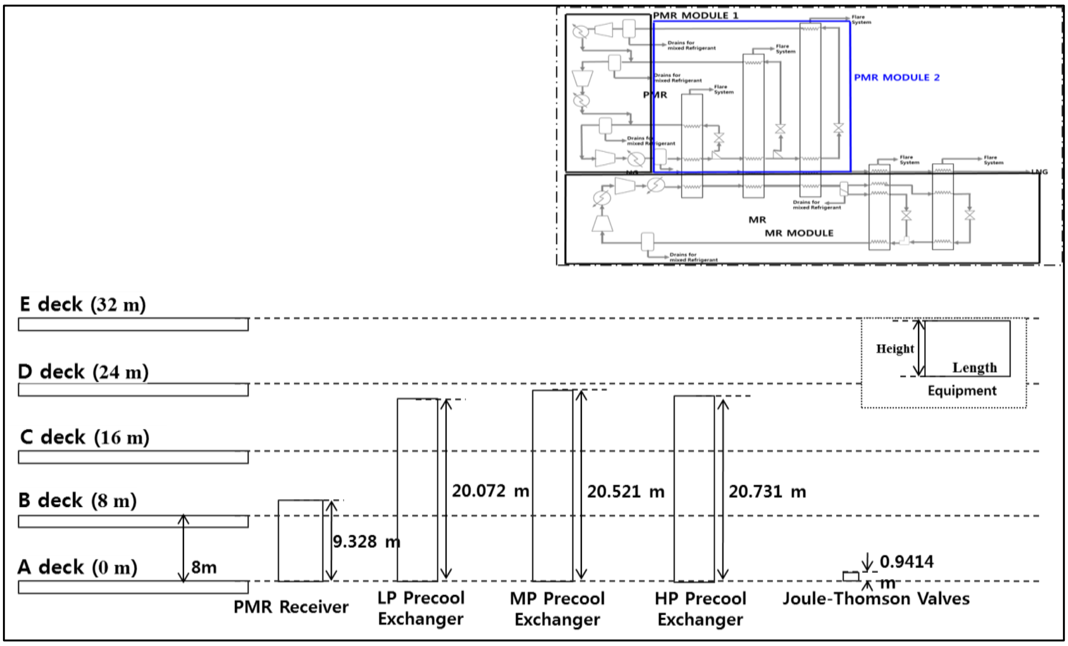

Figure 5-12 Elevated view of PMR module 2 of the DMR cycle

Table 5-17 Equipment sizes for PMR module 2 of the DMR cycle (4.0 MTPA)

No.	Name	Dimension of the Equipment			
		Length	Breadth /Diameter	Height	Module
1	PMR Receiver	3.957	3.957	9.328	PMR Module 2
2	LP Precool Exchanger	3.957	3.957	20.072	
3	MP Precool Exchanger	4.025	4.025	20.521	
4	HP Precool Exchanger	4.145	4.145	20.731	
5	Joule-Thomson Valve 1	0.9414	0.9414	0.9414	
6	Joule-Thomson Valve 2	0.9414	0.9414	0.9414	
7	Joule-Thomson Valve 3	0.9414	0.9414	0.9414	

Table 5-18 Equipment sizes for PMR module 2 of the DMR cycle (3.0 MTPA)

No.	Name	Dimension of the Equipment			
		Length	Breadth /Diameter	Height	Module
1	PMR Receiver	2.77	2.77	6.53	PMR Module 2
2	LP Precool Exchanger	2.77	2.77	14.05	
3	MP Precool Exchanger	2.82	2.82	14.37	
4	HP Precool Exchanger	2.90	2.90	14.51	
5	Joule-Thomson Valve 1	0.66	0.66	0.66	
6	Joule-Thomson Valve 2	0.66	0.66	0.66	
7	Joule-Thomson Valve 3	0.66	0.66	0.66	

Table 5-19 Equipment sizes for PMR module 2 of the DMR cycle (2.0 MTPA)

No.	Name	Dimension of the Equipment			
		Length	Breadth /Diameter	Height	Module
1	PMR Receiver	1.74	1.74	4.10	PMR Module 2
2	LP Precool Exchanger	1.74	1.74	8.83	
3	MP Precool Exchanger	1.77	1.77	9.03	
4	HP Precool Exchanger	1.82	1.82	9.12	

5	Joule-Thomson Valve 1	0.41	0.41	0.41	
6	Joule-Thomson Valve 2	0.41	0.41	0.41	
7	Joule-Thomson Valve 3	0.41	0.41	0.41	

Table 5-20 Equipment sizes for PMR module 2 of the DMR cycle (1.0 MTPA)

No.	Name	Dimension of the Equipment			
		Length	Breadth /Diameter	Height	Module
1	PMR Receiver	0.83	0.83	1.96	PMR Module 2
2	LP Precool Exchanger	0.83	0.83	4.22	
3	MP Precool Exchanger	0.85	0.85	4.31	
4	HP Precool Exchanger	0.87	0.87	4.35	
5	Joule-Thomson Valve 1	0.20	0.20	0.20	
6	Joule-Thomson Valve 2	0.20	0.20	0.20	
7	Joule-Thomson Valve 3	0.20	0.20	0.20	

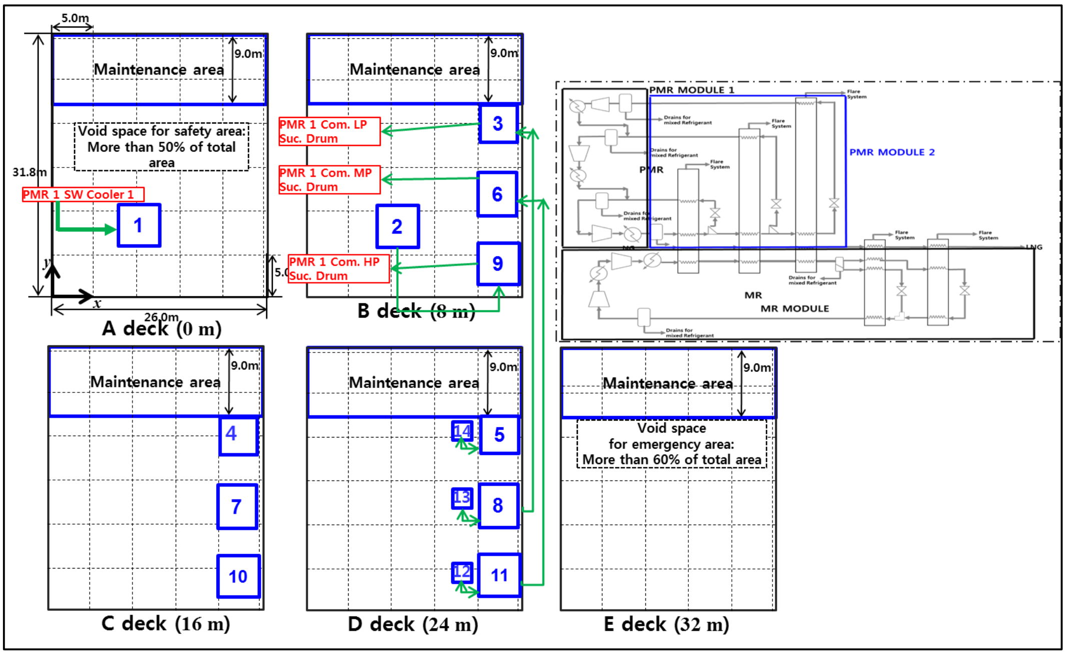

Figure 5-13 Connection information of PMR module 2 of the DMR cycle

The MR module, which takes care of the liquefaction and subcooling, has one compressor with two-stage compression using two impellers, one overhead crane, one dedicated compressor cooler, one suction drum, two seawater coolers, one heat exchanger, two JT valves, and one MR separator. The approximate sizes of this equipment are shown in Figure 5-14 and 5-21 and in Table 5-24.

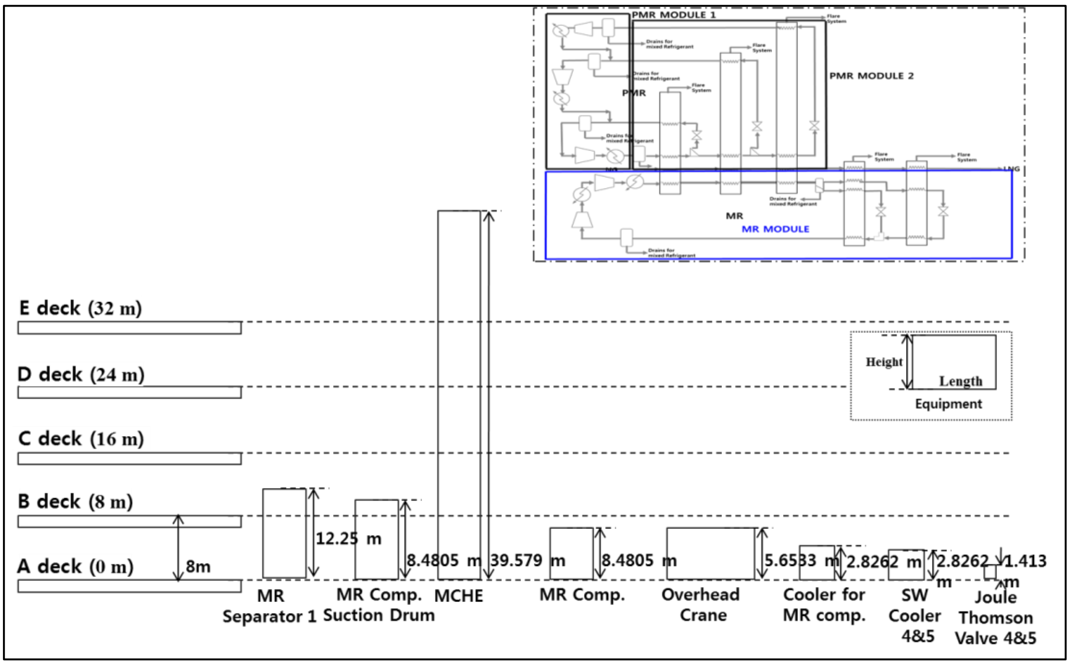

Figure 5-14 Elevated view of the MR module of the DMR cycle

Table 5-21 Equipment sizes for the MR module of the DMR cycle (4.0 MTPA)

No.	Name	Dimension of the Equipment			
		Length	Breadth /Diameter	Height	Module
1	MR Separator 1	4.2397	4.2397	12.25	MR Module
2	MCHE	5.3706	5.3706	39.579	
3	MR Comp. Suction Drum	5.1821	5.1821	8.4805	
4	MR Comp.	16.3022	5.6533	5.6533	
5	Cooler for MR comp.	2.8262	1.884	2.8262	
6	Overhead crane	21.6738	15.0771	5.6533	

7	SW cooler 4	3.7686	2.355	2.8262	
8	SW cooler 5	3.7686	2.355	2.8262	
9	Joule-Thomson Valve 4	1.413	1.413	1.413	
10	Joule-Thomson Valve 5	1.413	1.413	1.413	

Table 5-22 Equipment sizes for the MR module of the DMR cycle (3.0 MTPA)

No.	**Name**	**Dimension of the Equipment**			
		Length	**Breadth /Diameter**	**Height**	**Module**
1	MR Separator 1	2.97	2.97	8.58	MR Module
2	MCHE	3.76	3.76	27.71	
3	MR Comp. Suction Drum	3.63	3.63	5.94	
4	MR Comp.	11.41	3.96	3.96	
5	Cooler for MR comp.	1.98	1.32	1.98	
6	Overhead crane	15.17	10.56	3.96	
7	SW cooler 4	2.64	1.65	1.98	
8	SW cooler 5	2.64	1.65	1.98	
9	Joule-Thomson Valve 4	0.99	0.99	0.99	
10	Joule-Thomson Valve 5	0.99	0.99	0.99	

Table 5-23 Equipment sizes for the MR module of the DMR cycle (2.0 MTPA)

No.	**Name**	**Dimension of the Equipment**			
		Length	**Breadth /Diameter**	**Height**	**Module**
1	MR Separator 1	1.87	1.87	5.39	MR Module
2	MCHE	2.36	2.36	17.41	
3	MR Comp. Suction Drum	2.28	2.28	3.73	
4	MR Comp.	7.17	2.49	2.49	
5	Cooler for MR comp.	1.24	0.83	1.24	
6	Overhead crane	9.54	6.63	2.49	
7	SW cooler 4	1.66	1.04	1.24	
8	SW cooler 5	1.66	1.04	1.24	
9	Joule-Thomson Valve 4	0.62	0.62	0.62	
10	Joule-Thomson Valve 5	0.62	0.62	0.62	

Table 5-24 Equipment sizes for the MR module of the DMR cycle (1.0 MTPA)

No.	Name	Dimension of the Equipment			
		Length	Breadth /Diameter	Height	Module
1	MR Separator 1	0.89	0.89	2.57	MR Module
2	MCHE	1.13	1.13	8.31	
3	MR Comp. Suction Drum	1.09	1.09	1.78	
4	MR Comp.	3.42	1.19	1.19	
5	Cooler for MR comp.	0.59	0.40	0.59	
6	Overhead crane	4.55	3.17	1.19	
7	SW cooler 4	0.79	0.49	0.59	
8	SW cooler 5	0.79	0.49	0.59	
9	Joule-Thomson Valve 4	0.30	0.30	0.30	
10	Joule-Thomson Valve 5	0.30	0.30	0.30	

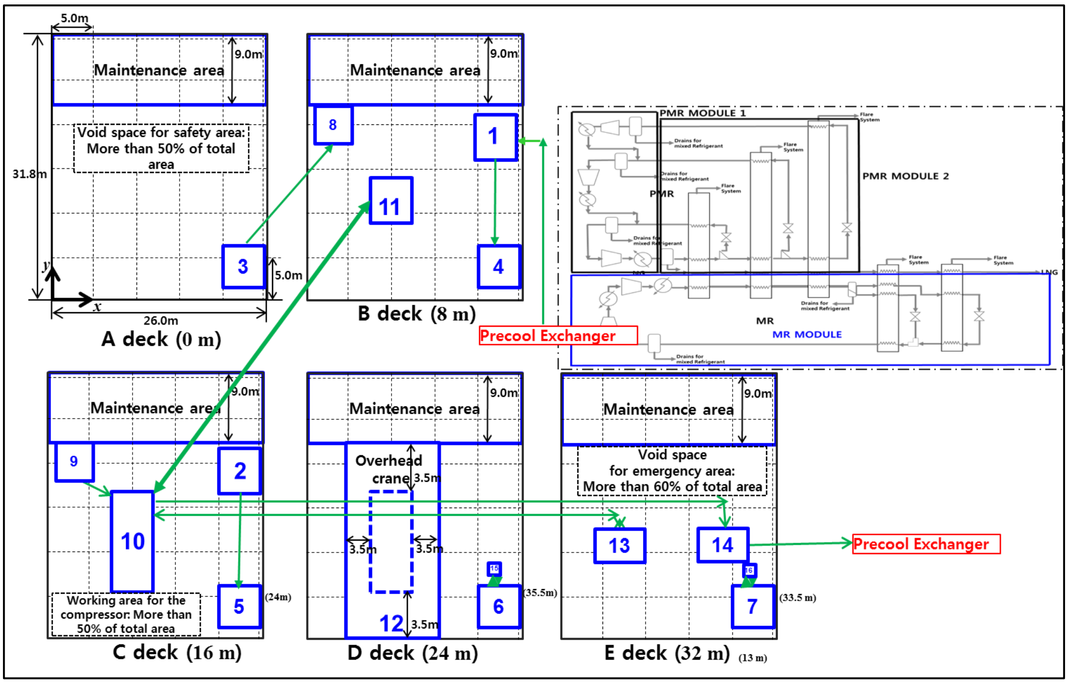

Figure 5-15 Connection information of the MR module of the DMR cycle

As shown in Figure 5-9, the DMR cycle is separately placed on three modules. The first pre-cooling module consists of a three-stage compression compressor, an overhead crane, a dedicated compressor cooler, three suction drums, and three seawater coolers. This module is called “PMR module 1.” The second pre-cooling module has a PMR receiver, three PMR heat exchangers, and three JT valves. It is called “PMR module 2.” The last module, the main cooling part, consists of a two-stage compression compressor, an overhead crane, a dedicated compressor cooler, a suction drum, two seawater coolers, an MCHE, two JT valves, and an MR separator. This module is called “MR module.”

Each module consists of multiple decks, each separated by an 8 m height. PMR module 2 and the MR module are available from deck A to deck E, and PMR module 1 is available from deck A to deck D.

5.2.3. C_3MR cycle

The C_3MR cycle widely used for onshore LNG plants is shown in Figure 5-16. The main equipment comprising the C_3MR cycle are compressors, heat exchangers, seawater coolers, an MR separator, JT valves, tees, and common headers. Additional equipment should be considered for the module layouts of the C_3MR cycle. First of all, a compressor suction drum, dedicated compressor coolers, and an overhead crane are the additional equipment for the compressors. The compressor suction drum is installed upstream of a compressor to remove the liquid refrigerant from the two-phase refrigerant to prevent compressor failure from the incoming liquid flow. The dedicated compressor coolers located at the bottom of a compressor can remove the heat from the compressor itself. An overhead crane installed at the upper deck of the compressor can be used to maneuver a very large compressor for maintenance. The additional equipment with respect to the heat exchangers is a PMR receiver. A PMR receiver installed between the compressors and heat exchangers has a buffer function, which enables it to continuously supply MRs to the heat exchangers for two to three minutes if the compressors are shut down, and which protects the pipelines from surge impact. In addition, the PMR receiver is used to replace the refrigerant lost through pipe and equipment leakage.

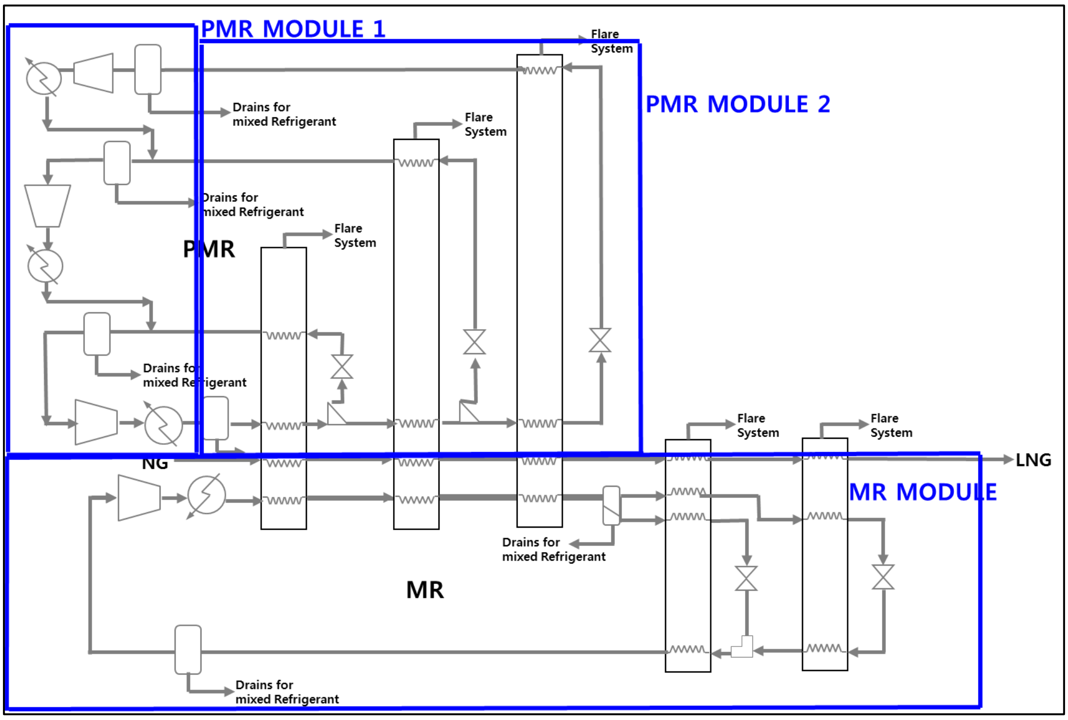

Figure 5-16 Equipment module configurations of the C_3MR cycle

Therefore, the following equipment is considered for the module layouts of the C_3MR cycle. In PMR modules 1 and 2, there is one compressor that has three-stage compression using three impellers, one overhead crane, one dedicated compressor cooler, three suction drums, three seawater coolers, one PMR receiver, three heat exchangers, and three JT valves. The approximate sizes and connection information of this equipment are shown in Figure 5-17 to 5-20 and in Table 5-25 to 5-32.

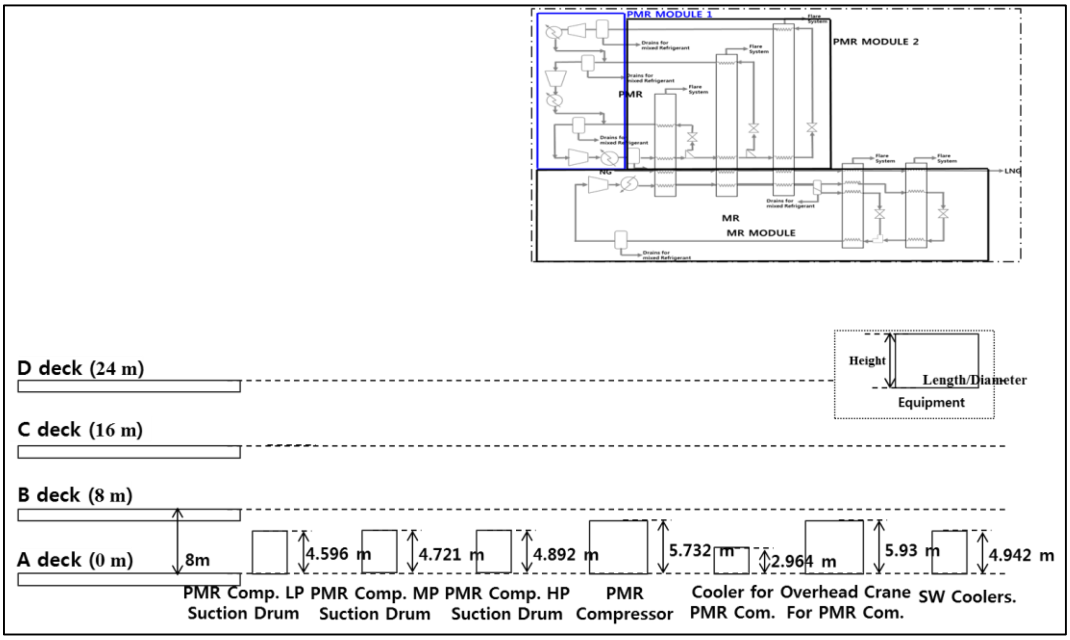

Figure 5-17 Elevated view of PMR module 1 of the C_3MR cycle

Table 5-25 Equipment sizes for PMR module 1 of the C_3MR cycle (4.0 MTPA)

No.	Name	Dimension of the Equipment			
		Length	Breadth /Diameter	Height	Module
1	PMR comp. LP suction drum	3.6075	3.608	4.596	PMR Module 1
2	PMR comp. MP suction drum	3.3723	3.372	4.721	
3	PMR comp. HP suction drum	3.2120	3.212	4.892	
4	PMR Compressor	18.7801	5.909	5.732	
5	Cooler for PMR com.	2.9643	1.976	2.964	
6	Overhead crane for PMR com.	22.734	15.815	5.93	
7	SW cooler 1	7.907	1.9762	4.942	
8	SW cooler 2	7.907	1.9762	4.942	
9	SW cooler 3	7.907	1.9762	4.942	

Table 5-26 Equipment sizes for PMR module 1 of the C_3MR cycle (3.0 MTPA)

No.	**Name**	**Dimension of the Equipment**			
		Length	**Breadth /Diameter**	**Height**	**Module**
1	PMR comp. LP suction drum	2.45	2.45	3.12	PMR Module 1
2	PMR comp. MP suction drum	2.29	2.29	3.21	
3	PMR comp. HP suction drum	2.18	2.18	3.32	
4	PMR Compressor	12.76	4.02	3.90	
5	Cooler for PMR com.	2.01	1.34	2.01	
6	Overhead crane for PMR com.	15.45	10.75	4.03	
7	SW cooler 1	5.37	1.34	3.36	
8	SW cooler 2	5.37	1.34	3.36	
9	SW cooler 3	5.37	1.34	3.36	

Table 5-27 Equipment sizes for PMR module 1 of the C_3MR cycle (2.0 MTPA)

No.	**Name**	**Dimension of the Equipment**			
		Length	**Breadth /Diameter**	**Height**	**Module**
1	PMR comp. LP suction drum	2.00	2.00	5.78	PMR Module 1
2	PMR comp. MP suction drum	2.53	2.53	18.68	
3	PMR comp. HP suction drum	2.45	2.45	4.00	
4	PMR Compressor	7.70	2.67	2.67	
5	Cooler for PMR com.	1.33	0.89	1.33	
6	Overhead crane for PMR com.	10.23	7.12	2.67	
7	SW cooler 1	1.78	1.11	1.33	
8	SW cooler 2	0.67	0.67	0.67	
9	SW cooler 3	0.67	0.67	0.67	

Table 5-28 Equipment sizes for PMR module 1 of the C_3MR cycle (1.0 MTPA)

No.	**Name**	**Dimension of the Equipment**			
		Length	**Breadth /Diameter**	**Height**	**Module**

1	PMR comp. LP suction drum	0.79	0.79	1.01	PMR Module 1
2	PMR comp. MP suction drum	0.74	0.74	1.04	
3	PMR comp. HP suction drum	0.71	0.71	1.08	
4	PMR Compressor	4.13	1.30	1.26	
5	Cooler for PMR com.	0.65	0.43	0.65	
6	Overhead crane for PMR com.	5.00	3.48	1.30	
7	SW cooler 1	1.74	0.43	1.09	
8	SW cooler 2	1.74	0.43	1.09	
9	SW cooler 3	1.74	0.43	1.09	

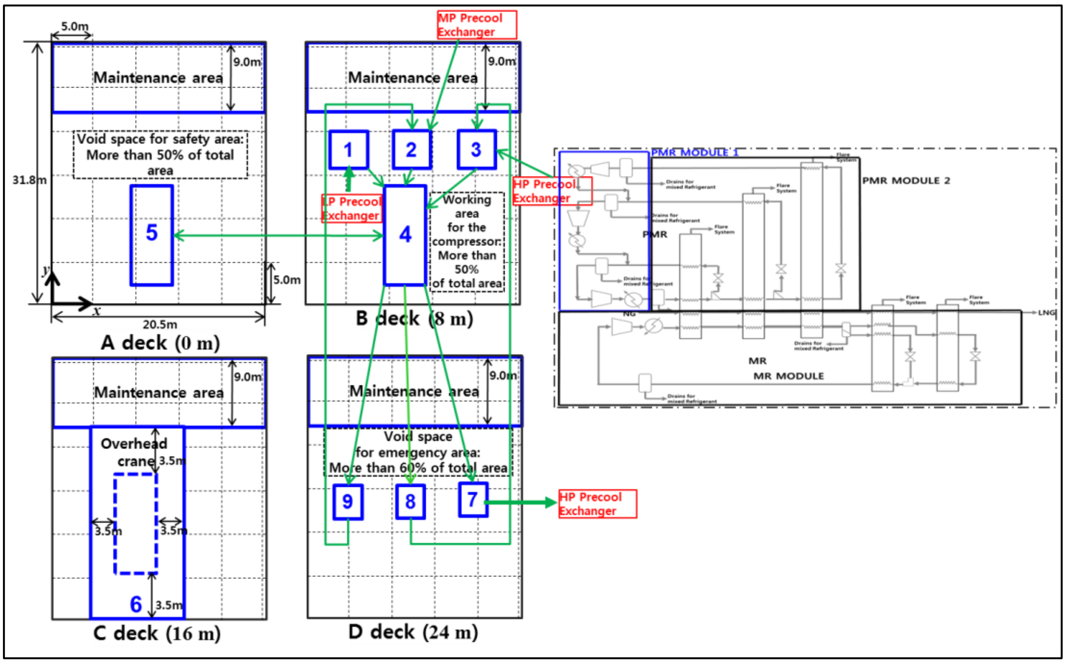

Figure 5-18 Connection information of PMR module 1 of the C_3MR cycle

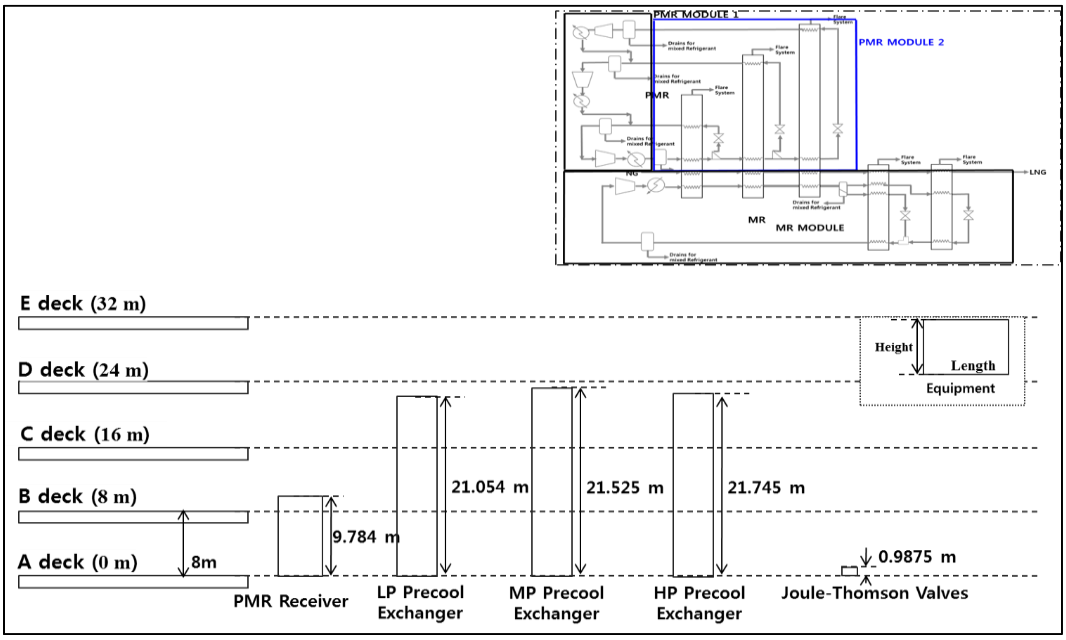

Figure 5-19 Elevated view of PMR module 2 of the C_3MR cycle

Table 5-29 Equipment sizes for PMR module 2 of the C_3MR cycle (4.0 MTPA)

No.	Name	Dimension of the Equipment			
		Length	Breadth /Diameter	Height	Module
1	PMR Receiver	4.151	4.151	9.784	PMR Module 2
2	LP Precool Exchanger	4.151	4.151	21.054	
3	MP Precool Exchanger	4.222	4.222	21.525	
4	HP Precool Exchanger	4.348	4.348	21.745	
5	Joule-Thomson Valve 1	0.987	0.9875	0.9875	
6	Joule-Thomson Valve 2	0.987	0.9875	0.9875	
7	Joule-Thomson Valve 3	0.987	0.9875	0.9875	

Table 5-30 Equipment sizes for PMR module 2 of the C_3MR cycle (3.0 MTPA)

No.	Name	Dimension of the Equipment			
		Length	Breadth /Diameter	Height	Module
1	PMR Receiver	2.82	2.82	6.65	PMR Module 2
2	LP Precool Exchanger	2.82	2.82	14.31	
3	MP Precool Exchanger	2.87	2.87	14.63	
4	HP Precool Exchanger	2.95	2.95	14.78	
5	Joule-Thomson Valve 1	0.67	0.67	0.67	
6	Joule-Thomson Valve 2	0.67	0.67	0.67	
7	Joule-Thomson Valve 3	0.67	0.67	0.67	

Table 5-31 Equipment sizes for PMR module 2 of the C_3MR cycle (2.0 MTPA)

No.	Name	Dimension of the Equipment			
		Length	Breadth /Diameter	Height	Module
1	PMR Receiver	1.87	1.87	4.40	PMR Module 2
2	LP Precool Exchanger	1.87	1.87	9.47	
3	MP Precool Exchanger	1.90	1.90	9.69	
4	HP Precool Exchanger	1.96	1.96	9.79	
5	Joule-Thomson Valve 1	0.44	0.44	0.44	
6	Joule-Thomson Valve 2	0.44	0.44	0.44	
7	Joule-Thomson Valve 3	0.44	0.44	0.44	

Table 5-32 Equipment sizes for PMR module 2 of the C_3MR cycle (1.0 MTPA)

No.	Name	Dimension of the Equipment			
		Length	Breadth /Diameter	Height	Module
1	PMR Receiver	0.91	0.91	2.15	PMR Module 2
2	LP Precool Exchanger	0.91	0.91	4.63	
3	MP Precool Exchanger	0.93	0.93	4.74	
4	HP Precool Exchanger	0.96	0.96	4.78	

5	Joule-Thomson Valve 1	0.22	0.22	0.22	
6	Joule-Thomson Valve 2	0.22	0.22	0.22	
7	Joule-Thomson Valve 3	0.22	0.22	0.22	

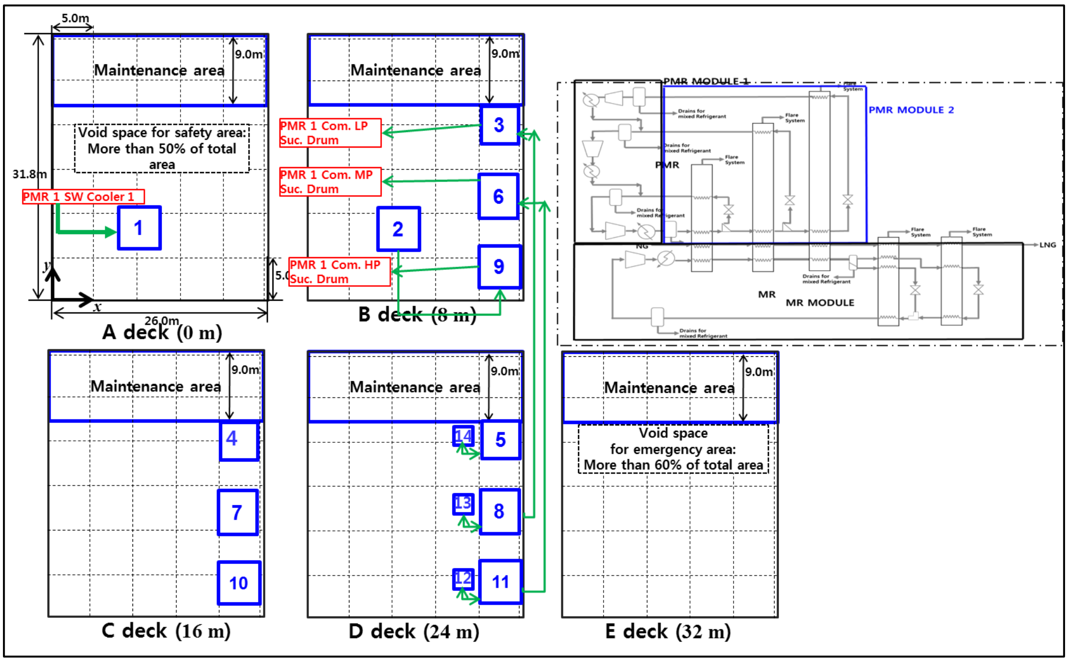

Figure 5-20 Connection information of PMR module 2 of the C_3MR cycle

The MR module, which takes care of the liquefaction and subcooling, has one compressor with two-stage compression using two impellers, one overhead crane, one dedicated compressor cooler, one suction drum, one seawater cooler, one heat exchanger, two JT valves, and one MR separator. The approximate sizes of this equipment are shown in Figure 5-21 and 5-22 and in Table 5-33 to 5-36.

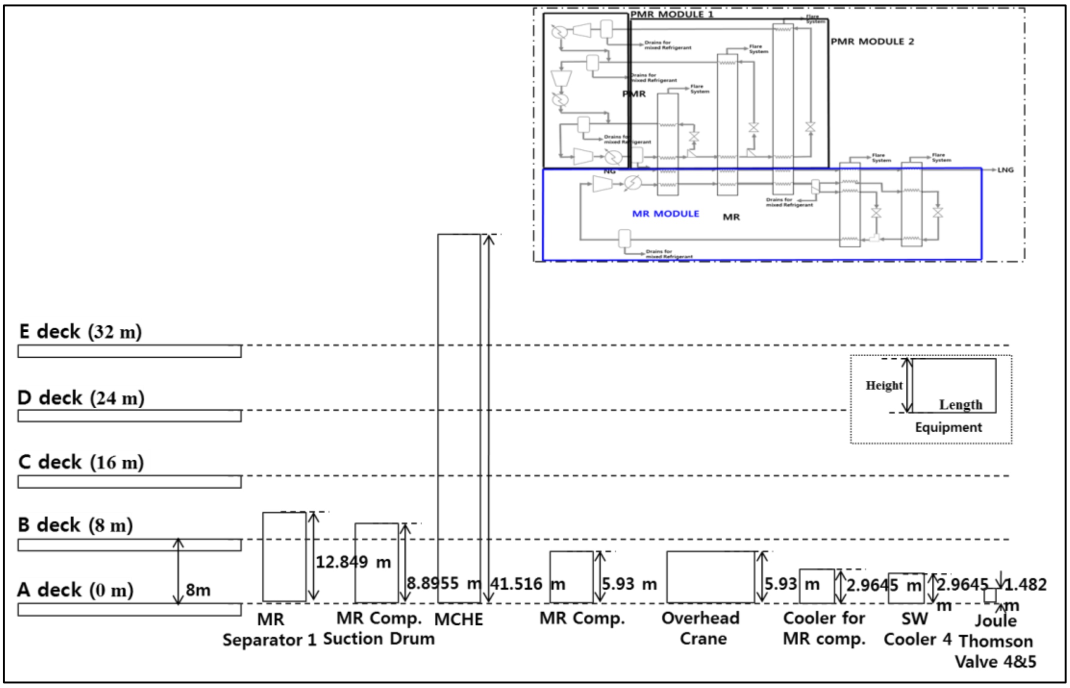

Figure 5-21 Elevated view of the MR module of the C_3MR cycle

Table 5-33 Equipment sizes for the MR module of the C_3MR cycle (4.0 MTPA)

No.	Name	Dimension of the Equipment			
		Length	**Breadth /Diameter**	**Height**	**Module**
1	MR Separator 1	4.447	4.447	12.849	MR Module
2	MCHE	5.633	5.633	41.516	
3	MR Comp. Suction Drum	5.436	5.436	8.8955	
4	MR Comp.	17.1	5.93	5.93	
5	Cooler for MR comp.	2.964	1.976	2.9645	
6	Overhead crane	22.734	15.815	5.93	
7	SW cooler 4	3.953	2.47	2.9645	
8	Joule-Thomson Valve 4	1.482	1.482	1.482	
9	Joule-Thomson Valve 5	1.482	1.482	1.482	

Table 5-34 Equipment sizes for the MR module of the C_3MR cycle (3.0 MTPA)

No.	Name	Dimension of the Equipment			
		Length	Breadth /Diameter	Height	Module
1	MR Separator 1	3.02	3.02	8.73	MR Module
2	MCHE	3.83	3.83	28.21	
3	MR Comp. Suction Drum	3.69	3.69	6.05	
4	MR Comp.	11.62	4.03	4.03	
5	Cooler for MR comp.	2.01	1.34	2.01	
6	Overhead crane	15.45	10.75	4.03	
7	SW cooler 4	2.69	1.68	2.01	
8	Joule-Thomson Valve 4	1.01	1.01	1.01	
9	Joule-Thomson Valve 5	1.01	1.01	1.01	

Table 5-35 Equipment sizes for the MR module of the C_3MR cycle (2.0 MTPA)

No.	Name	Dimension of the Equipment			
		Length	Breadth /Diameter	Height	Module
1	MR Separator 1	2.00	2.00	5.78	MR Module
2	MCHE	2.53	2.53	18.68	
3	MR Comp. Suction Drum	2.45	2.45	4.00	
4	MR Comp.	7.70	2.67	2.67	
5	Cooler for MR comp.	1.33	0.89	1.33	
6	Overhead crane	10.23	7.12	2.67	
7	SW cooler 4	1.78	1.11	1.33	
8	Joule-Thomson Valve 4	0.67	0.67	0.67	
9	Joule-Thomson Valve 5	0.67	0.67	0.67	

Table 5-36 Equipment sizes for the MR module of the C_3MR cycle (1.0 MTPA)

No.	Name	Dimension of the Equipment			
		Length	Breadth /Diameter	Height	Module
1	MR Separator 1	0.98	0.98	2.83	MR Module
2	MCHE	1.24	1.24	9.13	
3	MR Comp. Suction Drum	1.20	1.20	1.96	
4	MR Comp.	3.76	1.30	1.30	
5	Cooler for MR comp.	0.65	0.43	0.65	
6	Overhead crane	5.00	3.48	1.30	
7	SW cooler 4	0.87	0.54	0.65	
8	Joule-Thomson Valve 4	0.33	0.33	0.33	
9	Joule-Thomson Valve 5	0.33	0.33	0.33	

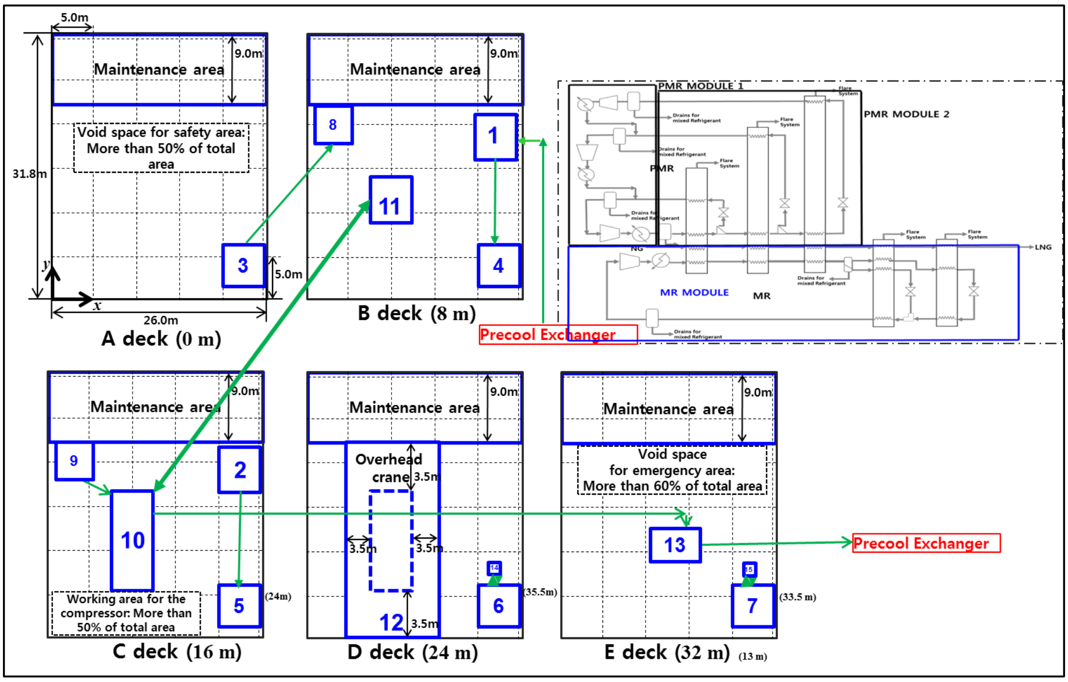

Figure 5-22 Connection information of the MR module of the C_3MR cycle

As shown in Figure 5-16, the C_3MR cycle is separately placed on three modules. The first pre-cooling module consists of a three-stage compression compressor, an overhead crane, a dedicated compressor cooler, three suction drums, and three seawater coolers. This module is called “PMR module 1.” The second pre-cooling module has a PMR receiver, three PMR heat exchangers, and three JT valves. It is called “PMR module 2.” The last module, the main cooling part, consists of a two-stage compression compressor, an overhead crane, a dedicated compressor cooler, a suction drum, a seawater cooler, an MCHE, two JT valves, and an MR separator. This module is called “MR module.”

Each module consists of multiple decks, each separated by an 8 m height. PMR module 2 and the MR module are available from deck A to deck E, and PMR module 1 is available from deck A to deck D.

5.2.4. Dual N2 expander cycle

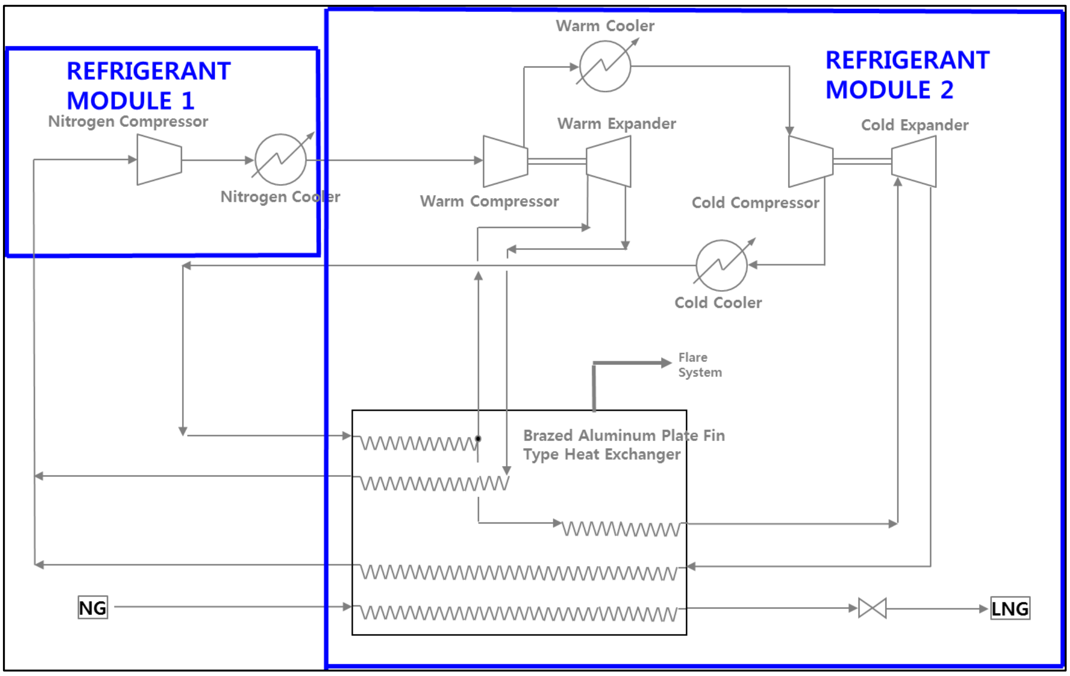

Figure 5-23 Equipment module configurations of the dual N_2 expander cycle

The dual N_2 expander cycle that is now being applied for FLEX LNG FPSO is shown in Figure 5-23. The main equipment comprising the dual N_2 expander cycle are compressors, heat exchangers, seawater coolers, expander, tees, and common headers. Additional equipment should be considered for the module layouts of the dual N_2 expander cycle. First of all, the dedicated compressor coolers and an overhead crane are the additional equipment for the compressors. The dedicated compressor coolers located at the bottom of a compressor can remove the heat from the compressor itself. An overhead crane installed at the upper deck of the compressor can be used to maneuver a very large compressor for maintenance.

Therefore, the following equipment is considered for the module layouts of the dual

N_2 expander cycle. In refrigerant module 1, there is one compressor that has one-stage compression using one impeller, one overhead crane, one dedicated compressor cooler, and a seawater cooler. The approximate sizes and connection information of this equipment are shown in Figure 5-24 and 5-25 and in Table 5-37 to 5-40.

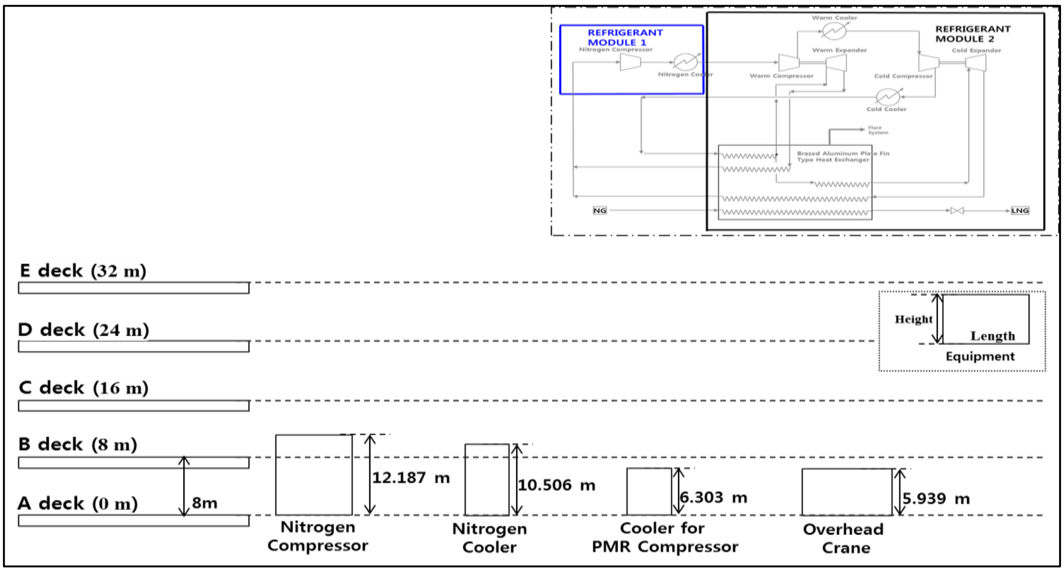

Figure 5-24 Elevated view of refrigerant module 1 of the dual N_2 expander cycle

Table 5-37 Equipment sizes for refrigerant module 1 of the dual N_2 expander cycle (4.0 MTPA)

No.	Name	Dimension of the Equipment			
		Length	Breadth /Diameter	Height	Module
1	Nitrogen Compressor	39.929	12.608	12.187	Refrigerant Module 1
2	Nitrogen Cooler	16.811	4.201	10.506	
3	Cooler for PMR com.	6.303	4.201	6.303	
4	Overhead crane for PMR com.	39.929	20.502	5.939	

Table 5-38 Equipment sizes for refrigerant module 1 of the dual N_2 expander cycle (3.0 MTPA)

No.	Name	Dimension of the Equipment			
		Length	Breadth /Diameter	Height	Module
1	Nitrogen Compressor	24.35	7.69	7.43	Refrigerant Module 1
2	Nitrogen Cooler	10.25	2.56	6.41	
3	Cooler for PMR com.	3.84	2.56	3.84	
4	Overhead crane for PMR com.	24.35	12.50	3.62	

Table 5-39 Equipment sizes for refrigerant module 1 of the dual N_2 expander cycle (2.0 MTPA)

No.	Name	Dimension of the Equipment			
		Length	Breadth /Diameter	Height	Module
1	Nitrogen Compressor	14.38	4.54	4.39	Refrigerant Module 1
2	Nitrogen Cooler	6.05	1.51	3.78	
3	Cooler for PMR com.	2.27	1.51	2.27	
4	Overhead crane for PMR com.	14.38	7.38	2.14	

Table 5-40 Equipment sizes for refrigerant module 1 of the dual N_2 expander cycle (1.0 MTPA)

No.	Name	Dimension of the Equipment			
		Length	Breadth /Diameter	Height	Module
1	Nitrogen Compressor	6.79	2.14	2.07	Refrigerant Module 1
2	Nitrogen Cooler	2.86	0.71	1.79	
3	Cooler for PMR com.	1.07	0.71	1.07	
4	Overhead crane for PMR com.	6.79	3.49	1.01	

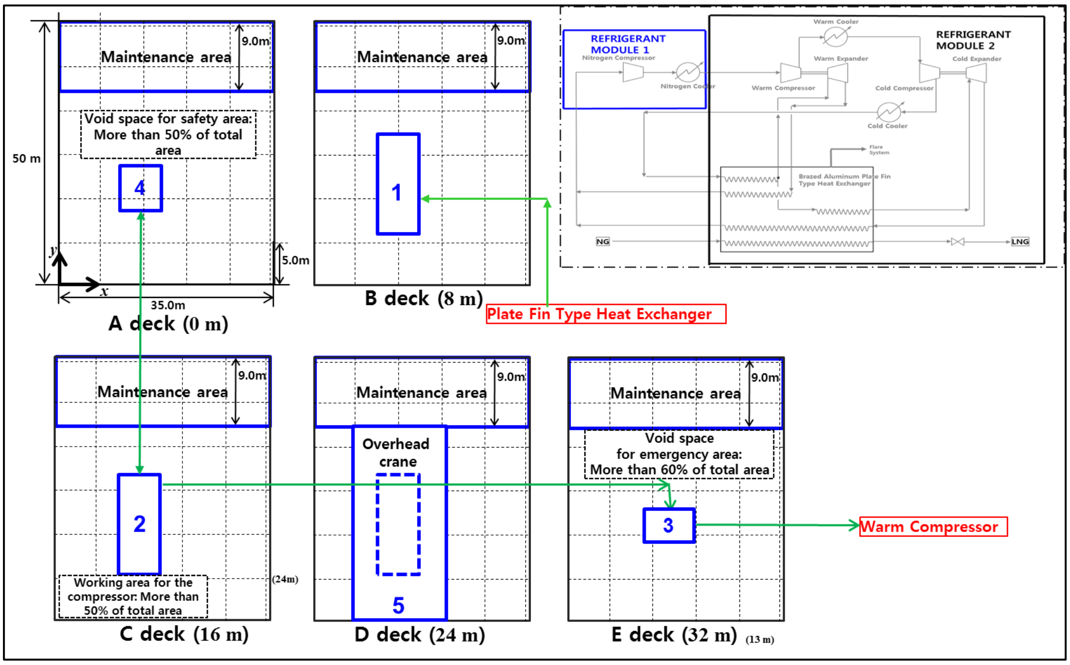

Figure 5-25 Connection information of refrigerant module 1 of the dual N_2 expander cycle

Refrigerant module 2 has two compressors, with each one-stage compression using one impeller, two expanders, two sea water coolers, and one heat exchanger. The approximate sizes of this equipment are shown in Figure 5-26 and 5-27 and in Table 5-41 to 5-44.

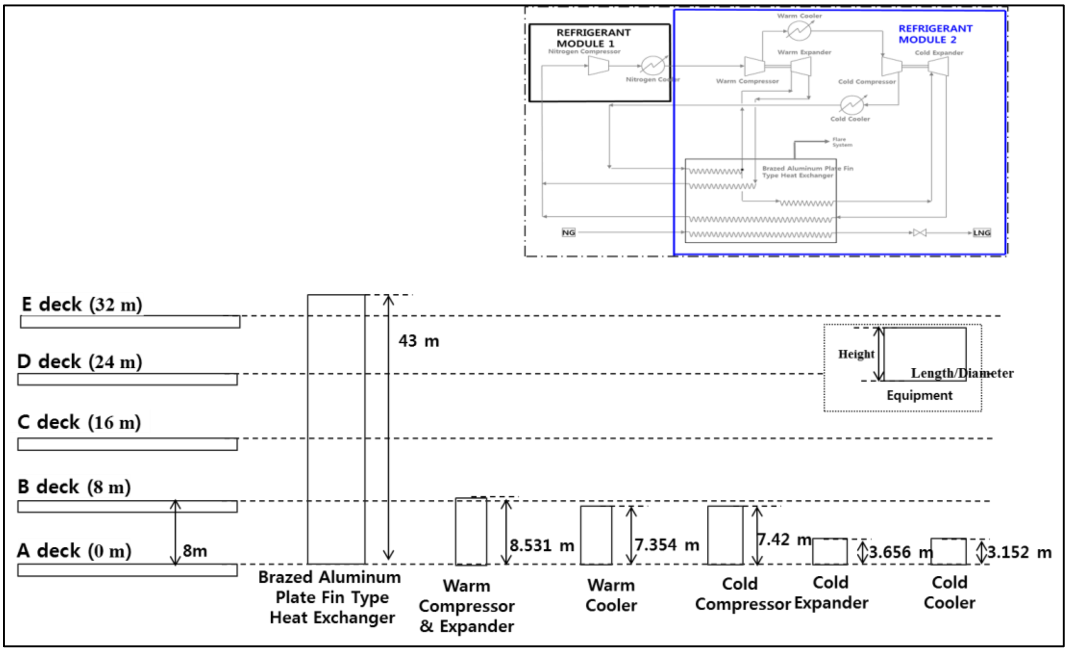

Figure 5-26 Elevated view of refrigerant module 2 of the dual N_2 expander cycle

Table 5-41 Equipment sizes for refrigerant module 2 of the dual N_2 expander cycle (4.0 MTPA)

No.	Name	Dimension of the Equipment			
		Length	Breadth /Diameter	Height	Module
1	Warm Compressor	27.95	8.825	8.531	
2	Warm Cooler	11.767	2.941	7.354	
3	Warm Expander	27.95	8.825	8.531	
4	Cold Compressor	25.01	7.52	7.42	Refrigerant Module 2
5	Cold Cooler	5.04	1.26	3.152	
6	Cold Expander	11.98	3.782	3.656	
7	Brazed Aluminum Plate Fin Type Heat Exchanger	17.1	17.1	43	

Table 5-42 Equipment sizes for refrigerant module 2 of the dual N_2 expander cycle (3.0 MTPA)

No.	Name	Dimension of the Equipment			
		Length	Breadth /Diameter	Height	Module
1	Warm Compressor	17.05	5.38	5.20	Refrigerant Module 2
2	Warm Cooler	7.18	1.79	4.49	
3	Warm Expander	17.05	5.38	5.20	
4	Cold Compressor	15.25	4.59	4.53	
5	Cold Cooler	3.07	0.77	1.92	
6	Cold Expander	7.31	2.31	2.23	
7	Brazed Aluminum Plate Fin Type Heat Exchanger	10.43	10.43	26.23	

Table 5-43 Equipment sizes for refrigerant module 2 of the dual N_2 expander cycle (2.0 MTPA)

No.	Name	Dimension of the Equipment			
		Length	Breadth /Diameter	Height	Module
1	Warm Compressor	10.06	3.18	3.07	Refrigerant Module 2
2	Warm Cooler	4.24	1.06	2.65	
3	Warm Expander	10.06	3.18	3.07	
4	Cold Compressor	9.00	2.71	2.67	
5	Cold Cooler	1.81	0.45	1.13	
6	Cold Expander	4.31	1.36	1.32	
7	Brazed Aluminum Plate Fin Type Heat Exchanger	6.16	6.16	15.48	

Table 5-44 Equipment sizes for refrigerant module 2 of the dual N_2 expander cycle (1.0 MTPA)

No.	Name	Dimension of the Equipment			
		Length	Breadth /Diameter	Height	Module
1	Warm Compressor	4.75	1.50	1.45	Refrigerant Module 2
2	Warm Cooler	2.00	0.50	1.25	

3	Warm Expander	4.75	1.50	1.45	
4	Cold Compressor	4.25	1.28	1.26	
5	Cold Cooler	0.86	0.21	0.54	
6	Cold Expander	2.04	0.64	0.62	
7	Brazed Aluminum Plate Fin Type Heat Exchanger	2.91	2.91	7.31	

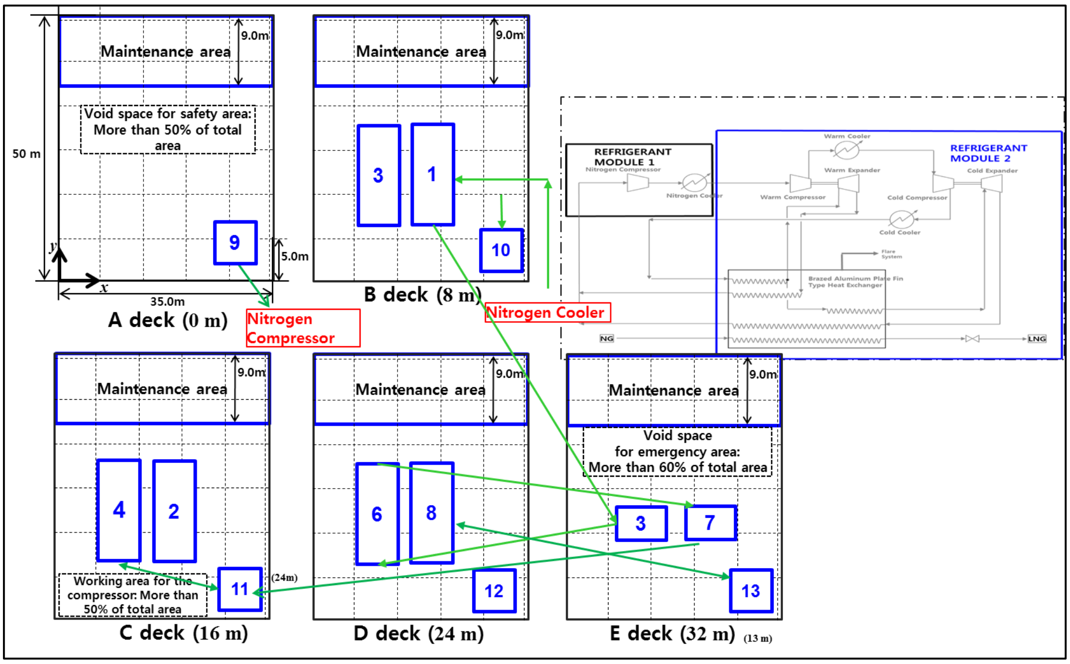

Figure 5-27 Connection information of refrigerant module 2 of the dual N_2 expander cycle

As shown in Figure 5-23, the dual N_2 expander cycle is separately placed on two modules. The first refrigerant module consists of a one-stage compression compressor, an overhead crane, a dedicated compressor cooler, and seawater cooler. This module is called “refrigerant module 1.” The second refrigerant module has a single-stage warm compressor, a warm cooler, a warm expander, a single-stage cold compressor, a cold cooler, a cold expander, and a heat exchanger. It is called “refrigerant module 2.” Each module consists of multiple decks, each separated by an 8 m height. Refrigerant modules 1 and 2 are available from decks A to E.

5.3. Mathematical Models for the Optimal Equipment Module Layout for the Potential Offshore Liquefaction Cycles

5.3.1. Potential MR liquefaction cycle (case 14)

Deck allocation, equipment position and orientation, and deck area are defined as design variables to determine the optimal liquefaction module layout, as follows (Patsiatzis, 2002):

(1) Design variables (Unknowns)

① Continuous variables

x_i, y_i: Coordinates of the geometrical center of equipment item *i*

z_i: Height from the bottom of equipment *i* to the piping connection point of equipment item *i*

$U_{i,j}$: Relative distance in the z-coordinates between equipment items *i* and *j* if *i* is higher than *j*

$TD_{i,j}$: Total rectilinear distance between equipment items *i* and *j*

FA: Deck area

X^{max}, Y^{max}: Dimensions of the deck area

② Binary variables

$V_{i,k}$: 1 if equipment item *i* is assigned to deck *k*; otherwise, 0

$Z_{i,j}$: 1 if equipment items *i* and *j* are allocated to the same deck; otherwise; 0

O_i: 1 if the length of equipment item *i* is equal to a_i (i.e., parallel to the x-axis); otherwise, 0

$E1_{i,j}$, $E2_{i,j}$: Non-overlapping binary variables (as used in Papageorgiou & Rotstein, 1998)

In addition, i, j: equipment number; and k: deck number.

When applied to the above, the MR and PMR module design variables can be summarized as follows:

Table 5-45 Design variables related with each equipment for PMR module 1 of the potential MR liquefaction cycle

Equipment		x_i [m]	y_i [m]	O_i	$V_{i,k}$		
No.	**Name**				$V_{i,1}$	**...**	$V_{i,4}$
1	PMR Comp. LP Suction Drum	x_1	y_1	O_1	$V_{1,1}$	...	$V_{1,4}$
2	PMR Comp. HP Suction Drum	x_2	y_2	O_2	$V_{2,1}$	...	$V_{2,4}$
3	PMR HP Compressor	x_3	y_3	O_3	$V_{3,1}$	...	$V_{3,4}$
4	Cooler for PMR Comp.	x_4	y_4	O_4	$V_{4,1}$	…	$V_{4,4}$
5	Overhead Crane	x_5	y_5	O_5	$V_{5,1}$	…	$V_{5,4}$
6	SW Cooler 1	x_6	y_6	O_6	$V_{6,1}$	…	$V_{6,4}$
7	SW Cooler 2	x_7	y_7	O_7	$V_{7,1}$	…	$V_{7,4}$

Table 5-46 Design variables related with each equipment for PMR module 2 of the potential MR liquefaction cycle

Equipment		x_i [*m*]	y_i [*m*]	O_i	$V_{i,k}$		
No	**Name**				$V_{i,1}$	...	$V_{i,5}$
1	PMR Receiver on the Lower Deck	x_1	y_1	O_1	$V_{1,1}$	...	$V_{1,5}$
2	PMR Receiver on the Upper Deck	x_2	y_2	O_2	$V_{2,1}$	...	$V_{2,5}$
3	LP Pre-cooling Heat Exchanger on Deck A	x_3	y_3	O_3	$V_{3,1}$	...	$V_{3,5}$
4	LP Pre-cooling Heat Exchanger on Deck B	x_4	y_4	O_4	$V_{4,1}$	...	$V_{4,5}$
5	LP Pre-cooling Heat Exchanger on Deck C	x_5	y_5	O_5	$V_{5,1}$	...	$V_{5,5}$
6	HP Pre-cooling Heat Exchanger on Deck A	x_6	y_6	O_6	$V_{6,1}$	…	$V_{6,5}$
7	HP Pre-cooling Heat Exchanger on Deck B	x_7	y_7	O_7	$V_{7,1}$	…	$V_{7,5}$
8	HP Pre-cooling Heat Exchanger on Deck C	x_8	y_8	O_8	$V_{8,1}$	…	$V_{8,5}$
9	JT Valve 1	x_9	y_9	O_9	$V_{9,1}$	…	$V_{9,5}$
10	JT Valve 2	x_{10}	y_{10}	O_{10}	$V_{10,1}$	…	$V_{10,5}$

Table 5-47 Design variables related with each equipment for the MR module of the potential MR liquefaction cycle

Equipment		x_i [m]	y_i [m]	O_i	$V_{i,k}$		
No.	Name				$V_{i,1}$	...	$V_{i,5}$
1	MR Separator 1 on the Lower Deck	x_1	y_1	O_1	$V_{1,1}$	...	$V_{1,5}$
2	MR Separator 1 on the Upper Deck	x_2	y_2	O_2	$V_{2,1}$	...	$V_{2,5}$
3	MCHE on Deck A	x_3	y_3	O_3	$V_{3,1}$	...	$V_{3,5}$
4	MCHE on Deck B	x_4	y_4	O_4	$V_{4,1}$	...	$V_{4,5}$
5	MCHE on Deck C	x_5	y_5	O_5	$V_{5,1}$	...	$V_{5,5}$
6	MCHE on Deck D	x_6	y_6	O_6	$V_{6,1}$	...	$V_{6,5}$
7	MCHE on Deck E	x_7	y_7	O_7	$V_{7,1}$	...	$V_{7,5}$
8	MR Comp. Suction Drum on the Lower Deck	x_8	y_8	O_8	$V_{8,1}$	…	$V_{8,5}$
9	MR Comp. Suction Drum on the Upper Deck	x_9	y_9	O_9	$V_{9,1}$	…	$V_{9,5}$
10	MR Comp.	x_{10}	y_{10}	O_{10}	$V_{10,1}$	…	$V_{10,5}$
11	Cooler for Comp.	x_{11}	y_{11}	O_{11}	$V_{11,1}$	…	$V_{11,5}$
12	Overhead Crane	x_{12}	y_{12}	O_{12}	$V_{12,1}$	…	$V_{12,5}$
13	SW Water 3	x_{13}	y_{13}	O_{13}	$V_{13,1}$	…	$V_{13,5}$
14	SW Water 4	x_{14}	y_{14}	O_{14}	$V_{14,1}$	…	$V_{14,5}$
15	JT Valve 3	x_{15}	y_{15}	O_{15}	$V_{15,1}$	…	$V_{15,5}$
16	JT Valve 4	x_{16}	y_{16}	O_{16}	$V_{16,1}$	…	$V_{16,5}$

Considering the deck area (*FA*) and its dimensions (X^{max}, Y^{max}), the design variables for the mathematical modeling of the potential MR liquefaction modules numbered 257.

(2) Equality constraints

① Deck constraints

Each piece of equipment should be assigned to one deck, and this can be expressed as follows (Patsiatzis, 2002). When applied to all the equipment on the potential MR liquefaction modules, a total of 158 constraints can be derived, as follows:

For PMR module 1 (28),

$$\sum_{k=1}^{NF} V_{i,k} = 1 , \qquad (5\text{-}1)$$

where i = 1,2,…,7, and NF: numbers of decks (4).

For PMR module 2 (50),

$$\sum_{k=1}^{NF} V_{i,k} = 1 , \qquad (5\text{-}2)$$

where i = 1,2,…,10, and NF: number of decks (5).

For the MR module (80),

$$\sum_{k=1}^{NF} V_{i,k} = 1 , \qquad (5\text{-}3)$$

where i = 1,2,…,16, and NF: number of decks (5).

② Land area constraints

The dimensions of the deck area (Xmax, Ymax) are used to calculate the deck area (FA). These values are related to the additional layout design constraint in the inequality constraints. In addition, the y-coordinate of the decks should be considered 9 m for the maintenance area.

$$FA = X^{\max}(Y^{\max} + 9) \tag{5-4}$$

③ Equipment constraints: Multi-decks

Some equipment height that exceeds the height of the decks (8 m) should be installed across two or more decks. In PMR module 1, there is no equipment that spans two or more decks. In PMR module 2, however, the PMR receiver is installed across two decks, and LP/HP pre-cooling heat exchangers are installed across three decks. In the MR module, the MR separator and MR refrigerant compressor suction drum are installed across two decks, and the MCHE is located across five decks. To consider the equipment's installation across multiple decks, the design variables for the amount of equipment include multi-deck situations, and the x- and y-axis of the multi-deck equipment are as follows:

For the PMR receiver in PMR module 2,

$x_1 = x_2$, and (5-5)

$y_1 = y_2$. (5-6)

For the LP pre-cooling heat exchanger in PMR module 2,

$x_i = x_{i+1}$, and (5-7)

$y_i = y_{i+1}$, (5-8)

where i = 3,4.

For the HP pre-cooling heat exchanger in PMR module 2,

$x_i = x_{i+1}$, and (5-9)

$y_i = y_{i+1}$, (5-10)

where i = 6,7.

For MR separator 1 in the MR module,

$x_1 = x_2$, and (5-11)

$y_1 = y_2$. (5-12)

For the MCHE in the MR module,

$x_i = x_{i+1}$, and (5-13)

$y_i = y_{i+1}$, (5-14)

where i = 3,4,5,6.

For the MR compressor suction drum in the MR module,

$x_8 = x_9$, and (5-15)

$y_8 = y_9$. (5-16)

The compressor cooler is installed under the MR compressor, and the overhead crane is located above the MR compressor. The x- and y-axis of the equipment are as follows:

$x_{10} = x_{11}$, (5-17)

$x_{10} = x_{12}$, (5-18)

$y_{10} = y_{11}$, and (5-19)

$y_{10} = x_{12}$. (5-20)

To consider that the same equipment is continuously allocated on the decks in the direction of the height, the following equality constraints are derived:

For the PMR compressor, compressor cooler, and overhead crane in PMR module 1,

$$\sum_{k=1}^{2} V_{3,k} V_{4,k+1} V_{5,k+2} = 1 \quad (5\text{-}21)$$

For the PMR receiver in PMR module 2,

$$\sum_{k=1}^{4} V_{1,k} V_{2,k+1} = 1 \quad (5\text{-}22)$$

For the LP pre-cooling heat exchanger in PMR module 2,

$$\sum_{k=1}^{3} V_{3,k} V_{4,k+1} V_{5,k+2} = 1 \quad . \tag{5-23}$$

For the HP pre-cooling heat exchanger in PMR module 2,

$$\sum_{k=1}^{3} V_{6,k} V_{7,k+1} V_{8,k+2} = 1 \quad . \tag{5-24}$$

For MR separator 1 in the MR module,

$$\sum_{k=1}^{4} V_{1,k} V_{2,k+1} = 1 \quad . \tag{5-25}$$

For the MCHE in the MR module,

$$V_{3,k} V_{4,k+1} V_{5,k+2} V_{6,k+3} V_{7,k+4} = 1 , \tag{5-26}$$

where k = 1.

For the MR compressor suction drum in the MR module,

$$\sum_{k=1}^{4} V_{8,k} V_{9,k+1} = 1 \quad . \tag{5-27}$$

For the MR compressor, compressor cooler, and overhead crane in the MR module,

$$\sum_{k=1}^{3} V_{10,k} V_{11,k+1} V_{12,k+2} = 1 \quad . \tag{5-28}$$

When applied to all the equipment on the potential MR liquefaction modules (three modules), a total of 34 constraints can be derived, as per the above equations. Therefore, the equality constraints for the mathematical modeling of the potential MR liquefaction modules numbered 193.

(3) Inequality constraints

① Non-overlapping constraints

If i and j are allocated to the same deck, non-overlapping is guaranteed if at least one of the following inequalities is active (Patsiatzis, 2002):

$$x_i - x_j \geq \frac{l_i + l_j}{2}, \tag{5-29}$$

where i = 1,2,…,N, and j = i +1,…,N+1;

$$x_j - x_i \geq \frac{l_i + l_j}{2}, \tag{5-30}$$

where i = 1,2,…,N, and j = i +1,…,N+1;

$$y_i - y_j \geq \frac{d_i + d_j}{2}, \tag{5-31}$$

where i = 1,2,…,N, and j = i +1,…,N+1; and

$$y_j - y_i \geq \frac{d_i + d_j}{2}, \tag{5-32}$$

where i = 1,2,…,N, and j = i +1,…,N+1.

These non-overlapping disjunctive conditions can be mathematically modeled by including appropriate “big M” constraints and introducing two additional sets of binary variables, $E1_{ij}$ and $E2_{ij}$. Each pair of values (0 or 1) for these variables determines which constraint from (5-29) to (5-32) is active.

$$x_i - x_j + M\left(1 - Z_{ij} + E1_{ij} + E2_{ij}\right) \geq \frac{l_i + l_j}{2}, \tag{5-33}$$

$$x_j - x_i + M\left(2 - Z_{ij} + E1_{ij} + E2_{ij}\right) \geq \frac{l_i + l_j}{2}, \tag{5-34}$$

$$y_i - y_j + M\left(2 - Z_{ij} + E1_{ij} - E2_{ij}\right) \geq \frac{d_i + d_j}{2}, \text{ and} \tag{5-35}$$

$$y_j - y_i + M\left(3 - Z_{ij} - E1_{ij} - E2_{ij}\right) \geq \frac{d_i + d_j}{2}, \tag{5-36}$$

where i = 1,2,…,N, and j = i +1,…,N+1.

For every i,j such that $j>i$ and $Z_{i,j}$=1, if constraint (5-29) is active, then $E1_{ij}$=0 and $E2_{ij}$=0; if constraint (5-30) is active, then $E1_{ij}$=1 and $E2_{ij}$=0; if constraint (5-31) is active, then $E1_{ij}$=0 and $E2_{ij}$=1; if constraint (5-32) is active, then $E1_{ij}$=1 and $E2_{ij}$=1.

In conclusion, considering the minimum distance between the equipment as 4 m, the non-overlapping constraints included in the model are:

$$x_i - x_j + M\left(1 - Z_{ij} + E1_{ij} + E2_{ij}\right) \geq \frac{l_i + l_j}{2} + 4, \tag{5-37}$$

$$x_j - x_i + M\left(2 - Z_{ij} + E1_{ij} + E2_{ij}\right) \geq \frac{l_i + l_j}{2} + 4, \tag{5-38}$$

$$y_i - y_j + M\left(2 - Z_{ij} + E1_{ij} - E2_{ij}\right) \geq \frac{d_i + d_j}{2} + 4, \text{ and} \tag{5-39}$$

$$y_j - y_i + M\left(3 - Z_{ij} - E1_{ij} - E2_{ij}\right) \geq \frac{d_i + d_j}{2} + 4, \tag{5-40}$$

where i = 1,2,…,N, and j = i +1,…,N+1.

When applied to all the equipment on the potential MR liquefaction modules, a total of 132 constraints can be derived, as follows:

For PMR module 1 (28),

$$x_i - x_j + M\left(1 - Z_{ij} + E1_{ij} + E2_{ij}\right) \geq \frac{l_i + l_j}{2} + 4, \tag{5-41}$$

$$x_j - x_i + M\left(2 - Z_{ij} + E1_{ij} + E2_{ij}\right) \geq \frac{l_i + l_j}{2} + 4, \tag{5-42}$$

$$y_i - y_j + M\left(2 - Z_{ij} + E1_{ij} - E2_{ij}\right) \geq \frac{d_i + d_j}{2} + 4, \text{ and} \tag{5-43}$$

$$y_j - y_i + M\left(3 - Z_{ij} - E1_{ij} - E2_{ij}\right) \geq \frac{d_i + d_j}{2} + 4, \tag{5-44}$$

where i = 1,2,…,7, and j = i +1,…,8.

For PMR module 2 (40),

$$x_i - x_j + M\left(1 - Z_{ij} + E1_{ij} + E2_{ij}\right) \geq \frac{l_i + l_j}{2} + 4, \tag{5-45}$$

$$x_j - x_i + M\left(2 - Z_{ij} + E1_{ij} + E2_{ij}\right) \geq \frac{l_i + l_j}{2} + 4, \tag{5-46}$$

$$y_i - y_j + M\left(2 - Z_{ij} + E1_{ij} - E2_{ij}\right) \geq \frac{d_i + d_j}{2} + 4, \text{ and} \tag{5-47}$$

$$y_j - y_i + M\left(3 - Z_{ij} - E1_{ij} - E2_{ij}\right) \geq \frac{d_i + d_j}{2} + 4, \tag{5-48}$$

where i = 1,2,…,10, and j = i +1,…,11.

For the MR module (64),

$$x_i - x_j + M\left(1 - Z_{ij} + E1_{ij} + E2_{ij}\right) \geq \frac{l_i + l_j}{2} + 4, \tag{5-49}$$

$$x_j - x_i + M\left(2 - Z_{ij} + E1_{ij} + E2_{ij}\right) \geq \frac{l_i + l_j}{2} + 4, \tag{5-50}$$

$$y_i - y_j + M\left(2 - Z_{ij} + E1_{ij} - E2_{ij}\right) \geq \frac{d_i + d_j}{2} + 4, \tag{5-51}$$

$$y_j - y_i + M\left(3 - Z_{ij} - E1_{ij} - E2_{ij}\right) \geq \frac{d_i + d_j}{2} + 4, \tag{5-52}$$

where i = 1,2,…,16, and j = i +1,…,17.

② Workspace area constraints

The workspace that is not related to the equipment or maintenance area is assumed to be more than 50% of the deck area (FA). When applied to all the equipment on the potential MR liquefaction modules, a total of 33 constraints can be derived, as follows:

For PMR module 1 (7),

$$FA-(\sum_{i=1}^{7}V_{i,1}a_ib_i+X^{\max}\times 9)\geq \frac{1}{2}FA \quad (5\text{-}53)$$

.

For PMR module 2 (10),

$$FA-(\sum_{i=1}^{10}V_{i,1}a_ib_i+X^{\max}\times 9)\geq \frac{1}{2}FA \quad (5\text{-}54)$$

.

For the MR module (16),

$$FA-(\sum_{i=1}^{16}V_{i,1}a_ib_i+X^{\max}\times 9)\geq \frac{1}{2}FA \quad (5\text{-}55)$$

.

③ Emergency area constraints

To consider safety for each module, safety facilities such as the PSV and blow down valve (BDV) are considered. Thus, the safety facility space at the highest decks for each module is assumed to be more than 60% of the deck area (FA). When applied to all the equipment on the potential MR liquefaction modules, a total of 33 constraints can be derived, as follows:

For PMR module 1 (7),

$$FA-(\sum_{i=1}^{7}V_{i,4}a_ib_i+X^{\max}\times 9)\geq 0.6FA \quad (5\text{-}56)$$

.

For PMR module 2 (10),

$$FA-(\sum_{i=1}^{10}V_{i,5}a_ib_i+X^{\max}\times 9)\geq 0.6FA \quad (5\text{-}57)$$

.

For the MR module (16),

$$FA-(\sum_{i=1}^{16}V_{i,5}a_ib_i+X^{\max}\times 9)\geq 0.6FA \quad (5\text{-}58)$$

.

④ Additional layout design constraints

In Figure 5-8, the distance between the equipment side and each deck side is assumed to be more than 3 m. When applied to all equipment on the potential MR liquefaction modules, a total of 132 constraints can be derived, as follows:

For PMR module 1 (28),

$$x_i\geq \frac{l_i}{2}+3 \quad (5\text{-}59)$$

,

$$y_i\geq \frac{b_i}{2}+3 \quad (5\text{-}60)$$

,

$$x_i+\frac{l_i}{2}+3\leq X^{\max} \quad (5\text{-}61)$$

, and

$$y_i+\frac{d_i}{2}\leq Y^{\max} \quad (5\text{-}62)$$

,

where i = 1,2,…,7.

For PMR module 2 (40),

$$x_i\geq \frac{l_i}{2}+3 \quad (5\text{-}63)$$

,

$$y_i\geq \frac{b_i}{2}+3 \quad (5\text{-}64)$$

,

$$x_i+\frac{l_i}{2}+3\leq X^{\max} \quad (5\text{-}65)$$

, and

$$y_i+\frac{d_i}{2}\leq Y^{\max} \quad (5\text{-}66)$$

,

where i = 1,2,…,10.

For the MR module (64),

$$x_i \geq \frac{l_i}{2} + 3 \quad , \tag{5-67}$$

$$y_i \geq \frac{b_i}{2} + 3 \quad , \tag{5-68}$$

$$x_i + \frac{l_i}{2} + 3 \leq X^{\max} \text{, and} \tag{5-69}$$

$$y_i + \frac{d_i}{2} \leq Y^{\max} \quad , \tag{5-70}$$

where i = 1,2,…,16.

Therefore, the inequality constraints for the mathematical modeling of the potential MR liquefaction modules numbered 330.

(4) Objective function

The overall objective function that was used for the plant layout problem is as follows (Patsiatzis, 2002):

$$W = \sum_{i} \sum_{j \neq i / f_{ij}=1} \left[C_{ij}^{c} TD_{ij} + C_{ij}^{v} D_{ij} + C_{ij}^{h} \left(R_{ij} + L_{ij} + A_{ij} + B_{ij} \right) \right] + FC1 \cdot NF + LC \cdot FA \quad , \tag{5-71}$$

where i = 1,2,…,16, and j = 1,2,…,16;

f_{ij}: 1 if the flow is from item i to item j; otherwise, 0;

C^{c}_{ij}: connection cost between items i and j;

C^{v}_{ij}: vertical pumping cost between items i and j;

C^{h}_{ij}: horizontal pumping cost between items i and j;

$FC1$: deck construction cost; and

LC: module cost.

In each module, there are high-pressure systems using compressors; pumps are not used in this study. The number of decks for each module is fixed. Thus, the deck construction cost is not required as an objective function in this study. In this paper, the connectivity cost, the construction cost proportional to the deck area, and the distance of the MCHEs and separators from the centerline of the hull are considered objective functions to be minimized. In conclusion, there is an objective function in this study, as follows:

$$W = \sum_{i}\sum_{j \neq i}\left[W_{1,ij}TD_{ij}\right] + W_2 FA + W_3 y_i \quad (5\text{-}72)$$

,

where $W_{1,ij}$: connection cost between items i and j;

W_2: construction cost;

W_3: motion impact cost;

i,j: equipment items;

TD_{ij}: total rectilinear distance between equipment items i and j;

FA: deck area; and

y_i: distance between the heat exchanger and the centerline;

$$TD_{ij} = \left|x_i - x_j\right| + \left|y_i - y_j\right| + U_{ij} \quad (5\text{-}73)$$

, and

$$U_{ij} = \left|H\sum_{k=1}^{NF} k\left(V_{ik} - V_{jk}\right) + z_i - z_j\right| \quad (5\text{-}74)$$

where

,

where k: deck number;

NF: number of decks (5);

H: height between the decks (8 m);

$V_{i,k}$: 1 if equipment item i is assigned to deck k; otherwise, 0; and

$U_{i,j}$: relative distance in the z-coordinates between equipment items i and j if i is higher than j.

(5) Summary of the mathematical model

Objective function: Minimize W

$$W = \sum_{i}\sum_{j \neq i}\left[W_{1,ij} TD_{ij}\right] + W_2 FA + W_3 y_i$$

Design variables [257]:

- Related to each equipment [49+80+128=257]

Constraints:

(Equality constraints) [193]

- Deck constraints [28+50+80=158]
- Land area constraints [1]
- Equipment constraints: multi-deck [34]

(Inequality constraints) [330]

- Non-overlapping constraints [132]
- Workspace area constraints [33]
- Emergency area constraints [33]
- Additional layout design constraint [132]

5.3.2. DMR cycle

Deck allocation, equipment position and orientation, and deck area are defined as design variables to determine the optimal liquefaction module layout, as follows (Patsiatzis, 2002):

(1) Design variables (unknowns)

① Continuous variables

x_i, y_i: Coordinates of the geometric center of equipment item i

z_i: Height from the bottom of equipment i to the piping connection point of equipment item i

$U_{i,j}$: Relative distance in the z-coordinates between equipment items i and j if i is higher than j

$TD_{i,j}$: Total rectilinear distance between equipment items i and j

FA: Deck area

X^{max}, Y^{max}: Dimensions of the deck area

② Binary variables

$V_{i,k}$: 1 if equipment item i is assigned to deck k; otherwise, 0

$Z_{i,j}$: 1 if equipment items i and j are allocated to the same deck; otherwise, 0

O_i: 1 if the length of equipment item i is equal to a_i (i.e., parallel to the x-axis); otherwise, 0

$E1_{i,j}$, $E2_{i,j}$: Non-overlapping binary variables (as used in Papageorgiou & Rotstein, 1998)

In addition, i, j: equipment number, and k: deck number.

When applied to the above, the MR and PMR module design variables can be summarized as follows:

Table 5-48 Design variables related with each equipment for PMR module 1 of the DMR cycle

Equipment		**x_i [m]**	**y_i [m]**	**O_i**	**$V_{i,k}$**		
No.	**Name**				**$V_{i,1}$**	**...**	**$V_{i,4}$**
1	PMR Comp. LP Suction Drum	x_1	y_1	O_1	$V_{1,1}$	...	$V_{1,4}$
2	PMR Comp. MP Suction Drum	x_2	y_2	O_2	$V_{2,1}$	...	$V_{2,4}$
3	PMR Comp. HP Suction Drum	x_3	y_3	O_3	$V_{3,1}$	...	$V_{3,4}$
4	PMR HP Compressor	x_4	y_4	O_4	$V_{4,1}$	…	$V_{4,4}$
5	Cooler for PMR Comp.	x_5	y_5	O_5	$V_{5,1}$	…	$V_{5,4}$
6	Overhead Crane	x_6	y_6	O_6	$V_{6,1}$	…	$V_{6,4}$
7	SW Cooler 1	x_7	y_7	O_7	$V_{7,1}$	…	$V_{7,4}$
8	SW Cooler 2	x_8	y_8	O_8	$V_{8,1}$	…	$V_{8,4}$
9	SW Cooler 3	x_9	y_9	O_9	$V_{9,1}$	…	$V_{9,4}$

Table 5-49 Design variables related with each equipment for PMR module 2 of the DMR cycle

Equipment		**x_i [m]**	**y_i [m]**	**O_i**	**$V_{i,k}$**		
No.	**Name**				**$V_{i,1}$**	**...**	**$V_{i,5}$**
1	PMR Receiver on the Lower Deck	x_1	y_1	O_1	$V_{1,1}$	...	$V_{1,5}$
2	PMR Receiver on the Upper Deck	x_2	y_2	O_2	$V_{2,1}$	...	$V_{2,5}$

3	LP Pre-cooling Heat Exchanger on Deck A	x_3	y_3	O_3	$V_{3,1}$	...	$V_{3,5}$
4	LP Pre-cooling Heat Exchanger on Deck B	x_4	y_4	O_4	$V_{4,1}$	...	$V_{4,5}$
5	LP Pre-cooling Heat Exchanger on Deck C	x_5	y_5	O_5	$V_{5,1}$	...	$V_{5,5}$
6	MP Pre-cooling Heat Exchanger on Deck A	x_6	y_6	O_6	$V_{6,1}$	…	$V_{6,5}$
7	MP Pre-cooling Heat Exchanger on Deck B	x_7	y_7	O_7	$V_{7,1}$	…	$V_{7,5}$
8	MP Pre-cooling Heat Exchanger on Deck C	x_8	y_8	O_8	$V_{8,1}$	…	$V_{8,5}$
9	HP Pre-cooling Heat Exchanger on Deck A	x_9	y_9	O_9	$V_{9,1}$	…	$V_{9,5}$
10	HP Pre-cooling Heat Exchanger on Deck B	x_{10}	y_{10}	O_{10}	$V_{10,1}$	…	$V_{10,5}$
11	HP Pre-cooling Heat Exchanger on Deck C	x_{11}	y_{11}	O_{11}	$V_{11,1}$	...	$V_{11,5}$

12	JT Valve 1	x_{12}	y_{12}	O_{12}	$V_{12,1}$	…	$V_{12,5}$
13	JT Valve 2	x_{13}	y_{13}	O_{13}	$V_{13,1}$	…	$V_{13,5}$
14	JT Valve 3	x_{14}	y_{14}	O_{14}	$V_{14,1}$	…	$V_{14,5}$

Table 5-50 Design variables related with each equipment for the MR module of the DMR cycle

Equipment		x_i **[m]**	y_i **[m]**	O_i	$V_{i,k}$		
No.	**Name**				$V_{i,1}$	**…**	$V_{i,5}$
1	MR Separator 1 on the Lower Deck	x_1	y_1	O_1	$V_{1,1}$	…	$V_{1,5}$
2	MR Separator 1 on the Upper Deck	x_2	y_2	O_2	$V_{2,1}$	…	$V_{2,5}$
3	MCHE on Deck A	x_3	y_3	O_3	$V_{3,1}$	…	$V_{3,5}$
4	MCHE on Deck B	x_4	y_4	O_4	$V_{4,1}$	…	$V_{4,5}$
5	MCHE on Deck C	x_5	y_5	O_5	$V_{5,1}$	…	$V_{5,5}$
6	MCHE on Deck D	x_6	y_6	O_6	$V_{6,1}$	…	$V_{6,5}$
7	MCHE on Deck E	x_7	y_7	O_7	$V_{7,1}$	…	$V_{7,5}$
8	MR Comp. Suction Drum on the Lower Deck	x_8	y_8	O_8	$V_{8,1}$	…	$V_{8,5}$
9	MR Comp. Suction	x_9	y_9	O_9	$V_{9,1}$	…	$V_{9,5}$

	Drum on the Upper Deck						
10	MR Comp.	x_{10}	y_{10}	O_{10}	$V_{10,1}$	…	$V_{10,5}$
11	Cooler for Comp.	x_{11}	y_{11}	O_{11}	$V_{11,1}$	…	$V_{11,5}$
12	Overhead Crane	x_{12}	y_{12}	O_{12}	$V_{12,1}$	…	$V_{12,5}$
13	SW Water 4	x_{13}	y_{13}	O_{13}	$V_{13,1}$	…	$V_{13,5}$
14	SW Water 5	x_{14}	y_{14}	O_{14}	$V_{14,1}$	…	$V_{14,5}$
15	JT Valve 4	x_{15}	y_{15}	O_{15}	$V_{15,1}$	…	$V_{15,5}$
16	JT Valve 5	x_{16}	y_{16}	O_{16}	$V_{16,1}$	…	$V_{16,5}$

Considering the deck area (FA) and its dimensions (X^{max}, Y^{max}), the design variables for the mathematical modeling of the DMR modules numbered 303.

(2) Equality constraints

① Deck constraints

Each piece of equipment should be assigned to one deck, and this can be expressed as follows (Patsiatzis, 2002). When applied to all the equipment on the DMR modules, a total of 186 constraints can be derived, as follows:

For PMR module 1 (36),

$$\sum_{k=1}^{NF} V_{i,k} = 1 \quad , \tag{5-75}$$

where i = 1,2,…,9, and NF: number of decks (4).

For PMR module 2 (70),

$$\sum_{k=1}^{NF} V_{i,k} = 1 \quad , \tag{5-76}$$

where i = 1,2,…,14, and NF: number of decks (5).

For the MR module (80),

$$\sum_{k=1}^{NF} V_{i,k} = 1 \quad , \tag{5-77}$$

where i = 1,2,…,16, and NF: number of decks (5).

② Land area constraints

The dimensions of the deck area (Xmax, Ymax) are used to calculate the deck area (FA). These values are related to the additional layout design constraint in the inequality constraints. In addition, the y-coordinate of the decks should be considered 9 m for the maintenance area.

$$FA = X^{\max}(Y^{\max} + 9) \tag{5-78}$$

③ Equipment constraints: Multi-decks

Some equipment height that exceeds the height of the decks (8 m) should be installed across two or more decks. In PMR module 1, there is no equipment that spans two or more decks. In PMR module 2, however, the PMR receiver is installed across two decks, and LP/MP/HP pre-cooling heat exchangers are installed across three decks. In the MR module, the MR separator and MR refrigerant compressor suction drum are installed across two decks, and the MCHE is located across five decks. To consider the equipment’s installation across multiple decks, the design variables for the amount of equipment include multi-deck situations, and the x- and y-axis of the multi-deck equipment are as follows:

For the PMR receiver in PMR module 2,

$$x_1 = x_2 \text{, and} \quad (5\text{-}79)$$

$$y_1 = y_2 . \quad (5\text{-}80)$$

For the LP pre-cooling heat exchanger in PMR module 2,

$$x_i = x_{i+1} \text{, and} \quad (5\text{-}81)$$

$$y_i = y_{i+1} , \quad (5\text{-}82)$$

where i = 3,4.

For the MP pre-cooling heat exchanger in PMR module 2,

$$x_i = x_{i+1} \text{, and} \quad (5\text{-}83)$$

$$y_i = y_{i+1} , \quad (5\text{-}84)$$

where i = 6,7.

For the HP pre-cooling heat exchanger in PMR module 2,

$$x_i = x_{i+1} \text{, and} \quad (5\text{-}85)$$

$$y_i = y_{i+1} , \quad (5\text{-}86)$$

where i = 9,10.

For MR separator 1 in the MR module,

$$x_1 = x_2 \text{, and} \quad (5\text{-}87)$$

$$y_1 = y_2 . \quad (5\text{-}88)$$

For the MCHE in the MR module,

$$x_i = x_{i+1} \text{, and} \quad (5\text{-}89)$$

$$y_i = y_{i+1} , \quad (5\text{-}90)$$

where i = 3,4,5,6.

For the MR compressor suction drum in the MR module,

$x_8 = x_9$, and (5-91)

$y_8 = y_9$. (5-92)

The compressor cooler is installed under the MR compressor, and the overhead crane is located above the MR compressor. The x- and y-axis of the equipment are as follows:

$x_{10} = x_{11}$, (5-93)

$x_{10} = x_{12}$, (5-94)

$y_{10} = y_{11}$, and (5-95)

$y_{10} = x_{12}$. (5-96)

To consider that the same equipment is continuously allocated on the decks in the direction of the height, the following equality constraints are derived:

For the PMR compressor, compressor cooler, and overhead crane in PMR module 1,

$$\sum_{k=1}^{2} V_{4,k} V_{5,k+1} V_{6,k+2} = 1 \quad (5\text{-}97)$$

For the PMR receiver in PMR module 2,

$$\sum_{k=1}^{4} V_{1,k} V_{2,k+1} = 1 \quad (5\text{-}98)$$

For the LP pre-cooling heat exchanger in PMR module 2,

$$\sum_{k=1}^{3} V_{3,k} V_{4,k+1} V_{5,k+2} = 1 \quad (5\text{-}99)$$

For the MP pre-cooling heat exchanger in PMR module 2,

$$\sum_{k=1}^{3} V_{6,k} V_{7,k+1} V_{8,k+2} = 1 \quad (5\text{-}100)$$

For the HP pre-cooling heat exchanger in PMR module 2,

$$\sum_{k=1}^{3} V_{9,k} V_{10,k+1} V_{11,k+2} = 1 \quad . \tag{5-101}$$

For MR separator 1 in the MR module,

$$\sum_{k=1}^{4} V_{1,k} V_{2,k+1} = 1 \quad . \tag{5-102}$$

For the MCHE in the MR module,

$$V_{3,k} V_{4,k+1} V_{5,k+2} V_{6,k+3} V_{7,k+4} = 1 \, , \tag{5-103}$$

where k = 1.

For the MR compressor suction drum in the MR module,

$$\sum_{k=1}^{4} V_{8,k} V_{9,k+1} = 1 \quad . \tag{5-104}$$

For the MR compressor, compressor cooler, and overhead crane in the MR module,

$$\sum_{k=1}^{3} V_{10,k} V_{11,k+1} V_{12,k+2} = 1 \quad . \tag{5-105}$$

When applied to all the equipment on the DMR modules (three modules), a total of 39 constraints can be derived, as per the above equations. Therefore, the equality constraints for the mathematical modeling of the DMR modules numbered 226.

(3) Inequality constraints

① Non-overlapping constraints

If i and j are allocated to the same deck, non-overlapping is guaranteed if at least one of the following inequalities is active (Patsiatzis, 2002):

$$x_i - x_j \geq \frac{l_i + l_j}{2} \, , \tag{5-106}$$

where i = 1,2,…,N, and j = i +1,…,N+1;

$$x_j - x_i \geq \frac{l_i + l_j}{2}, \quad (5\text{-}107)$$

where i = 1,2,…,N, and $j = i$ +1,…,N+1;

$$y_i - y_j \geq \frac{d_i + d_j}{2}, \quad (5\text{-}108)$$

where i = 1,2,…,N, and $j = i$ +1,…,N+1; and

$$y_j - y_i \geq \frac{d_i + d_j}{2}, \quad (5\text{-}109)$$

where i = 1,2,…,N, and $j = i$ +1,…,N+1.

These non-overlapping disjunctive conditions can be mathematically modeled by including appropriate "big M" constraints and introducing two additional sets of binary variables, $E1_{ij}$ and $E2_{ij}$. Each pair of values (0 or 1) for these variables determines which constraint from (5-106) to (5-109) is active.

$$x_i - x_j + M\left(1 - Z_{ij} + E1_{ij} + E2_{ij}\right) \geq \frac{l_i + l_j}{2}, \quad (5\text{-}110)$$

$$x_j - x_i + M\left(2 - Z_{ij} + E1_{ij} + E2_{ij}\right) \geq \frac{l_i + l_j}{2}, \quad (5\text{-}111)$$

$$y_i - y_j + M\left(2 - Z_{ij} + E1_{ij} - E2_{ij}\right) \geq \frac{d_i + d_j}{2}, \text{ and} \quad (5\text{-}112)$$

$$y_j - y_i + M\left(3 - Z_{ij} - E1_{ij} - E2_{ij}\right) \geq \frac{d_i + d_j}{2}, \quad (5\text{-}113)$$

where i = 1,2,…,N, and $j = i$ +1,…,N+1.

For every i,j such that $j>i$ and $Z_{i,j}$=1, if constraint (5-106) is active, then $E1_{ij}$=0 and $E2_{ij}$=0; if constraint (5-107) is active, then $E1_{ij}$=1 and $E2_{ij}$=0; if constraint (5-108) is active, then $E1_{ij}$=0 and $E2_{ij}$=1; if constraint (5-109) is active, then $E1_{ij}$=1 and $E2_{ij}$=1.

In conclusion, considering the minimum distance between the equipment as 4 m, the non-overlapping constraints included in the model are

$$x_i - x_j + M\left(1 - Z_{ij} + E1_{ij} + E2_{ij}\right) \geq \frac{l_i + l_j}{2} + 4, \quad (5\text{-}114)$$

$$x_j - x_i + M\left(2 - Z_{ij} + E1_{ij} + E2_{ij}\right) \geq \frac{l_i + l_j}{2} + 4, \quad (5\text{-}115)$$

$$y_i - y_j + M\left(2 - Z_{ij} + E1_{ij} - E2_{ij}\right) \geq \frac{d_i + d_j}{2} + 4, \text{ and} \quad (5\text{-}116)$$

$$y_j - y_i + M\left(3 - Z_{ij} - E1_{ij} - E2_{ij}\right) \geq \frac{d_i + d_j}{2} + 4, \quad (5\text{-}117)$$

where i = 1,2,…,N, and j = i +1,…,N+1.

When applied to all the equipment on the DMR modules, a total of 156 constraints can be derived, as follows:

For PMR module 1 (36),

$$x_i - x_j + M\left(1 - Z_{ij} + E1_{ij} + E2_{ij}\right) \geq \frac{l_i + l_j}{2} + 4, \quad (5\text{-}118)$$

$$x_j - x_i + M\left(2 - Z_{ij} + E1_{ij} + E2_{ij}\right) \geq \frac{l_i + l_j}{2} + 4, \quad (5\text{-}119)$$

$$y_i - y_j + M\left(2 - Z_{ij} + E1_{ij} - E2_{ij}\right) \geq \frac{d_i + d_j}{2} + 4, \text{ and} \quad (5\text{-}120)$$

$$y_j - y_i + M\left(3 - Z_{ij} - E1_{ij} - E2_{ij}\right) \geq \frac{d_i + d_j}{2} + 4, \quad (5\text{-}121)$$

where i = 1,2,…,9, and j = i +1,…,10.

For PMR module 2 (56),

$$x_i - x_j + M\left(1 - Z_{ij} + E1_{ij} + E2_{ij}\right) \geq \frac{l_i + l_j}{2} + 4, \quad (5\text{-}122)$$

$$x_j - x_i + M\left(2 - Z_{ij} + E1_{ij} + E2_{ij}\right) \geq \frac{l_i + l_j}{2} + 4, \quad (5\text{-}123)$$

$$y_i - y_j + M\left(2 - Z_{ij} + E1_{ij} - E2_{ij}\right) \geq \frac{d_i + d_j}{2} + 4, \text{ and} \quad (5\text{-}124)$$

$$y_j - y_i + M\left(3 - Z_{ij} - E1_{ij} - E2_{ij}\right) \geq \frac{d_i + d_j}{2} + 4, \quad (5\text{-}125)$$

where i = 1,2,…,14, and j = i +1,…,15.

For the MR module (64),

$$x_i - x_j + M\left(1 - Z_{ij} + E1_{ij} + E2_{ij}\right) \geq \frac{l_i + l_j}{2} + 4, \quad (5\text{-}126)$$

$$x_j - x_i + M\left(2 - Z_{ij} + E1_{ij} + E2_{ij}\right) \geq \frac{l_i + l_j}{2} + 4, \quad (5\text{-}127)$$

$$y_i - y_j + M\left(2 - Z_{ij} + E1_{ij} - E2_{ij}\right) \geq \frac{d_i + d_j}{2} + 4, \text{ and} \quad (5\text{-}128)$$

$$y_j - y_i + M\left(3 - Z_{ij} - E1_{ij} - E2_{ij}\right) \geq \frac{d_i + d_j}{2} + 4, \quad (5\text{-}129)$$

where i = 1,2,…,16, and j = i +1,…,17.

② Workspace area constraints

The workspace that is not related to the equipment or maintenance area is assumed to be more than 50% of the deck area (FA). When applied to all the equipment on the DMR modules, a total of 39 constraints can be derived, as follows:

For PMR module 1 (9),

$$FA - \left(\sum_{i=1}^{9} V_{i,1} a_i b_i + X^{\max} \times 9\right) \geq \frac{1}{2} FA. \quad (5\text{-}130)$$

For PMR module 2 (14),

$$FA - \left(\sum_{i=1}^{14} V_{i,1} a_i b_i + X^{\max} \times 9\right) \geq \frac{1}{2} FA. \quad (5\text{-}131)$$

For the MR module (16),

$$FA-(\sum_{i=1}^{16}V_{i,1}a_ib_i+X^{\max}\times 9)\geq \frac{1}{2}FA \quad (5\text{-}132)$$

③ Emergency area constraints

To consider safety for each module, safety facilities such as the PSV and BDV are considered. Thus, the safety facility space at the highest decks for each module is assumed to be more than 60% of the deck area (FA). When applied to all the equipment on the DMR modules, a total of 39 constraints can be derived, as follows:

For PMR module 1 (9),

$$FA-(\sum_{i=1}^{9}V_{i,4}a_ib_i+X^{\max}\times 9)\geq 0.6FA \quad (5\text{-}133)$$

For PMR module 2 (14),

$$FA-(\sum_{i=1}^{14}V_{i,5}a_ib_i+X^{\max}\times 9)\geq 0.6FA \quad (5\text{-}134)$$

For the MR module (16),

$$FA-(\sum_{i=1}^{16}V_{i,5}a_ib_i+X^{\max}\times 9)\geq 0.6FA \quad (5\text{-}135)$$

④ Additional layout design constraints

In Figure 5-8, the distance between the equipment side and each deck side is assumed to be more than 3 m. When applied to all the equipment on the DMR modules, a total of 156 constraints can be derived, as follows:

For PMR module 1 (36),

$$x_i \geq \frac{l_i}{2} + 3 \quad , \tag{5-136}$$

$$y_i \geq \frac{b_i}{2} + 3 \quad , \tag{5-137}$$

$$x_i + \frac{l_i}{2} + 3 \leq X^{\max} \quad \text{, and} \tag{5-138}$$

$$y_i + \frac{d_i}{2} \leq Y^{\max} \quad , \tag{5-139}$$

where i = 1,2,…,9.

For PMR module 2 (56),

$$x_i \geq \frac{l_i}{2} + 3 \quad , \tag{5-140}$$

$$y_i \geq \frac{b_i}{2} + 3 \quad , \tag{5-141}$$

$$x_i + \frac{l_i}{2} + 3 \leq X^{\max} \quad \text{, and} \tag{5-142}$$

$$y_i + \frac{d_i}{2} \leq Y^{\max} \quad , \tag{5-143}$$

where i = 1,2,…,14.

For the MR module (64),

$$x_i \geq \frac{l_i}{2} + 3 \quad , \tag{5-144}$$

$$y_i \geq \frac{b_i}{2} + 3 \quad , \tag{5-145}$$

$$x_i + \frac{l_i}{2} + 3 \leq X^{\max} \quad \text{, and} \tag{5-146}$$

$$y_i + \frac{d_i}{2} \leq Y^{\max} \quad , \tag{5-147}$$

where i = 1,2,…,16.

Therefore, the inequality constraints for the mathematical modeling of the DMR modules numbered 390.

(4) Objective function

The overall objective function that was used for the plant layout problem is as follows (Patsiatzis, 2002):

$$W = \sum_{i} \sum_{j \neq i / f_{ij}=1} \left[C_{ij}^{c} TD_{ij} + C_{ij}^{v} D_{ij} + C_{ij}^{h} \left(R_{ij} + L_{ij} + A_{ij} + B_{ij} \right) \right] + FC1 \cdot NF + LC \cdot FA \quad , \tag{5-148}$$

where i = 1,2,…,16, and j = 1,2,…,16;

f_{ij}: 1 if the flow is from item i to item j; otherwise, 0;

C^{c}_{ij}: connection cost between items i and j;

C^{v}_{ij}: vertical pumping cost between items i and j;

C^{h}_{ij}: horizontal pumping cost between items i and j;

$FC1$: deck construction cost; and

LC: module cost.

In each module, there are high-pressure systems using compressors; pumps are not used in this study. The number of decks for each module is fixed. Thus, the deck construction cost is not required as an objective function in this study. In this paper, the connectivity cost, the construction cost proportional to the deck area, and the distance of the MCHEs and separators from the centerline of the hull are considered objective functions to be minimized. In conclusion, there is an objective function in this study, as follows:

$$W = \sum_{i} \sum_{j \neq i} \left[W_{1,ij} TD_{ij} \right] + W_2 FA + W_3 y_i \quad , \tag{5-149}$$

where $W_{1,ij}$: connection cost between items i and j;

W_2: construction cost;

W_3: motion impact cost;

i,*j*: equipment items;

TD_{ij}: total rectilinear distance between equipment items *i* and *j*;

FA: deck area; and

y_i: distance between the heat exchanger and the centerline,

$$TD_{ij} = \left|x_i - x_j\right| + \left|y_i - y_j\right| + U_{ij} \quad , \tag{5-150}$$

where

$$U_{ij} = \left| H \sum_{k=1}^{NF} k\left(V_{ik} - V_{jk}\right) + z_i - z_j \right| \quad , \tag{5-151}$$

where *k*: deck number;

NF: number of decks (5);

H: height between the decks (8 m);

$V_{i,k}$: 1 if equipment item *i* is assigned to deck *k*; otherwise, 0; and

$U_{i,j}$: relative distance in the z-coordinates between equipment items *i* and *j* if *i* is higher than *j*.

(5) Summary of the mathematical model

Objective function: Minimize W

$$W = \sum_i \sum_{j \neq i} \left[W_{1,ij} TD_{ij} \right] + W_2 FA + W_3 y_i$$

Design variables [303]:

- Related to each equipment [63+112+128=303]

Constraints:

(Equality constraints) [226]

- Deck constraints [36+70+80=186]
- Land area constraints [1]
- Equipment constraints: multi-deck [39]

(Inequality constraints) [390]

- Non-overlapping constraints [156]
- Workspace area constraints [39]
- Emergency area constraints [39]
- Additional layout design constraint [156]

5.3.3. C_3MR cycle

Deck allocation, equipment position and orientation, and deck area are defined as design variables to determine the optimal liquefaction module layout, as follows (Patsiatzis, 2002):

(1) Design variables (unknowns)

① Continuous variables

x_i, y_i: Coordinates of the geometric center of equipment item *i*

z_i: Height from the bottom of equipment *i* to the piping connection point of equipment item *i*

$U_{i,j}$: Relative distance in the z-coordinates between equipment items *i* and *j* if *i* is higher than *j*

$TD_{i,j}$: Total rectilinear distance between equipment items *i* and *j*

FA: Deck area

X^{max}, Y^{max}: Dimensions of the deck area

② Binary variables

$V_{i,k}$: 1 if equipment item *i* is assigned to deck *k*; otherwise, 0

$Z_{i,j}$: 1 if equipment items *i* and *j* are allocated to the same deck; otherwise, 0

O_i: 1 if the length of equipment item *i* is equal to a_i (i.e., parallel to the x-axis); otherwise, 0

$E1_{i,j}$, $E2_{i,j}$: Non-overlapping binary variables (as used in Papageorgiou & Rotstein, 1998)

In addition, *i*, *j*: equipment number, and *k*: deck number.

When applied to the above, the MR and PMR module design variables can be summarized as follows:

Table 5-51 Design variables related with each equipment for PMR module 1 of the C_3MR cycle

Equipment		x_i [m]	y_i [m]	O_i	$V_{i,k}$		
No.	**Name**				$V_{i,1}$	**...**	$V_{i,4}$
1	PMR Comp. LP Suction Drum	x_1	y_1	O_1	$V_{1,1}$	...	$V_{1,4}$
2	PMR Comp. MP Suction Drum	x_2	y_2	O_2	$V_{2,1}$	...	$V_{2,4}$
3	PMR Comp. HP Suction Drum	x_3	y_3	O_3	$V_{3,1}$	...	$V_{3,4}$
4	PMR HP Compressor	x_4	y_4	O_4	$V_{4,1}$	…	$V_{4,4}$
5	Cooler for PMR Comp.	x_5	y_5	O_5	$V_{5,1}$	…	$V_{5,4}$
6	Overhead Crane	x_6	y_6	O_6	$V_{6,1}$	…	$V_{6,4}$
7	SW Cooler 1	x_7	y_7	O_7	$V_{7,1}$	…	$V_{7,4}$
8	SW Cooler 2	x_8	y_8	O_8	$V_{8,1}$	…	$V_{8,4}$
9	SW Cooler 3	x_9	y_9	O_9	$V_{9,1}$	…	$V_{9,4}$

Table 5-52 Design variables related with each equipment for PMR module 2 of the C_3MR cycle

Equipment		x_i [m]	y_i [m]	O_i	$V_{i,k}$		
No.	**Name**				$V_{i,1}$	**...**	$V_{i,5}$
1	PMR Receiver on the Lower Deck	x_1	y_1	O_1	$V_{1,1}$	...	$V_{1,5}$
2	PMR Receiver on the Upper Deck	x_2	y_2	O_2	$V_{2,1}$	...	$V_{2,5}$

3	LP Pre-cooling Heat Exchanger on Deck A	x_3	y_3	O_3	$V_{3,1}$	...	$V_{3,5}$
4	LP Pre-cooling Heat Exchanger on Deck B	x_4	y_4	O_4	$V_{4,1}$	...	$V_{4,5}$
5	LP Pre-cooling Heat Exchanger on Deck C	x_5	y_5	O_5	$V_{5,1}$	...	$V_{5,5}$
6	MP Pre-cooling Heat Exchanger on Deck A	x_6	y_6	O_6	$V_{6,1}$	…	$V_{6,5}$
7	MP Pre-cooling Heat Exchanger on Deck B	x_7	y_7	O_7	$V_{7,1}$	…	$V_{7,5}$
8	MP Pre-cooling Heat Exchanger on Deck C	x_8	y_8	O_8	$V_{8,1}$	…	$V_{8,5}$
9	HP Pre-cooling Heat Exchanger on Deck A	x_9	y_9	O_9	$V_{9,1}$	…	$V_{9,5}$
10	HP Pre-cooling Heat Exchanger on Deck B	x_{10}	y_{10}	O_{10}	$V_{10,1}$	…	$V_{10,5}$
11	HP Pre-cooling Heat Exchanger on Deck C	x_{11}	y_{11}	O_{11}	$V_{11,1}$	...	$V_{11,5}$

12	JT Valve 1	x_{12}	y_{12}	O_{12}	$V_{12,1}$	…	$V_{12,5}$
13	JT Valve 2	x_{13}	y_{13}	O_{13}	$V_{13,1}$	…	$V_{13,5}$
14	JT Valve 3	x_{14}	y_{14}	O_{14}	$V_{14,1}$	…	$V_{14,5}$

Table 5-53 Design variables related with each equipment for the MR module of the C_3MR cycle

Equipment		**x_i [m]**	**y_i [m]**	**O_i**	**$V_{i,k}$**		
No.	**Name**				**$V_{i,1}$**	**...**	**$V_{i,5}$**
1	MR Separator 1 on the Lower Deck	x_1	y_1	O_1	$V_{1,1}$	…	$V_{1,5}$
2	MR Separator 1 on the Upper Deck	x_2	y_2	O_2	$V_{2,1}$	…	$V_{2,5}$
3	MCHE on Deck A	x_3	y_3	O_3	$V_{3,1}$	…	$V_{3,5}$
4	MCHE on Deck B	x_4	y_4	O_4	$V_{4,1}$	…	$V_{4,5}$
5	MCHE on Deck C	x_5	y_5	O_5	$V_{5,1}$	…	$V_{5,5}$
6	MCHE on Deck D	x_6	y_6	O_6	$V_{6,1}$	…	$V_{6,5}$
7	MCHE on Deck E	x_7	y_7	O_7	$V_{7,1}$	…	$V_{7,5}$
8	MR Comp. Suction Drum on the Lower Deck	x_8	y_8	O_8	$V_{8,1}$	…	$V_{8,5}$
9	MR Comp. Suction	x_9	y_9	O_9	$V_{9,1}$	…	$V_{9,5}$

	Drum on the Upper Deck						
10	MR Comp.	x_{10}	y_{10}	O_{10}	$V_{10,1}$	…	$V_{10,5}$
11	Cooler for Comp.	x_{11}	y_{11}	O_{11}	$V_{11,1}$	…	$V_{11,5}$
12	Overhead Crane	x_{12}	y_{12}	O_{12}	$V_{12,1}$	…	$V_{12,5}$
13	SW Water 4	x_{13}	y_{13}	O_{13}	$V_{13,1}$	…	$V_{13,5}$
14	JT Valve 4	x_{14}	y_{14}	O_{14}	$V_{14,1}$	…	$V_{14,5}$
15	JT Valve 5	x_{15}	y_{15}	O_{15}	$V_{15,1}$	…	$V_{15,5}$

Considering the deck area (FA) and its dimensions (X^{max}, Y^{max}), the design variables for the mathematical modeling of the C_3MR modules numbered 295.

(2) Equality constraints

① Deck constraints

Each piece of equipment should be assigned to one deck, and this can be expressed as follows (Patsiatzis, 2002). When applied to all the equipment on the C_3MR modules, a total of 181constraints can be derived, as follows:

For PMR module 1 (36),

$$\sum_{k=1}^{NF} V_{i,k} = 1 \quad , \tag{5-152}$$

where i = 1,2,…,9, and NF: number of decks (4).

For PMR module 2 (70),

$$\sum_{k=1}^{NF} V_{i,k} = 1 \quad , \tag{5-153}$$

where i = 1,2,…,14, and NF: number of decks (5).

For the MR module (75),

$$\sum_{k=1}^{NF} V_{i,k} = 1 \quad , \qquad (5\text{-}154)$$

where i = 1,2,…,15, and NF: number of decks (5).

② Land area constraints

The dimensions of the deck area (Xmax, Ymax) are used to calculate the deck area (FA). These values are related to the additional layout design constraint in the inequality constraints. In addition, the y-coordinate of the decks should be considered 9 m for the maintenance area.

$$FA = X^{\max}(Y^{\max} + 9) \qquad (5\text{-}155)$$

③ Equipment constraints: Multi-decks

Some equipment height that exceeds the height of the decks (8 m) should be installed across two or more decks. In PMR module 1, there is no equipment that spans two or more decks. In PMR module 2, however, the PMR receiver is installed across two decks, and LP/MP/HP pre-cooling heat exchangers are installed across three decks. In the MR module, the MR separator and MR refrigerant compressor suction drum are installed across two decks, and the MCHE is located across five decks. To consider the equipment's installation across multiple decks, the design variables for the amount of equipment include multi-deck situations, and the x- and y-axis of the multi-deck equipment are as follows:

For the PMR receiver in PMR module 2,

$$x_1 = x_2 \text{, and} \quad (5\text{-}156)$$

$$y_1 = y_2 . \quad (5\text{-}157)$$

For the LP pre-cooling heat exchanger in PMR module 2,

$$x_i = x_{i+1} \text{, and} \quad (5\text{-}158)$$

$$y_i = y_{i+1} , \quad (5\text{-}159)$$

where i = 3,4.

For the MP pre-cooling heat exchanger in PMR module 2,

$$x_i = x_{i+1} \text{, and} \quad (5\text{-}160)$$

$$y_i = y_{i+1} , \quad (5\text{-}161)$$

where i = 6,7.

For the HP pre-cooling heat exchanger in PMR module 2,

$$x_i = x_{i+1} \text{, and} \quad (5\text{-}162)$$

$$y_i = y_{i+1} , \quad (5\text{-}163)$$

where i = 9,10.

For MR separator 1 in the MR module,

$$x_1 = x_2 \text{, and} \quad (5\text{-}164)$$

$$y_1 = y_2 . \quad (5\text{-}165)$$

For the MCHE in the MR module,

$$x_i = x_{i+1} \text{, and} \quad (5\text{-}166)$$

$$y_i = y_{i+1} , \quad (5\text{-}167)$$

where i = 3,4,5,6.

For the MR compressor suction drum in the MR module,

$$x_8 = x_9 \text{, and} \quad (5\text{-}168)$$

$$y_8 = y_9 . \quad (5\text{-}169)$$

The compressor cooler is installed under the MR compressor, and the overhead crane is located above the MR compressor. The x- and y-axis of the equipment are as follows:

$$x_{10} = x_{11} , \quad (5\text{-}170)$$

$$x_{10} = x_{12} , \quad (5\text{-}171)$$

$$y_{10} = y_{11} \text{, and} \quad (5\text{-}172)$$

$$y_{10} = x_{12} . \quad (5\text{-}173)$$

To consider that the same equipment is continuously allocated on the decks in the direction of the height, the following equality constraints are derived:

For the PMR compressor, compressor cooler, and overhead crane in PMR module 1,

$$\sum_{k=1}^{2} V_{4,k} V_{5,k+1} V_{6,k+2} = 1 . \quad (5\text{-}174)$$

For the PMR receiver in PMR module 2,

$$\sum_{k=1}^{4} V_{1,k} V_{2,k+1} = 1 . \quad (5\text{-}175)$$

For the LP pre-cooling heat exchanger in PMR module 2,

$$\sum_{k=1}^{3} V_{3,k} V_{4,k+1} V_{5,k+2} = 1 . \quad (5\text{-}176)$$

For the MP pre-cooling heat exchanger in PMR module 2,

$$\sum_{k=1}^{3} V_{6,k} V_{7,k+1} V_{8,k+2} = 1 . \quad (5\text{-}177)$$

For the HP pre-cooling exchanger in PMR module 2,

$$\sum_{k=1}^{3} V_{9,k} V_{10,k+1} V_{11,k+2} = 1 . \quad (5\text{-}178)$$

For MR separator 1 in the MR module,

$$\sum_{k=1}^{4} V_{1,k} V_{2,k+1} = 1 \quad . \tag{5-179}$$

For the MCHE in the MR module,

$$V_{3,k} V_{4,k+1} V_{5,k+2} V_{6,k+3} V_{7,k+4} = 1 , \tag{5-180}$$

where k = 1.

For the MR compressor suction drum in the MR module,

$$\sum_{k=1}^{4} V_{8,k} V_{9,k+1} = 1 \quad . \tag{5-181}$$

For the MR compressor, compressor cooler, and overhead crane in the MR module,

$$\sum_{k=1}^{3} V_{10,k} V_{11,k+1} V_{12,k+2} = 1 \quad . \tag{5-182}$$

When applied to all the equipment on the C_3MR modules (three modules), a total of 39 constraints can be derived, as per the above equations. Therefore, the equality constraints for the mathematical modeling of the C_3MR modules numbered 221.

(3) Inequality constraints

① Non-overlapping constraints

If i and j are allocated to the same deck, non-overlapping is guaranteed if at least one of the following inequalities is active (Patsiatzis, 2002):

$$x_i - x_j \geq \frac{l_i + l_j}{2} , \tag{5-183}$$

where i = 1,2,…,N, and j = i +1,…,N+1;

$$x_j - x_i \geq \frac{l_i + l_j}{2} , \tag{5-184}$$

where i = 1,2,…,N, and j = i +1,…,N+1;

$$y_i - y_j \geq \frac{d_i + d_j}{2}, \tag{5-185}$$

where i = 1,2,…,N, and j = i +1,…,N+1; and

$$y_j - y_i \geq \frac{d_i + d_j}{2}, \tag{5-186}$$

where i = 1,2,…,N, and j = i +1,…,N+1.

These non-overlapping disjunctive conditions can be mathematically modeled by including appropriate "big M" constraints and introducing two additional sets of binary variables, $E1_{ij}$ and $E2_{ij}$. Each pair of values (0 or 1) for these variables determines which constraint from (5-183) to (5-186) is active.

$$x_i - x_j + M\left(1 - Z_{ij} + E1_{ij} + E2_{ij}\right) \geq \frac{l_i + l_j}{2}, \tag{5-187}$$

$$x_j - x_i + M\left(2 - Z_{ij} + E1_{ij} + E2_{ij}\right) \geq \frac{l_i + l_j}{2}, \tag{5-188}$$

$$y_i - y_j + M\left(2 - Z_{ij} + E1_{ij} - E2_{ij}\right) \geq \frac{d_i + d_j}{2}, \text{ and} \tag{5-189}$$

$$y_j - y_i + M\left(3 - Z_{ij} - E1_{ij} - E2_{ij}\right) \geq \frac{d_i + d_j}{2}, \tag{5-190}$$

where i = 1,2,…,N, and j = i +1,…,N+1.

For every i,j such that $j>i$ and $Z_{i,j}=1$, if constraint (5-183) is active, then $E1_{ij}=0$ and $E2_{ij}=0$; if constraint (5-184) is active, then $E1_{ij}=1$ and $E2_{ij}=0$; if constraint (5-185) is active, then $E1_{ij}=0$ and $E2_{ij}=1$; if constraint (5-186) is active, then $E1_{ij}=1$ and $E2_{ij}=1$.

In conclusion, considering the minimum distance between the equipment as 4 m, the non-overlapping constraints included in the model are

$$x_i - x_j + M\left(1 - Z_{ij} + E1_{ij} + E2_{ij}\right) \geq \frac{l_i + l_j}{2} + 4, \tag{5-191}$$

$$x_j - x_i + M\left(2 - Z_{ij} + E1_{ij} + E2_{ij}\right) \geq \frac{l_i + l_j}{2} + 4, \tag{5-192}$$

$$y_i - y_j + M\left(2 - Z_{ij} + E1_{ij} - E2_{ij}\right) \geq \frac{d_i + d_j}{2} + 4 \text{, and} \tag{5-193}$$

$$y_j - y_i + M\left(3 - Z_{ij} - E1_{ij} - E2_{ij}\right) \geq \frac{d_i + d_j}{2} + 4 \text{,} \tag{5-194}$$

where i = 1,2,…,N, and $j = i$ +1,…,N+1.

When applied to all the equipment on the C_3MR modules, a total of 152 constraints can be derived, as follows:

For PMR module 1 (36),

$$x_i - x_j + M\left(1 - Z_{ij} + E1_{ij} + E2_{ij}\right) \geq \frac{l_i + l_j}{2} + 4 \text{,} \tag{5-195}$$

$$x_j - x_i + M\left(2 - Z_{ij} + E1_{ij} + E2_{ij}\right) \geq \frac{l_i + l_j}{2} + 4 \text{,} \tag{5-196}$$

$$y_i - y_j + M\left(2 - Z_{ij} + E1_{ij} - E2_{ij}\right) \geq \frac{d_i + d_j}{2} + 4 \text{, and} \tag{5-197}$$

$$y_j - y_i + M\left(3 - Z_{ij} - E1_{ij} - E2_{ij}\right) \geq \frac{d_i + d_j}{2} + 4 \text{,} \tag{5-198}$$

where i = 1,2,…,9, and $j = i$ +1,…,10.

For PMR module 2 (56),

$$x_i - x_j + M\left(1 - Z_{ij} + E1_{ij} + E2_{ij}\right) \geq \frac{l_i + l_j}{2} + 4 \text{,} \tag{5-199}$$

$$x_j - x_i + M\left(2 - Z_{ij} + E1_{ij} + E2_{ij}\right) \geq \frac{l_i + l_j}{2} + 4 \text{,} \tag{5-200}$$

$$y_i - y_j + M\left(2 - Z_{ij} + E1_{ij} - E2_{ij}\right) \geq \frac{d_i + d_j}{2} + 4 \text{, and} \tag{5-201}$$

$$y_j - y_i + M\left(3 - Z_{ij} - E1_{ij} - E2_{ij}\right) \geq \frac{d_i + d_j}{2} + 4 \text{,} \tag{5-202}$$

where i = 1,2,…,14, and $j = i$ +1,…,15.

For the MR module (60),

$$x_i - x_j + M\left(1 - Z_{ij} + E1_{ij} + E2_{ij}\right) \geq \frac{l_i + l_j}{2} + 4 , \tag{5-203}$$

$$x_j - x_i + M\left(2 - Z_{ij} + E1_{ij} + E2_{ij}\right) \geq \frac{l_i + l_j}{2} + 4 , \tag{5-204}$$

$$y_i - y_j + M\left(2 - Z_{ij} + E1_{ij} - E2_{ij}\right) \geq \frac{d_i + d_j}{2} + 4 \text{, and} \tag{5-205}$$

$$y_j - y_i + M\left(3 - Z_{ij} - E1_{ij} - E2_{ij}\right) \geq \frac{d_i + d_j}{2} + 4 , \tag{5-206}$$

where $i = 1,2,\ldots,15$, and $j = i+1,\ldots,16$.

② Workspace area constraints

The workspace that is not related to the equipment or maintenance area is assumed to be more than 50% of the deck area (FA). When applied to all the equipment on the C_3MR modules, a total of 38 constraints can be derived, as follows:

For PMR module 1 (9),

$$FA - \left(\sum_{i=1}^{9} V_{i,1} a_i b_i + X^{\max} \times 9\right) \geq \frac{1}{2} FA . \tag{5-207}$$

For PMR module 2 (14),

$$FA - \left(\sum_{i=1}^{14} V_{i,1} a_i b_i + X^{\max} \times 9\right) \geq \frac{1}{2} FA . \tag{5-208}$$

For the MR module (15),

$$FA - \left(\sum_{i=1}^{15} V_{i,1} a_i b_i + X^{\max} \times 9\right) \geq \frac{1}{2} FA . \tag{5-209}$$

③ Emergency area constraints

To consider safety for each module, safety facilities such as the PSV and BDV are considered. Thus, the safety facility space at the highest decks for each module is assumed to be more than 60% of the deck area (FA). When applied to all the equipment on the C_3MR modules, a total of 38 constraints can be derived, as follows:

For PMR module 1 (9),

$$FA-(\sum_{i=1}^{9} V_{i,4} a_i b_i + X^{\max} \times 9) \geq 0.6FA \tag{5-210}$$

For PMR module 2 (14),

$$FA-(\sum_{i=1}^{14} V_{i,5} a_i b_i + X^{\max} \times 9) \geq 0.6FA \tag{5-211}$$

For the MR module (15),

$$FA-(\sum_{i=1}^{15} V_{i,5} a_i b_i + X^{\max} \times 9) \geq 0.6FA \tag{5-212}$$

④ Additional layout design constraints

In Figure 5-8, the distance between the equipment side and each deck side is assumed to be more than 3 m. When applied to all the equipment on the C_3MR modules, a total of 152 constraints can be derived, as follows:

For PMR module 1 (36),

$$x_i \geq \frac{l_i}{2} + 3 , \tag{5-213}$$

$$y_i \geq \frac{b_i}{2} + 3, \quad (5\text{-}214)$$

$$x_i + \frac{l_i}{2} + 3 \leq X^{\max}, \text{ and} \quad (5\text{-}215)$$

$$y_i + \frac{d_i}{2} \leq Y^{\max}, \quad (5\text{-}216)$$

where $i = 1,2,\ldots,9$.

For PMR module 2 (56),

$$x_i \geq \frac{l_i}{2} + 3, \quad (5\text{-}217)$$

$$y_i \geq \frac{b_i}{2} + 3, \quad (5\text{-}218)$$

$$x_i + \frac{l_i}{2} + 3 \leq X^{\max}, \text{ and} \quad (5\text{-}219)$$

$$y_i + \frac{d_i}{2} \leq Y^{\max}, \quad (5\text{-}220)$$

where $i = 1,2,\ldots,14$.

For the MR module (60),

$$x_i \geq \frac{l_i}{2} + 3, \quad (5\text{-}221)$$

$$y_i \geq \frac{b_i}{2} + 3, \quad (5\text{-}222)$$

$$x_i + \frac{l_i}{2} + 3 \leq X^{\max}, \text{ and} \quad (5\text{-}223)$$

$$y_i + \frac{d_i}{2} \leq Y^{\max}, \quad (5\text{-}224)$$

where $i = 1,2,\ldots,15$.

Therefore, the inequality constraints for the mathematical modeling of the C_3MR modules numbered 380.

(4) Objective function

The overall objective function that was used for the plant layout problem is as follows (Patsiatzis, 2002):

$$W = \sum_{i} \sum_{j \neq i / f_{ij}=1} \left[C_{ij}^{c} TD_{ij} + C_{ij}^{v} D_{ij} + C_{ij}^{h} \left(R_{ij} + L_{ij} + A_{ij} + B_{ij} \right) \right] + FC1 \cdot NF + LC \cdot FA \quad , \tag{5-225}$$

where $i = 1,2,\ldots,15$, and $j = 1,2,\ldots,15$;

f_{ij}: 1 if the flow is from item i to item j; otherwise, 0;

C^{c}_{ij}: connection cost between items i and j;

C^{v}_{ij}: vertical pumping cost between items i and j;

C^{h}_{ij}: horizontal pumping cost between items i and j;

$FC1$: deck construction cost; and

LC: module cost.

In each module, there are high-pressure systems using compressors; pumps are not used in this study. The number of decks for each module is fixed. Thus, the deck construction cost is not required as an objective function in this study. In this paper, the connectivity cost, the construction cost proportional to the deck area, and the distance of the MCHEs and separators from the centerline of the hull are considered objective functions to be minimized. In conclusion, there is an objective function in this study, as follows:

$$W = \sum_{i} \sum_{j \neq i} \left[W_{1,ij} TD_{ij} \right] + W_2 FA + W_3 y_i \quad , \tag{5-226}$$

where $W_{1,ij}$: connection cost between items i and j;

W_2: construction cost;

W_3: motion impact cost;

i,j: equipment items;

TD_{ij}: total rectilinear distance between equipment items i and j;

FA: deck area; and

y_i: distance between the heat exchanger and the centerline,

$$TD_{ij} = |x_i - x_j| + |y_i - y_j| + U_{ij} \quad , \tag{5-227}$$

$$U_{ij} = \left| H \sum_{k=1}^{NF} k \left(V_{ik} - V_{jk} \right) + z_i - z_j \right| \quad , \tag{5-228}$$

where

where k: deck number;

NF: number of decks (5);

H: height between the decks (8 m);

$V_{i,k}$: 1 if equipment item i is assigned to deck k; otherwise, 0; and

$U_{i,j}$: relative distance in the z-coordinates between equipment items i and j if i is higher than j.

(5) Summary of the mathematical model

Objective function: Minimize W

$$W = \sum_i \sum_{j \neq i} \left[W_{1,ij} TD_{ij} \right] + W_2 FA + W_3 y_i$$

Design variables [295]:

- Related to each equipment [63+112+120=295]

Constraints:

(Equality constraints) [221]

- Deck constraints [36+70+75=181]
- Land area constraints [1]
- Equipment constraints: multi-deck [39]

(Inequality constraints) [380]

- Non-overlapping constraints [152]
- Workspace area constraints [38]
- Emergency area constraints [38]
- Additional layout design constraint [152]

5.3.4. Dual N_2 expander cycle

Deck allocation, equipment position and orientation, and deck area are defined as design variables to determine the optimal liquefaction module layout, as follows (Patsiatzis, 2002):

(1) Design variables (unknowns)

① Continuous variables

x_i, y_i: Coordinates of the geometric center of equipment item i

z_i: Height from the bottom of equipment item i to the piping connection point of equipment item i

$U_{i,j}$: Relative distance in the z-coordinates between equipment items i and j if i is higher than j

$TD_{i,j}$: Total rectilinear distance between equipment items i and j

FA: Deck area

X^{max}, Y^{max}: Dimensions of the deck area

② Binary variables

$V_{i,k}$: 1 if equipment item i is assigned to deck k; otherwise, 0

$Z_{i,j}$: 1 if equipment items i and j are allocated to the same deck; otherwise, 0

O_i: 1 if the length of equipment item i is equal to a_i (i.e., parallel to the x-axis); otherwise, 0

$E1_{i,j}$, $E2_{i,j}$: Non-overlapping binary variables (as used in Papageorgiou & Rotstein, 1998)

In addition, i, j: equipment number, and k: deck number.

When applied to the above, the refrigerant module design variables can be summarized as follows:

Table 5-54 Design variables related with each equipment for refrigerant module 1 of the dual N_2 expander cycle

Equipment		**x_i [m]**	**y_i [m]**	**O_i**	**$V_{i,k}$**		
No.	**Name**				**$V_{i,1}$**	**...**	**$V_{i,5}$**
1	Nitrogen Compressor on the Lower Deck	x_1	y_1	O_1	$V_{1,1}$	...	$V_{1,5}$
2	Nitrogen Compressor on the Upper Deck	x_2	y_2	O_2	$V_{2,1}$	...	$V_{2,5}$
3	Nitrogen Cooler	x_3	y_3	O_3	$V_{3,1}$	...	$V_{3,5}$
4	Cooler for PMR Compressor	x_4	y_4	O_4	$V_{4,1}$	...	$V_{4,5}$
5	Overhead Crane for PMR Compressor	x_5	y_5	O_5	$V_{5,1}$	...	$V_{5,5}$

Table 5-55 Design variables related with each equipment for refrigerant module 2 of the dual N_2 expander cycle

Equipment		$\boldsymbol{x_i}$ **[*m*]**	$\boldsymbol{y_i}$ **[*m*]**	$\boldsymbol{O_i}$	$\boldsymbol{V_{i,k}}$		
No.	**Name**				$\boldsymbol{V_{i,1}}$	**...**	$\boldsymbol{V_{i,5}}$
1	Warm Compressor on the Lower Deck	x_1	y_1	O_1	$V_{1,1}$	...	$V_{1,5}$
2	Warm Compressor on the Upper Deck	x_2	y_2	O_2	$V_{2,1}$	...	$V_{2,5}$
3	Warm Cooler	x_3	y_3	O_3	$V_{3,1}$	...	$V_{3,5}$
4	Warm Expander on the Lower Deck	x_4	y_4	O_4	$V_{4,1}$	...	$V_{4,5}$
5	Warm Expander on the Upper Deck	x_5	y_5	O_5	$V_{5,1}$	...	$V_{5,5}$
6	Cold Compressor	x_6	y_6	O_6	$V_{6,1}$	...	$V_{6,5}$
7	Cold Cooler	x_7	y_7	O_7	$V_{7,1}$	...	$V_{7,5}$
8	Cold Expander	x_8	y_8	O_8	$V_{8,1}$	…	$V_{8,5}$
9	MCHE on Deck A	x_9	y_9	O_9	$V_{9,1}$	…	$V_{9,5}$
10	MCHE on Deck B	x_{10}	y_{10}	O_{10}	$V_{10,1}$	…	$V_{10,5}$
11	MCHE on Deck C	x_{11}	y_{11}	O_{11}	$V_{11,1}$	…	$V_{11,5}$
12	MCHE on Deck D	x_{12}	y_{12}	O_{12}	$V_{12,1}$	…	$V_{12,5}$
13	MCHE on Deck E	x_{13}	y_{13}	O_{13}	$V_{13,1}$	…	$V_{13,5}$

Considering the deck area (FA) and its dimensions (X^{max}, Y^{max}), the design variables for the mathematical modeling of the dual N_2 expander modules numbered 144.

(2) Equality constraints

① Deck constraints

Each piece of equipment should be assigned to one deck, and this can be expressed as follows (Patsiatzis, 2002). When applied to all the equipment on the dual N_2 expander modules, a total of 90 constraints can be derived, as follows:

For refrigerant module 1 (25),

$$\sum_{k=1}^{NF} V_{i,k} = 1 , \tag{5-229}$$

Where i = 1,2,…,5, and NF: number of decks (5).

For refrigerant module 2 (65),

$$\sum_{k=1}^{NF} V_{i,k} = 1 , \tag{5-230}$$

where i = 1,2,…,13, and NF: number of decks (5).

② Land area constraints

The dimensions of the deck area (Xmax, Ymax) are used to calculate the deck area (FA). These values are related to the additional layout design constraint in the inequality constraints. In addition, the y-coordinate of the decks should be considered 9 m for the maintenance area.

$$FA = X^{\max}(Y^{\max} + 9) \tag{5-231}$$

③ Equipment constraints: Multi-decks

Some equipment height that exceeds the height of the decks (8 m) should be installed across two or more decks. In refrigerant module 1, the nitrogen compressor and the nitrogen cooler are installed across two decks. In refrigerant module 2, the warm compressor and warm expander are installed across two decks, and the MCHE is located across five decks. To consider the equipment's installation across multiple decks, the design variables for the amount of equipment include the multi-deck situations, and the x- and y-axis of the multi-deck equipment are as follows:

For the nitrogen compressor in refrigerant module 1,

$$x_1 = x_2 \text{, and} \tag{5-232}$$

$$y_1 = y_2 . \tag{5-233}$$

For the warm compressor in refrigerant module 2,

$$x_1 = x_2 \text{, and} \tag{5-234}$$

$$y_1 = y_2 . \tag{5-235}$$

For the warm expander in refrigerant module 2,

$$x_4 = x_5 \text{, and} \tag{5-236}$$

$$y_4 = y_5 . \tag{5-237}$$

For the MCHE in refrigerant module 2,

$$x_i = x_{i+1} \text{, and} \tag{5-238}$$

$$y_i = y_{i+1} , \tag{5-239}$$

where i = 9,10,11,12.

The compressor cooler is installed under the nitrogen compressor, and the overhead crane is located above the MR compressor. The x- and y-axis of the equipment are as follows:

$$x_1 = x_4 ,\tag{5-240}$$

$$x_1 = x_5 ,\tag{5-241}$$

$$y_1 = y_4 \text{, and}\tag{5-242}$$

$$y_1 = x_5 .\tag{5-243}$$

To consider that the same equipment is continuously allocated on the decks in the direction of the height, the following equality constraints are derived:

For the nitrogen compressor, compressor cooler, and overhead crane in refrigerant module 1,

$$\sum_{k=1}^{3} V_{1,k} V_{4,k+1} V_{5,k+2} = 1 .\tag{5-244}$$

For the nitrogen compressor in refrigerant module 1,

$$\sum_{k=1}^{4} V_{1,k} V_{2,k+1} = 1 .\tag{5-245}$$

For the warm compressor in refrigerant module 2,

$$\sum_{k=1}^{4} V_{1,k} V_{2,k+1} = 1 .\tag{5-246}$$

For the warm expander in refrigerant module 2,

$$\sum_{k=1}^{4} V_{4,k} V_{5,k+1} = 1 .\tag{5-247}$$

For the MCHE in refrigerant module 2,

$$V_{9,k} V_{10,k+1} V_{11,k+2} V_{12,k+3} V_{13,k+4} = 1 ,\tag{5-248}$$

where $k = 1$.

When applied to all the equipment on the dual N_2 expander modules (two modules), a total of 23 constraints can be derived, as per the above equations. Therefore, the equality constraints for the mathematical modeling of the dual N_2 expander modules numbered 114.

(3) Inequality constraints

① Non-overlapping constraints

If i and j are allocated to the same deck, non-overlapping is guaranteed if at least one of the following inequalities is active (Patsiatzis, 2002):

$$x_i - x_j \geq \frac{l_i + l_j}{2}, \tag{5-249}$$

where i = 1,2,…,N, and j = i +1,…,N+1;

$$x_j - x_i \geq \frac{l_i + l_j}{2}, \tag{5-250}$$

where i = 1,2,…,N, and j = i +1,…,N+1;

$$y_i - y_j \geq \frac{d_i + d_j}{2}, \tag{5-251}$$

where i = 1,2,…,N, j = i +1,…,N+1; and

$$y_j - y_i \geq \frac{d_i + d_j}{2}, \tag{5-252}$$

where i = 1,2,…,N, and j = i +1,…,N+1.

These non-overlapping disjunctive conditions can mathematically be modeled by including appropriate “big M” constraints and introducing two additional sets of binary variables, $E1_{ij}$ and $E2_{ij}$. Each pair of values (0 or 1) for these variables determines which constraint from (5-249) to (5-252) is active.

$$x_i - x_j + M\left(1 - Z_{ij} + E1_{ij} + E2_{ij}\right) \geq \frac{l_i + l_j}{2}, \tag{5-253}$$

$$x_j - x_i + M\left(2 - Z_{ij} + E1_{ij} + E2_{ij}\right) \geq \frac{l_i + l_j}{2}, \tag{5-254}$$

$$y_i - y_j + M\left(2 - Z_{ij} + E1_{ij} - E2_{ij}\right) \geq \frac{d_i + d_j}{2} \text{, and} \qquad (5\text{-}255)$$

$$y_j - y_i + M\left(3 - Z_{ij} - E1_{ij} - E2_{ij}\right) \geq \frac{d_i + d_j}{2}, \qquad (5\text{-}256)$$

where i = 1,2,…,N, and $j = i$ +1,…,N+1.

For every i,j such that $j>i$ and $Z_{i,j}$=1, if constraint (5-249) is active, then $E1_{ij}$=0 and $E2_{ij}$=0; if constraint (5-250) is active, then $E1_{ij}$=1 and $E2_{ij}$=0; if constraint (5-251) is active, then $E1_{ij}$=0 and $E2_{ij}$=1; if constraint (5-252) is active, then $E1_{ij}$=1 and $E2_{ij}$=1.

In conclusion, considering the minimum distance between the equipment as 4 m, the non-overlapping constraints included in the model are

$$x_i - x_j + M\left(1 - Z_{ij} + E1_{ij} + E2_{ij}\right) \geq \frac{l_i + l_j}{2} + 4, \qquad (5\text{-}257)$$

$$x_j - x_i + M\left(2 - Z_{ij} + E1_{ij} + E2_{ij}\right) \geq \frac{l_i + l_j}{2} + 4, \qquad (5\text{-}258)$$

$$y_i - y_j + M\left(2 - Z_{ij} + E1_{ij} - E2_{ij}\right) \geq \frac{d_i + d_j}{2} + 4 \text{, and} \qquad (5\text{-}259)$$

$$y_j - y_i + M\left(3 - Z_{ij} - E1_{ij} - E2_{ij}\right) \geq \frac{d_i + d_j}{2} + 4, \qquad (5\text{-}260)$$

where i = 1,2,…,N, and $j = i$ +1,…,N+1.

When applied to all the equipment on the dual N_2 expander modules, a total of 72 constraints can be derived, as follows:

For refrigerant module 1 (20),

$$x_i - x_j + M\left(1 - Z_{ij} + E1_{ij} + E2_{ij}\right) \geq \frac{l_i + l_j}{2} + 4, \qquad (5\text{-}261)$$

$$x_j - x_i + M\left(2 - Z_{ij} + E1_{ij} + E2_{ij}\right) \geq \frac{l_i + l_j}{2} + 4, \qquad (5\text{-}262)$$

$$y_i - y_j + M\left(2 - Z_{ij} + E1_{ij} - E2_{ij}\right) \geq \frac{d_i + d_j}{2} + 4 \text{, and} \qquad (5\text{-}263)$$

$$y_j - y_i + M\left(3 - Z_{ij} - E1_{ij} - E2_{ij}\right) \geq \frac{d_i + d_j}{2} + 4 , \tag{5-264}$$

where i = 1,2,…,5, and j = i +1,…,6.

For refrigerant module 2 (52),

$$x_i - x_j + M\left(1 - Z_{ij} + E1_{ij} + E2_{ij}\right) \geq \frac{l_i + l_j}{2} + 4 , \tag{5-265}$$

$$x_j - x_i + M\left(2 - Z_{ij} + E1_{ij} + E2_{ij}\right) \geq \frac{l_i + l_j}{2} + 4 , \tag{5-266}$$

$$y_i - y_j + M\left(2 - Z_{ij} + E1_{ij} - E2_{ij}\right) \geq \frac{d_i + d_j}{2} + 4 \text{, and} \tag{5-267}$$

$$y_j - y_i + M\left(3 - Z_{ij} - E1_{ij} - E2_{ij}\right) \geq \frac{d_i + d_j}{2} + 4 , \tag{5-268}$$

where i = 1,2,…,13, and j = i +1,…,14.

② Workspace area constraints

The workspace that is not related to the equipment or maintenance area is assumed to be more than 50% of the deck area (FA). When applied to all the equipment on the dual N_2 expander modules, a total of 18 constraints can be derived, as follows:

For refrigerant module 1 (5),

$$FA - \left(\sum_{i=1}^{5} V_{i,1} a_i b_i + X^{\max} \times 9\right) \geq \frac{1}{2} FA . \tag{5-269}$$

For refrigerant module 2 (13),

$$FA - \left(\sum_{i=1}^{13} V_{i,1} a_i b_i + X^{\max} \times 9\right) \geq \frac{1}{2} FA . \tag{5-270}$$

③ Emergency area constraints

To consider safety for each module, safety facilities such as the PSV and BDV are considered. Thus, the safety facility space at the highest decks for each module is assumed to be more than 60% of the deck area (FA). When applied to all the equipment on the dual N_2 expander modules, a total of 18 constraints can be derived, as follows:

For refrigerant module 1 (5),

$$FA-(\sum_{i=1}^{5}V_{i,4}a_ib_i + X^{\max}\times 9) \geq 0.6FA \quad (5\text{-}271)$$

For refrigerant module 2 (13),

$$FA-(\sum_{i=1}^{13}V_{i,5}a_ib_i + X^{\max}\times 9) \geq 0.6FA \quad (5\text{-}272)$$

④ Additional layout design constraints

In Figure 5-8, the distance between the equipment side and each deck side is assumed to be more than 3 m. When applied to all the equipment on the dual N_2 expander modules, a total of 72 constraints can be derived, as follows:

For refrigerant module 1 (20),

$$x_i \geq \frac{l_i}{2}+3, \quad (5\text{-}273)$$

$$y_i \geq \frac{b_i}{2}+3, \quad (5\text{-}274)$$

$$x_i + \frac{l_i}{2}+3 \leq X^{\max}, \text{ and} \quad (5\text{-}275)$$

$$y_i + \frac{d_i}{2} \leq Y^{\max}, \quad (5\text{-}276)$$

where i = 1,2,…,5.

For refrigerant module 2 (52),

$$x_i \geq \frac{l_i}{2} + 3, \qquad (5\text{-}277)$$

$$y_i \geq \frac{b_i}{2} + 3, \qquad (5\text{-}278)$$

$$x_i + \frac{l_i}{2} + 3 \leq X^{\max}, \text{ and} \qquad (5\text{-}279)$$

$$y_i + \frac{d_i}{2} \leq Y^{\max}, \qquad (5\text{-}280)$$

where i = 1,2,…,13.

Therefore, the inequality constraints for the mathematical modeling of the dual N_2 expander modules numbered 180.

(4) Objective function

The overall objective function that was used for the plant layout problem is as follows (Patsiatzis, 2002):

$$W = \sum_i \sum_{j \neq i / f_{ij}=1} \left[C^c_{ij} TD_{ij} + C^v_{ij} D_{ij} + C^h_{ij} \left(R_{ij} + L_{ij} + A_{ij} + B_{ij} \right) \right] + FC1 \cdot NF + LC \cdot FA, \qquad (5\text{-}281)$$

where i = 1,2,…,13, j = 1,2,…,13;

f_{ij}: 1 if the flow is from item i to item j; otherwise, 0;

C^c_{ij}: connection cost between items i and j;

C^v_{ij}: vertical pumping cost between items i and j;

C^h_{ij}: horizontal pumping cost between items i and j;

$FC1$: deck construction cost; and

LC: module cost.

In each module, there are high-pressure systems using compressors; pumps are not used in this study. The number of decks for each module is fixed. Thus, the deck construction cost is not required as an objective function in this study. In this paper, the connectivity cost, the construction cost proportional to the deck area, and the distance of the MCHEs and separators from the centerline of the hull are considered objective functions to be minimized. In conclusion, there is an objective function in this study, as follows:

$$W = \sum_i \sum_{j \neq i} \left[W_{1,ij} TD_{ij} \right] + W_2 FA + W_3 y_i \quad , \tag{5-282}$$

where $W_{1,ij}$: connection cost between items i and j;

W_2: construction cost;

W_3: motion impact cost;

i,j: equipment items;

TD_{ij}: total rectilinear distance between equipment items i and j;

FA: deck area; and

y_i: distance between the heat exchanger and the centerline,

$$TD_{ij} = \left| x_i - x_j \right| + \left| y_i - y_j \right| + U_{ij} \tag{5-283}$$

$$U_{ij} = \left| H \sum_{k=1}^{NF} k \left(V_{ik} - V_{jk} \right) + z_i - z_j \right| \quad , \tag{5-284}$$

where

where k: deck number;

NF: number of decks (5);

H: height between the decks (8 m);

$V_{i,k}$: 1 if equipment item i is assigned to deck k; otherwise, 0; and

$U_{i,j}$: relative distance in the z-coordinates between equipment items i and j if i is higher than j.

(5) Summary of the mathematical model

Objective function: Minimize W

$$W = \sum_{i} \sum_{j \neq i} \left[W_{1,ij} TD_{ij} \right] + W_2 FA + W_3 y_i$$

Design variables [144]:

- Related to each equipment [40+104=144]

Constraints:

(Equality constraints) [114]

- Deck constraints [25+65=90]
- Land area constraints [1]
- Equipment constraints: multi-deck [23]

(Inequality constraints) [180]

- Non-overlapping constraints [72]
- Workspace area constraints [18]
- Emergency area constraints [18]

Additional layout design constraint [72]

5.4. Determination of the Optimal Equipment Module Layout for the Potential Offshore Liquefaction Cycles

Based on the mathematical models formulated herein, the optimal equipment module layouts for the potential offshore liquefaction cycles were obtained using MINLP.

5.4.1. Potential MR liquefaction cycle (case 14)

The results for the 3D view, plane views, and design variables for each module are shown in Figure 5-28 to 5-42 and in Table 5-56 to 5-67, respectively.

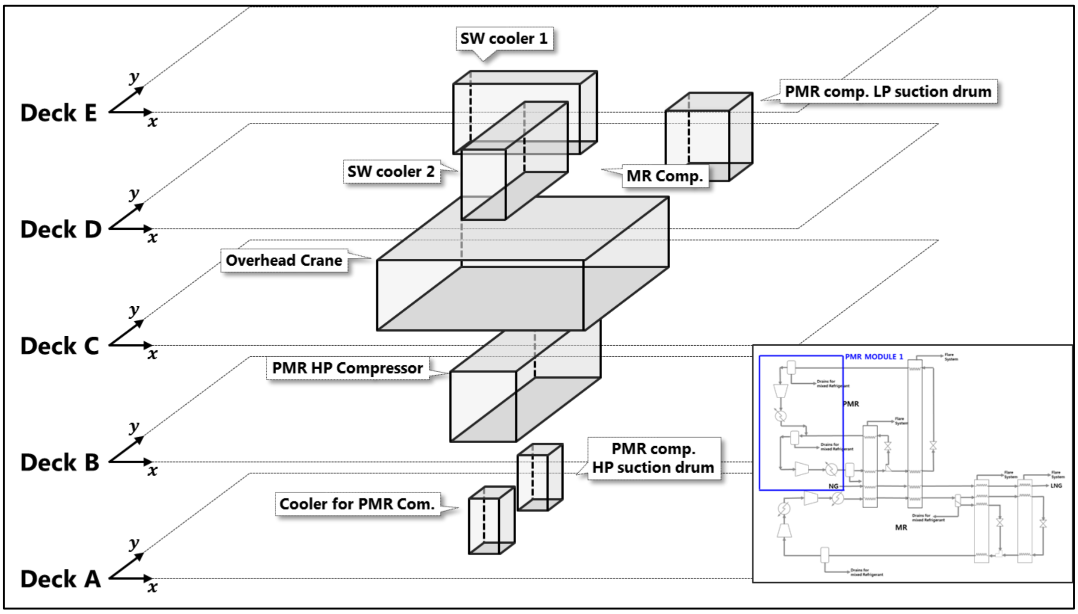

Figure 5-28 3D view of PMR module 1 of the potential MR liquefaction cycle

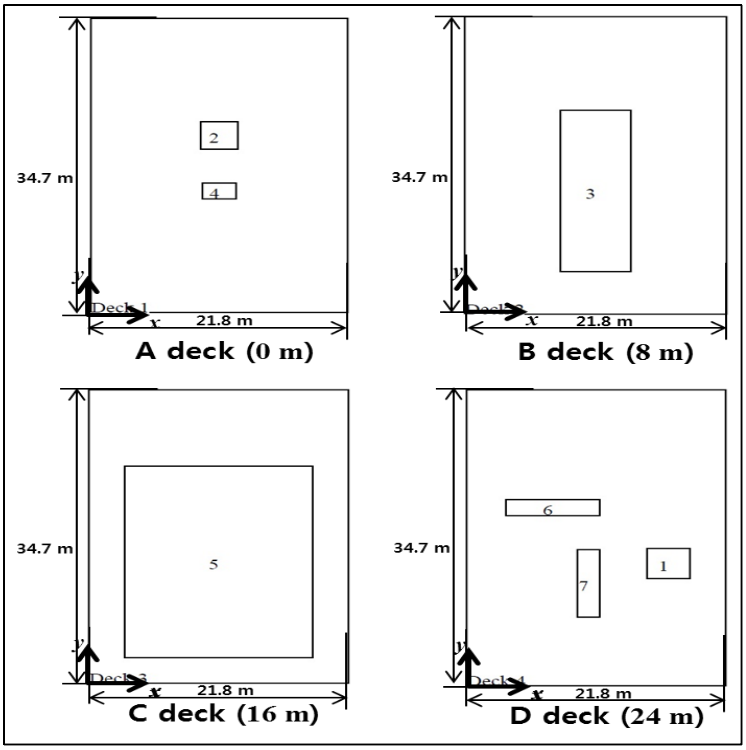

Figure 5-29 Plane view of PMR module 1 of the potential MR liquefaction cycle (4.0 MTPA)

Table 5-56 Design variables of PMR module 1 of the potential MR liquefaction cycle (4.0 MTPA)

Equipment		x_i [m]	y_i [m]	O_i	$V_{i,k}$			
No.	Name				$V_{i,1}$	$V_{i,2}$	$V_{i,3}$	$V_{i,4}$
1	PMR comp. LP suction drum	17	14.35	0	0	0	0	1
2	PMR comp. HP suction drum	10.872	20.9	0	1	0	0	0
3	PMR HP Compressor	10.9	14.35	1	0	1	0	0
4	Cooler for PMR Com.	10.9	14.35	0	1	0	0	0
5	Overhead Crane	10.9	14.35	1	0	0	1	0
6	SW cooler 1	7.25	20.9	0	0	0	0	1
7	SW cooler 2	10.25	12	1	0	0	0	1

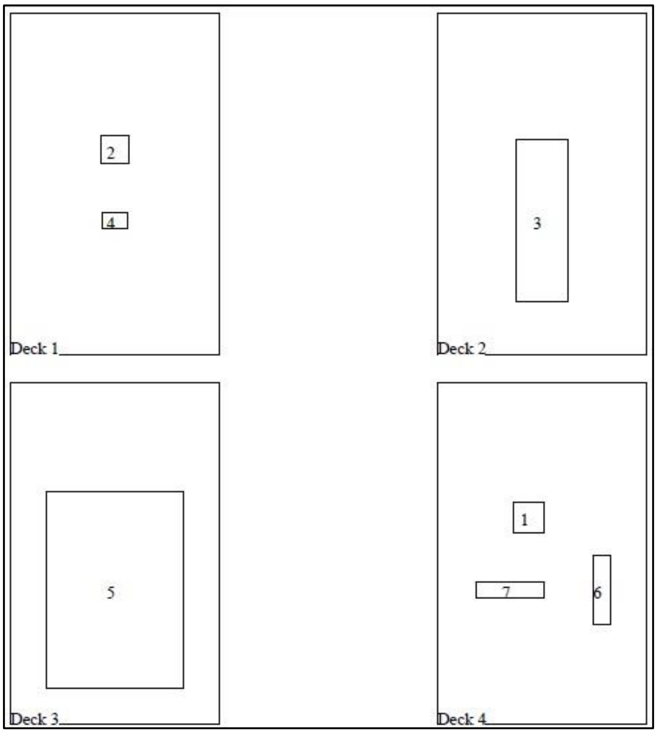

Figure 5-30 Plane view of PMR module 1 of the potential MR liquefaction cycle (3.0 MTPA)

Table 5-57 Design variables of PMR module 1 of the potential MR liquefaction cycle (3.0 MTPA)

Equipment		x_i [m]	y_i [m]	O_i	$V_{i,k}$			
No.	Name				$V_{i,1}$	$V_{i,2}$	$V_{i,3}$	$V_{i,4}$
1	PMR comp. LP suction drum	7.560	17.060	0	0	0	0	1
2	PMR comp. HP suction drum	8.620	16.920	0	1	0	0	0
3	PMR HP Compressor	8.620	11.080	1	0	1	0	0
4	Cooler for PMR Com.	8.620	11.080	0	1	0	0	0
5	Overhead Crane	8.620	11.080	1	0	0	1	0
6	SW cooler 1	13.540	11.080	1	0	0	0	1
7	SW cooler 2	6.030	11.080	0	0	0	0	1

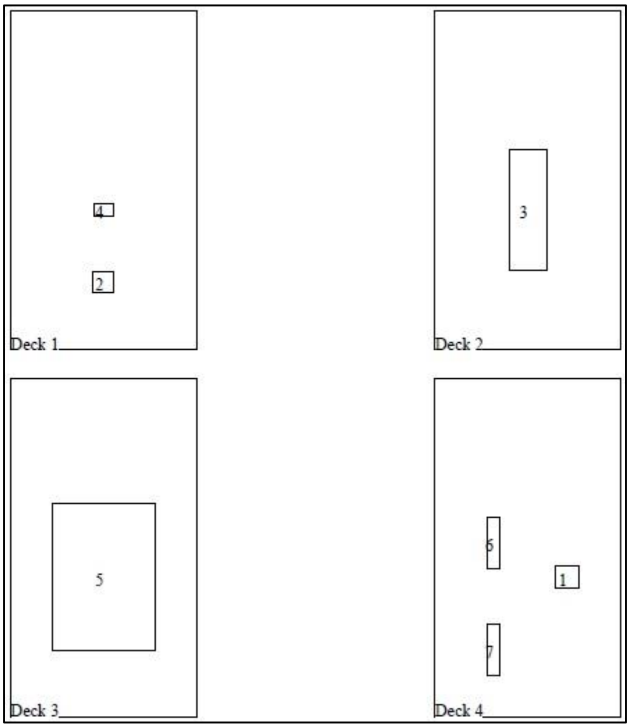

Figure 5-31 Plane view of PMR module 1 of the potential MR liquefaction cycle (2.0 MTPA)

Table 5-58 Design variables of PMR module 1 of the potential MR liquefaction cycle (2.0 MTPA)

Equipment		x_i [m]	y_i [m]	O_i	$V_{i,k}$			
No.	Name				$V_{i,1}$	$V_{i,2}$	$V_{i,3}$	$V_{i,4}$
1	PMR comp. LP suction drum	9.46	10.015	0	0	0	0	1
2	PMR comp. HP suction drum	6.645	4.820	0	1	0	0	0
3	PMR HP Compressor	6.645	10.015	1	0	1	0	0
4	Cooler for PMR Com.	6.645	10.015	0	1	0	0	0
5	Overhead Crane	6.645	10.015	1	0	0	1	0
6	SW cooler 1	4.175	12.460	1	0	0	0	1
7	SW cooler 2	4.175	4.820	1	0	0	0	1

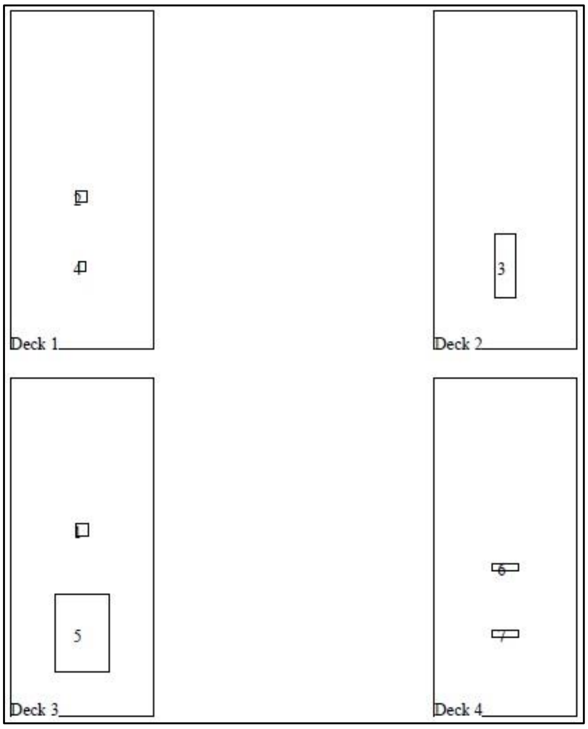

Figure 5-32 Plane view of PMR module 1 of the potential MR liquefaction cycle (1.0 MTPA)

Table 5-59 Design variables of PMR module 1 of the potential MR liquefaction cycle (1.0 MTPA)

Equipment		x_i $[m]$	y_i $[m]$	O_i	$V_{i,k}$			
No.	Name				$V_{i,1}$	$V_{i,2}$	$V_{i,3}$	$V_{i,4}$
1	PMR comp. LP suction drum	4.820	12.655	0	0	0	1	0
2	PMR comp. HP suction drum	4.820	10.330	0	1	0	0	0
3	PMR HP Compressor	4.820	5.620	1	0	1	0	0
4	Cooler for PMR Com.	4.820	5.620	1	1	0	0	0
5	Overhead Crane	4.820	5.620	1	0	0	1	0
6	SW cooler 1	4.820	10.080	0	0	0	0	1
7	SW cooler 2	4.820	5.620	0	0	0	0	1

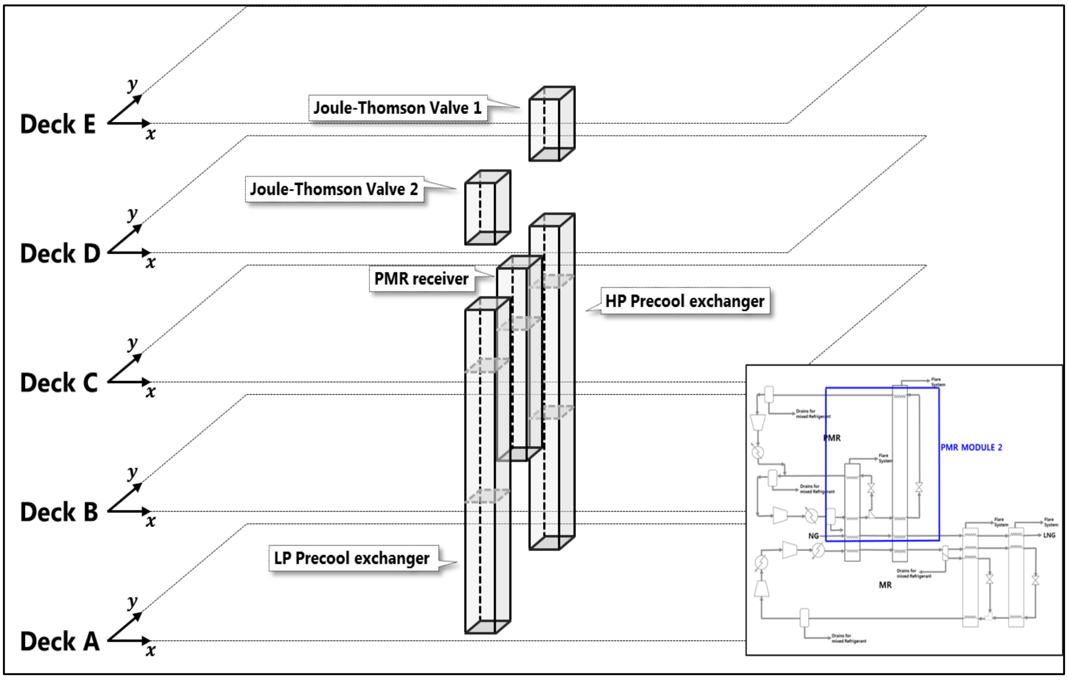

Figure 5-33 3D view of PMR module 2 of the potential MR liquefaction cycle.

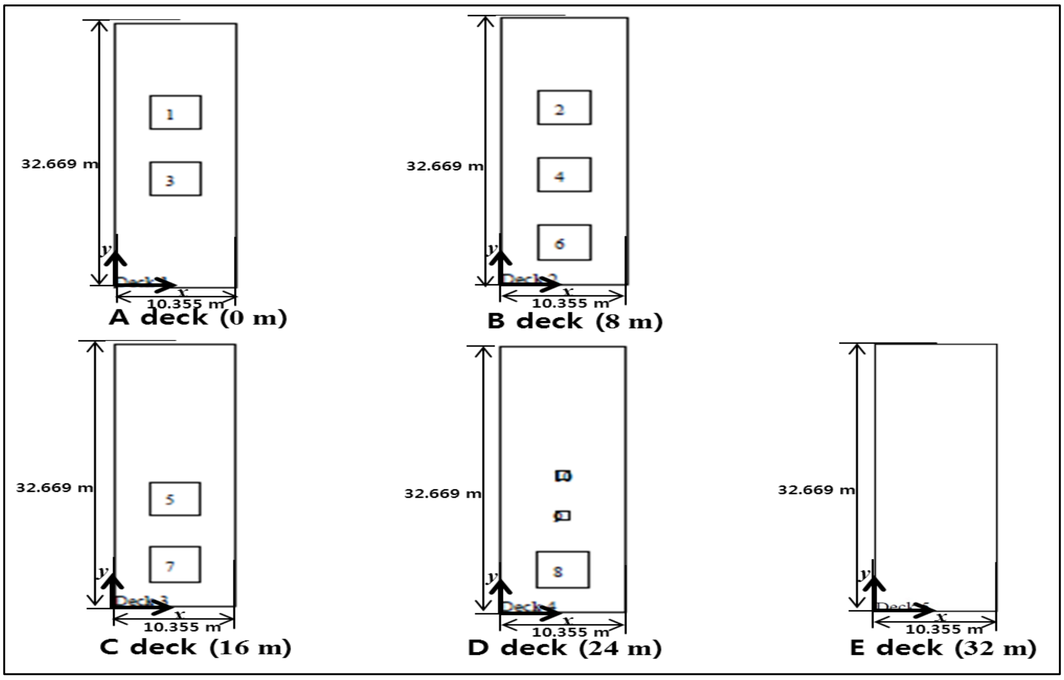

Figure 5-34 Plane view of PMR module 2 of the potential MR liquefaction cycle (4.0 MTPA)

Table 5-60 Design variables of PMR module 2 of the potential MR liquefaction cycle (4.0 MTPA)

Equipment		x_i [m]	y_i [m]	O_i	$V_{i,k}$				
No	Name				$V_{i,1}$	$V_{i,2}$	$V_{i,3}$	$V_{i,4}$	$V_{i,5}$
1	PMR receiver on lower deck	5.177	21.591	1	1	0	0	0	0
2	PMR receiver on upper deck	5.177	21.591	1	0	1	0	0	0
3	LP precool exchanger on A deck	5.177	13.434	1	1	0	0	0	0
4	LP precool exchanger on B deck	5.177	13.434	1	0	1	0	0	0
5	LP precool exchanger	5.177	13.434	1	0	0	1	0	0

	on C deck								
6	HP precool exchanger on A deck	5.177	5.177	0	0	1	0	0	0
7	HP precool exchanger on B deck	5.177	5.177	0	0	0	1	0	0
8	HP precool exchanger on C deck	5.177	5.177	0	0	0	0	1	0
9	Joule-Thomson Valve 1	5.177	11.850	0	0	0	0	1	0
10	Joule-Thomson Valve 2	5.177	16.839	0	0	0	0	1	0

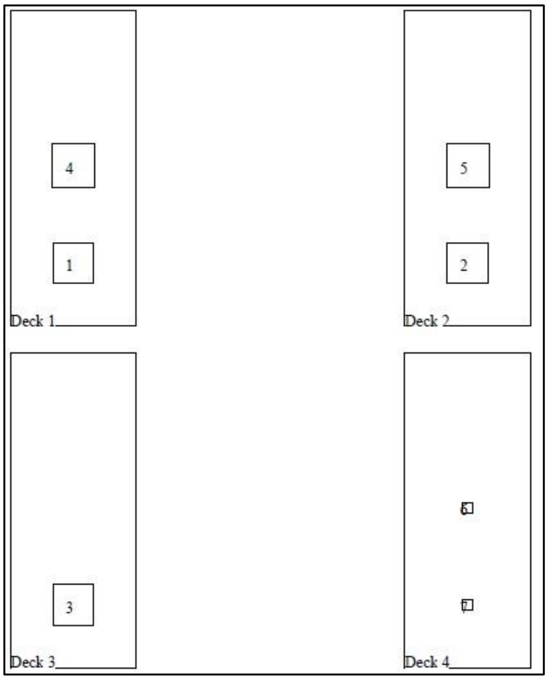

Figure 5-35 Plane view of PMR module 2 of the potential MR liquefaction cycle (3.0 MTPA)

Table 5-61 Design variables of PMR module 2 of the potential MR liquefaction cycle (3.0 MTPA)

Equipment		x_i [m]	y_i [m]	O_i	$V_{i,k}$				
No	Name				$V_{i,1}$	$V_{i,2}$	$V_{i,3}$	$V_{i,4}$	$V_{i,5}$
1	PMR receiver	4.545	4.545	0	1	0	0	0	0
2	LP precool exchanger on B deck	4.545	4.545	0	0	1	0	0	0
3	LP precool exchanger on C deck	4.545	4.545	0	0	0	1	0	0
4	HP precool exchanger on A deck	4.545	11.563	0	1	0	0	0	0
5	HP precool	4.545	11.563	0	0	1	0	0	0

	exchanger on B deck								
6	Joule-Thomson Valve 1	4.545	11.563	0	0	0	0	1	0
7	Joule-Thomson Valve 2	4.545	4.545	0	0	0	0	1	0

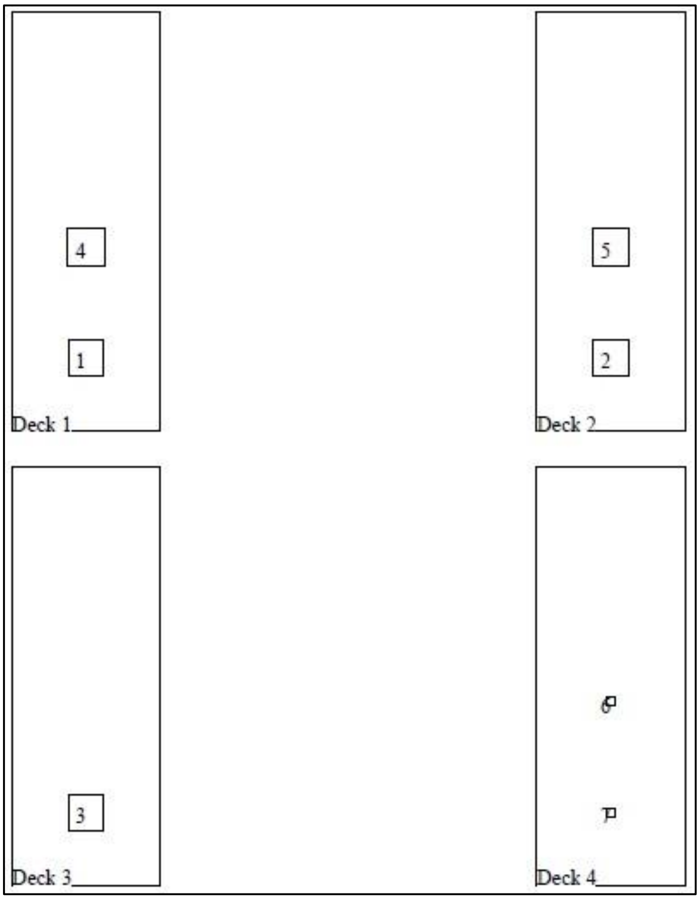

Figure 5-36 Plane view of PMR module 2 of the potential MR liquefaction cycle (2.0 MTPA)

Table 5-62 Design variables of PMR module 2 of the potential MR liquefaction cycle (2.0 MTPA)

Equipment		x_i [m]	y_i [m]	O_i	$V_{i,k}$				
No	Name				$V_{i,1}$	$V_{i,2}$	$V_{i,3}$	$V_{i,4}$	$V_{i,5}$
1	PMR receiver	4.000	3.955	0	1	0	0	0	0
2	LP precool exchanger on B deck	3.984	3.955	0	0	1	0	0	0
3	LP precool exchanger	3.984	3.955	0	0	0	1	0	0

	on C deck								
4	HP precool exchanger on A deck	4.000	9.910	0	1	0	0	0	0
5	HP precool exchanger on B deck	4.000	9.910	0	0	1	0	0	0
6	Joule-Thomson Valve 1	4.000	9.910	0	0	0	0	1	0
7	Joule-Thomson Valve 2	3.984	3.955	0	0	0	0	1	0

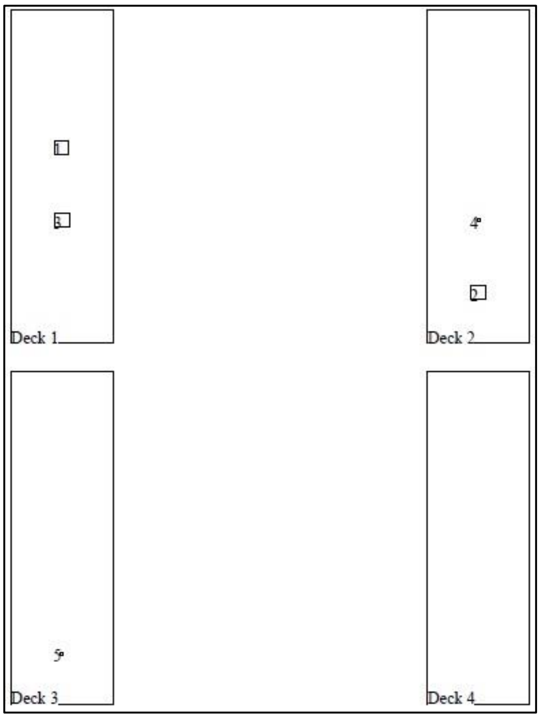

Figure 5-37 Plane view of PMR module 2 of the potential MR liquefaction cycle (1.0 MTPA)

Table 5-63 Design variables of PMR module 2 of the potential MR liquefaction cycle (1.0 MTPA)

Equipment		x_i [m]	y_i [m]	O_i	$V_{i,k}$				
No	Name				$V_{i,1}$	$V_{i,2}$	$V_{i,3}$	$V_{i,4}$	$V_{i,5}$
1	PMR receiver	3.500	13.440	0	1	0	0	0	0
2	LP precool exchanger on B deck	3.480	3.480	0	0	1	0	0	0
3	HP precool exchanger on A deck	3.500	8.460	0	1	0	0	0	0
4	Joule-Thomson Valve 1	3.500	8.460	0	0	1	0	0	0
5	Joule-Thomson Valve 2	3.480	3.480	0	0	0	1	0	0

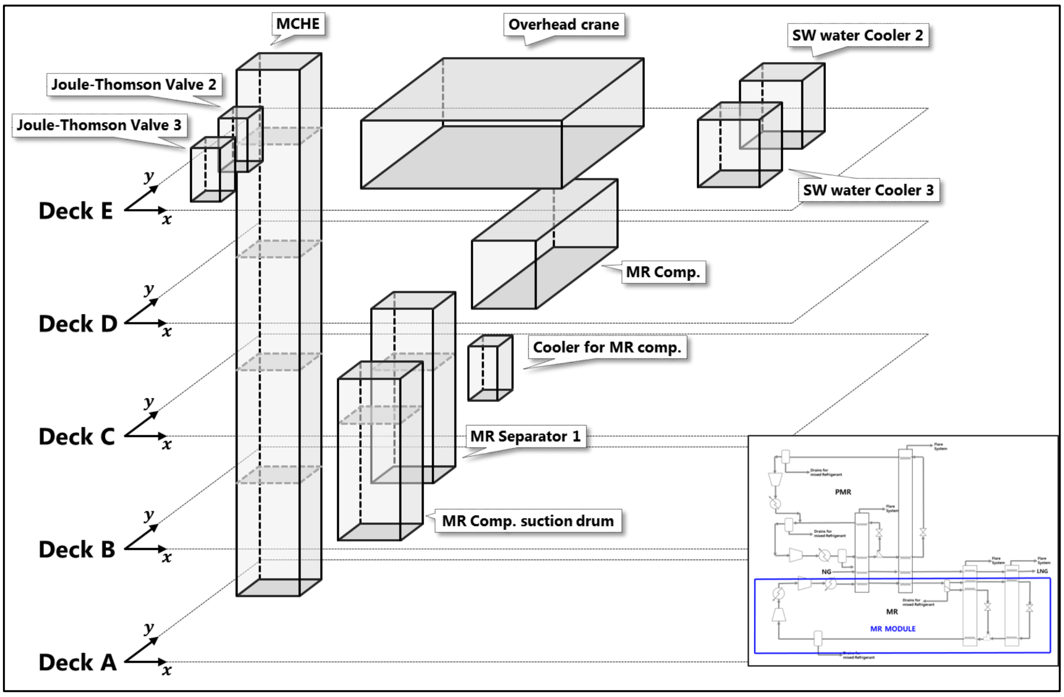

Figure 5-38 3D view of the MR module of the potential MR liquefaction cycle

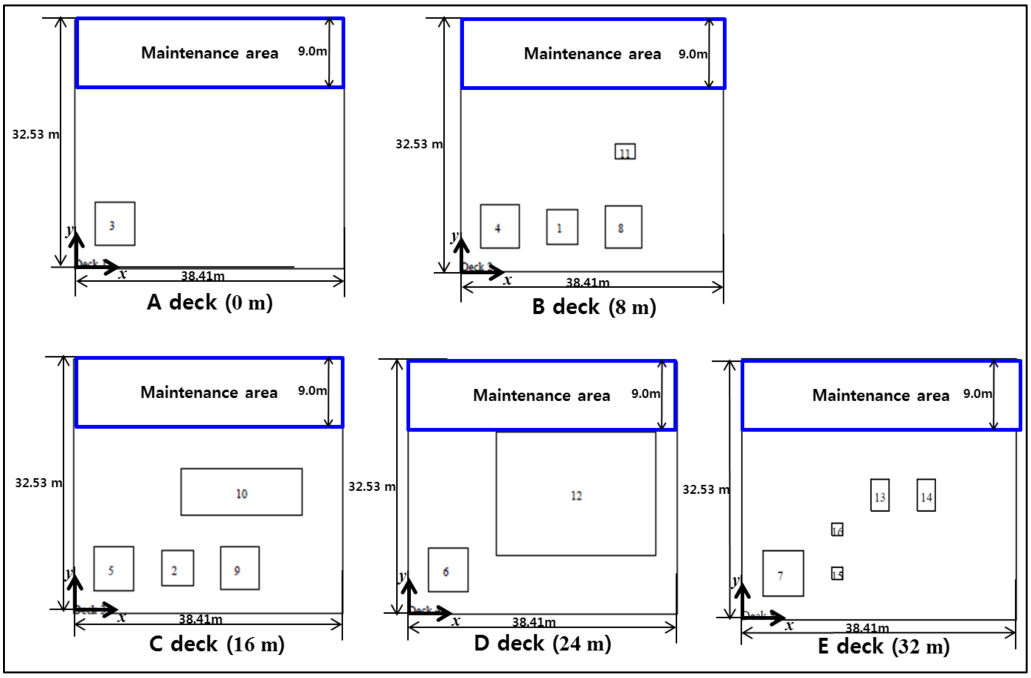

Figure 5-39 Plane view of the MR module of the potential MR liquefaction cycle (4.0 MTPA)

Table 5-64 Design variables of the MR module of the potential MR liquefaction cycle (4.0 MTPA)

Equipment		x_i [m]	y_i [m]	O_i	$V_{i,k}$				
No.	Name				$V_{i,1}$	$V_{i,2}$	$V_{i,3}$	$V_{i,4}$	$V_{i,5}$
1	MR separator 1 on lower deck	14.865	5.820	0	0	1	0	0	0
2	MR separator 1 on upper deck	14.865	5.820	0	0	0	1	0	0
3	MCHE on A deck	5.820	5.820	0	1	0	0	0	0
4	MCHE on B deck	5.820	5.820	0	0	1	0	0	0
5	MCHE on C deck	5.820	5.820	0	0	0	1	0	0
6	MCHE on D deck	5.820	5.820	0	0	0	0	1	0
7	MCHE	5.820	5.820	0	0	0	0	0	1

	on E deck								
8	MR Comp. suction drum on lower deck	23.810	5.821	0	0	1	0	0	0
9	MR Comp. suction drum on upper deck	23.810	5.821	0	0	0	1	0	0
10	MR Comp.	24.025	15.610	0	0	0	1	0	0
11	Cooler for comp.	24.025	15.610	0	0	1	0	0	0
12	Overhead crane	24.025	15.610	0	0	0	0	1	0
13	SW water 3	19.355	15.610	1	0	0	0	0	1
14	SW water 4	25.825	15.610	1	0	0	0	0	1
15	Joule-Thomson Valve 3	13.380	5.820	0	0	0	0	0	1
16	Joule-Thomson Valve 4	13.380	11.300	0	0	0	0	0	1

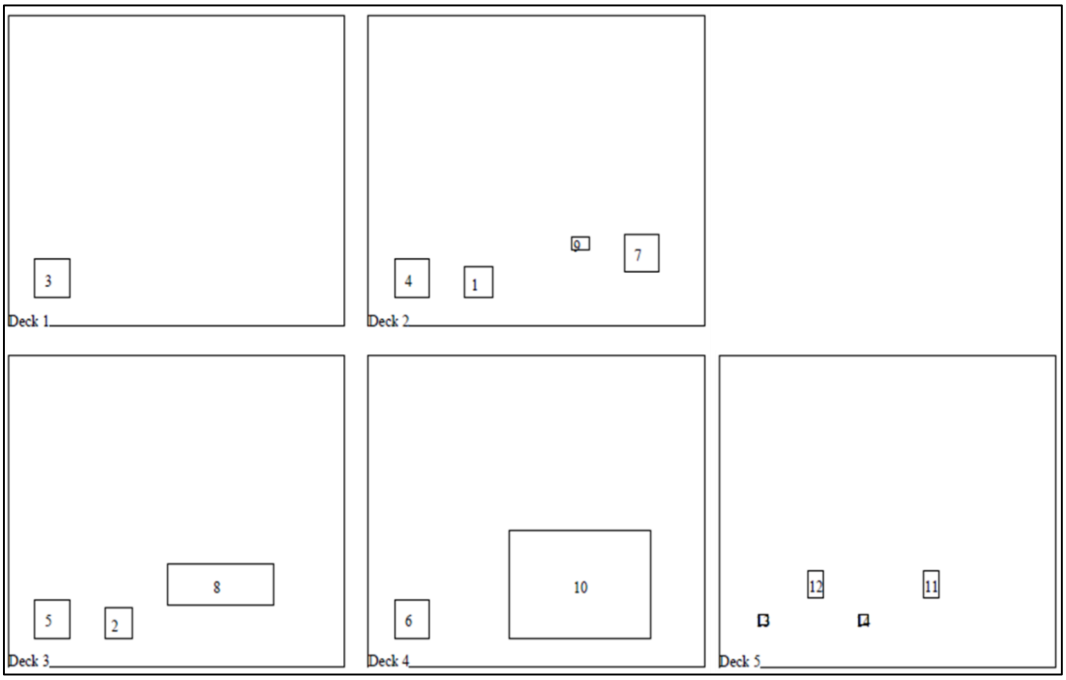

Figure 5-40 Plane view of the MR module of the potential MR liquefaction cycle (3.0 MTPA)

Table 5-65 Design variables of the MR module of the potential MR liquefaction cycle (3.0 MTPA)

Equipment		x_i [m]	y_i [m]	O_i	$V_{i,k}$				
No.	Name				$V_{i,1}$	$V_{i,2}$	$V_{i,3}$	$V_{i,4}$	$V_{i,5}$
1	MR separator 1 on lower deck	12.590	4.580	0	0	1	0	0	0
2	MR separator 1 on upper deck	12.590	4.580	0	0	0	1	0	0
3	MCHE on A deck	5.005	5.005	0	1	0	0	0	0
4	MCHE on B deck	5.005	5.005	0	0	1	0	0	0
5	MCHE on C deck	5.005	5.005	0	0	0	1	0	0
6	MCHE on D deck	5.005	5.005	0	0	0	0	1	0
7	MR Comp.	31.235	7.639	0	0	1	0	0	0

	suction drum								
8	MR Comp.	24.250	8.620	0	0	0	1	0	0
9	Cooler for comp.	24.250	8.620	0	0	1	0	0	0
10	Overhead crane	24.250	8.620	0	0	0	0	1	0
11	SW water 3	24.250	8.620	1	0	0	0	0	1
12	SW water 4	11.037	8.620	1	0	0	0	0	1
13	Joule-Thomson Valve 3	5.005	5.005	0	0	0	0	0	1
14	Joule-Thomson Valve 4	16.442	5.005	0	0	0	0	0	1

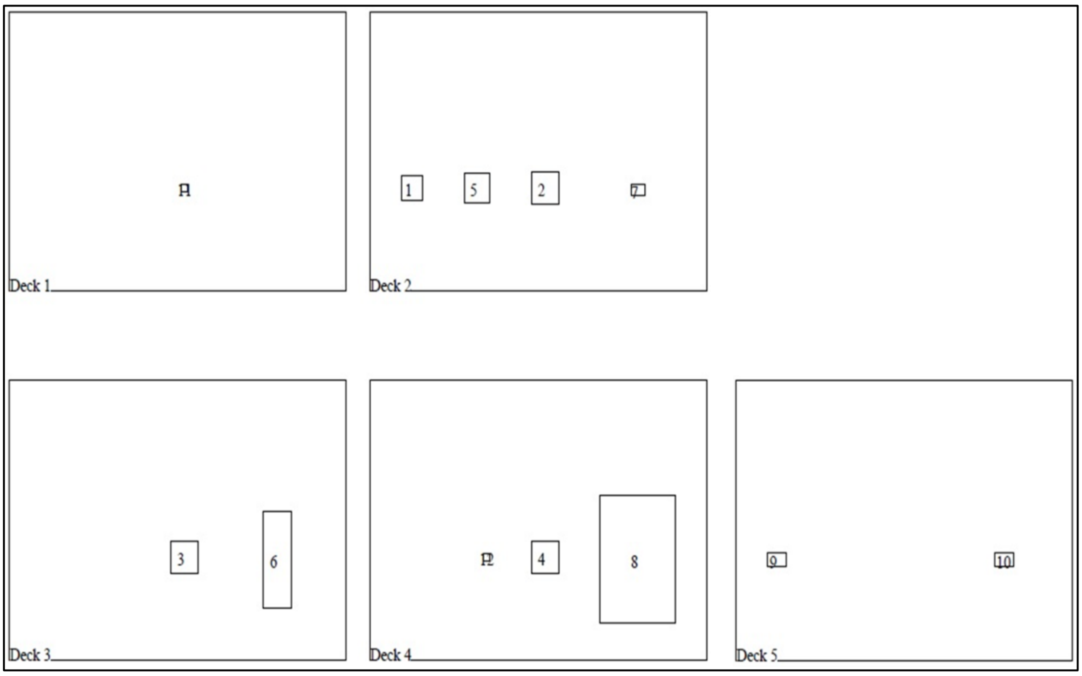

Figure 5-41 Plane view of the MR module of the potential MR liquefaction cycle (2.0 MTPA)

Table 5-66 Design variables of the MR module of the potential MR liquefaction cycle (2.0 MTPA)

Equipment		x_i $[m]$	y_i $[m]$	O_i	$V_{i,k}$				
No.	Name				$V_{i,1}$	$V_{i,2}$	$V_{i,3}$	$V_{i,4}$	$V_{i,5}$
1	MR separator 1	4.475	8.235	0	0	1	0	0	0
2	MCHE on B deck	10.800	8.235	0	0	1	0	0	0
3	MCHE on C deck	10.800	8.235	0	0	0	1	0	0
4	MCHE on D deck	10.800	8.235	0	0	0	0	1	0
5	MR Comp. suction drum	4.250	8.235	0	0	0	0	1	0
6	MR Comp.	19.745	8.235	1	0	0	1	0	0
7	Cooler for MR comp.	19.745	8.235	0	0	1	0	0	0
8	Overhead crane	19.745	8.235	1	0	0	0	1	0
9	SW water 3	22.480	8.235	0	0	0	0	0	1
10	SW water 4	16.660	8.235	0	0	0	0	0	1
11	Joule-Thomson Valve 3	6.172	8.235	0	1	0	0	0	0
12	Joule-Thomson Valve 4	10.852	8.235	0	1	0	0	0	0

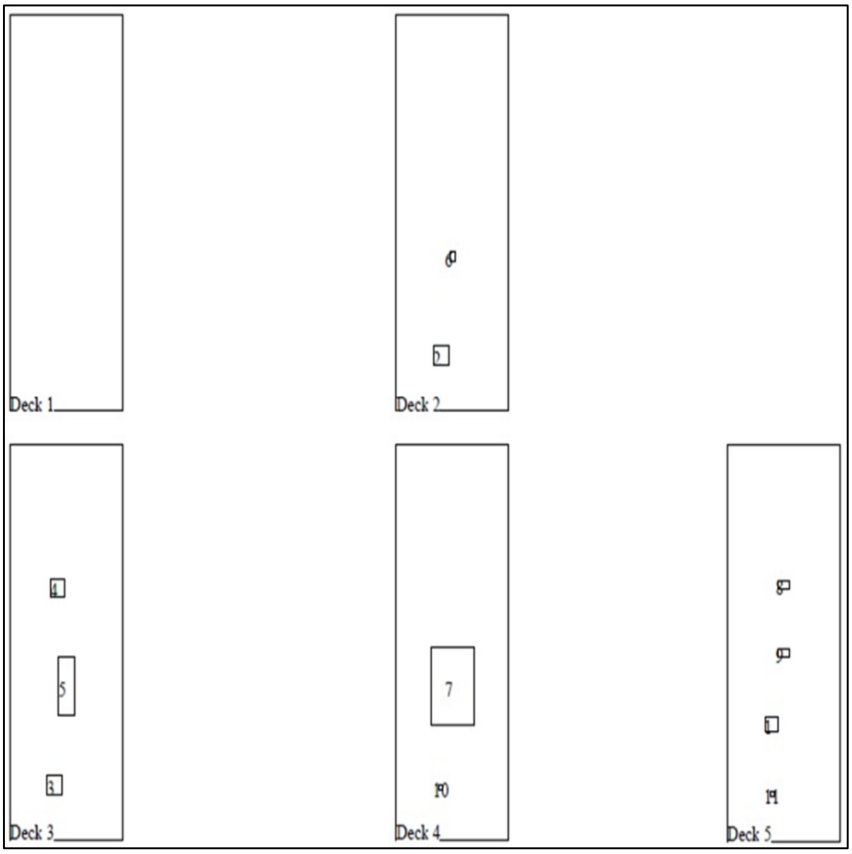

Figure 5-42 Plane view of the MR module of the potential MR liquefaction cycle (1.0 MTPA)

Table 5-67 Design variables of the MR module of the potential MR liquefaction cycle (1.0 MTPA)

Equipment		x_i [m]	y_i [m]	O_i	$V_{i,k}$				
No.	Name				$V_{i,1}$	$V_{i,2}$	$V_{i,3}$	$V_{i,4}$	$V_{i,5}$
1	MR separator 1	3.820	7.845	0	0	0	0	0	1
2	MCHE on B deck	3.819	3.650	0	0	1	0	0	0
3	MCHE on C deck	3.819	3.650	0	0	0	1	0	0
4	MR Comp. suction drum	4.095	16.860	0	0	0	1	0	0
5	MR Comp.	4.815	10.270	1	0	0	1	0	0

6	Cooler for comp.	4.815	10.270	1	0	1	0	0	0
7	Overhead crane	4.815	10.270	1	0	0	0	1	0
8	SW water 3	4.815	17.190	0	0	0	0	0	1
9	SW water 4	4.815	12.630	0	0	0	0	0	1
10	Joule-Thomson Valve 3	3.819	3.485	0	0	0	0	1	0
11	Joule-Thomson Valve 4	3.819	3.170	1	0	0	0	0	1

5.4.2. DMR cycle

The results for the 3D view, plan views and design variables for each module are shown in Figures 5-43~5-57, and Tables 5-68~79, respectively.

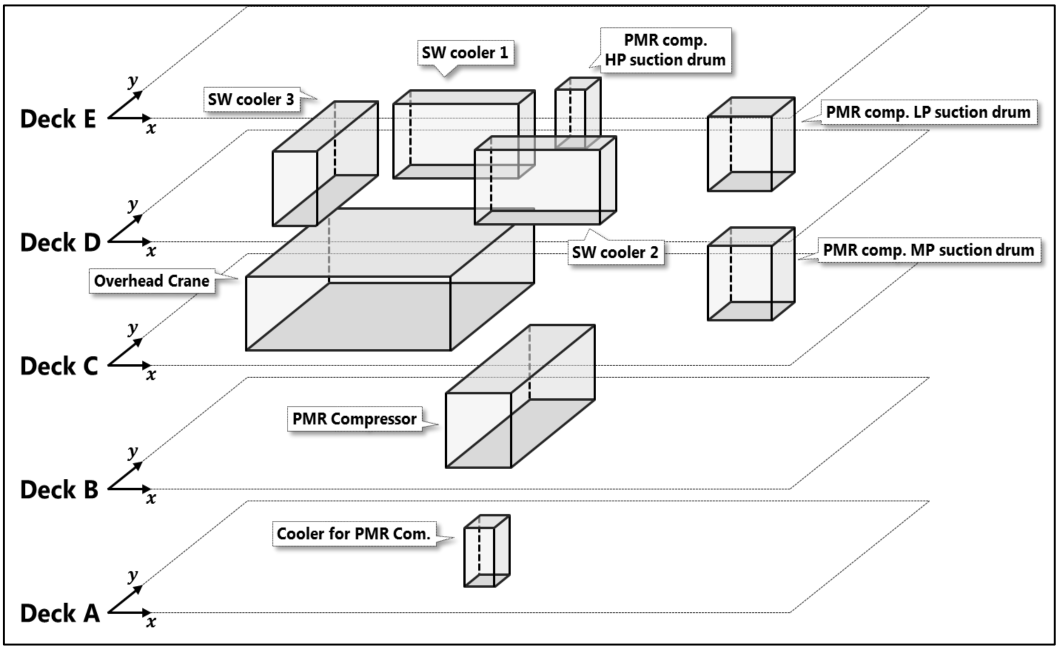

Figure 5-43 3D view of PMR module 1 of the DMR cycle

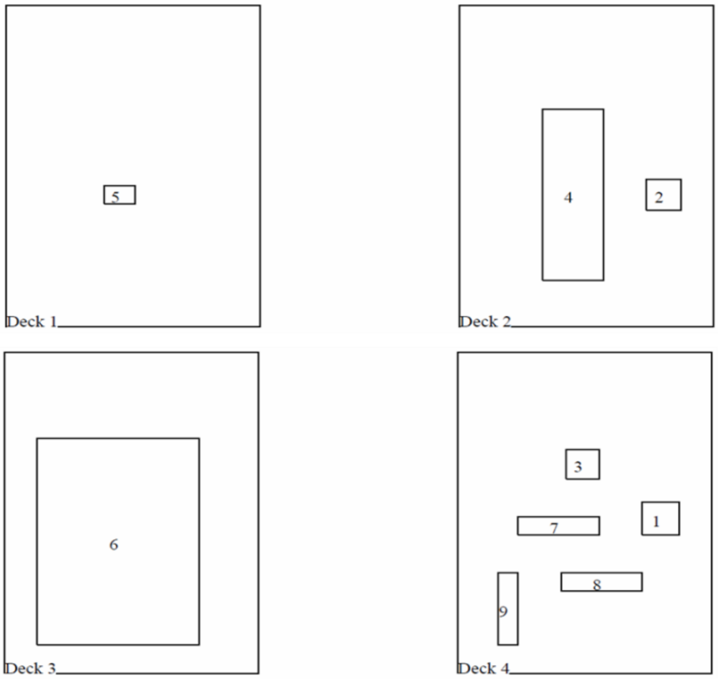

Figure 5-44 Plane view of PMR module 1 of the DMR cycle (4.0 MTPA)

Table 5-68 Design variables of PMR module 1 of the DMR cycle (4.0 MTPA)

Equipment		x_i $[m]$	y_i $[m]$	O_i	$V_{i,k}$			
No.	Name				$V_{i,1}$	$V_{i,2}$	$V_{i,3}$	$V_{i,4}$
1	PMR comp. LP suction drum	18.855	16.262	0	0	0	0	1
2	PMR comp. MP suction drum	18.965	13.835	0	0	1	0	0
3	PMR comp. HP suction drum	11.605	21.952	0	0	0	0	1
4	PMR HP Compressor	10.540	13.835	1	0	1	0	0
5	Cooler for PMR Com.	10.540	13.835	0	1	0	0	0
6	Overhead Crane	10.540	13.835	1	0	0	1	0
7	SW cooler 1	9.365	15.482	0	0	0	0	1
8	SW cooler 2	13.353	9.602	0	0	0	0	1
9	SW cooler 3	4.643	6.772	1	0	0	0	1

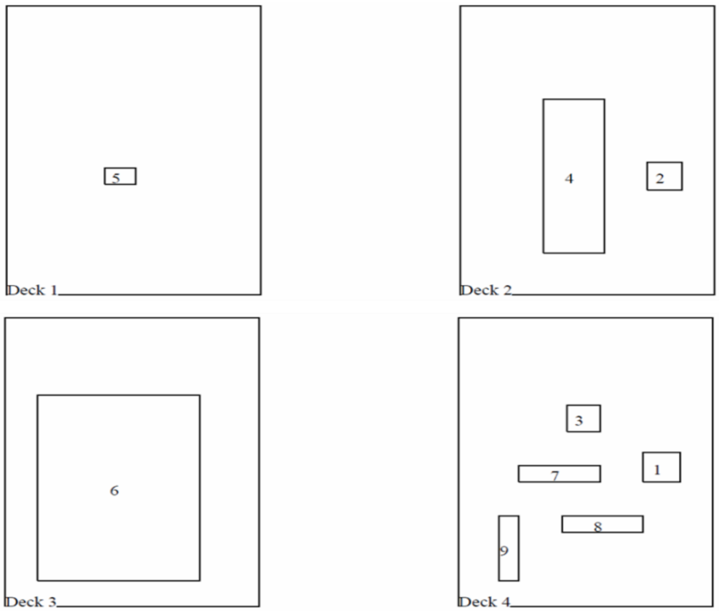

Figure 5-45 Plane view of PMR module 1 of the DMR cycle (3.0 MTPA)

Table 5-69 Design variables of PMR module 1 of the DMR cycle (3.0 MTPA)

Equipment		x_i $[m]$	y_i $[m]$	O_i	$V_{i,k}$			
No.	Name				$V_{i,1}$	$V_{i,2}$	$V_{i,3}$	$V_{i,4}$
1	PMR comp. LP suction drum	18.855	16.262	0	0	0	0	1
2	PMR comp. MP suction drum	18.965	13.835	0	0	1	0	0
3	PMR comp. HP suction drum	11.605	21.952	0	0	0	0	1
4	PMR HP Compressor	10.540	13.835	1	0	1	0	0
5	Cooler for PMR Com.	10.540	13.835	0	1	0	0	0
6	Overhead Crane	10.540	13.835	1	0	0	1	0
7	SW cooler 1	9.365	15.482	0	0	0	0	1
8	SW cooler 2	13.353	9.602	0	0	0	0	1
9	SW cooler 3	4.643	6.772	1	0	0	0	1

The layout results for this case are assumed to the same results for PMR module 1 of the DMR cycle (4.0 MTPA) due to internal problems in MINLP. It will be updated according to the actual results for 3.0 MTPA.

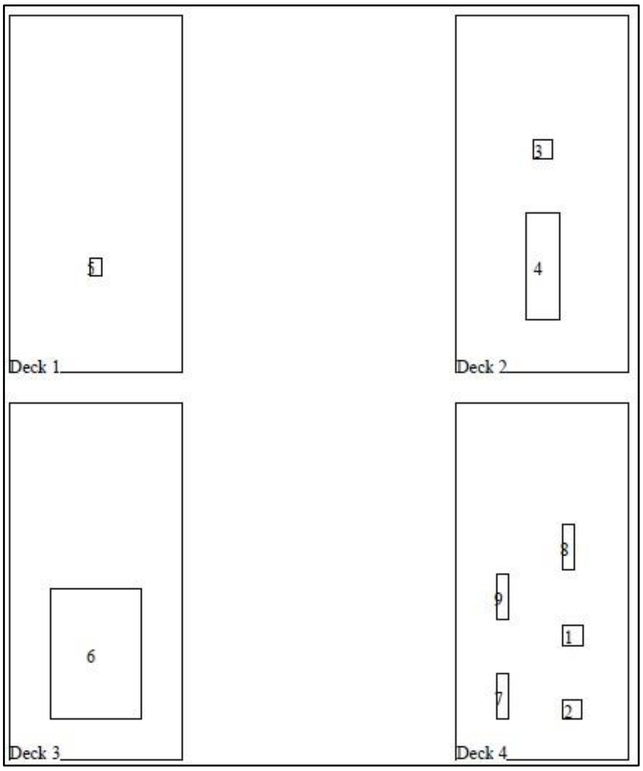

Figure 5-46 Plane view of PMR module 1 of the DMR cycle (2.0 MTPA)

Table 5-70 Design variables of PMR module 1 of the DMR cycle (2.0 MTPA)

Equipment		x_i [m]	y_i [m]	O_i	$V_{i,k}$			
No.	Name				$V_{i,1}$	$V_{i,2}$	$V_{i,3}$	$V_{i,4}$
1	PMR comp. LP suction drum	8.585	9.165	0	0	0	0	1
2	PMR comp. MP suction drum	8.535	3.705	0	0	0	0	1
3	PMR comp. HP suction drum	6.341	16.385	0	0	1	0	0
4	PMR HP Compressor	6.315	7.770	1	0	1	0	0
5	Cooler for PMR Com.	6.315	7.770	1	1	0	0	0
6	Overhead Crane	6.315	7.770	1	0	0	1	0

7	SW cooler 1	3.415	4.660	1	0	0	0	1
8	SW cooler 2	8.245	15.580	1	0	0	0	1
9	SW cooler 3	3.415	11.980	1	0	0	0	1

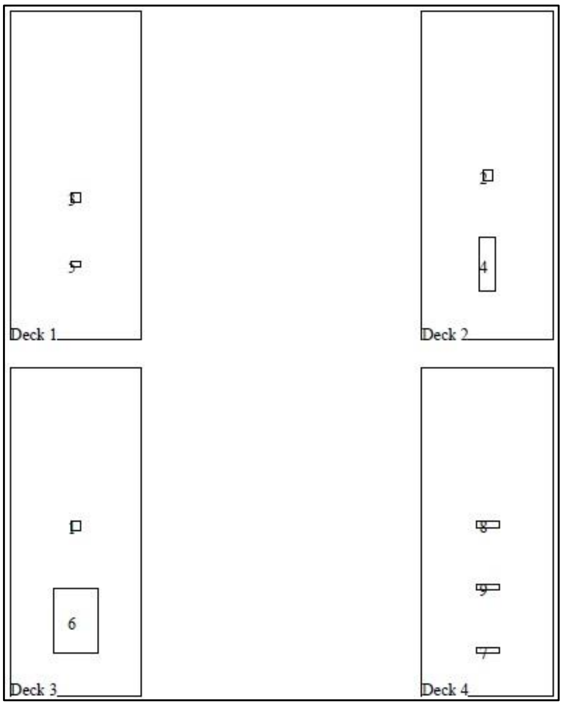

Figure 5-47 Plane view of PMR module 1 of the DMR cycle (1.0 MTPA)

Table 5-71 Design variables of PMR module 1 of the DMR cycle (1.0 MTPA)

Equipment		x_i [m]	y_i [m]	O_i	$V_{i,k}$			
No.	Name				$V_{i,1}$	$V_{i,2}$	$V_{i,3}$	$V_{i,4}$
1	PMR comp. LP suction drum	4.585	11.910	0	0	0	1	0
2	PMR comp. MP suction drum	4.585	11.495	0	0	1	0	0
3	PMR comp. HP suction drum	4.585	9.970	0	1	0	0	0
4	PMR HP Compressor	4.585	5.275	1	0	1	0	0

5	Cooler for PMR Com.	4.585	5.275	0	1	0	0	0
6	Overhead Crane	4.585	5.275	1	0	0	1	0
7	SW cooler 1	4.585	3.200	0	0	0	0	1
8	SW cooler 2	4.585	12.000	0	0	0	0	1
9	SW cooler 3	4.585	7.600	0	0	0	0	1

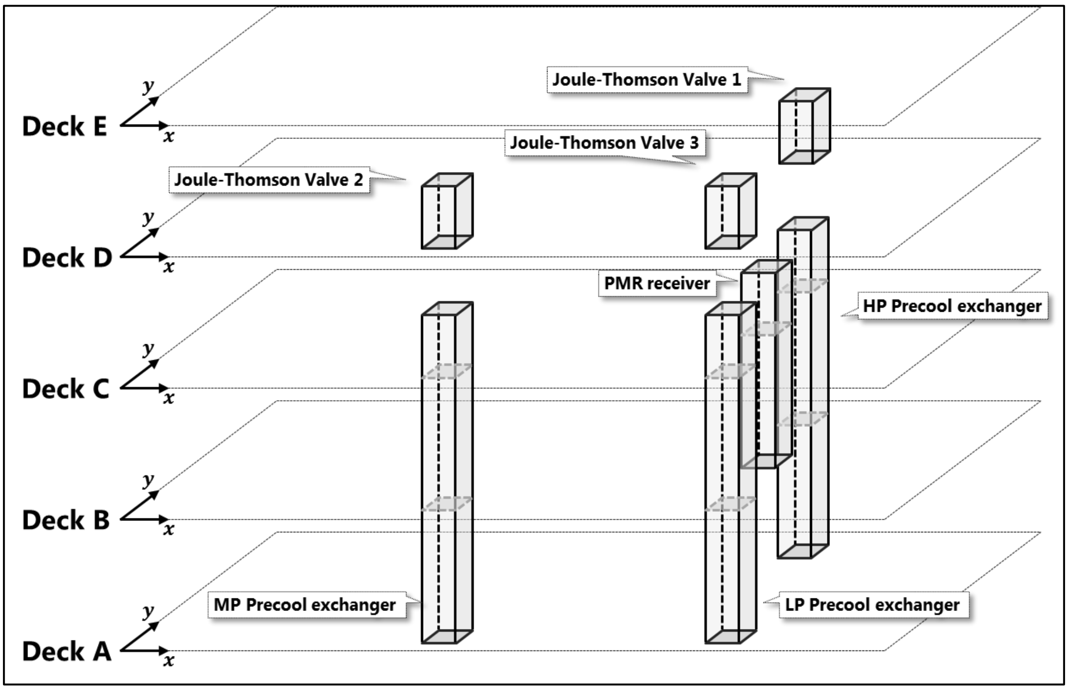

Figure 5-48 3D view of PMR module 2 of the DMR cycle

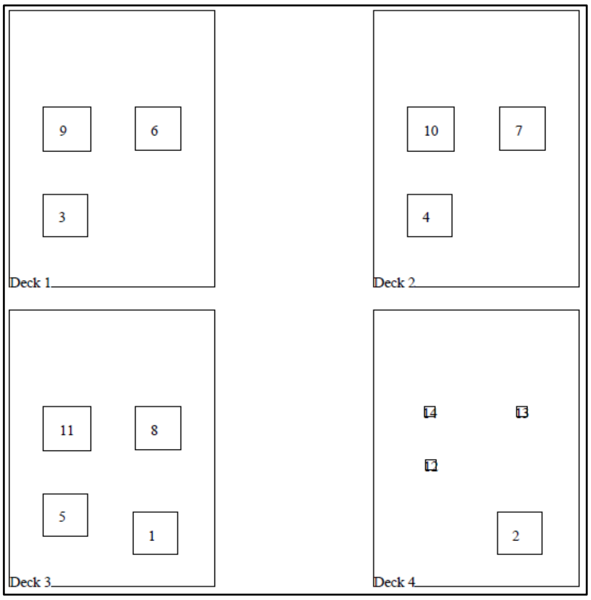

Figure 5-49 Plane view of PMR module 2 of the DMR cycle (4.0 MTPA)

Table 5-72 Design variables of PMR module 2 of the DMR cycle (4.0 MTPA)

Equipment		x_i [m]	y_i [m]	O_i	$V_{i,k}$				
No	Name				$V_{i,1}$	$V_{i,2}$	$V_{i,3}$	$V_{i,4}$	$V_{i,5}$
1	PMR receiver on lower deck	12.925	4.980	0	0	0	1	0	0
2	PMR receiver on upper deck	12.925	4.980	0	0	0	0	1	0
3	LP precool exchanger on A deck	4.975	6.710	0	1	0	0	0	0
4	LP precool exchanger on B deck	4.975	6.710	0	0	1	0	0	0
5	LP precool exchanger on C deck	4.975	6.710	0	0	0	1	0	0
6	MP precool exchanger	13.165	14.825	0	1	0	0	0	0

	on A deck								
7	MP precool exchanger on B deck	13.165	14.825	0	0	1	0	0	0
8	MP precool exchanger on C deck	13.165	14.825	0	0	0	1	0	0
9	HP precool exchanger on A deck	5.075	14.765	0	1	0	0	0	0
10	HP precool exchanger on B deck	5.075	14.765	0	0	1	0	0	0
11	HP precool exchanger on C deck	5.075	14.765	0	0	0	1	0	0
12	Joule-Thomson Valve 1	5.075	11.430	0	0	0	0	1	0
13	Joule-Thomson Valve 2	13.165	16.370	0	0	0	0	1	0
14	Joule-Thomson Valve 3	4.975	16.370	0	0	0	0	1	0

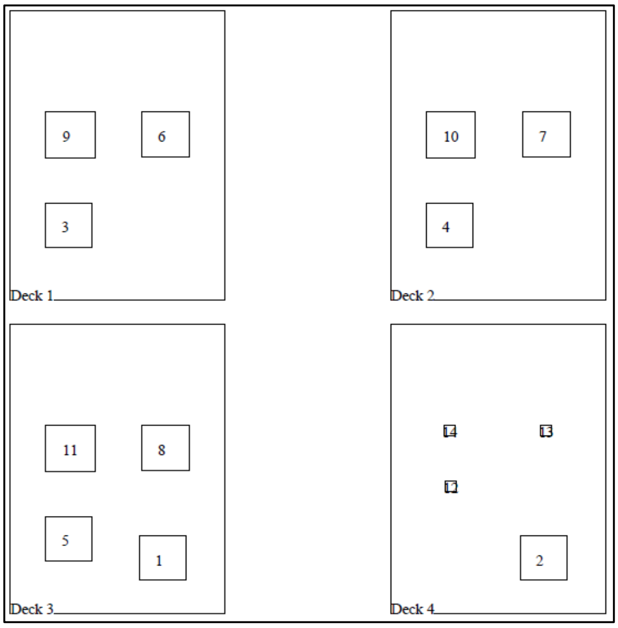

Figure 5-50 Plane view of PMR module 2 of the DMR cycle (3.0 MTPA)

Table 5-73 Design variables of PMR module 2 of the DMR cycle (3.0 MTPA)

Equipment		x_i	y_i	O_i	$V_{i,k}$				
No	Name	[m]	[m]		$V_{i,1}$	$V_{i,2}$	$V_{i,3}$	$V_{i,4}$	$V_{i,5}$
1	PMR receiver on lower deck	12.925	4.980	0	0	0	1	0	0
2	PMR receiver on upper deck	12.925	4.980	0	0	0	0	1	0
3	LP precool exchanger on A deck	4.975	6.710	0	1	0	0	0	0
4	LP precool exchanger on B deck	4.975	6.710	0	0	1	0	0	0
5	LP precool exchanger on C deck	4.975	6.710	0	0	0	1	0	0
6	MP precool exchanger	13.165	14.825	0	1	0	0	0	0

	on A deck								
7	MP precool exchanger on B deck	13.165	14.825	0	0	1	0	0	0
8	MP precool exchanger on C deck	13.165	14.825	0	0	0	1	0	0
9	HP precool exchanger on A deck	5.075	14.765	0	1	0	0	0	0
10	HP precool exchanger on B deck	5.075	14.765	0	0	1	0	0	0
11	HP precool exchanger on C deck	5.075	14.765	0	0	0	1	0	0
12	Joule-Thomson Valve 1	5.075	11.430	0	0	0	0	1	0
13	Joule-Thomson Valve 2	13.165	16.370	0	0	0	0	1	0
14	Joule-Thomson Valve 3	4.975	16.370	0	0	0	0	1	0

The layout results for this case are assumed to the same results for PMR module 2 of the DMR cycle (4.0 MTPA) due to internal problems in MINLP. It will be updated according to the actual results for 3.0 MTPA.

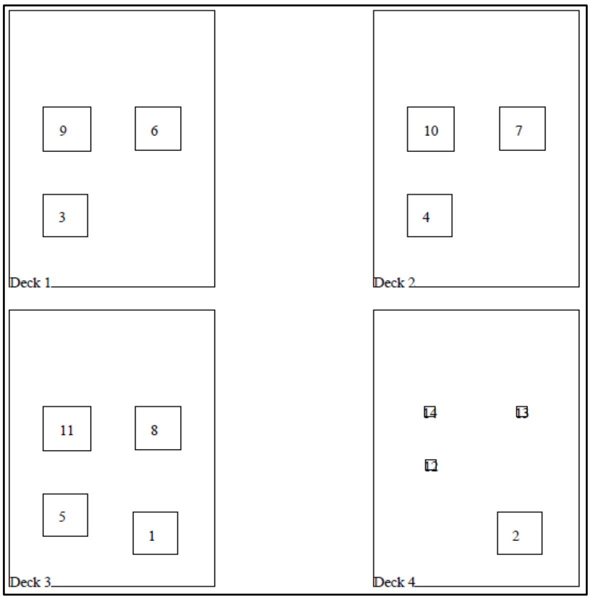

Figure 5-51 Plane view of PMR module 2 of the DMR cycle (2.0 MTPA)

Table 5-74 Design variables of PMR module 2 of the DMR cycle (2.0 MTPA)

Equipment		x_i [m]	y_i [m]	O_i	$V_{i,k}$				
No	Name				$V_{i,1}$	$V_{i,2}$	$V_{i,3}$	$V_{i,4}$	$V_{i,5}$
1	PMR receiver on lower deck	12.925	4.980	0	0	0	1	0	0
2	PMR receiver on upper deck	12.925	4.980	0	0	0	0	1	0
3	LP precool exchanger on A deck	4.975	6.710	0	1	0	0	0	0
4	LP precool exchanger on B deck	4.975	6.710	0	0	1	0	0	0
5	LP precool exchanger on C deck	4.975	6.710	0	0	0	1	0	0
6	MP precool exchanger	13.165	14.825	0	1	0	0	0	0

	on A deck								
7	MP precool exchanger on B deck	13.165	14.825	0	0	1	0	0	0
8	MP precool exchanger on C deck	13.165	14.825	0	0	0	1	0	0
9	HP precool exchanger on A deck	5.075	14.765	0	1	0	0	0	0
10	HP precool exchanger on B deck	5.075	14.765	0	0	1	0	0	0
11	HP precool exchanger on C deck	5.075	14.765	0	0	0	1	0	0
12	Joule-Thomson Valve 1	5.075	11.430	0	0	0	0	1	0
13	Joule-Thomson Valve 2	13.165	16.370	0	0	0	0	1	0
14	Joule-Thomson Valve 3	4.975	16.370	0	0	0	0	1	0

The layout results for this case are assumed to the same results for PMR module 2 of the DMR cycle (4.0 MTPA) due to internal problems in MINLP. It will be updated according to the actual results for 2.0 MTPA.

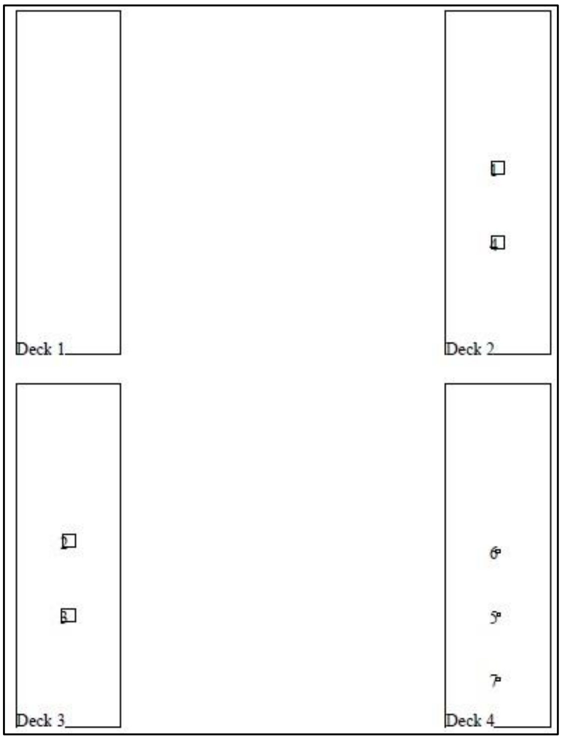

Figure 5-52 Plane view of PMR module 2 of the DMR cycle (1.0 MTPA)

Table 5-75 Design variables of PMR module 2 of the DMR cycle (1.0 MTPA)

Equipment		x_i [m]	y_i [m]	O_i	$V_{i,k}$				
No	Name				$V_{i,1}$	$V_{i,2}$	$V_{i,3}$	$V_{i,4}$	$V_{i,5}$
1	PMR receiver	3.435	12.210	0	0	1	0	0	0
2	LP precool exchanger on C deck	3.425	12.200	0	0	0	1	0	0
3	MP precool exchanger on C deck	3.425	7.360	0	0	0	1	0	0
4	HP precool exchanger on B deck	3.435	7.360	0	0	1	0	0	0
5	Joule-Thomson Valve 1	3.435	7.360	0	0	0	0	1	0

6	Joule-Thomson Valve 2	3.425	11.560	0	0	0	0	1	0
7	Joule-Thomson Valve 3	3.425	3.160	0	0	0	0	1	0

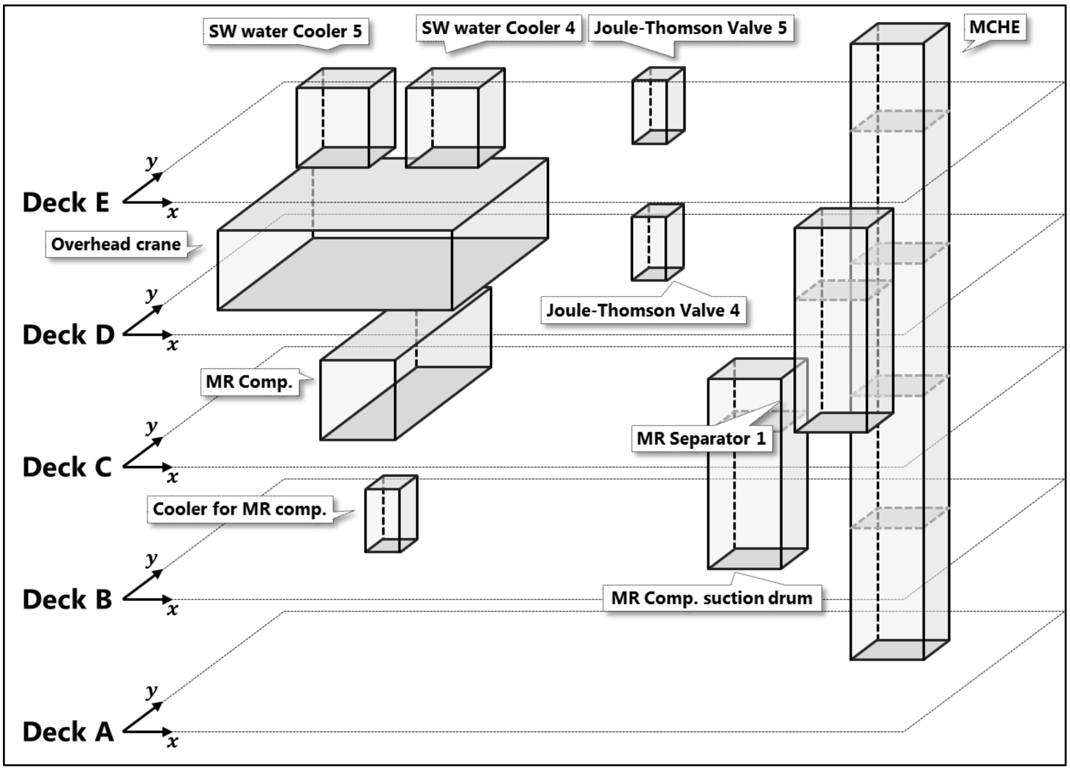

Figure 5-53 3D view of the MR module of the DMR cycle

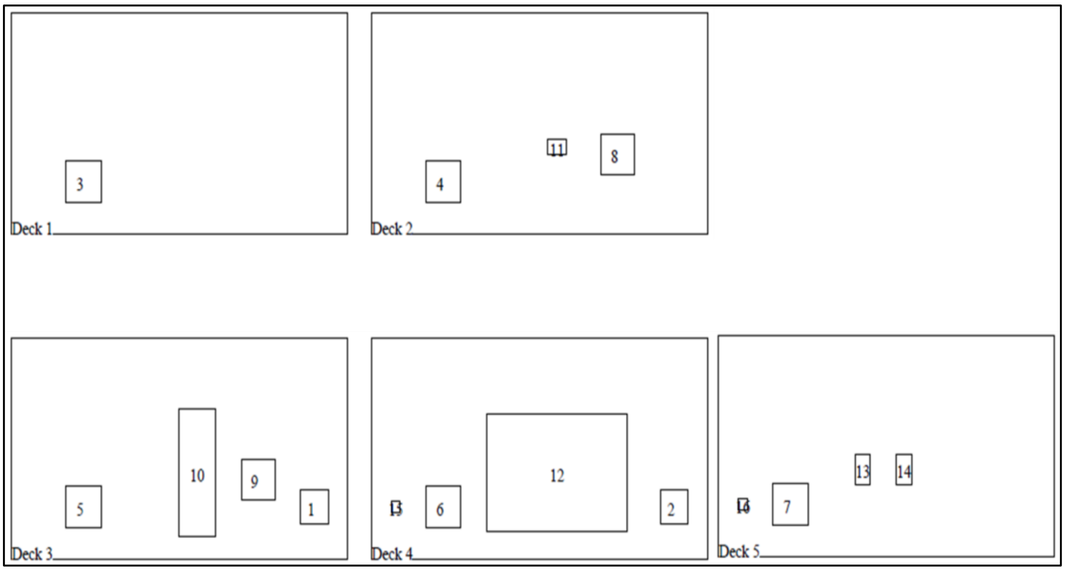

Figure 5-54 Plane view of the MR module of the DMR cycle (4.0 MTPA)

Table 5-76 Design variables of the MR module of the DMR cycle (4.0 MTPA)

Equipment		x_i [m]	y_i [m]	O_i	$V_{i,k}$				
No.	Name				$V_{i,1}$	$V_{i,2}$	$V_{i,3}$	$V_{i,4}$	$V_{i,5}$
1	MR separator 1 on lower deck	46.740	6.753	0	0	0	1	0	0
2	MR separator 1 on upper deck	46.740	6.753	0	0	0	0	1	0
3	MCHE on A deck	11.095	6.753	0	1	0	0	0	0
4	MCHE on B deck	11.095	6.753	0	0	1	0	0	0
5	MCHE on C deck	11.095	6.753	0	0	0	1	0	0
6	MCHE on D deck	11.095	6.753	0	0	0	0	1	0
7	MCHE on E deck	11.095	6.753	0	0	0	0	0	1
8	MR Comp. suction drum on lower deck	38.030	10.244	0	0	1	0	0	0
9	MR Comp. suction drum on upper deck	38.030	10.244	0	0	0	1	0	0
10	MR Comp.	28.615	11.150	1	0	0	1	0	0
11	Cooler for comp.	28.615	11.150	0	0	1	0	0	0
12	Overhead crane	28.615	11.150	0	0	0	0	1	0
13	SW water 4	22.261	11.150	1	0	0	0	0	1
14	SW water 5	28.621	11.150	1	0	0	0	0	1
15	Joule-Thomson Valve 4	3.705	6.753	0	0	0	0	1	0
16	Joule-Thomson Valve 5	3.705	6.753	0	0	0	0	0	1

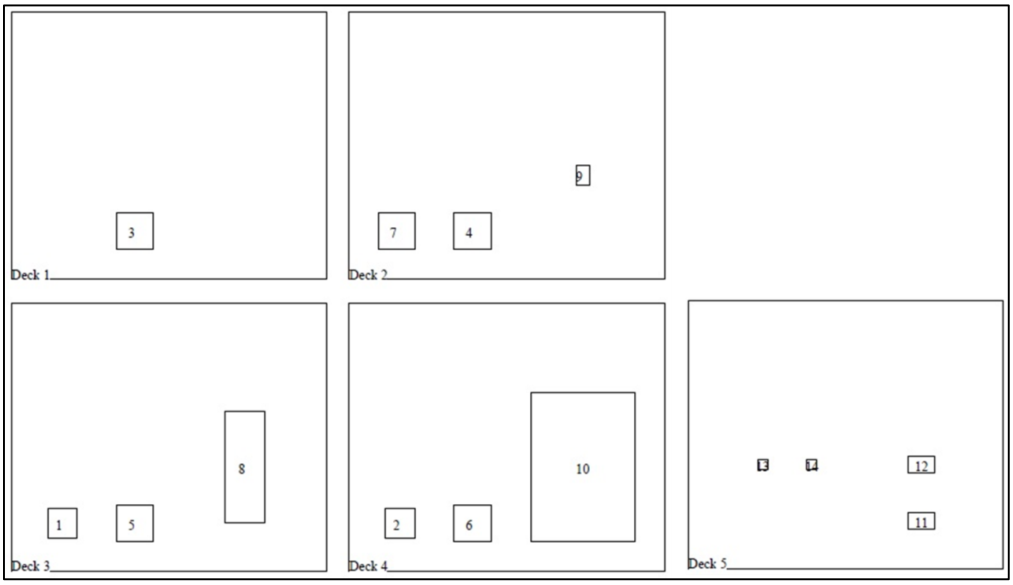

Figure 5-55 Plane view of the MR module of the DMR cycle (3.0 MTPA)

Table 5-77 Design variables of the MR module of the DMR cycle (3.0 MTPA)

Equipment		x_i [m]	y_i [m]	O_i	$V_{i,k}$				
No.	Name				$V_{i,1}$	$V_{i,2}$	$V_{i,3}$	$V_{i,4}$	$V_{i,5}$
1	MR separator 1 on lower deck	5.145	4.880	0	0	0	1	0	0
2	MR separator 1 on upper deck	5.145	4.880	0	0	0	0	1	0
3	MCHE on A deck	12.510	4.880	0	1	0	0	0	0
4	MCHE on B deck	12.510	4.880	0	0	1	0	0	0
5	MCHE on C deck	12.510	4.880	0	0	0	1	0	0
6	MCHE on D deck	12.510	4.880	0	0	0	0	1	0
7	MR Comp. suction drum	4.815	4.880	0	0	1	0	0	0
8	MR Comp.	23.670	10.585	1	0	0	1	0	0

9	Cooler for comp.	23.670	10.585	1	0	1	0	0	0
10	Overhead crane	23.670	10.585	1	0	0	0	1	0
11	SW water 4	23.670	4.881	0	0	0	0	0	1
12	SW water 5	23.670	10.585	0	0	0	0	0	1
13	Joule-Thomson Valve 4	7.556	10.585	0	0	0	0	0	1
14	Joule-Thomson Valve 5	12.546	10.585	0	0	0	0	0	1

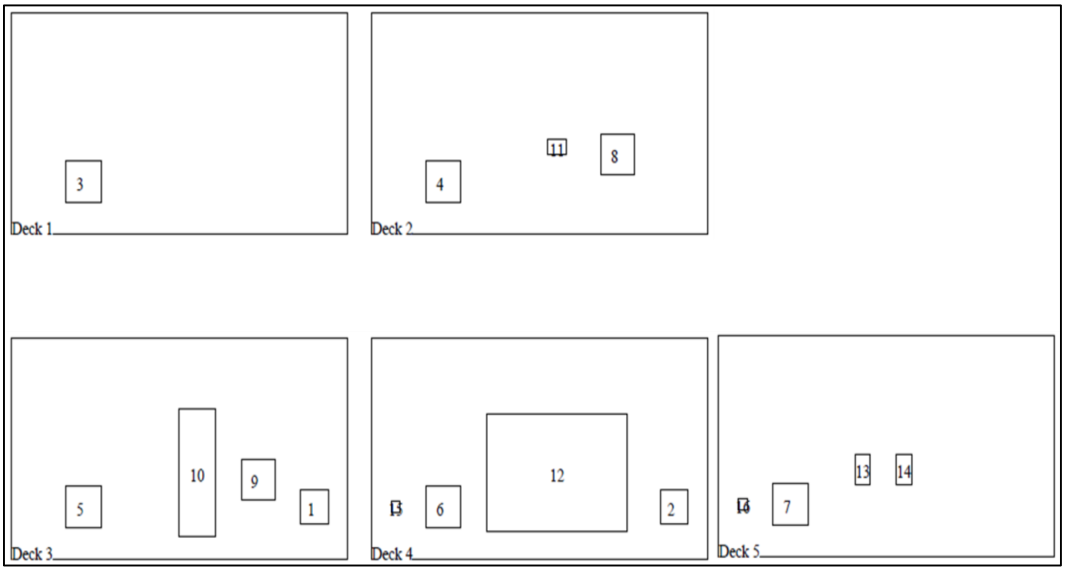

Figure 5-56 Plane view of the MR module of the DMR cycle (2.0 MTPA)

Table 5-78 Design variables of the MR module of the DMR cycle (2.0 MTPA)

Equipment		x_i [m]	y_i [m]	O_i	$V_{i,k}$				
No.	Name				$V_{i,1}$	$V_{i,2}$	$V_{i,3}$	$V_{i,4}$	$V_{i,5}$
1	MR separator 1 on lower deck	5.145	4.880	0	0	0	1	0	0
2	MR separator 1 on upper deck	5.145	4.880	0	0	0	0	1	0
3	MCHE on A deck	12.510	4.880	0	1	0	0	0	0
4	MCHE on B deck	12.510	4.880	0	0	1	0	0	0
5	MCHE on C deck	12.510	4.880	0	0	0	1	0	0
6	MCHE on D deck	12.510	4.880	0	0	0	0	1	0
7	MR Comp. suction drum	4.815	4.880	0	0	1	0	0	0
8	MR Comp.	23.670	10.585	1	0	0	1	0	0
9	Cooler for comp.	23.670	10.585	1	0	1	0	0	0
10	Overhead crane	23.670	10.585	1	0	0	0	1	0
11	SW water 4	23.670	4.881	0	0	0	0	0	1
12	SW water 5	23.670	10.585	0	0	0	0	0	1
13	Joule-Thomson Valve 4	7.556	10.585	0	0	0	0	0	1
14	Joule-Thomson Valve 5	12.546	10.585	0	0	0	0	0	1

The layout results for this case are assumed to the same results for case MR module of the DMR cycle (3.0 MTPA) due to internal problems in MINLP. It will be updated according to the actual results for 2.0 MTPA.

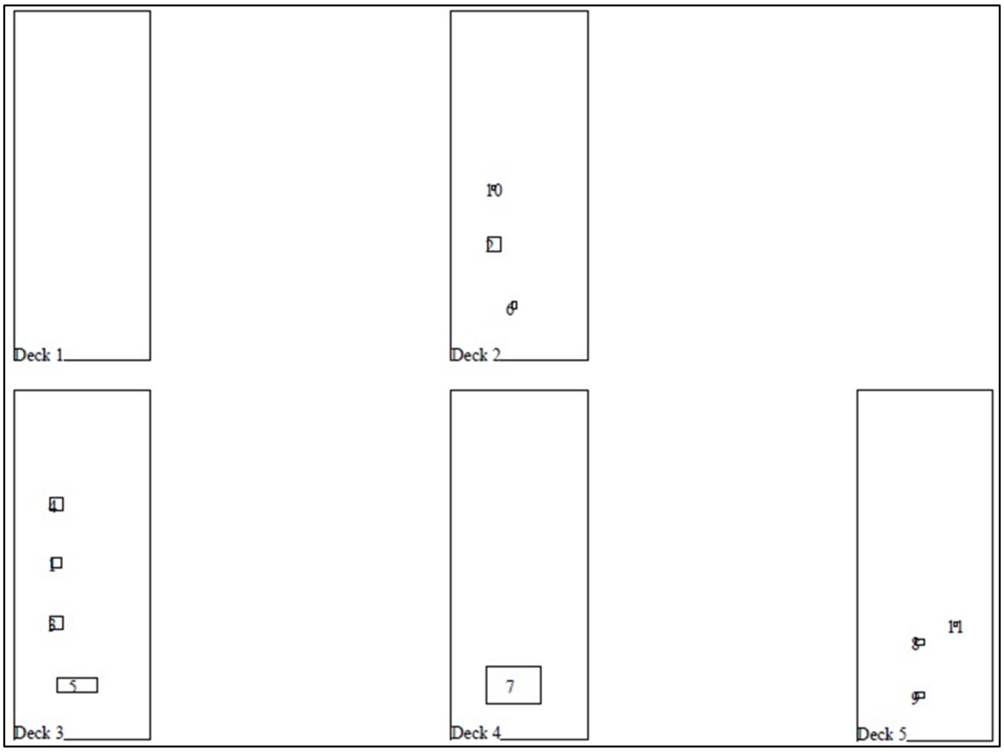

Figure 5-57 Plane view of the MR module of the DMR cycle (1.0 MTPA)

Table 5-79 Design variables of the MR module of the DMR cycle (1.0 MTPA)

Equipment		x_i [m]	y_i [m]	O_i	$V_{i,k}$				
No.	Name				$V_{i,1}$	$V_{i,2}$	$V_{i,3}$	$V_{i,4}$	$V_{i,5}$
1	MR separator 1	3.568	14.750	0	0	0	1	0	0
2	MCHE on B deck	3.565	9.740	1	0	1	0	0	0
3	MCHE on C deck	3.565	9.740	0	0	0	1	0	0
4	MR Comp. suction drum	3.585	19.730	0	0	0	1	0	0
5	MR Comp.	5.275	4.580	0	0	0	1	0	0
6	Cooler for MR comp.	5.275	4.580	1	0	1	0	0	0
7	Overhead crane	5.275	4.580	0	0	0	0	1	0

8	SW water 4	5.275	8.262	0	0	0	0	0	1
9	SW water 5	5.275	3.767	0	0	0	0	0	1
10	Joule-Thomson Valve 4	3.565	14.460	0	0	1	0	0	0
11	Joule-Thomson Valve 5	8.280	9.740	0	0	0	1	0	0

5.4.3. C_3MR cycle

The results for the 3D view, plane views, and design variables for each module are shown in Figure 5-58 to 5-72 and in Table 5-80 to 5-91, respectively.

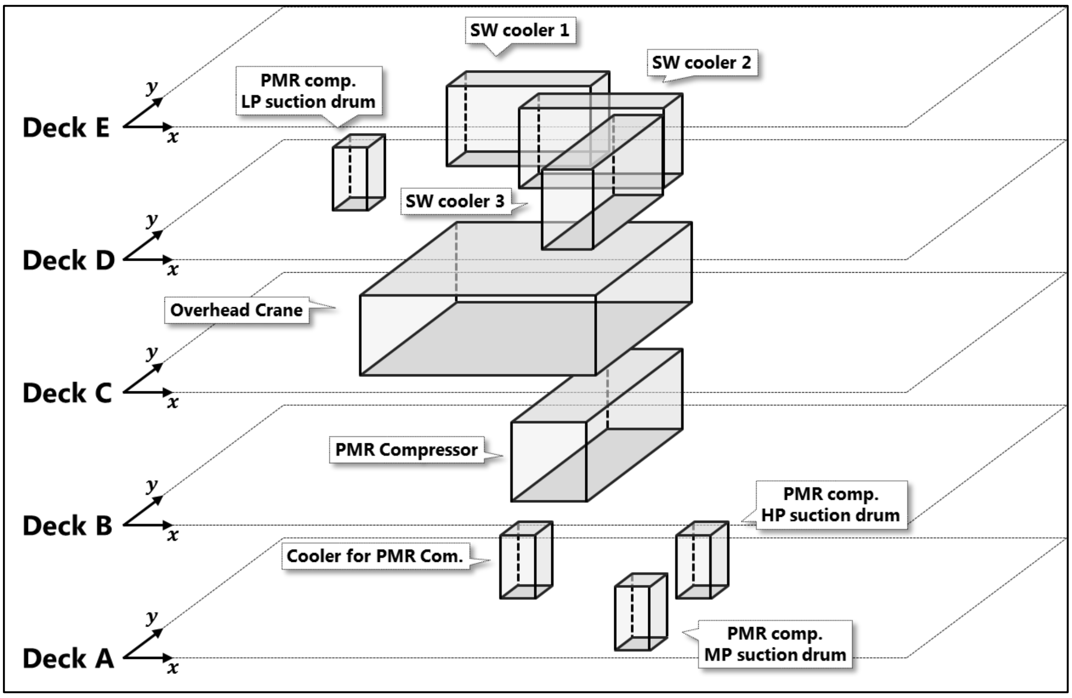

Figure 5-58 3D view of PMR module 1 of the C_3MR cycle

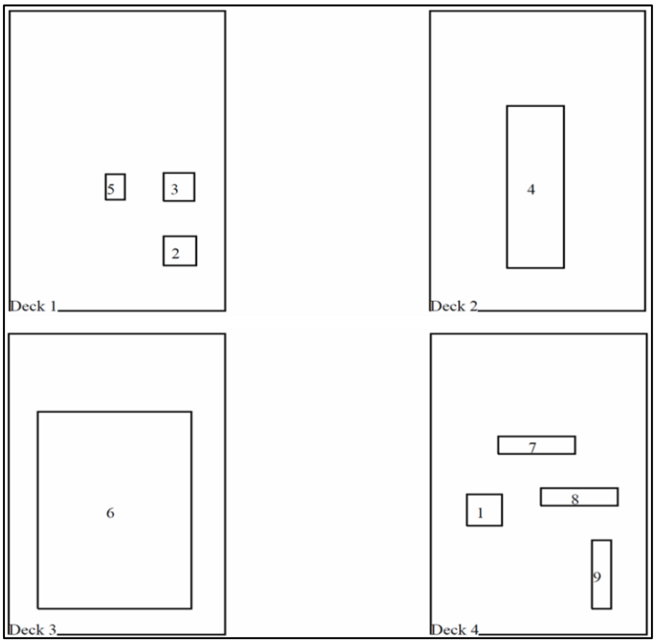

Figure 5-59 Plane view of PMR module 1 of the C_3MR cycle (4.0 MTPA)

Table 5-80 Design variables of PMR module 1 of the C_3MR cycle (4.0 MTPA)

Equipment		x_i [m]	y_i [m]	O_i	$V_{i,k}$			
No.	Name				$V_{i,1}$	$V_{i,2}$	$V_{i,3}$	$V_{i,4}$
1	PMR comp. LP suction drum	5.550	14.365	1	0	0	0	1
2	PMR comp. MP suction drum	17.580	6.955	1	1	0	0	0
3	PMR comp. HP suction drum	17.500	14.365	1	1	0	0	0
4	PMR HP Compressor	10.910	14.365	1	0	1	0	0
5	Cooler for PMR Com.	10.910	14.365	1	1	0	0	0
6	Overhead Crane	10.910	14.365	1	0	0	1	0
7	SW cooler 1	10.910	21.880	0	0	0	0	1
8	SW cooler 2	15.305	15.900	0	0	0	0	1

9	SW cooler 3	17.580	6.966	1	0	0	0	1

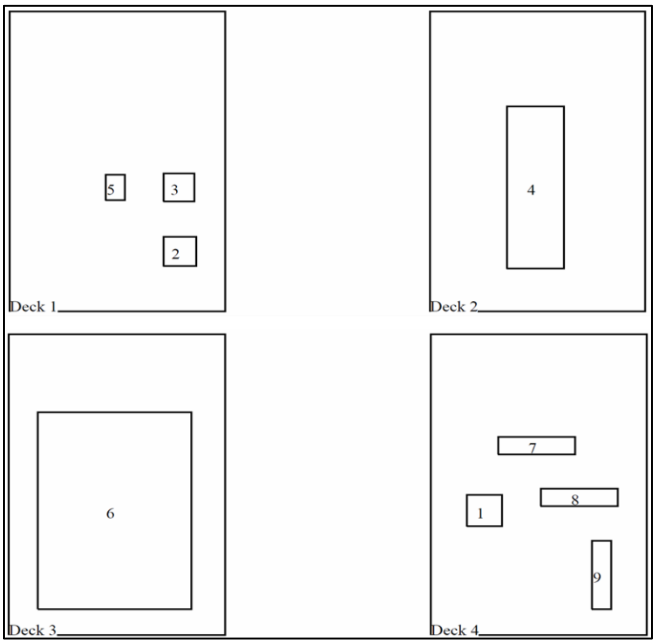

Figure 5-60 Plane view of PMR module 1 of the C_3MR cycle (3.0 MTPA)

Table 5-81 Design variables of PMR module 1 of the C_3MR cycle (3.0 MTPA)

Equipment		x_i $[m]$	y_i $[m]$	O_i	$V_{i,k}$			
No.	Name				$V_{i,1}$	$V_{i,2}$	$V_{i,3}$	$V_{i,4}$
1	PMR comp. LP suction drum	5.550	14.365	1	0	0	0	1
2	PMR comp. MP suction drum	17.580	6.955	1	1	0	0	0
3	PMR comp. HP suction drum	17.500	14.365	1	1	0	0	0
4	PMR HP Compressor	10.910	14.365	1	0	1	0	0
5	Cooler for PMR Com.	10.910	14.365	1	1	0	0	0
6	Overhead Crane	10.910	14.365	1	0	0	1	0

7	SW cooler 1	10.910	21.880	0	0	0	0	1
8	SW cooler 2	15.305	15.900	0	0	0	0	1
9	SW cooler 3	17.580	6.966	1	0	0	0	1

The layout results for this case are assumed to the same results for PMR module 1 of the C_3MR cycle (4.0 MTPA) due to internal problems in MINLP. It will be updated according to the actual results for 3.0 MTPA.

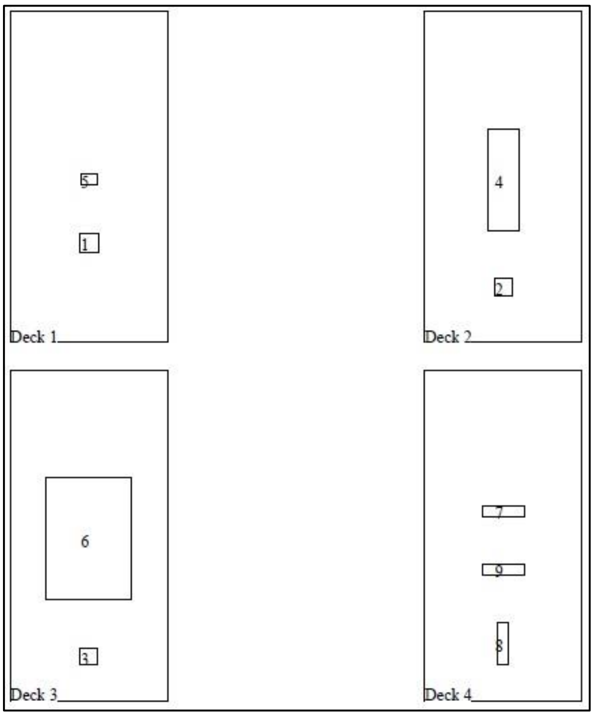

Figure 5-61 Plane view of PMR module 1 of the C_3MR cycle (2.0 MTPA)

Table 5-82 Design variables of PMR module 1 of the C_3MR cycle (2.0 MTPA)

Equipment		x_i [m]	y_i [m]	O_i	$V_{i,k}$			
No.	Name				$V_{i,1}$	$V_{i,2}$	$V_{i,3}$	$V_{i,4}$
1	PMR comp. LP suction drum	6.560	8.310	0	1	0	0	0
2	PMR comp. MP suction drum	6.560	4.580	0	0	1	0	0
3	PMR comp. HP	6.560	3.725	0	0	0	1	0

	suction drum							
4	PMR HP Compressor	6.560	13.565	1	0	1	0	0
5	Cooler for PMR Com.	6.560	13.565	0	1	0	0	0
6	Overhead Crane	6.560	13.565	1	0	0	1	0
7	SW cooler 1	6.560	15.895	0	0	0	0	1
8	SW cooler 2	6.560	4.780	1	0	0	0	1
9	SW cooler 3	6.560	11.005	0	0	0	0	1

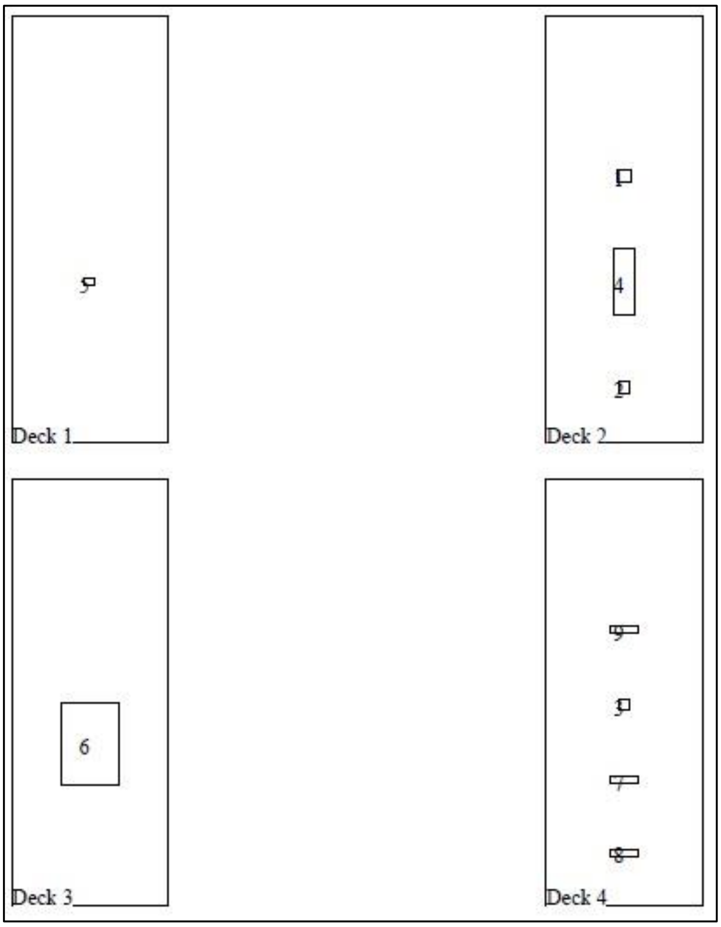

Figure 5-62 Plane view of PMR module 1 of the C_3MR cycle (1.0 MTPA)

Table 5-83 Design variables of PMR module 1 of the C_3MR cycle (1.0 MTPA)

Equipment		x_i [m]	y_i [m]	O_i	$V_{i,k}$			
No.	Name				$V_{i,1}$	$V_{i,2}$	$V_{i,3}$	$V_{i,4}$
1	PMR comp. LP suction drum	4.740	16.265	0	0	1	0	0
2	PMR comp. MP suction drum	4.740	3.370	0	0	1	0	0
3	PMR comp. HP suction drum	4.740	12.215	0	0	0	0	1
4	PMR HP Compressor	4.740	9.805	1	0	1	0	0
5	Cooler for PMR Com.	4.740	9.805	0	1	0	0	0
6	Overhead Crane	4.740	9.805	1	0	0	1	0
7	SW cooler 1	4.740	7.645	0	0	0	0	1
8	SW cooler 2	4.740	3.215	0	0	0	0	1
9	SW cooler 3	4.740	16.785	0	0	0	0	1

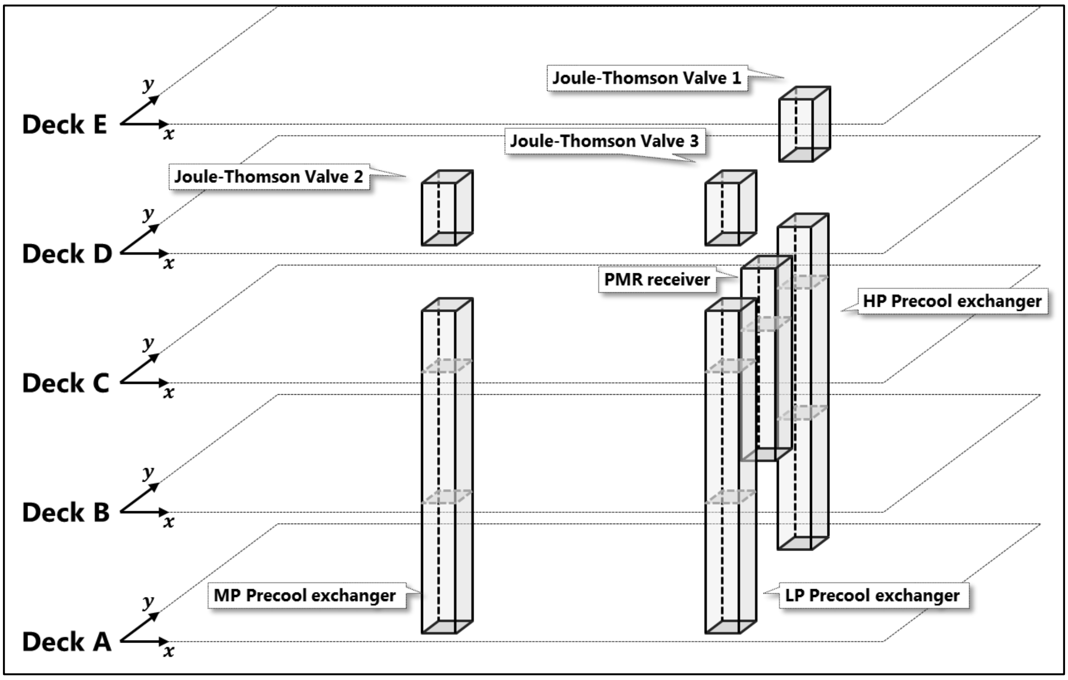

Figure 5-63 3D view of PMR module 2 of the C_3MR cycle

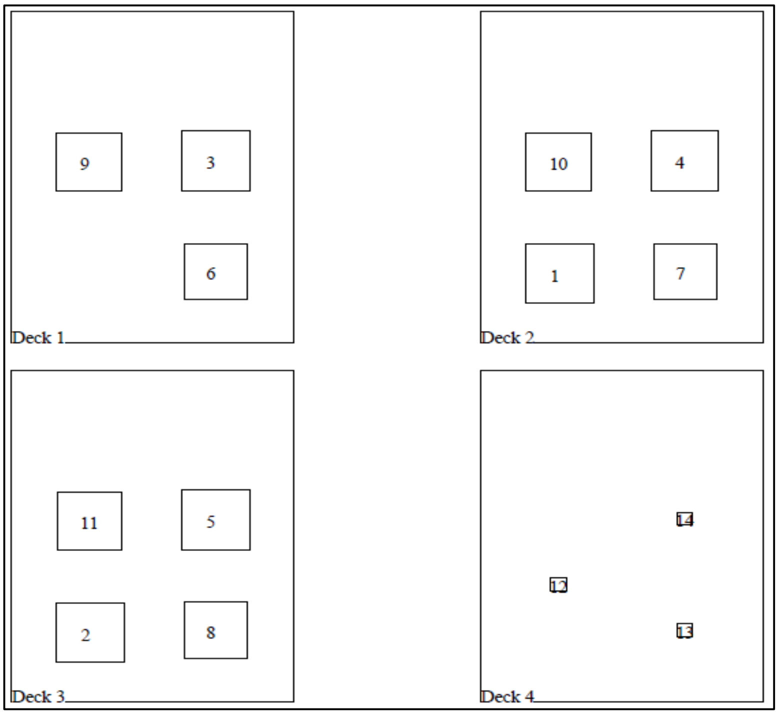

Figure 5-64 Plane view of PMR module 2 of the C_3MR cycle (4.0 MTPA)

Table 5-84 Design variables of PMR module 2 of the C_3MR cycle (4.0 MTPA)

Equipment		x_i [m]	y_i [m]	O_i	$V_{i,k}$				
No	Name				$V_{i,1}$	$V_{i,2}$	$V_{i,3}$	$V_{i,4}$	$V_{i,5}$
1	PMR receiver on lower deck	5.255	5.265	1	0	1	0	0	0
2	PMR receiver on upper deck	5.255	5.265	1	0	0	1	0	0
3	LP precool exchanger on A deck	13.605	13.790	1	1	0	0	0	0
4	LP precool exchanger on B deck	13.605	13.790	1	0	1	0	0	0
5	LP precool exchanger on C deck	13.605	13.790	1	0	0	1	0	0

6	MP precool exchanger on A deck	13.610	5.420	1	1	0	0	0	0
7	MP precool exchanger on B deck	13.610	5.420	1	0	1	0	0	0
8	MP precool exchanger on C deck	13.610	5.420	1	0	0	1	0	0
9	HP precool exchanger on A deck	5.175	13.705	0	1	0	0	0	0
10	HP precool exchanger on B deck	5.175	13.705	1	0	1	0	0	0
11	HP precool exchanger on C deck	5.175	13.705	1	0	0	1	0	0
12	Joule-Thomson Valve 1	5.175	8.876	1	0	0	0	1	0
13	Joule-Thomson Valve 2	13.610	5.420	0	0	0	0	1	0
14	Joule-Thomson Valve 3	13.605	13.866	1	0	0	0	1	0

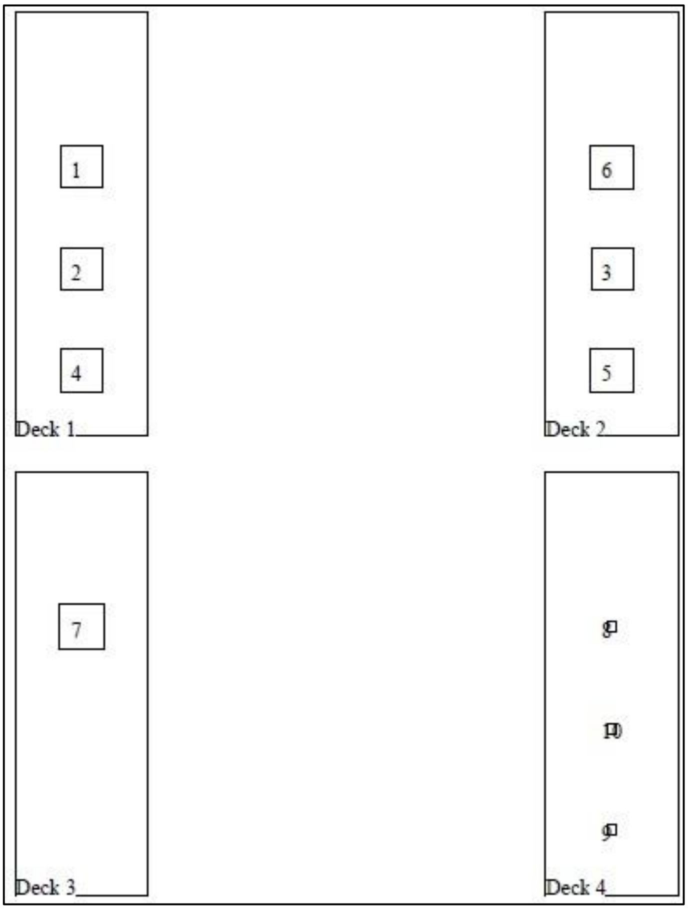

Figure 5-65 Plane view of PMR module 2 of the C_3MR cycle (3.0 MTPA)

Table 5-85 Design variables of PMR module 2 of the C_3MR cycle (3.0 MTPA)

Equipment		x_i [m]	y_i [m]	O_i	$V_{i,k}$				
No	Name				$V_{i,1}$	$V_{i,2}$	$V_{i,3}$	$V_{i,4}$	$V_{i,5}$
1	PMR receiver	4.475	18.165	0	1	0	0	0	0
2	LP precool exchanger on A deck	4.475	11.280	0	1	0	0	0	0
3	LP precool exchanger on B deck	4.475	11.280	0	0	1	0	0	0
4	MP precool	4.475	4.435	0	1	0	0	0	0

	exchanger on A deck								
5	MP precool exchanger on B deck	4.475	4.435	0	0	1	0	0	0
6	HP precool exchanger on B deck	4.475	18.165	0	0	1	0	0	0
7	HP precool exchanger on C deck	4.475	18.165	0	0	0	1	0	0
8	Joule-Thomson Valve 1	4.475	18.165	0	0	0	0	1	0
9	Joule-Thomson Valve 2	4.475	4.435	0	0	0	0	1	0
10	Joule-Thomson Valve 3	4.475	11.280	0	0	0	0	1	0

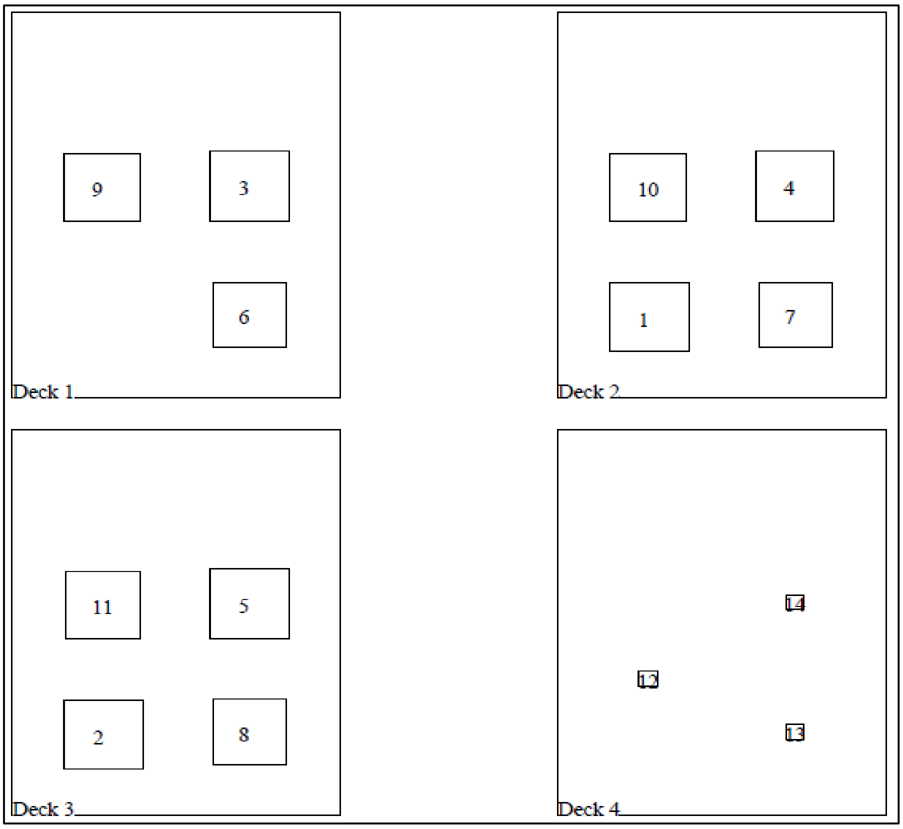

Figure 5-66 Plane view of PMR module 2 of the C_3MR cycle (2.0 MTPA)

Table 5-86 Design variables of PMR module 2 of the C_3MR cycle (2.0 MTPA)

Equipment		x_i [m]	y_i [m]	O_i	$V_{i,k}$				
No	Name				$V_{i,1}$	$V_{i,2}$	$V_{i,3}$	$V_{i,4}$	$V_{i,5}$
1	PMR receiver	4.475	18.165	0	1	0	0	0	0
2	LP precool exchanger on A deck	4.475	11.280	0	1	0	0	0	0
3	LP precool exchanger on B deck	4.475	11.280	0	0	1	0	0	0
4	MP precool exchanger on A deck	4.475	4.435	0	1	0	0	0	0

5	MP precool exchanger on B deck	4.475	4.435	0	0	1	0	0	0
6	HP precool exchanger on B deck	4.475	18.165	0	0	1	0	0	0
7	HP precool exchanger on C deck	4.475	18.165	0	0	0	1	0	0
8	Joule-Thomson Valve 1	4.475	18.165	0	0	0	0	1	0
9	Joule-Thomson Valve 2	4.475	4.435	0	0	0	0	1	0
10	Joule-Thomson Valve 3	4.475	11.280	0	0	0	0	1	0
The layout results for this case are assumed to the same results for PMR module 2 of the C_3MR cycle (3.0 MTPA) due to internal problems in MINLP. It will be updated according to the actual results for 2.0 MTPA.									

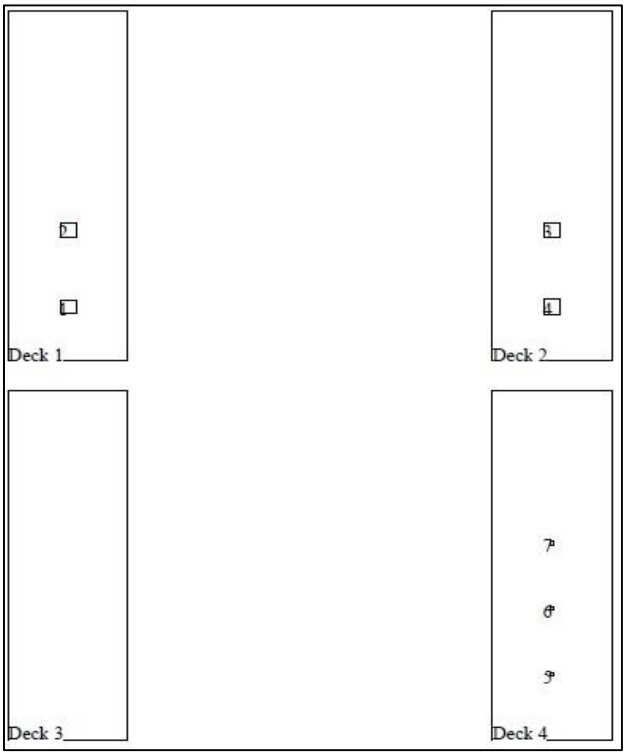

Figure 5-67 Plane view of PMR module 2 of the C_3MR cycle (1.0 MTPA)

Table 5-87 Design variables of PMR module 2 of the C_3MR cycle (1.0 MTPA)

Equipment		x_i [m]	y_i [m]	O_i	$V_{i,k}$				
No	Name				$V_{i,1}$	$V_{i,2}$	$V_{i,3}$	$V_{i,4}$	$V_{i,5}$
1	PMR receiver	3.480	3.480	0	1	0	0	0	0
2	LP precool exchanger	3.480	8.425	0	1	0	0	0	0
3	MP precool exchanger	3.480	8.425	0	0	1	0	0	0
4	HP precool exchanger	3.480	3.480	0	0	1	0	0	0
5	Joule-Thomson Valve 1	3.480	4.248	0	0	0	0	1	0
6	Joule-Thomson Valve 2	3.480	8.468	0	0	0	0	1	0

7	Joule-Thomson Valve 3	3.480	12.688	0	0	0	0	1	0

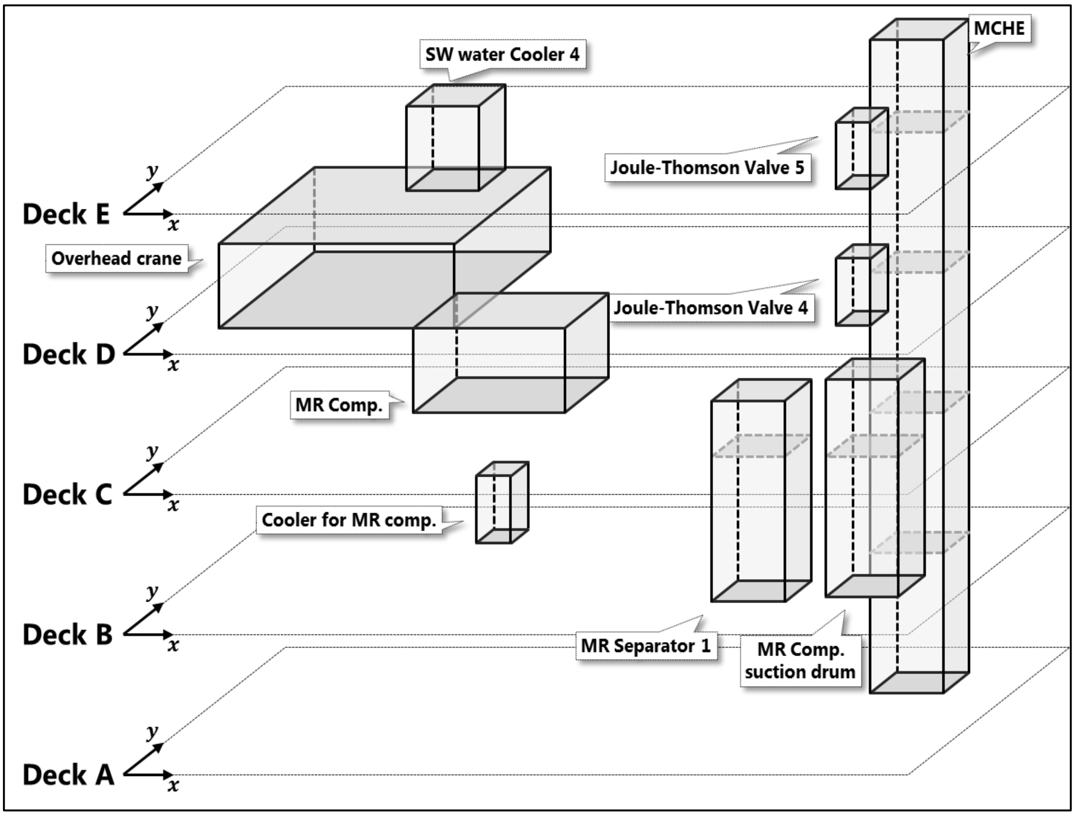

Figure 5-68 3D view of the MR module of the C_3MR cycle

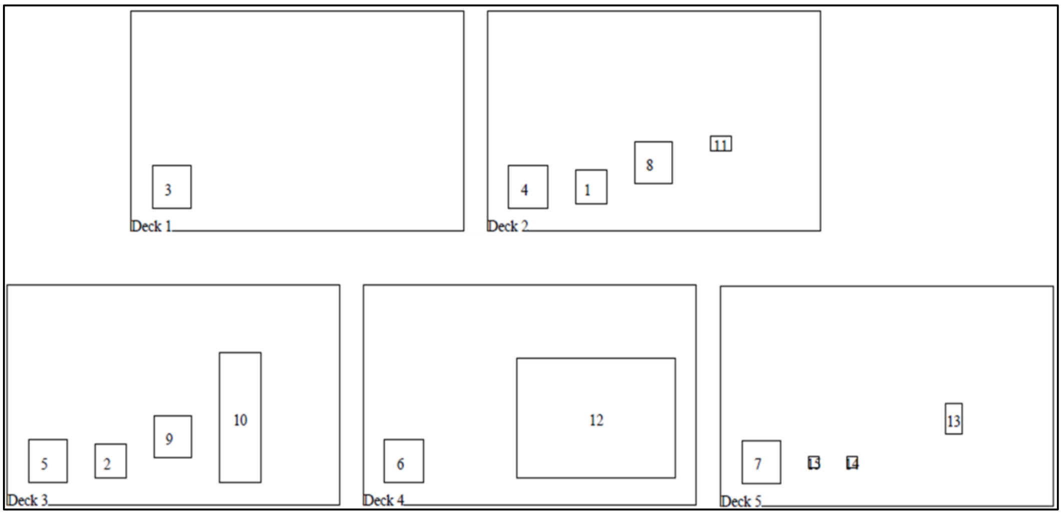

Figure 5-69 Plane view of the MR module of the C_3MR cycle (4.0 MTPA)

Table 5-88 Design variables of the MR module of the C_3MR cycle (4.0 MTPA)

Equipment		x_i [m]	y_i [m]	O_i	$V_{i,k}$				
No.	Name				$V_{i,1}$	$V_{i,2}$	$V_{i,3}$	$V_{i,4}$	$V_{i,5}$
1	MR separator 1 on lower deck	14.855	5.815	0	0	1	0	0	0
2	MR separator 1 on upper deck	14.855	5.815	0	0	0	1	0	0
3	MCHE on A deck	5.815	5.815	0	1	0	0	0	0
4	MCHE on B deck	5.815	5.815	0	0	1	0	0	0
5	MCHE on C deck	5.815	5.815	0	0	0	1	0	0
6	MCHE on D deck	5.815	5.815	0	0	0	0	1	0
7	MCHE on E deck	5.815	5.815	0	0	0	0	0	1
8	MR Comp. suction drum on lower deck	23.800	9.038	0	0	1	0	0	0

9	MR Comp. suction drum on upper deck	23.800	9.038	0	0	0	1	0	0
10	MR Comp.	33.485	11.550	1	0	0	1	0	0
11	Cooler for comp.	33.485	11.550	0	0	1	0	0	0
12	Overhead crane	33.485	11.550	0	0	0	0	1	0
13	SW water 4	33.485	11.550	1	0	0	0	0	1
14	Joule-Thomson Valve 4	18.850	5.815	0	0	0	0	0	1
15	Joule-Thomson Valve 5	13.370	5.815	0	0	0	0	0	1

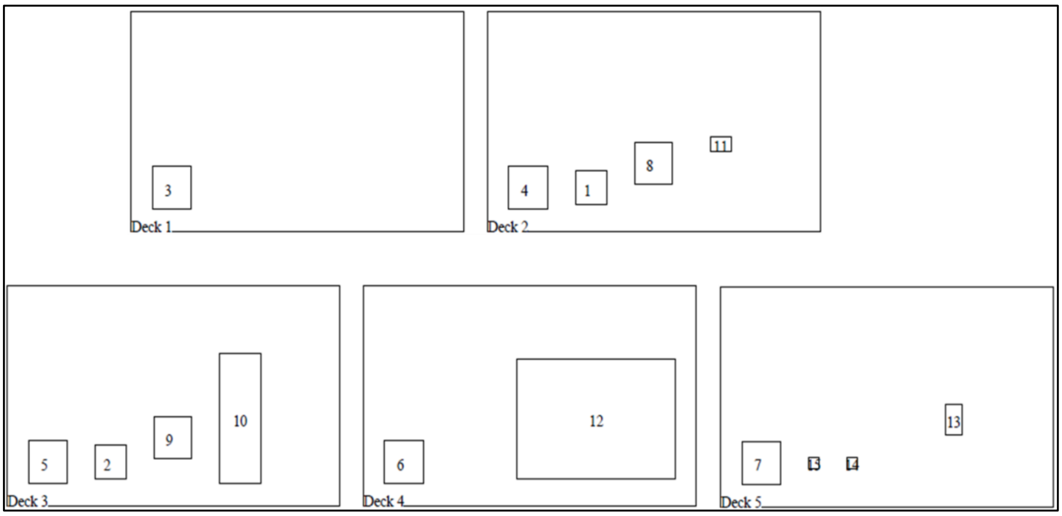

Figure 5-70 Plane view of the MR module of the C_3MR cycle (3.0 MTPA)

Table 5-89 Design variables of the MR module of the C_3MR cycle (3.0 MTPA)

Equipment		x_i [m]	y_i [m]	O_i	$V_{i,k}$				
No.	Name				$V_{i,1}$	$V_{i,2}$	$V_{i,3}$	$V_{i,4}$	$V_{i,5}$
1	MR separator 1 on lower deck	14.855	5.815	0	0	1	0	0	0
2	MR separator 1	14.855	5.815	0	0	0	1	0	0

	on upper deck								
3	MCHE on A deck	5.815	5.815	0	1	0	0	0	0
4	MCHE on B deck	5.815	5.815	0	0	1	0	0	0
5	MCHE on C deck	5.815	5.815	0	0	0	1	0	0
6	MCHE on D deck	5.815	5.815	0	0	0	0	1	0
7	MCHE on E deck	5.815	5.815	0	0	0	0	0	1
8	MR Comp. suction drum on lower deck	23.800	9.038	0	0	1	0	0	0
9	MR Comp. suction drum on upper deck	23.800	9.038	0	0	0	1	0	0
10	MR Comp.	33.485	11.550	1	0	0	1	0	0
11	Cooler for comp.	33.485	11.550	0	0	1	0	0	0
12	Overhead crane	33.485	11.550	0	0	0	0	1	0
13	SW water 4	33.485	11.550	1	0	0	0	0	1
14	Joule-Thomson Valve 4	18.850	5.815	0	0	0	0	0	1
15	Joule-Thomson Valve 5	13.370	5.815	0	0	0	0	0	1

The layout results for this case are assumed to the same results for MR module of the C_3MR cycle (4.0 MTPA) due to internal problems in MINLP. It will be updated according to the actual results for 3.0 MTPA.

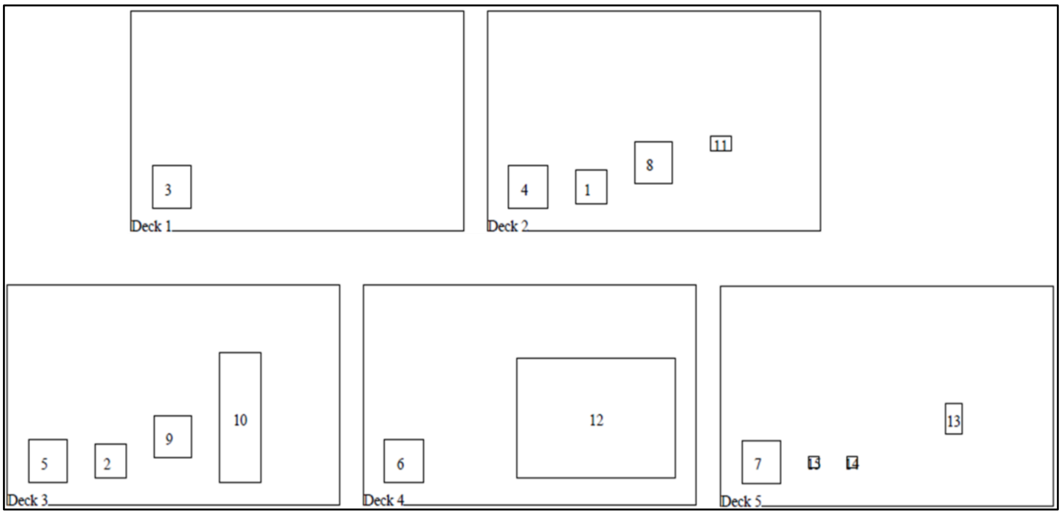

Figure 5-71 Plane view of the MR module of the C_3MR cycle (2.0 MTPA)

Table 5-90 Design variables of the MR module of the C_3MR cycle (2.0 MTPA)

Equipment		x_i [m]	y_i [m]	O_i	$V_{i,k}$				
No.	Name				$V_{i,1}$	$V_{i,2}$	$V_{i,3}$	$V_{i,4}$	$V_{i,5}$
1	MR separator 1 on lower deck	14.855	5.815	0	0	1	0	0	0
2	MR separator 1 on upper deck	14.855	5.815	0	0	0	1	0	0
3	MCHE on A deck	5.815	5.815	0	1	0	0	0	0
4	MCHE on B deck	5.815	5.815	0	0	1	0	0	0
5	MCHE on C deck	5.815	5.815	0	0	0	1	0	0
6	MCHE on D deck	5.815	5.815	0	0	0	0	1	0
7	MCHE on E deck	5.815	5.815	0	0	0	0	0	1
8	MR Comp. suction drum on lower deck	23.800	9.038	0	0	1	0	0	0

9	MR Comp. suction drum on upper deck	23.800	9.038	0	0	0	1	0	0
10	MR Comp.	33.485	11.550	1	0	0	1	0	0
11	Cooler for comp.	33.485	11.550	0	0	1	0	0	0
12	Overhead crane	33.485	11.550	0	0	0	0	1	0
13	SW water 4	33.485	11.550	1	0	0	0	0	1
14	Joule-Thomson Valve 4	18.850	5.815	0	0	0	0	0	1
15	Joule-Thomson Valve 5	13.370	5.815	0	0	0	0	0	1
The layout results for this case are assumed to the same results for MR module of the C_3MR cycle (4.0 MTPA) due to internal problems in MINLP. It will be updated according to the actual results for 2.0 MTPA.									

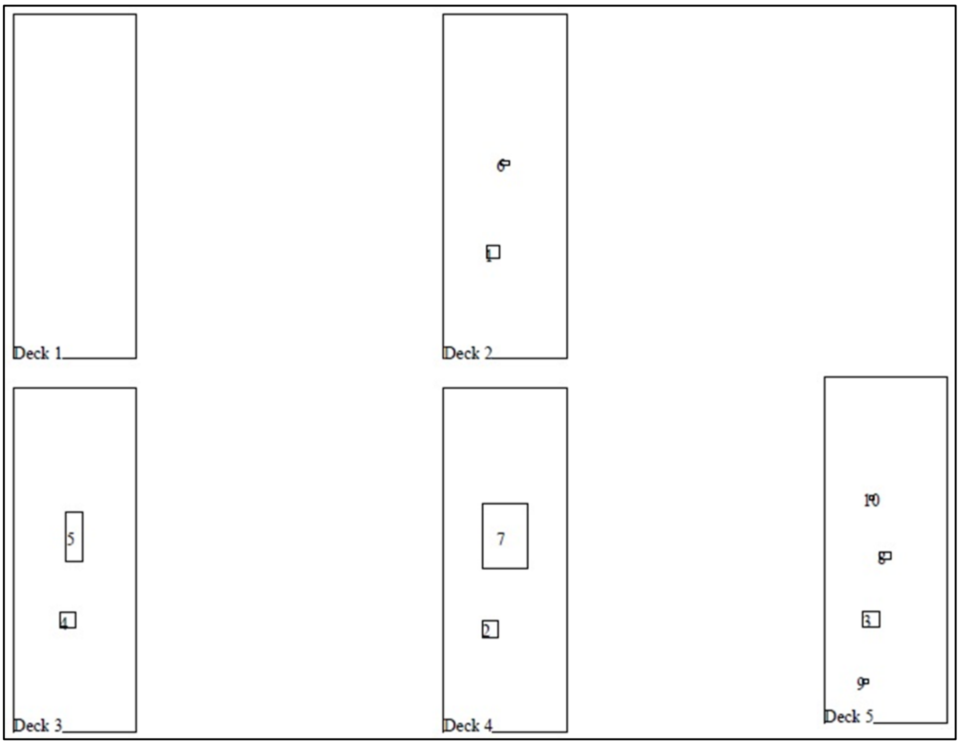

Figure 5-72 Plane view of the MR module of the C_3MR cycle (1.0 MTPA)

Table 5-91 Design variables of the MR module of the C_3MR cycle (1.0 MTPA)

Equipment		x_i [m]	y_i [m]	O_i	$V_{i,k}$				
No.	Name				$V_{i,1}$	$V_{i,2}$	$V_{i,3}$	$V_{i,4}$	$V_{i,5}$
1	MR separator 1	3.827	8.177	0	0	1	0	0	0
2	MCHE on D deck	3.620	7.950	0	0	0	0	1	0
3	MCHE on E deck	3.620	7.950	0	0	0	0	0	1
4	MR Comp. suction drum	4.221	8.590	0	0	0	1	0	0
5	MR Comp.	4.740	15.070	1	0	0	1	0	0
6	Cooler for comp.	4.740	15.070	0	0	1	0	0	0
7	Overhead crane	4.740	15.070	1	0	0	0	1	0
8	SW water 4	4.740	12.840	0	0	0	0	0	1
9	Joule-Thomson Valve 4	3.165	3.165	0	0	0	0	0	1
10	Joule-Thomson Valve 5	3.620	17.275	0	0	0	0	0	1

5.4.4. Dual N_2 expander cycle

The results for the 3D view, plane views, and design variables for each module are shown in Figure 5-73 to 5-82 and in Table 5-92 to 5-99, respectively.

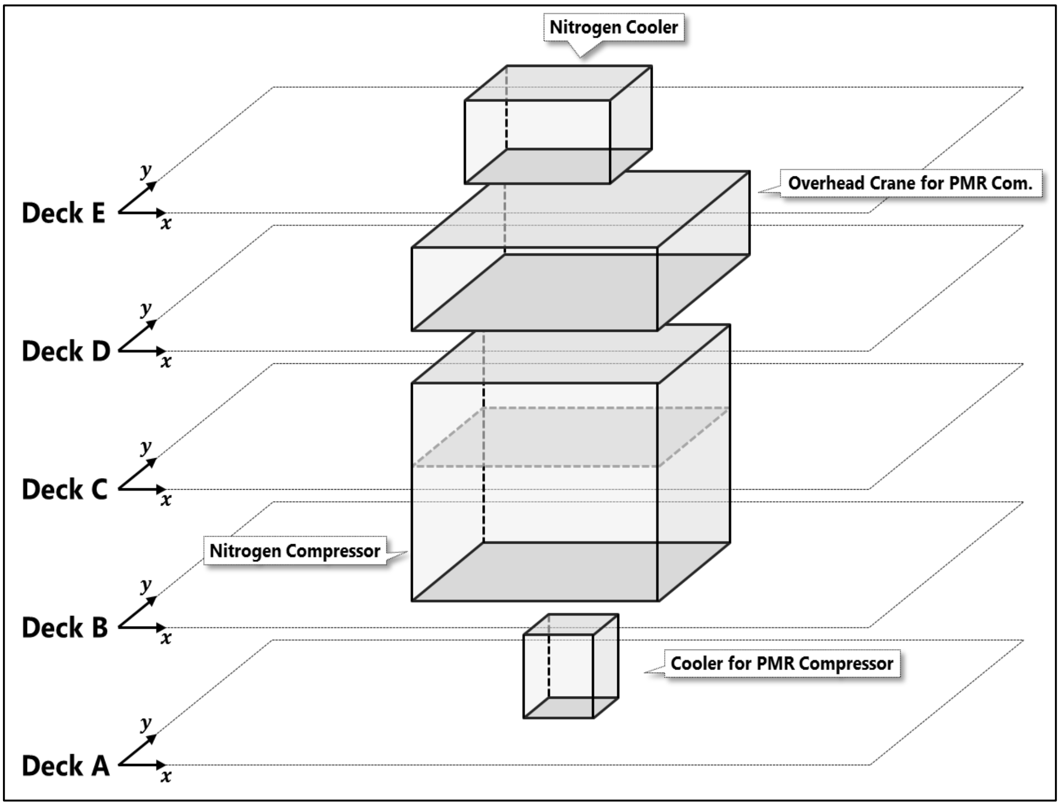

Figure 5-73 3D view of refrigerant module 1 of the dual N_2 expander cycle

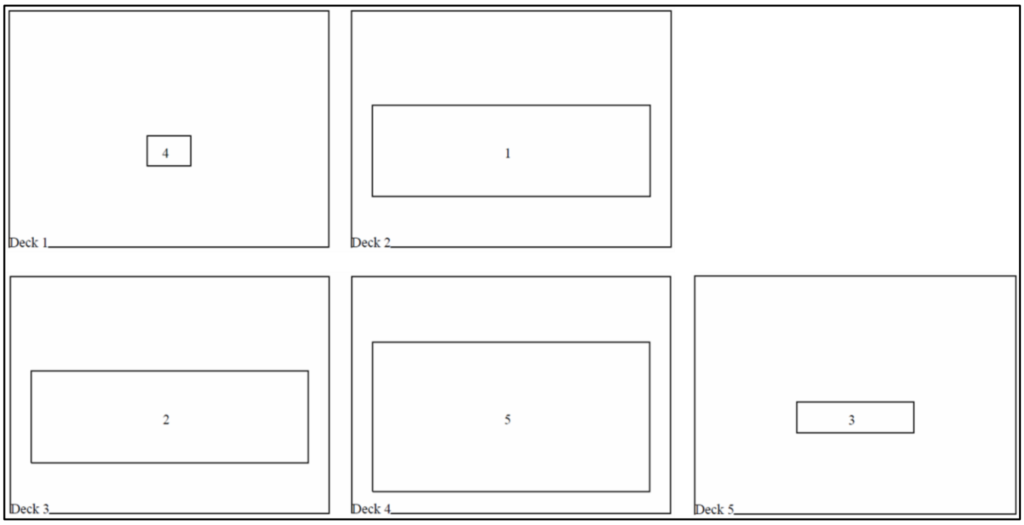

Figure 5-74 Plane view of refrigerant module 1 of the dual N_2 expander cycle (4.0 MTPA)

Table 5-92 Design variables of refrigerant module 1 of the dual N_2 expander cycle (4.0 MTPA)

Equipment		x_i	y_i	O_i	$V_{i,k}$				
No	Name	[m]	[m]		$V_{i,1}$	$V_{i,2}$	$V_{i,3}$	$V_{i,4}$	$V_{i,5}$
1	Nitrogen Compressor on lower deck	20.965	11.250	0	0	1	0	0	0
2	Nitrogen Compressor on upper deck	20.965	11.250	0	0	0	1	0	0
3	Nitrogen Cooler	20.965	11.250	0	0	0	0	0	1
4	Cooler for PMR Compressor	20.965	11.250	0	1	0	0	0	0
5	Overhead Crane for PMR Compressor	20.965	11.250	0	0	0	0	1	0

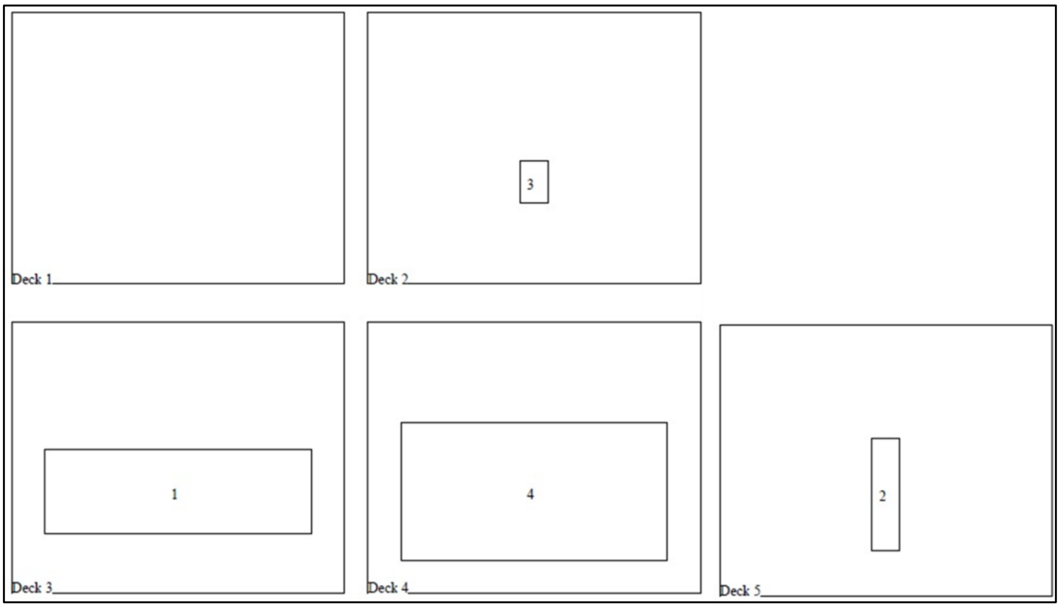

Figure 5-75 Plane view of refrigerant module 1 of the dual N_2 expander cycle (3.0 MTPA)

Table 5-93 Design variables of refrigerant module 1 of the dual N_2 expander cycle (3.0 MTPA)

Equipment	x_i	y_i	O_i	$V_{i,k}$

No	Name	[m]	[m]		$V_{i,1}$	$V_{i,2}$	$V_{i,3}$	$V_{i,4}$	$V_{i,5}$
1	Nitrogen Compressor	15.175	9.251	0	0	0	1	0	0
2	Nitrogen Cooler	15.175	9.251	1	0	0	0	0	1
3	Cooler for PMR Compressor	15.175	9.251	1	0	1	0	0	0
4	Overhead Crane for PMR Compressor	15.175	9.251	0	0	0	0	1	0

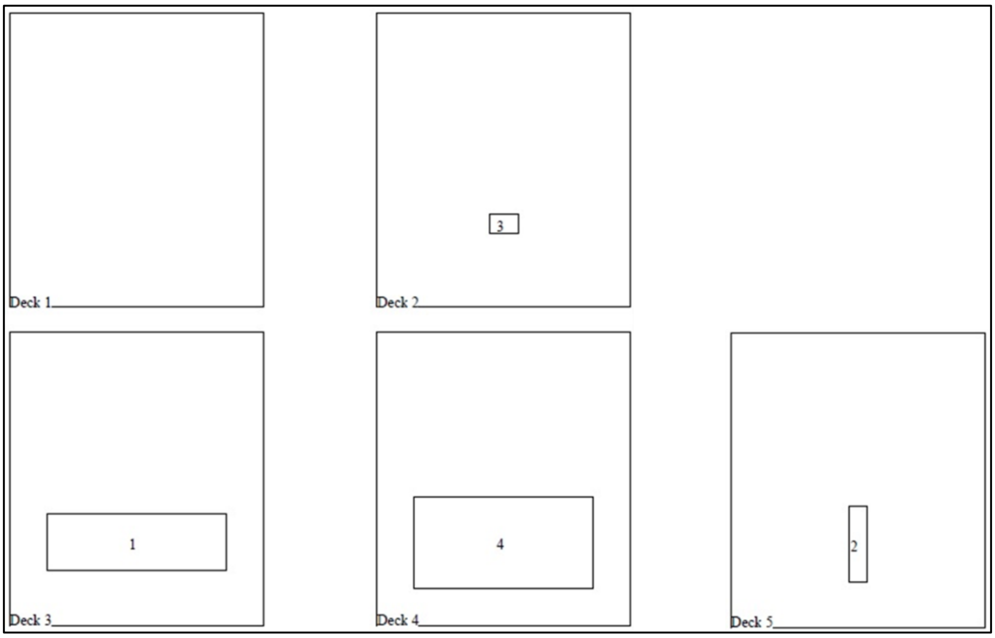

Figure 5-76 Plane view of refrigerant module 1 of the dual N_2 expander cycle (2.0 MTPA)

Table 5-94 Design variables of refrigerant module 1 of the dual N_2 expander cycle (2.0 MTPA)

Equipment		x_i [m]	y_i [m]	O_i	$V_{i,k}$				
No	Name				$V_{i,1}$	$V_{i,2}$	$V_{i,3}$	$V_{i,4}$	$V_{i,5}$
1	Nitrogen Compressor	10.190	6.690	0	0	0	1	0	0
2	Nitrogen Cooler	10.190	6.690	1	0	0	0	0	1
3	Cooler for PMR	10.190	6.690	0	0	1	0	0	0

	Compressor								
4	Overhead Crane for PMR Compressor	10.190	6.690	0	0	0	0	1	0

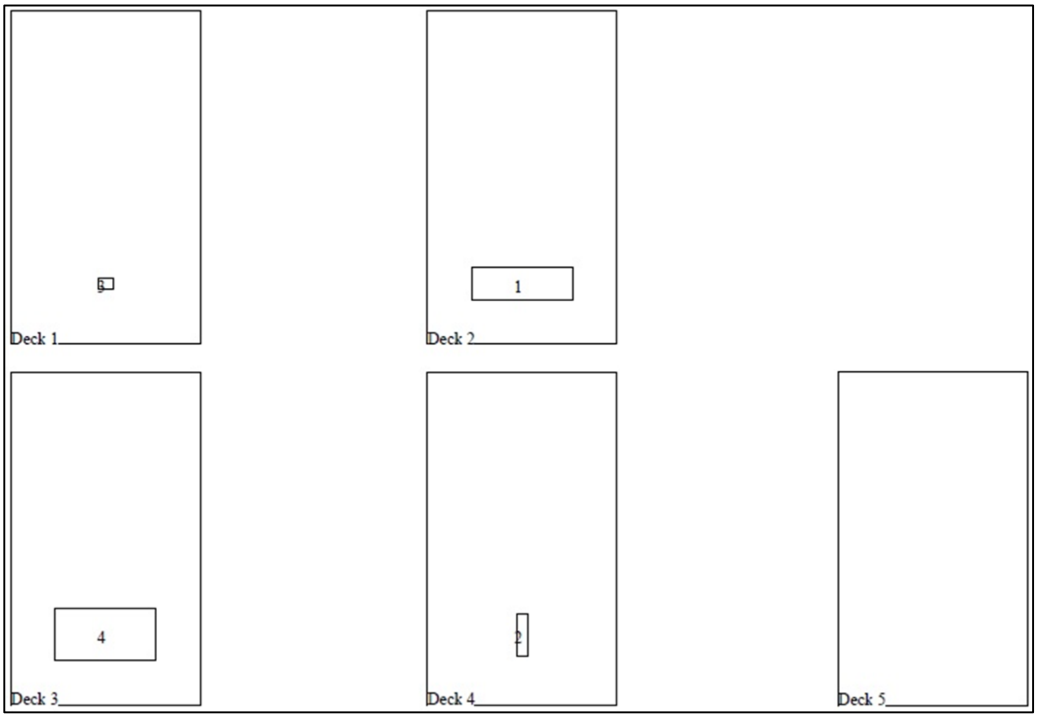

Figure 5-77 Plane view of refrigerant module 1 of the dual N_2 expander cycle (1.0 MTPA)

Table 5-95 Design variables of refrigerant module 1 of the dual N_2 expander cycle (1.0 MTPA)

Equipment		x_i [m]	y_i [m]	O_i	$V_{i,k}$				
No	Name				$V_{i,1}$	$V_{i,2}$	$V_{i,3}$	$V_{i,4}$	$V_{i,5}$
1	Nitrogen Compressor on lower deck	6.395	4.070	0	0	1	0	0	0
2	Nitrogen Cooler	6.395	4.745	1	0	0	0	1	0
3	Cooler for PMR Compressor	6.395	4.070	0	1	0	0	0	0
4	Overhead Crane	6.395	4.745	0	0	0	1	0	0

	for PMR Compressor								

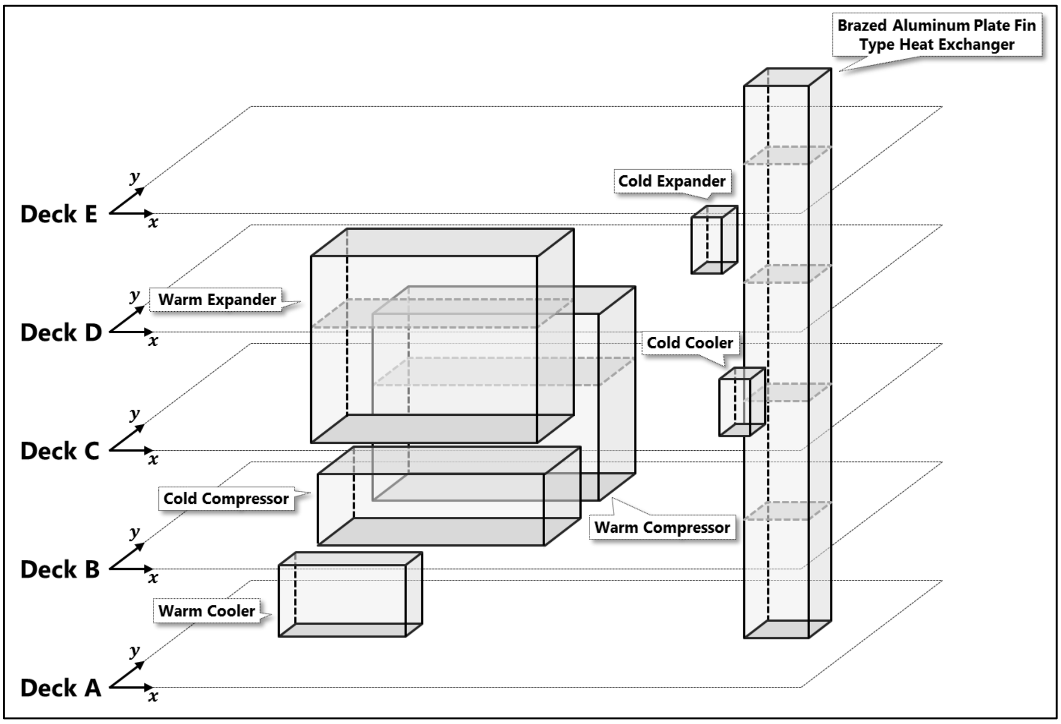

Figure 5-78 3D view of refrigerant module 2 of the dual N_2 expander cycle

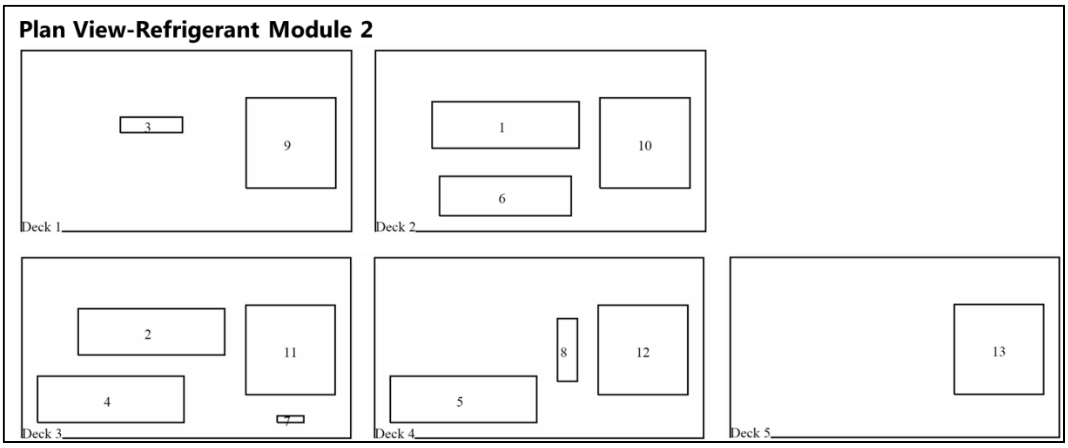

Figure 5-79 Plane view of refrigerant module 2 of the dual N_2 expander cycle (4.0 MTPA)

Table 5-96 Design variables of refrigerant module 2 of the dual N_2 expander cycle (4.0 MTPA)

Equipment		x_i [m]	y_i [m]	O_i	$V_{i,k}$				
No.	Name				$V_{i,1}$	$V_{i,2}$	$V_{i,3}$	$V_{i,4}$	$V_{i,5}$
1	Warm Compressor on lower deck	14.975	5.415	0	0	1	0	0	0
2	Warm Compressor on upper deck	14.975	5.415	0	0	0	1	0	0
3	Warm Cooler	25.325	15.245	0	1	0	0	0	0
4	Warm Expander on lower deck	14.975	15.245	0	0	0	1	0	0
5	Warm Expander on upper deck	14.975	15.245	0	0	0	0	1	0
6	Cold Compressor	25.325	23.010	0	0	1	0	0	0
7	Cold Cooler	30.580	23.010	0	0	0	1	0	0
8	Cold Expander	52.200	15.245	1	0	0	0	1	0
9	MCHE on A deck	40.760	9.700	0	1	0	0	0	0
10	MCHE	40.760	9.700	0	0	1	0	0	0

	on B deck								
11	MCHE on C deck	40.760	9.700	0	0	0	1	0	0
12	MCHE on D deck	40.760	9.700	0	0	0	0	1	0
13	MCHE on E deck	40.760	9.700	0	0	0	0	0	1

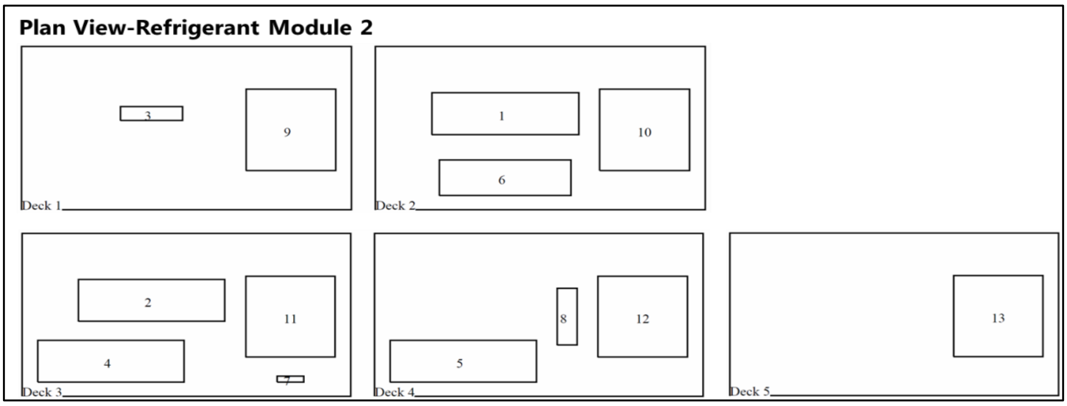

Figure 5-80 Plane view of refrigerant module 2 of the dual N_2 expander cycle (3.0 MTPA)

Table 5-97 Design variables of refrigerant module 2 of the dual N_2 expander cycle (3.0 MTPA)

Equipment		x_i [m]	y_i [m]	O_i	$V_{i,k}$				
No.	Name				$V_{i,1}$	$V_{i,2}$	$V_{i,3}$	$V_{i,4}$	$V_{i,5}$
1	Warm Compressor on lower deck	14.975	5.415	0	0	1	0	0	0
2	Warm Compressor on upper deck	14.975	5.415	0	0	0	1	0	0
3	Warm Cooler	25.325	15.245	0	1	0	0	0	0
4	Warm Expander on lower deck	14.975	15.245	0	0	0	1	0	0
5	Warm Expander	14.975	15.245	0	0	0	0	1	0

	on upper deck								
6	Cold Compressor	25.325	23.010	0	0	1	0	0	0
7	Cold Cooler	30.580	23.010	0	0	0	1	0	0
8	Cold Expander	52.200	15.245	1	0	0	0	1	0
9	MCHE on A deck	40.760	9.700	0	1	0	0	0	0
10	MCHE on B deck	40.760	9.700	0	0	1	0	0	0
11	MCHE on C deck	40.760	9.700	0	0	0	1	0	0
12	MCHE on D deck	40.760	9.700	0	0	0	0	1	0
13	MCHE on E deck	40.760	9.700	0	0	0	0	0	1
The layout results for this case are assumed to the same results for the refrigerant module 2 of the dual N_2 expander cycle (4.0 MTPA) due to internal problems in MINLP. It will be updated according to the actual results for 3.0 MTPA.									

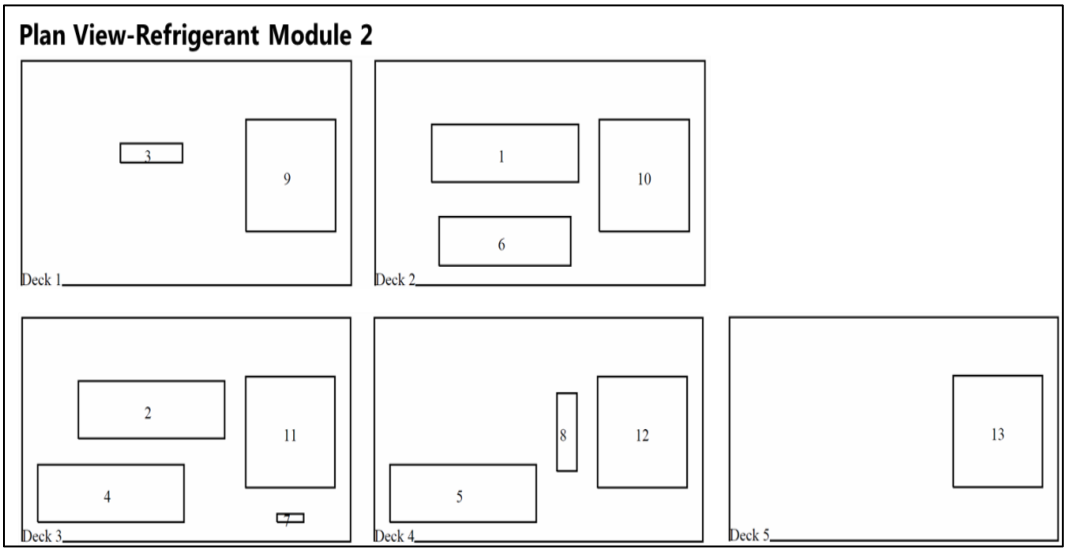

Figure 5-81 Plane view of refrigerant module 2 of the dual N_2 expander cycle (2.0 MTPA)

Table 5-98 Design variables of refrigerant module 2 of the dual N_2 expander cycle (2.0 MTPA)

Equipment		x_i [m]	y_i [m]	O_i	$V_{i,k}$				
No.	Name				$V_{i,1}$	$V_{i,2}$	$V_{i,3}$	$V_{i,4}$	$V_{i,5}$
1	Warm Compressor on lower deck	14.975	5.415	0	0	1	0	0	0
2	Warm Compressor on upper deck	14.975	5.415	0	0	0	1	0	0
3	Warm Cooler	25.325	15.245	0	1	0	0	0	0
4	Warm Expander on lower deck	14.975	15.245	0	0	0	1	0	0
5	Warm Expander on upper deck	14.975	15.245	0	0	0	0	1	0
6	Cold Compressor	25.325	23.010	0	0	1	0	0	0
7	Cold Cooler	30.580	23.010	0	0	0	1	0	0
8	Cold Expander	52.200	15.245	1	0	0	0	1	0
9	MCHE on A deck	40.760	9.700	0	1	0	0	0	0
10	MCHE on B deck	40.760	9.700	0	0	1	0	0	0
11	MCHE on C deck	40.760	9.700	0	0	0	1	0	0
12	MCHE on D deck	40.760	9.700	0	0	0	0	1	0
13	MCHE on E deck	40.760	9.700	0	0	0	0	0	1

The layout results for this case are assumed to the same results for the refrigerant module 2 of the dual N_2 expander cycle (4.0 MTPA) due to internal problems in MINLP. It will be updated according to the actual results for 2.0 MTPA.

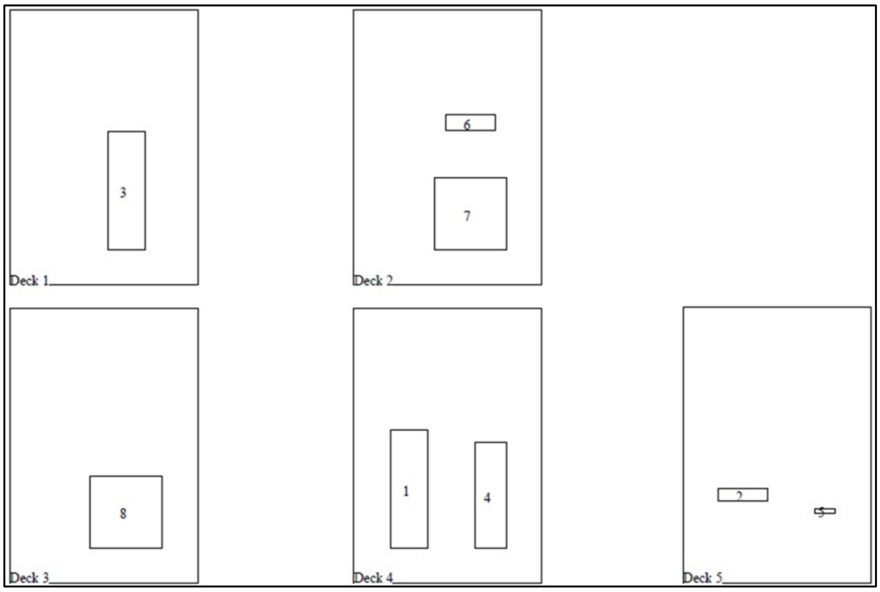

Figure 5-82 Plane view of refrigerant module 2 of the dual N_2 expander cycle (1.0 MTPA)

Table 5-99 Design variables of refrigerant module 2 of the dual N_2 expander cycle (1.0 MTPA)

Equipment		x_i [m]	y_i [m]	O_i	$V_{i,k}$				
No.	Name				$V_{i,1}$	$V_{i,2}$	$V_{i,3}$	$V_{i,4}$	$V_{i,5}$
1	Warm Compressor	4.750	8.030	1	0	0	0	1	0
2	Warm Cooler	5.120	7.509	0	0	0	0	0	1
3	Warm Expander	9.969	8.030	1	1	0	0	0	0
4	Cold Compressor	11.695	7.500	1	0	0	0	1	0
5	Cold Cooler	12.145	6.152	0	0	0	0	0	1
6	Cold Expander	9.969	13.840	0	0	1	0	0	0
7	MCHE on B deck	9.969	6.080	0	0	1	0	0	0
8	MCHE on C deck	9.969	6.080	0	0	0	1	0	0

5.5. Simplicity Analysis of the Preliminary Equipment Module Layouts

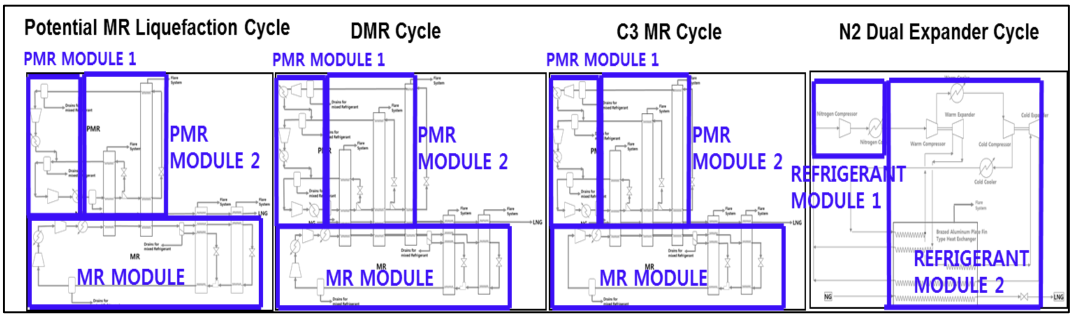

Figure 5-83 Potential offshore liquefaction cycles

Table 5-100 Comparison of simplicity for the potential offshore liquefaction cycles (4.0 MTPA)

Cases	**Required Area (m^2)**	**Simplicity Ranking**
Potential MR Liquefaction Cycle	2,344	1
DMR Cycle	2,731	3
C_3MR Cycle	2,638	2
Dual N_2 Expander Cycle	3,249	4

Table 5-101 Comparison of simplicity for the potential offshore liquefaction cycles (3.0 MTPA)

Cases	**Required Area (m^2)**	**Simplicity Ranking**
Potential MR Liquefaction Cycle	1,869	1
DMR Cycle	2,132	2
C_3MR Cycle	2,422	3
Dual N_2 Expander Cycle	2,719	4
The layout results for some modules (3.0 MTPA) are assumed due to internal problems in MINLP. So, the layout results and required area (3.0 MTPA) will be updated according to the actual results for them.		

Table 5-102 Comparison of simplicity for the potential offshore liquefaction cycles (2.0 MTPA)

Cases	**Required Area (m^2)**	**Simplicity Ranking**
Potential MR Liquefaction Cycle	1,108	1
DMR Cycle	1,669	2
C_3MR Cycle	2,012	3
Dual N_2 Expander Cycle	2,452	4
The layout results for some modules (2.0 MTPA) are assumed due to internal problems in MINLP. So, the layout results and required area (2.0 MTPA) will be updated according to the actual results for them.		

Table 5-103 Comparison of simplicity for the potential offshore liquefaction cycles (1.0 MTPA)

Cases	Required Area (m^2)	Simplicity Ranking
Potential MR Liquefaction Cycle	637	1
DMR Cycle	823	4
C_3MR Cycle	655	2
Dual N_2 Expander Cycle	665	3

Table 5-100 to 5-103 show the required area for each potential offshore liquefaction cycle based on the results from the optimal equipment module layout. The required area is the sum of each deck's sizes for them. For offshore application on the offshore liquefaction cycles, their simplicity, which is the critical offshore factor, should be considered based on the above required area. From the offshore simplicity viewpoint, the potential MR liquefaction cycle is considered the optimal liquefaction cycle for LNG FPSO.

For actual application for LNG FPSO, the trade-offs between simplicity and efficiency is addressed in the next chapter.

6. Offshore Trade-offs between Liquefaction Simplicity and Efficiency

6.1. Offshore Liquefaction Process Cycle Selection Criteria

For liquefaction offshore, the criteria for technology selection differ from those for onshore liquefaction, and this leads to an interesting conclusion regarding the best choice of technology. The most important criterion offshore is to minimize the space required for a safe plant due to the effect on the overall vessel size and overall cost. Offshore plants must also be insensitive to vessel motion, simple to operate, and flexible to the changes in the feed gas rate or rapid start-up after shutdowns or when moving between fields. In contrast to onshore liquefaction, where energy efficiency has a large effect on the overall cost, energy efficiency is of secondary importance offshore.

The feasibility studies for LNG FPSO conducted by the major international companies date back to the late 1980s, with the paper studies going back to the 1970s. David Wood was involved in evaluating the late 1980s' feasibility studies conducted by Mobil for potential deployment offshore, particularly in the Persian Gulf and Papua New Guinea. Shell also invested heavily in research and technical designs during the early and mid-1990s for potential deployment in a number of international locations. None of these projects materialized, however, due to the unfavorable economics (high breakeven LNG sales price) and the high level of technical risk. The key technical challenges that LNG FPSO will have to combat have been the subject of extensive research and have received development attention for more than a decade now (Eriksen et al., 2002):

① Space and weight requirements

- Floating systems are constrained by the available deck and marine vessel space.
- LNG FPSO requires additional safety systems for onshore LNG facilities.
- High equipment density to overcome the space and weight constraints

② Ease of operation/ start-up/ shutdown

- Bad weather and rough sea conditions require the ability for rapid plant shutdown. For this reason, LNG FPSO solutions are presently targeted for benign waters. Liquefaction process trains are most efficient when operated continuously with infrequent shutdowns. An increase in operational interruptions should be expected offshore, and this could adversely impact the operational efficiency.

③ Flexibility and Efficiency

- LNG FPSO requires process flexibility vs. efficiency, reliability, ease of installation, operation, and maintenance. Designs that enable gas input from different fields with varying gas compositions (gathering associated gas from several producing fields) are the most attractive because they offer some flexibility in terms of operating capacity and feed gas quality.

④ Safety

- The safe offloading of liquefied gas products to visiting LNG carriers under demanding environmental conditions require more robust mooring and loading arm technologies than those developed for sheltered, land-based ports. The transfer of LNG at cryogenic temperatures through hoses and loading arms is challenging.

- The control of process-related hazards (mechanical integrity of the process equipment, ignition source control systems, and explosion overpressure) requires more robust designs and operating systems offshore.
- Avoidance of vessel collision hazards (visiting LNG carriers, merchant vessel traffic, supply vessels and tugs) and other standard marine safety requirements add to the complexity of the safety management and emergency response procedures of such facilities.

⑤ Vessel motions

- Moving decks are challenging for process equipment operability and efficiency.
- Sloshing stresses in partly filled tanks require containment. The relative motions between an LNG FPSO and LNG carriers during loading and offloading operations are key design issues. Vessel motion is the key limiting factor in deploying floating facilities in harsh environments. The recent advances in ship-to-ship LNG transfers and the cryogenic pipework for use in such transfers are evidence that such issues can be satisfactorily resolved.

⑥ Chemical process systems

- Cooling system complexity and the fact that some liquefaction processes are obliged to manage substantial inventories of hydrocarbon refrigerants represent significant offshore handling hazards, adding to the safety concerns and cost.

- Process-related accidental hydrocarbon releases (both the refrigerants and the partially processed natural gas) are additional hazards to resolve.

From the foregoing, it is clear that offshore natural gas liquefaction has process requirements different from those of the traditional onland baseload plants. While thermodynamic efficiency is the key technical process selection criterion for large onshore natural-gas liquefiers, the high-efficiency precooled mixed refrigerant and optimized cascade plants that dominate onshore LNG installations are unlikely to meet the diverse technical and safety needs of LNG FPSO.

The offshore liquefaction technology developers are rightly focusing on process simplicity, low weight, and small footprint. Some technologies already deployed and proven to be effective for onshore peak-shaving applications are attractive in this regard. Considering that all process technologies deal with the thermodynamic constraints imposed by natural-gas compositions, the technologies that best fit the tried and tested machinery are those that are most likely to succeed commercially. The key criteria that influence process selection and plant optimization for offshore liquefaction unavoidably lead to some trade-offs and compromises between efficiency and simplicity.

Table 6-1 shows a summary of the offshore liquefaction process cycle selection criteria.

Table 6-1 Offshore liquefaction process cycle selection criteria

Offshore Liquefaction Process Cycle Selection Criteria	**Key Selection Criteria**	**Notes**
Equipment Module Layout	Simplicity	Numerical Values
Equipment Counts		
Compressor Power	Efficiency	
CAPEX	Other Criteria	Non-numerical Values
Flexibility		
Refrigerant Storage Hazard		
Proven Technology		
Vessel Motions		
Safety		
Simplicity of Operation		
Ease of Start-up/Shutdown		

6.2. Optimal Liquefaction Cycle for Actual Offshore Application

Based on the results from the optimal synthesis (compressor powers, equipment counts) and optimal equipment module layout (required area) in this paper, trade-offs are performed to select the optimal liquefaction cycle for LNG FPSO, as per Table 6-2.

Table 6-2 Trade-offs for the potential offshore liquefaction cycles

Cases	**Compressor Power (kW)**	**Equipment Counts**	**Equipment Module Layout (4.0 MTPA)**	**Equipment Module Layout (3.0 MTPA)**	**Equipment Module Layout (2.0 MTPA)**	**Equipment Module Layout (1.0 MTPA)**
Category	Efficiency	Simplicity				
Potential MR Liquefaction	133,100	22	2344	1625	1375	1010
DMR	126,700	26	2731	2105	1585	1225
C_3MR	132,900	25	2638	1975	1410	1195
Dual N_2 Expander	225,210	10	3249	2295	1390	895

In this paper, efficiency and simplicity are mainly considered for selecting the optimal liquefaction cycle for LNG FPSO. In conclusion, the potential MR liquefaction cycle has been selected for actual offshore application.

7. Conclusions

Optimization methods and offshore criteria for selecting the optimal liquefaction process system are proposed to contribute to future FEED engineering on LNG FPSO projects.

The goal of the process FEED method for LNG FPSO is to determine the potential feasibility of well development by estimating the final process FEED results, which include the total costs, weights, and layout of LNG FPSO. The specifications of all the equipment, instruments, and pipes, which are the main components of LNG FPSO, are determined to estimate the final process FEED results, In this paper, an offshore process FEED method was introduced and reviewed to efficiently obtain the final process FEED results.

The key criteria that influence the process selection and plant optimization for the offshore liquefaction cycle lead to some trade-offs and compromises between efficiency and simplicity. In addition, other criteria for offshore liquefaction cycles should be considered, such as flexibility, safety, vessel motion, refrigerant storage hazard, proven technology, simplicity of operation, ease of start-up/shutdown, and capital cost. This paper mainly focuses on two key factors: efficiency and simplicity.

From the efficiency viewpoint, this paper introduces the configurations and underlying principles of the liquefaction cycle. In addition, it addresses the configuration strategies of the liquefaction cycle, which are used to change the amount and association of the equipment making up the liquefaction cycle to within a feasible range. The four strategies described are the single cycle with regeneration, multi-stage compression with intercooling, multi-stage compression refrigeration, and multi-stage refrigeration. Based on these four strategies, a generic MR liquefaction cycle is proposed. The 27 feasible MR liquefaction cycles derived from such generic MR liquefaction cycle are configured for optimal synthesis, for use in the optimal liquefaction cycle. In these 27 cycles, all the optimal operating conditions, such as the pressure, temperature, volume, flow rate, and compositions of the refrigerant at the inlet and outlet of each piece of equipment, are calculated to minimize the power required by the compressors. Based on the optimal synthesis, the top 10 MR liquefaction cycles are selected for offshore application. Then one MR liquefaction cycle is selected, based on simplicity, among such 10 MR process cycles, and this is called the “potential MR liquefaction cycle.”

Second, three additional offshore liquefaction cycles — DMR for SHELL LNG FPSO, C_3MR for onshore projects, and the dual N_2 expander for FLEX LNG FPSO — are considered for comparison with the potential MR liquefaction cycle for the selection of the optimal offshore liquefaction cycle. Such four cycles can be considered potential offshore liquefaction cycles. The potential offshore liquefaction cycles are compared based on simplicity and efficiency in this paper.

In the efficiency aspect for the potential offshore liquefaction cycles, the optimal operating conditions for them with four LNG capacities (4.0, 3.0, 2.0, and 1.0 MTPA) are calculated with the minimum amount of power required for the compressors. Then the preliminary equipment sizes for them are assumed according to the proportion to the baseline design.

For the simplicity aspect for the potential offshore liquefaction cycles, the preliminary equipment module layout for the four cycles is designed as multi-deck instead of single-deck. This equipment module layout should be optimized to reduce the area occupied by the topside equipment at the FEED stage. In this paper, the connectivity cost, the construction cost proportional to the deck area, and the distance of the MCHE and separators from the centerline of the hull are considered objective functions to be minimized. Moreover, constraints are proposed to ensure safety and considering the deck penetration of long equipment across several decks. By considering the above, mathematical models are formulated for them. For example, the potential MR liquefaction cycle has a mathematical model consisting of 257 unknowns, 193 equality constraints, and 330 inequality constraints. Based on the mathematical model formulated herein, the preliminary optimal equipment module layouts with four LNG capacities (4.0, 3.0, 2.0, and 1.0 MTPA) are then obtained using mixed-integer nonlinear programming (MINLP).

Based on the above optimal operating conditions and equipment module layouts for the potential offshore liquefaction cycles, trade-offs between simplicity and efficiency are performed for actual offshore application, and finally, the potential MR liquefaction cycle is selected for the optimal liquefaction cycle for LNG FPSO.

Future work on the selection of the optimal liquefaction cycle will focus on blinded engineering methods for offshore equipment vendors to reduce uncertainties of equipment sizes. It would be tremendously contribute to get exact results of equipment module layout that lead to have more realistic offshore application on LNG liquefaction process systems.

In addition, the optimization of MR compositions and multi objective functions will be considered for future subjects on the optimal liquefaction cycle for offshore application.

References

[1] Michelle M. F., 2007. "An overview on liquefied natural gas, its properties, organization of LNG in industry", School of geosciences, University of Austin, Texas, Energy economic research.

[2] Mokhateb S., Finn A.J., and Shah K., 2008. "Offshore LNG industry developments, Petroleum Technology Quarterly", pp. 105, Q4.

[3] Hwang J., Roh M., and Lee K., 2013. "Determination of the optimal operating conditions of the dual mixed refrigerant cycle for the LNG FPSO topside liquefaction process", Computers and Chemical Engineering, vol.49, pp. 25-36.

[4] Shukri T., 2004. "LNG technology selection", Hydrocarbon Engineering.

[5] McLachlan G., Ayres C., Vink K., and AlMukhainy M., 2002. "Efficient operation of LNG from the oman LNG project", Gastech 2002, Doha, Qatar.

[6] DOE/EIA, 2003. "The global liquefied natural gas market: Status and outlook, Energy information administration", U.S. dept. of Energy, DOE/EIA-0637.

[7] Meyer M., 2004, "LNG liquefaction process-Why the big fuss about selection", IChemE London SONG meeting.

[8] Sheffield J., 2001. "The challenges of floating LNG facilities", Proc. of the GPA spring meeting.

[9] Faber F., Resweber L., Jones P., and Bliault A., 2002. "Floating LNG solutions from the drawing board to reality", Offshore technology conference, Houston, Texas.

[10] Technip, 2012. http://www.technip.com.

[11] Mustang engineering, 2012. http://www.mustangeng.com.

[12] Doris engineering, 2012. http://www.doris-engineering.com.

[13] Shin H.K., Lee H.Y., Lim C.G., Shin H.S., and Park I.G., 2000. “Motion of a very large floating structure in irregular waves”, Trans. Soc. Naval Architect Korea, 37(4), pp. 75-81.

[14] Lee H.Y., Shin H.K., Lim C.G., Kim O.H., Kang J.M., and Yoon M.C., 2000. “Hydroelastic responses for a very large floating structure with a breakwater”, Trans. Soc. Naval Architect Korea, 38(2), pp. 26-32.

[15] Lee J.O., Lee H.Y., Suh Y.S., and Yoon J.H., 1998. “Reliability of fatigue life predictions for fixed offshore structures”, Trans. Soc. Naval architect Korea, 35(2), pp. 74-82.

[16] Kim H.S., Jun S.H., Shim C.S., Lee G.Y., Nam H.S., Kang J.K., Shin Y.G., and Heo J.H., 2004. “The study on local strength analysis for floater type offshore structure”, Proceedings of the annual autumn meeting, The Society of Naval Architects of Korea, Sancheong, Korea.

[17] Na J.H., Shim W.S., Lee I.H., Moon J.S., Kim J.W., and Shin H.S., 2004, “FPSO quay mooring analysis in typhoon condition”, Proceedings of the annual autumn meeting, The Society of Naval Architects of Korea, Sancheong, Korea.

[18] Kim J.H., Cho S.K., Hong S.Y., and Kim Y.S., 2006. “Experimental study on a dolphin-fender mooring system for pontoon-type structure”, Trans. Soc. Naval Architect Korea, 42(1), pp. 43-49.

[19] Lake M., He H., Troesch A.W., Perlin M., and Thiagarajan K.P., 2000. “Hydrodynamic coefficients estimation for TLP and spar structures”, Joural of

Offshore Mech. Arct., 122(2), pp. 118-124.

[20] Newman J.N., and Lee C.H., 2002. “Boundary-element methods in offshore structure analysis”, Jouranl of Offshore Mech. Arct., 124(2), pp. 81-89.

[21] Matsuura J.P., and Bernitsas, M.M., 2006. “Routes to large amplitude motions of mooring systems due to slowly varying driff”, Jouranl of Offshore Mech. Arct., 128(4), pp. 280-285.

[22] Chang H.M., Park J.H., Woo H.S, Lee S., and Choe K.H., 2010. “New concept of natural gas liquefaction cycle with combined refrigerants”, International Cryogenic Engineering Conference.

[23] Finn A.J., Johnson G.L., and Tomlinson T.R., 2000. “LNG technology for offshore and mid-scale plants”, Proceedings of the 79th Ann GPA Convention, Atlanta.

[24] Lee J., Kim W., Kim H., and Park C., 2010a. “Comparison between the LNG liquefaction plant for the ships and large LNG liquefaction plant process”, Proceeding of the Annual Spring Meeting, the Society of Naval Architecture of Korea, pp. 956-960.

[25] Lee S., Cha K., Park C., Lee C., Cho Y., and Yang Y., 2010b. “The study on natural gas liquefaction cycle development”, Proceedings of the 9th ISOPE Pacific/Asian Offshore Mechanics Symposium, Busan, Korea.

[26] Lim W., Tak K., Moon I., and Choi K., 2010. “Simulation comparison of liquefaction technologies for LNG offshore plant design”, Proceedings of the 9th ISOPE Pacific/Asian Offshore Mechanics Symposium, Busan, Korea, pp. 34-37.

[27] Nogal F.D., Kim J.K., Perry S., and Smith R., 2008. “Optimal design of mixed refrigerant cycles”, Industrial & Engineering Chemistry Research, 47:pp. 8724-

8740.

[28] Remeljej C.W., Hoadley AFA., 2006. “An exergy analysis of small-scale liquefied natural gas (LNG) liquefaction processes”, Energy, 31:pp. 2005-2019.

[29] Chang H.M., Chung M.J., Kim M.J., and Park S.B., 2009. “Thermodynamic design of methane liquefaction system based on reversed-brayton cycle”, Cryogenics, 49(6):pp. 226-234.

[30] Jensen JB., 2008. Optimal operation of refrigeration cycles. Ph.D. Thesis, Norweglan University of Science and Technology.

[31] Kim H., Park C., Lee J., and Kim W., 2010. “Optimal degree of superheating of the liquefaction process for application of LNG FPSO”, Proceeding of the Annual Spring Meeting, the Society of Naval Architecture of Korea, pp. 961-965.

[32] Lee G.C., Smith R., and Zhu X., 2002. “Optimal synthesis of mixed refrigerant systems for low temperature processes”, Industrial & Engineering Chemistry Research, 41:pp. 5016-5028.

[33] Venkatarathnam G., 2008. Cryogenic mixed refrigerant processes, New York: Springer.

[34] Rangaiah G.P., 2008. “Multi-objective optimization techniques and applications in chemical engineering”, World scientific pulishing company, USA.

[35] Nogal F.D., 2006. Optimal design and integration of refrigeration and power systems, Ph.D. Thesis, The University of Manchester, UK.

[36] Penteado, F.D., and Ciric, A.R., 1996. “An MINLP approach for safe process plant layout”, Industrial and Engineering Chemistry Research 35, pp. 1354-1361.

[37] Patsiatzis, D.I. and Papageorgiou, L.G., 2002. "Optimal multi-floor process plant layout", Computer and Chemical Engineering 26, pp. 575-583.

[38] Park K., Koo J., Shin D., Lee C.J., and Yoon, E.S., 2011. "Optimal multi-floor plant layout with consideration of safety distance based on mathematical programming and modified consequence analysis", Korean Journal of Chemical Engineering 28(4), pp. 1009-1018.

[39] Georgiadis M.C., Schilling G., Rotstein G.E., and Macchietto, S., 1999. "A general mathematical programming approach for process plant layout", Computers and Chemical Engineering 23, pp. 823-840.

[40] Hwang J., Min J., Ahn Y., Kim H., Roh M., and Lee K., 2008. "Optimized methodology to build an integrated solution to offshore topside process engineering", International Society of Offshore and Polar Engineers (ISOPE) 2008, Vancouver, Canada.

[41] Hwang J., Ku N., Lee J., Roh M., and Lee K., 2012. "Optimal synthesis of LNG FPSO liquefaction cycles", International Society of Offshore and Polar Engineers (ISOPE) 2012, Rodos, Greece.

[42] Cengel Y.A., Boles M.A., 2011. Thermodynamics-an engineering approach, 7th edition, McGraw-Hill.

[43] Choi S.G., Hong S.E., 2008. Refrigeration engineering, Keonkiwon, Korea.

[44] Li Q.Y., Ju Y.L., 2010. "Design and analysis of liquefaction process for offshore associated gas resources", Applied Thermal Engineering 30, pp. 2518-2525.

[45] Mecklenburgh J.C., 1985. Process plant layout, George Godwin London and New Your.

[46] Eriksen R., Brandstorp J.M., and Cramer E., 2002. "Evaluating the viability of offshore LNG production and storage", paper presented at the GasTech 2002 conference, Doha, Qutar.

국문 초록

해양 모듈 배치를 고려한 FEED 단계에서의 LNG FPSO 용 최적 액화 프로세스 시스템 선정 연구

본 논문에서는 향후 LNG FPSO에 적용 가능한 최적 액화 프로세스 시스템 선정에 관한 연구를 수행 하였다. 이는 향후 LNG 액화 프로세스 시스템의 FEED 설계에 큰 기여를 할 수 있을 것으로 기대 한다.

해양 적용을 위한 액화 프로세스 시스템은 육상에 적용하는 액화 프로세스 시스템과는 큰 차이가 있다. 육상에 적용하기 위한 액화 프로세스 사이클을 선정하는데 있어 가장 중요한 요소는 열역학적 효율 이다. 그로 인하여 열효율이 높은 Pre-cooled mixed refrigerant 사이클과 optimized cascade 사이클을 적용한 액화 사이클들이 육상 LNG 액화 플랜트에 주를 이루었다. 이런 열효율이 높은 육상용 LNG 액화 사이클들은 해양적용을 위해서는 여러가지 기술적인 문제들로 인하여 적절치 않을 수 있다. 해양 적용을 위한 액화 프로세스 사이클은 열역학적 효율과 더불어 사이클이 간결해야 하며 무게가 가볍고 차지 하는 면적이 작아야 한다는 해양 환경을 고려한 추가적인 중요한 요소들이 있다. 그러므로 해양에 적용가능한 최적 액화 프로세스 사이클을 선정하기 위해서는 육상 적용 시 가장 중요한 요소인 효율(Efficiency)과 해양 적용시 추가적으로

고려해야 될 중요한 요소들인 간결성(Simplicity) 사이에 Trade-offs와 절충이 필요하다.

그 외에도 해양 적용 시 고려해야 될 요소들로는 유연성(Flexibility), 안전(Safety), 배의 움직임(Vessel Motion), 냉매 탱크 위험성(Refrigerant Storage Hazard), 검증된 기술(Proven Technology), 운전의 간결성(Simplicity of Operation), 초기 운전/운전 정지의 용이성(Ease of Start-Up/Shutdown)과 자본(Capital Cost) 등을 고려할 수 있다. 본 논문에서는 LNG FPSO 적용 가능한 최적 액화 프로세스 사이클 선정을 위해서 효율(Efficieny)과 간결성(Simplicity)을 고려하였으며 이를 위해 다음과 같은 연구들을 진행 하였다.

첫번째로, Generic MR(mixed Refrigerant) 액화 사이클을 제안하였으며 이를 근거로 기계적으로 실현 가능한 27개 MR 액화 사이클들을 최적 합성 하였다. 27개 MR 사이클들 중 효율(Efficiency) 측면에서 압축기 소요 동력을 최소로 하는 최적 운전 조건들을 구하여 상위 10개 MR 액화 사이클들을 선정 하였다. 그 후 10개 MR 사이클들 중 간결성(Simplicity) 측면에서 한가지 MR 액화 사이클을 선정 하였으며 선정된 한가지 액화 사이클을 잠재적 MR 액화 사이클로 명명 하였다. 이 단계에서 고려할 수 있는 간결성(Simplicity) 측면은 장비 개수가 유일하여 이를 기준으로 하였다. 이후, 여기서 선정된 잠재적 MR 액화 사이클과 추가적으로 고려한 해양 액화 사이클들에 대한 간결성(Simplicity)연구는 각 사이클들에 대한 최적 장비 모듈 배치(Optimal Equipment Module Layout)를 구하여 보다 실제적인 간결성에 대한 연구를 진행 하였다.

두번째로, 선정된 잠재적 MR 액화 사이클과 추가적으로 3가지 해양 액화 사이클들을 선정하여 이들 사이에 LNG FPSO 용 최적 액화 사이클을 선정하기 위한 효율(Efficiency) 과 간결성(Simplicity) 에 대한 연구를 진행 하였다. 추

가적으로 고려한 3가지 해양 액화 사이클들로는 현재 실제 LNG FPSO에 적용 중인 DMR 사이클, Dual N2 Expander 사이클과 육상에서 가장 널리 사용되는 C3 MR 사이클들 이다. 총 4가지 사이클들에 대한 효율(Efficiency) 측면에서는 각 사이클을 구성하는 장비들 중 압축기 소요 동력을 최소화하는 기준으로 4가지 LNG 생산 용량(4.0 MTPA, 3.0 MTPA, 2.0 MTPA, and 1.0 MTPA)에 대한 각 사이클들을 비교 분석 하였다. 다음으로 해양 적용 시 가장 중요한 간결성(Simplicity) 측면에 대한 연구를 언급 하겠다. 이 단계에서 4가지 사이클들의 실제적인 간결성(Simplicity) 차원의 연구를 진행하기 위하여 장비 모듈 배치 최적화 연구를 진행하여 각 사이클들이 차지하는 면적들을 구함으로써 각 사이클들을 비교 분석을 할 수 있었다.

본 논문에서는 배관 연결 비용(Connectivity Cost), 장비들이 차지하는 면적에 비례하는 생산 비용(Construction Cost), 배의 운동에 가장 민감한 장비들(Main Cryogenic Heat Exchanger, Phase Separator)의 배의 운동으로 인한 효율 감소로 인한 비용들을 목적함수로 정의 하였으며 이를 최소화 하였다. 여기서 목적함수를 통해 알 수 있듯이 해양 환경을 고려하여 배의 운동에 민감한 장비들에 대하여 효율에 최대한 덜 영향을 주기 위해 배의 중심 라인에 배치될 수 있도록 하였다. 또한 해양 환경 제약 조건들을 고려하여 FEED 단계에서 각 사이클들을 구성하는 장비들이 차지하는 면적을 최소로 하였다. 제약 조건들로는 안전을 고려한 제약 조건들과 길이 방향으로 긴 장비들이 여러 층을 관통하는 조건들 및 해양 환경상 특별히 고려해야될 제약 조건들에 대하여 정의 하였다. 이런 제약 조건들과 목적함수를 고려하여 4가지 사이클들에 대한 수학적 모델링들을 도출하였으며 Mixed Integer NonLinear Programming(MINLP)를 이용하여 4가지 LNG 생산 용량에 대한 각 사이클들의 최적화 문제들을 풀었다. 그 결과 최적 장비 모듈 배치들을 구하여 결국 각 사이클들이 차지하는 면적들을

구할 수 있었다.

실제 LNG FPSO에 적용을 위하여 상기 4가지 사이클들의 효율(Efficiency) 측면에서 최적 운전 조건들과 간결성(Simplicity) 측면에서 장비 모듈 배치 결과값들을 근거로 효율과 간결측 측면에서 Trade-offs 를 수행 하였다. 그 결과, Generic MR 액화 사이클로부터 선정된 잠재적 MR 액화 사이클이 LNG FPSO용 최적 액화 사이클로 선정 하였다.

본 연구에서는 해양 관련 가장 최신 기술인 액화 공정에 대해서 진행 하였으며 이는 해양 관련 모든 시스템들에도 적용 가능할 것이며 이를 통해서 결국 Topsides 전체 시스템들이 배 위에 차지하는 최적화된 면적들을 구할 수 있게 됨으로써 최종적으로 최적화된 배의 크기를 구할 수 있을 것으로 기대된다.

Keywords: 최적 액화 사이클 선정, 해양 적용, 효율, 간결성, 최적 합성, 최적 운전 조건, 최적 장비 모듈 배치, Generic MR 액화 사이클, LNG FPSO, FEED

Student number: 2007-30176

후기

휴스턴 시각으로 2013 년 2 월 1 일 오후 7 시 정각 박사 학위 후기를 작성하기 시작 하였다. 후기를 시작하기 전 어떤 말로 적절하게 시작해야 될지 많은 고민과 고민들을 거듭하였는데 결국 작성하고자 서재에 앉으니 일반적인 말들 밖에 떠오르지가 않는다. 1 시간이 흘렀다. 도저히 할 말이 떠오르지가 않는다. 이유로는 후기를 쓴다는 것이 현실일까, 꿈이 아닐까, 내가 정말 졸업을 하는 것인가 라는 먼가 와 닿지 않는 현실이라는 것과 이로 인해 아직 생각이 정리가 되지 않는 것이 가장 큰 이유인 듯 하다. 현재 머리 상태로는 박사 학위 논문 작성하는 것 보다도 후기 작성하는 것이 나에게는 더 어려운 일인 거 같다. 결국 와이프인 미영 에게 고민 상담을 시작하였고 후기에 대한 방향 설정을 할 수 있었다.

먼저 우리 나라 해양플랜트 엔지니어링에 제 박사 학위 논문이 밑거름이 될 수 있었으면 하는 바램이 가장 먼저 떠오르는 생각이고 바램이다. 몇 년 전 2 개의 미국 회사들과 1 개의 유럽 회사로부터 잡 오퍼를 받았다. 이 곳 휴스턴으로 취업하여 물 건너 온 후 회사 사업 특성 상 Oil FPSO Topsides 와 Turret FEED / EPCI 프로세스 엔지니어링 수행 및 LNG FPSO (FLNG) Topsides 프로세스 연구를 회사 네덜란드 본사 측과 공동으로 수행 중이다. 또한 휴스턴

프로세스 시스템 엔지니어링 부서 안에서 시니어 프로세스 엔지니어로써 많은 노력들과 경험들을 하고자 하루 하루 피나는 노력들을 하였다. 가장 기억에 남는 일은 휴스턴으로 와서 처음 수행한 쉘 사에서 발주한 Oil FPSO Topsides FEED 프로세스 결과물이 다른 경쟁자들보다 기술적인 우위를 점해 EPCI 수주까지 이어진 것으로 이로 인해 회사 내부적인 입지를 더 다질 수 있는 계기가 될 수 있었던 것이 가장 첫번째로 떠오르는 일이다. 올해에는 코노코필립스 사에서 발주 예정인 LNG FPSO (FLNG) Turret FEED 프로젝트의 리더 프로세스 엔지니어 역할을 수행할 예정이다. 그 이 전에 프랑스 파리에서는 쉘사에서 발주한 LNG FPSO (FLNG) Topsides FEED 프로젝트를 수행하면서 해양 플랜트 선진 엔지니어링 회사들의 Know-how 와 기술력들을 습득하고자 매일 저녁에서 시작하여 새벽까지 피나는 노력들을 했던 소중한 추억들이 떠 오른다. 이런 노력들과 경험들을 기초로 박사 학위 논문 주제가 정해졌으며 SCI 논문도 3 편이 통과하게 되었다. 여기서 중요한 사실이 있다. 지도 교수님이신 이규열 교수님, 평생 고마운 마음을 간직할 것이며 은사로 모시고 살 것 이다. 해양 플랜트 실무 기술적인 부분들을 학문적으로 승화 시킬 수 있게 열정적으로 지도해 주셨으며 이로 인한 결과들이 SCI 논문들이 되었다. 이규열 교수님을 만나지 못했다면 이런 결과물 들 뿐 만 아니라 지금 이런

후기를 쓰는 꿈 같은 현실은 없었을 것이다. 또한, 박사 학위 과정 중 해양 플랜트 특성 상 해외 선진 기술들을 많이 습득하여 이를 학문적으로 승화 시킬 수 있게 연구실을 떠나 미국 취업까지 이해해 주셔서 이런 결과들이 나올 수 있었다고 생각 한다. 이규열 교수님, 다시 한번 더 고개 숙여 감사 드리며 초심을 잃지 않고 교수님 제자로서 해양 플랜트 엔지니어링에 큰 획을 그을 수 있는 엔지니어가 되겠습니다. 또한, 추후 한국에도 교수님 제자로써 기여할 수 있는 값진 일들을 할 수 있도록 하겠습니다.

먼저, 한달 동안 한국에서 박사 논문 심사 기간 중 박사 논문에 대한 무엇과도 바꿀 수 없는 값진 조언들과 심사를 맡아 주셨던 아래 심사위원님들에 대한 감사의 글을 올리고자 한다.

양영순 교수님, 제 박사 논문 심사위원장님직을 맡으시며 여러가지로 값진 조언들을 해주셔서 감사 드립니다. 박사 논문 심사 기간 중 많은 조언들과 박사 논문 심사가 잘 진행될 수 있도록 여러가지 측면에서 큰 도움들을 주셔서 감사 드립니다. 특히, 값진 조언들이 제 박사 논문에 한정 지어진 것이 아니라 향후 우리나라 해양플랜트 엔지니어링 더 나아가 해저 엔지니어링 분야까지 걱정하시며 이에 대한 여러가지 조언들을 해주셔서 제 인생의 목표 및 길을

다시 한번 더 생각할 수 있게 해주셔서 감사 드립니다. 교수님 말씀대로 여기서 피나는 노력들과 값진 경험들을 한 후 가치 있고 의미 있는 삶을 살 수 있도록 하겠습니다. 또한, 이렇게 양영순 교수님과 인연을 맺게 되어 큰 영광이며 앞으로도 계속해서 자주 연락 드리겠습니다.

한종훈 교수님, 처음 제 박사 논문 심사위원님으로 선정되셨을 때 두가지 기분이 교차 하였습니다. 첫번째 기분은 화학공학 분야의 최고 권위자 중 한명이신 분이 제 박사 논문 심사를 한다는 생각에 말로 표현하기 힘든 영광스러운 기분이였습니다. 두번째 기분은 이로 인하여 큰 부담감 또한 작용하여 한동안 긴장하며 박사 논문 심사를 준비 하였습니다. 박사 논문 심사 기간 동안 한종훈 교수님 만나 뵙고 제 논문이 서울대학교 박사 학위 논문 수준이 될 수 있도록 전체적인 방향 설정 및 소중한 조언들을 많이 해주셔서 진심으로 감사드립니다. 또한, 한종훈 교수님께서 말씀하셨듯이 우리 나라 해양플랜트 분야에 큰 획을 그을 수 있는 인재가 되겠으며 향후 한종훈 교수님 연구실과도 많은 발전적 교류들이 있을 수 있도록 하겠습니다.

문일 교수님, 박사 학위 논문 연구 중 문일 교수님 연구실에서 LNG 액화 공정 관련 연구들을 활발히 진행한다는 사실을 알게 되었습니다. 그 후 제 박사

학위 외부 논문 심사 위원님으로 선정되신 후 이런 생각을 하였습니다. 우리나라 화공 프로세스 시스템 분야의 최고 권위자들 이신 문일 교수님과 한종훈 교수님이 제 박사 논문 심사 위원님으로 선정된 것은 한편으로는 큰 부담으로 작용되었지만 다른 한편으로는 많은 지도와 가르침을 받은 후 향후 계속해서 좋은 인맥과 연구 관련 교류들을 할 수 있는 기회를 만들었다는 점에 큰 기대감으로 작용되었습니다. 그 후 저희 이규열 지도교수님께서 하신 말씀이 기억에 남습니다. 지도교수님께서 강조하셨던 말씀이 저희 연구실에서 박사를 받기 위해서는 무조건 정면돌파를 하여야 되며 우리 나라 최고 권위자들을 통해서 박사 논문이 검증 후 통과될 시 향후 더 큰 미래를 볼 때 개인적으로도 큰 도움이 된다는 것이 였습니다. 저 역시 그 말씀을 크게 깨닫게 되었으며 박사 학위 종심 마친 후 문일 교수님 연구실 제자들을 저에게 소개 시켜 주시며 향후 많은 교류들이 있기를 바란다고 말씀 하셨을 때 큰 영광이였습니다. 향후 해양플랜트 연구 관련 문일 교수님 연구실과 많은 교류가 있을 수 있도록 하겠습니다. 또한, 심사 기간 중 예리하시고 많은 값진 조언들을 해주셔서 감사 드립니다.

장범선 교수님, 장범선 교수님과는 인연이 꽤 오래 된 듯싶습니다. 삼성중공업 에서 처음 만나 Oil FPSO 개조 사업에 대한 사업성 조사를

장교수님과 잠시 같이 수행한 때가 생각 됩니다. 그 때 장 교수님께서 업무 진행하시는 내용을 보고 서울대학교 박사가 정말 대단하구나라는 생각을 하였으며 내 자신을 다시 한번 더 돌아 보는 계기가 되었습니다. 공교롭게도 그 당시 Oil FPSO 사업성 조사할 당시 Oil FPSO 세계 1 위 기업으로 조사되었던 SBM Offshore 로 현재 제가 이직하게 되었습니다. 미국으로 이직 결정할 당시, 미국 오일 메이져 회사 중 한 곳과 현재 직장 중 선택하여야 되었으며 최종 마음의 결정을 내릴 때 그 당시 장범선 교수님께서 자료 조사하신 내용이 크게 도움이 되었고 입사한 후로도 프로세스 엔지니어로써 제 선택이 옳았다라는 생각을 하게 되었습니다. 미국으로 취업되어 넘어갈 당시에도 많은 격려와 힘들을 주셔서 진심으로 감사드리며 이 연인이 제 박사 논문 심사로 까지 이어지게 되어 큰 영광이였습니다. 박사 학위 논문 심사 기간 중 예리하시면서도 제 박사 논문 수준을 더 끌어올리기 위한 값진 조언들을 많이 해주셔서 다시 한번 더 감사 드립니다. 앞으로도 지속적으로 연락 드리며 한국에 갈 때 마다 찾아 뵙겠습니다. 그리고 휴스턴 출장 나오시면 제가 1 순위라고 약조를 하셨으니 저희 집에서 저녁식사를 꼭 하셔야 됩니다.

다음으로는 박사 논문 연구 기간 중 큰 도움과 신세를 진 제 연구실 ASDAL 선배님들께 감사의 글을 남기고자 한다.

노명일 교수님, 2006 년 연말 정도에 학교 세미나 하러 가서 처음 인연을 맺게 된 후 벌써 6 년이라는 시간이 흘렀습니다. 6 년 이라는 시간 동안 많은 변화들이 있었습니다. 많은 변화들 속에서도 꾸준히 학문적인 지도와 조언을 해주셔서 이렇게 박사 학위 논문을 마무리할 수 있게 되었습니다. 처음 연구실에 들어 와서 학술진흥재단에 제안하였던 해양플랜트 3 년 과제가 최종 심의 결과 채택 되어 해양플랜트 프로세스 엔지니어링 관련 과제를 정부로부터 지원 받으면서 저희 연구가 시작되었을 때가 가장 기억에 많이 남습니다. 천재적인 노 교수님 지도로 인해 무사히 3 년 과제를 잘 마무리 하여 좋은 성과를 낼 수 있게 해주셔서 진심으로 감사 드립니다. 저는 노명일 교수님을 뵙고 정말 세상에는 천재가 있구나라는 것을 깨닫게 되었으며 세상을 보는 시각이 많이 넓어 질 수 있었습니다.

조두연 교수님, 조 교수님과는 정말 짧은 시간 동안 잠시 연구실에서 볼 수 있었으며 기억 상으로 정말 교수 스타일 말투와 지식, 특히, 겨울 방학 때 같이 공학수학 세미나에 참석했을 때 예리한 질문들과 수학적 설명들에 큰 감명을 받았습니다. 저 역시 조 교수님 같은 학자가 될 수 있도록 이 곳에서 꾸준히 노력하여 나중에 한국에서 같은 연구 과제를 진행할 수 있는 날을 손꼽아 기다리겠습니다.

박광필 박사님, 대우조선해양 3 대 과장(그 당시 에는 과장이였고 지금은 차장님 이시지만) 중 한명이라고 이규열 교수님께서 소개 해주셨을 때가 기억 납니다. 분명, 대우조선해양에서 사장까지 하실 분이라는 것을 확신하고 있으며 박 박사님을 볼 때 마다 사람이 예리하다는 것이 무었인지를 깨달을 수 있었습니다. 저 역시 이런 점들을 보고 배워서 계속해서 발전하는 사람이 될 수 있도록 하겠습니다.

차주환 교수님, 주환이를 항상 보면서 형이 생각하기를 모든 것이 완벽한 남자라고 생각 했단다. 인물이며 학문적 지식이며 명석한 두뇌며 엄청난 발표 자료 작성과 환상적인 발표 능력이며, 인간이라고 말하기에는 단점이 없는 초능력적인 사람이라고 생각 했단다. 다음에 한국에서 볼 때는 형한테 말도 편하게 하고 향후 발전적인 교류들이 많이 있었으면 하구나.

구남국 박사님, 남국아 형은 이번 박사 논문 심사를 위하여 한달간 한국에 체류하면서 너에게 큰 신세를 지었다고 생각한단다. 사람은 은혜를 받았으면 나중에 배풀줄 알아야 한다고 생각하며 앞으로도 형과 많은 교류들을 하였으면 하구나. 박사 논문 심사 기간 중 형과 같이 많은 밤을 세우면서도 한번도 불평 불만하지 않고 묵묵히 형 옆에서 많은 도움들을 주었던 점 너무 고맙고

감사하게 생각한다. 특히, 이제 갓 신혼 인데 남편 시간을 많이 빼앗게 되어 제수씨에게 미안하고 고마운 마음을 전해주고 싶구나. 앞으로 형과 좋은 관계를 계속 유지할 수 있었으면 하구나. 또한, 빠른 시일 내에 교수님이 되어 구교수님 이라고 불러 보고 싶구나.

하솔 박사님, 솔아, 이번에 한달 동안 형과 연구실에서 매일 밤샘을 하며 너의 특유한 좋은 성격으로 인하여 형이 힘들 때 마다 큰 힘이 되었단다. 너는 그 것을 잘 못 느낄 수가 있겠지만 한달 간 형이 너를 통해서 심적인 안정을 많이 찾을 수 있었단다. 그리고, 솔이도 박사 논문 심사 하랴 논문 쓰랴 바쁠 건데 형 박사 논문 관련해서 행정적인 서류 절차들 및 여러가지로 많은 도움들을 줘서 정말 고맙구나. 형과 같이 졸업한 후 향후 계획들에 대해서 많은 대화를 나누어 보도록 하자. 솔이가 어떤 결정을 내리고 미래가 어떻게 될지는 알 수 없지만 형이 도와 줄 수 있는 부분들이 있다면 최선을 다해 도와 줄께.

이준채, 준채와 형의 관계는 한 때 형 와이프가 과연 한국에 준채라는 사람이 있느냐라고 오해를 했을 정도의 각별한(?) 사이 였다고 생각한다. 파리에서 너와 국제 전화를 한 참 할 때 엄청한 전화 요금으로 인해서 이런 오해가 있었다고 생각하구나. 준채 너 졸업할 때까지 형과 정말 많은 전화와 대화를 했고 이로

인해 형과는 정말 특별한 관계가 되었던 거 같구나. 너와는 항상 한국에 한번씩 들어 갈 때 마다 개인적으로 만나서 많은 대화도 나누었던 거 같구나. 준채가 정말 잘해 줘서 정말 고맙고 형이 자주 말했지만 넌 정말 똑똑하고 향후 우리 나라를 이끌어갈 인재 중 인재야.

조아라씨, 아라씨와는 연구 분야도 틀리고 같이 시간을 많이 보내지 못한 것이 많이 아쉽군요. 조만간에 결혼하셔서 행복한 가정 꾸리시기 바라며 커리어 우먼으로써 우리 나라 해양 산업에 큰 임팩트를 끼칠수 있는 여성 엔지니어가 되실 것으로 믿으며 나아가 여성 최초 CEO 되기를 기대 합니다.

함승호, 사실 형이 승호를 만나고 승호의 머리는 어떤 것들로 구성되어 있을까 너무 궁금하였단다. 말이 석사를 졸업했지 박사 못지 않은 연구 결과들과 학무적인 성취도를 보며 항상 감탄했던 기억이 나구나. 형은 승호도 나중에 박사 학위 마친 후 대학 교수가 될 거 라는 개인적인 믿음을 가지고 있으며 향후 형과도 많은 교류들을 하며 너의 머리를 잠깐씩 빌릴 수 있었으면 하구나.

그 외에 3 분의 ASDAL 박사 졸업하신 분들과 많은 ASDAL 석사 졸업생들께서 계시지만 저와 실질적인 시간들을 보낼 기회들이 가지지 못하여

글로 표현하지 못하게 되어 미안한 마음이 듭니다. 향후 ASDAL 졸업생들끼리 많은 발전적 교류들이 있을 것으로 기대하며 ASDAL 졸업생 중 한명으로써 또한 이규열 교수님 제자로써 이에 걸맞는 세계적인 해양 플랜트 프로세스 엔지니어가 될 수 있도록 하겠습니다.

이제부터 내 인생에 있어서 고마운 분들에 대해서 감사의 글을 남기고자 한다.

내 영원한 친구 이자 와이프 홍미영, 벌써 우리 가족이 해외 생활을 한지가 4 년이 넘었고 많은 나라들을 돌아 다녔는데 남편 믿고 모든 집안일들과 우리 딸 혜주 관련 각 나라별 수업 내용들 파악하여 잘 가르치는 모습을 보고 너무 고맙다. 남편이 외국인들 사이에 많은 스트레스 받고 집에 돌아 오면 오로지 박사 학위 논문 연구만 할 수 있게 모든 배려들과 인내심들이 지금의 박사 학위를 무사히 마치고 졸업할 수 있게 된 큰 원동력이 되었다고 생각한다. 내 인생에 있어 가장 축복받은 것이 미영이를 만난 것이라고 생각한다. 지금까지 걸어온 길들을 보면 전부 미영이가 선견지명 있게 조언해 준 대로 하였고 결과적으로 잘 되었다고 생각한다. 박사 학위를 시작할 때와 중간에 시련, 프랑스에서의 힘들 때, 미국 취업 결심, 미국 적응, 박사 학위 진행 등에 있어서

모든 중요한 결정들을 하는데 있어서 미영이의 선택이 결국은 다 옳았다고 생각하며 나는 다시 한번 더 생각 하게 된다. 남자는 와이프를 잘 만나야 된다고 생각하며 박사 학위를 받는데 있어 모든 내조들을 해준 미영이에게 감사한다.

우리 하나 밖에 없는 딸 황혜주, 이 곳 미국에서는 엘리라는 이름만 부르긴 하지만 아빠 박사 학위 논문에는 혜주라는 이름을 쓰도록 할께. 아빠는 솔직히 걱정을 많이 했고 미안한 마음이 앞서구나. 유치원 때 한국을 떠나 올해 미국 초등학교 4 학년에 올라가는데 여러 나라들을 돌아 다닌다고 안정적이고 체계적인 교육을 받는데 어려움들이 있지 않았나 라는 생각이 많이 드는 구나. 5 학년 때 까지만 놀고 주니어 하이 스쿨 올라가면 아빠랑 같이 본격적으로 공부를 시작해 보자. 아빠도 책임감을 가지고 혜주 공부하는데 도움이 될 수 있도록 할께. 지금까지 회사 마친 후 와 주말에는 박사 학위 논문 연구로 혜주랑 시간을 거의 보내지 못해 항상 미안했는데 올해부터는 보다 많은 시간을 보낼 수 있도록 할께. 아빠는 지금까지 혜주랑 많은 시간들을 보내지 못해 항상 미안해 하고 있었단다. 이제부터는 아빠로써의 모습들을 보일 수 있도록 하겠다는 다짐과 아빠가 약속한 대로 올해부터는 일주일에 2 번씩 수영장에 같이 가도록 하자. 그리고, 미국 생활에 잘 적응하고 친구들과도 잘 지내는 모습들을 보니 정말 대견하고 고맙다.

형님과 형수님, 너무 오랫동안 한국을 떠나 있게 되어 자주 뵙지 못해 죄송한 마음이 앞섭니다. 집안 중요한 일들이 있을 때 마다 따뜻한 마음으로 많은 일들을 처리해 주시고 박사 학위 기간 중 동생 가족 신경 안쓰게 많은 배려들을 해주셔서 감사드립니다. 박사 학위 논문 진행하는데 있어서 심적으로도 많은 도움들을 주셔서 감사 드리며 한국에 복귀하는 날이 올 때는 보다 많은 가족들 간의 교류들이 있을 수 있도록 하겠습니다.

다경이와 세중이, 다경이가 태어날 때도 그렇고 세중이가 태어날 때도 그렇고 작은 아빠가 항상 멀리 있어서 미안한 마음이 들구나. 늦게 조카가 생겨서 너무 좋기도 하고 좋다 보니 눈물까지 흘릴 정도 였단다. 형과 형수님 닮았으니 명석한 두뇌를 가진 것은 명백하고 행복하고 항상 밝고 즐겁게 생활하였으면 하구나. 미국 작은 아빠 집에도 시간 될 때 놀러 와서 좋은 시간들을 보낼 수 있었으면 한단다.

처남, 매형으로써 많은 이야기들과 상담들을 해 주었어야 되는데 항상 바쁘다는 핑계로 그렇게 해주지 못해서 미안한 마음이 앞서구나. 이제 안정적인 직장을 구해서 잘 적응해서 생활한다고 하니 정말 축하하고 한국에 가게 되면 자주 만나고 즐거운 시간들을 보낼 수 있도록 하자.

건이네 집, 프랑스 파리에 오래 동안 거주할 당시 많이 외로웠을 때 한국에서 유학오신 건이네 집을 만나는 행운을 얻을 수 있었습니다. 그 당시에는 회사에서 큰 스트레스를 받고 새벽까지 박사 논문 연구로 큰 스트레스를 받을 때 한번씩 오형님과 김지나 형수님, 그리고, 건이와 윤이를 만날 수 있어 저에게는 정신적으로 큰 도움이 되었습니다. 특히, 제 와이프가 가장 좋아하는 김지나 형수님을 만나 뵙고 아직까지도 계속해서 연락을 취하며 정신적으로 의지할 수 있게 되어 너무 감사 합니다. 나중에 한국으로 돌아가더라도 형님 집 주위에 집을 얻을 계획까지 세우고 있답니다. 형님은 한국은행 에서 CEO 까지 되실 거라는 것에 확신하며 옛날 형님과 함께 파리에서 마셨던 와인들에 대한 소중한 추억들을 추후 다시 한번 더 파리에서 가질 수 있었으면 합니다.

정기자님 집, 얼마 전 알게된 소식인데 완전히 프랑스 파리 특파원으로 발령났다는 소식을 접하게 되었습니다. 진심으로 축하드리며 정기자님을 보면서 정말 파리를 사랑하시는 멋진 형님이다라고 생각 했었습니다. 옛날에 파리에서의 소중한 추억들이 지금도 가끔씩 떠 오릅니다. 심영 형수님도 현재 한국에서 잘나가는 엔터테이먼트 사 CEO 를 하고 계시는 것으로 알고 있습니다. 사업에 승승장구를 하시기를 기원하며 다음에 꼭 한번 뵙겠습니다. 윤하와 다형이도 잘 지내고 있을 것이라 생각하고 윤하는 이번에 아빠 따라 프랑스

파리로 가면 완전히 프랑스 시민권자가 되겠구나. 윤하가 사랑하는 파리에서 좋은 결과물을 얻을 수 있었으면 하구나. 그리고 다형이는 정말 사랑스러운 장난꾸러기 였던 기억이 나는데 파리에 갈 일이 있으면 이쁜 선물 가지고 꼭 찾아 가도록 할께.

그리고, 박사 학위 과정 동안 파리에서 인연을 맺게 된 애드워드 교수님, 클라우즈, 테크닙 프로세스 엔지니어들, 쉘 프로세스 엔지니어들과, 할라기 교수님, 현 직장에 있는 앤드류 이하 우리 프로세스 엔지니어 동료들, 네덜란드 본사 및 모나코 프로세스 엔지니어들 및 엑슨모빌 웬루, 엑슨모빌 프로세스 엔지니어들, 쉐브론 프로세스 엔지니어들에게 감사의 마음을 표시하고자 한다. 또한, 이전 직장 이였던 삼성중공업, 대우조선해양, 및 처음 프로세스 엔지니어로써 길을 걷게 해준 현대중공업에서 인연을 맺었던 동료들에게도 감사의 마음을 전하고자 한다.

마지막으로 현재 황지현, 홍미영, 황혜주가 있게 해주신 양가 부모님들에게 큰 고마움을 남기고자 한다.

장인어르신과 장모님, 훌륭한 따님을 저에게 주셔서 제일 감사 드리며 저희가 처음 사회 생활 시작할 때 혜주를 맡아 키워주시며 사회 초년생 시절 빨리

경제적으로 안정화 할 수 있게 해주서서 항상 마음 속 깊이 감사드리고 있습니다. 이런 밑거름들이 사위가 현재 나아가는 길에 있어서 정말 큰 주춤돌들이 되었으며 기대하시는 바에 충족할 수 있는 큰 아들이 되겠습니다.

아버지 어머니, 항상 이 두마디를 부르면 먼지 모르게 가슴이 찡한 느낌이 듭니다. 저를 나아 주셔서 이렇게까지 키워 주셔서 진심으로 감사 드립니다. 처음 시작할 때는 미흡했지만 이렇게 박사 학위를 받게 된 것은 아버지, 어머니의 보이는, 그리고 보이지 않는 노력들이 있었기 때문이라고 생각 합니다. 아버지, 어머지 둘째 아들로써 해양플랜트 엔지니어링에 있어 세계적으로 독보적인 박사가 될 수 있도록 하여 세계적으로 이름을 날릴 수 있는 자랑스러운 아들이 될 수 있도록 하겠습니다.

이제 후기를 마칠려고 하니 많은 아쉬움들이 남는다. 처음 후기를 쓸 때는 재밌고 코믹하게 쓸려고 했는데 막상 작성을 시작해 보니 지금까지 걸어 오며 만났던 인연들, 그리고 가족들에 대한 고마움에 대한 글쓰기가 되어 버렸다. 그렇지만 만족스럽다.

후기를 마치기 전 글로 꼭 남기고 싶은 말이 떠 올랐다. 이는 해양플랜트 엔지니어링이 독자적으로 우리나라에서 수행되기를 간절히 바라며 이를 위해

향후 해양플랜트 엔지니어들을 꿈꾸는 후배들을 위해 꼭 해주고 싶은 말이다. 해양플랜트 엔지니어링을 하기 위해서는 3 가지 필수적인 요소들이 선행되어야 된다고 본다. 3 가지 필수적인 요소들로는 기술력, 인프라, 세계화 이다. 이들 중 한가지라도 충족되지 않으면 해양플랜트 엔지니어링을 수행하는데 있어서 사실상 어렵다고 본다.

먼저, 기술력에 대해서 이야기 하고자 한다. 해양 플랜트 엔지니어링 특성 상 기술력들은 일반적으로 참고할 수 있는 서적들을 통해서 얻는 것은 매우 한정적이다. 최선의 방법은 실제 엔지니어링을 수행하는 것이다. 여기서 중요한 것이 자신이 실제로 수행해 보는 것으로써 남들이 해 놓은 엔지니어링 결과물들을 어깨 넘어로 보고 와서 엔지니어링에 대해서 논하는 오류를 범해서는 안된다. 아무리 쉬운 결과물이라도 해도 백지 상태에서 실제 수행해 보고 나온 결과물을 신뢰할 수 있는 기관을 통해서 검증이 되어야만 실제적인 기술력이 쌓인다고 본다. 여기서 모순이 있다. 그럼, 실제 엔지니어링을 수행하기 위한 방법이 무엇일까? 현재까지 최선의 방법은 실제로 해양플랜트 엔지니어링을 수행하는 해외 회사들에 취업을 하는 길이다. 그 엔지니어링 회사들의 정직원으로 그 조직의 일원이 되어야만 가능한 일이다. 단지, 한국에서 파견 등의 형식으로 그 엔지니어링 회사들로 가는 것은 도움이 되지 못한다.

앞서 말한 어깨 넘어로 보는 것과 실제로 하는 것과는 정말 큰 차이가 있기 때문이다. 그럼, 여기서, 그런 해양플랜트 엔지니이링 회사들로 취업하는 길은 무었일까? 여기서 중요한 사실이 있다. 이런 해양플랜트 회사들이 큰 매력을 가질 수 있는 자기 만의 무기가 있어야 된다는 것이다. 보통, 해양플랜트 회사들은 유럽과 미국에 집중되어 있다. 이런, 회사들이 외국인을 자기 회사로 뽑기 위해서는 자국 내 일자리를 보호하기 위해 만든 까다로운 법규들에 충족되어야만 된다. 따라서, 자기들 나라에 도움이 되고 자국민들 보다 뛰어난 꼭 필요한 인재들에 한하여 취업 허가가 나온다. 따라서, 이런 측면에서 자기 만이 할 수 있고 큰 매력을 느낄 수 있는 무기들을 꼭 준비하여 미래에 이 곳 휴스턴 뿐만 아니라 유럽 등지에 한국 국적의 많은 엔지니어들이 진출하여 추후 한국내 해양 플랜트 엔지니어링 발전에 큰 기여를 하는 날이 꼭 오기를 바란다.

두번째로 인프라 구축이다. 기술력만 개인적으로 뛰어나다고 해도 설계 인프라 구축이 되어 있지 않으면 사실상 엔지니어링이 불가능하다. 이런 설계 인프라 구축은 각 해외 회사들마다 자기들 만의 오래된 경험들에 의하여 구축된 자산들이다. 이런 인프라 구축이 잘 되어 있으면 신입 사원이 입사를 하여도 구축된 인프라에 따라 최종 결과물이 나올 수 있게 된다. 물론, 이런 경우 리더 엔지니어들의 역할이 매우 중요하게 되지만 이 부분은 언급하지 않겠다. 이런,

인프라 구축을 위해서는 앞서 말한대로 해외 엔지니어링 회사들에서 많은 경험과 노하우들을 습득하여 이를 자신만의 고유한 인프라로 재구축하는 방법이 최선이라고 본다. 무에서 유가 나올 수 없다고 본다. 기존에 있는 유를 어떻게 자신만의 유로 만드느냐가 관건이라고 본다.

마지막으로 세계화에 대해서 말하고자 한다. 본인이 말하고자 하는 세계화는 언어와 문화이다. 만약, 우리나라가 미국과 같은 전세계적인 영향력을 가지고 있으면 이런 걱정은 할 필요가 전혀 없다. 그렇지만, 현실을 직시해 보자. 그 현실을 해양플랜트 엔지니어링에 한정지어 보면 모든 해외 오일 메이져 사들은 유럽과 미국 등지에 있다. 이들이 실제적인 힘들을 가지고 있으며 그들이 사용하는 언어와 살아가는 문화들이 있다. 따라서, 이에 맞추지 못한다면 사실상 해양플랜트 엔지니어링 시장에 들어올 수가 없다. 실제로 해외 오일 메이져 사들이 한국과 거래하는데 기피하는 이유들 중 일부가 언어적인 문제와 문화적인 차이로 인한 부분들 이라고 한다. 현재 만국 공통어는 영어 이다. 또한 언어는 문화이기 때문에 해외 문화를 무시할 수가 없다. 영어와 문화에 대해서 본인의 경험을 이야기 해보고자 한다. 본인은 영어 공부를 열심히 하였고 한국에 있을 당시 영어에 정말 자신이 있었다. 소위 한국에서 말하는 영어 능력 측정 기준들인 토익 950 점, 오픽 AL 등급, 영어 웅변 대회 부서 내 1 등을

하였다. 이로 인해 영어에 대한 자신감 또한 충만 하였다. 이런 자심감으로 인해 해외 회사들 취업 시 현지 인터뷰들을 볼 때도 기술적인 질문들 외에도 기술 외적인 질문들도 정말 자신 있게 말하여 강한 인상들을 심어 주었다고 본다. 그런데, 미국으로 취업하여 넘어 온 후 처음 몇 달 동안은 미국 문화를 너무 몰라서 많이 힘들었다. 이로 인해 자심감들도 떨어져 영어 사용 함에 있어서 소심해 지는 시기가 있었다. 결국, 문화에 대한 오픈 마인들을 가지고자 노력하였으며 또한 끊임 없는 영어에 대한 노력들로 현재 자심감을 되찾을 수 있었으며 이로 인해 정말 활발한 활동들을 많이 하고 있다. 여기서 느낀 것이 있다. 언어는 문화 이며 문화와 언어는 연결되어 있어 어느 하나라도 충족하지 못한다면 이는 자심감과도 연결되어 있어 자신이 가진 능력들을 발휘하지 못하게 된다는 것이다. 미래 해양플랜트 엔지니어를 꿈꾸는 후배들께 꼭 해주고 싶은 말은 영어 공부에 대해서는 절대 왕도가 있을 수가 없으며 끊임 없이 피나는 자신과의 싸움이 유일한 방법이라는 것이다. 자기 모국어가 아닌 이상 언어에는 마스트가 없다고 본다. 죽을 때까지 공부하고 공부하는 것이 유일한 방법이라고 본다. 문화적인 측면은 개인적인 성향이 크게 좌우되기 때문에 평소 오픈 마인드를 가질 수 있도록 노력하는 방법이 좋을 것으로 본다. 또한, 어떤 일들을 함에 있어서 자신감을 잃지 말라는 말을 해주고 싶다. 본인은 이렇게

생각한다. 자신감을 잃으면 모든 것을 잃는 것이라고. 내 자신의 경우를 봐도 그렇다. 자신감을 잃었을 때는 외국인들과 미팅함에 있어서 긴장감에 힘들어 했지만, 자심감을 찾았을 때는 많은 외국인들이 들어 오는 미팅에서도 주도적으로 미팅을 진행하며 미팅을 즐긴다. 즉 자신감이 전혀 다른 사람이 된 주된 원인이라고 본다. 절대 자신감을 잃지 말고 모든 일들을 하였으면 한다. 다만, 자신감이 자만심이 되지 않도록만 자신을 잘 조절할 수만 있으면 된다.

마지막으로 나는 꿈을 꾸고 있는 것이 있다. 지금은 먼 나라에 와 있다. 매일 아침 5 시에 기상하여 하루 일과를 확인 후 회사로 출근한다. 그리고, 여러 인종들이 섞여 있는 외국인들과 매일 매일 힘겨루기를 하고 있다. 한국 사람은 내 주위에 아무도 없다. 회사 정책과 해양 프로세스 업무 특성 상 한국과 교류할 일들도 전혀 없다. 때로는 너무 외롭다. 때로는 이런 생각들을 한다. 미국, 인도, 중국, 정말 인맥 파워가 막강하고 기술력 또한 훌륭하다. 나의 조국 대한민국, 이곳 휴스턴 현지 회사에 해양플랜트 관련 한국 인맥은 거의 없다. 특히 해양 프로세스 관련 엔지니어는 현재 내가 유일하다. 어디 기댈 곳도 없다. 오로지 실력으로만 버텨야 된다. 미국, 인도, 중국 엔지니어들은 회사 마치고 개인 여가 생활들을 보낸다. 그렇지만 나는 퇴근해서도 매일 노력한다. 정말 노력한다. 때로는 힘들다. 한때는 이렇게 생각했다. 불공평하다. 그렇지만

깨달았다. 불공평하다고 불평만 하면 나아지는 것은 아무것도 없다는 것을. 그 상황에 맞추어 피나는 노력만이 살길이며 이 것이 결국 미국, 인도, 중국 엔지니어들보다 결론적으로는 내가 더 클 수 있다는 것을. 나는 바란다. 이런 값진 경험들과 노력들이 나중에 언젠가는 한국에 돌아가서 큰 기여를 할 수 있는 순간이 올 수 있기를…… 오늘도 밤 12 시에 잠이 들며 생각한다.

(휴스턴 집 서재에서 글을 마무리 하며)